Supplementary Material

New Lanostane-Type Triterpenes with Anti-Inflammatory Activity from the Epidermis of *Wolfporia cocos*

Te-Ri-Gen Bao[a], Guo-Qing Long[a], Yong Wang[a], Qian Wang[b], Xuan-Li Liu[a], Gao-Sheng Hu[a], Xiao-Xu Gao[a,†], An-Hua Wang[a, †], Jing-Ming Jia[a,†]

[a] *Teaching and Research Department of Chinese Materia Medica Resources, College of Chinese Materia Medica, Shenyang Pharmaceutical University, Shenyang 110016, People's Republic of China*

[b] *College of Pharmacy, Shenyang Pharmaceutical University, Shenyang 110016, People's Republic of China*

ABSTRACT

A chemical study on the epidermis of cultivated edible mushroom *Wolfiporia cocos* resulted in the isolation and identification of 46 lanostane triterpenoids, containing 17 new compounds (**1-17**). An experimental determination of their anti-inflammatory activity showed that poricoic acid GM (**39**) most strongly inhibited NO production in LPS-induced RAW264.7 murine macrophages with an IC_{50} value at 9.73 μM. Furthermore, poricoic acid GM induced HO-1 protein expression and inhibited iNOS and COX2 protein expression as well as the release of PGE_2, IL-1β, IL-6, TNF-α and reactive oxygen species (ROS) in LPS-induced RAW264.7 cells. Mechanistically, poricoic acid GM suppressed the phosphorylation of the IκBα protein, which prevented NF-κB from entering the nucleus to lose transcriptional activity and inhibited the dissociation of Keap1 from Nrf2, thereby activating Nrf2 into the nucleus to regulate antioxidant genes. Furthermore, the MAPK signaling pathway may play a significant role in poricoic acid GM-induced elimination of inflammation. This work further confirms that lanostane triterpenoids are key ingredients responsible for the anti-inflammatory properties of the edible medicinal mushroom *W. cocos*.

Keywords: *Wolfiporia cocos*; *triterpene acid*; *anti-inflammatory activity*; *NF-κB signaling pathway*; *Keap1-Nrf2 signaling pathway; MAPK signaling pathway*

† **Corresponding author.** E-mail addresses: jiajingming@163.com **(J.-M. Jia);** sywanganhua@163.com **(A.-H. Wang);** 18842643805@163.com **(X.-X. Gao).**

Catalogue

1. Materials and methods

1.1. General experimental procedures

UV spectra were recorded on a JASCO V-650 UV spectrophotometer. Optical rotations were measured on a JASCO P2000 automatic polarimeter. 1D- and 2D-NMR spectra were recorded on a Bruker Avance 600 spectrometer with solvent peaks as references. HRESIMS data were obtained with an Agilent 1290 Infinity liquid chromatography system and an Agilent 6540 UHD Accurate-Mass Q-TOF mass spectrometer. High-performance liquid chromatography (HPLC) data were recorded on an Agilent 1260 instrument equipped with a photo-diode array (PDA) and a YMC C_{18} column (250 × 4.6 mm, 5 μM). Preparative HPLC was performed on Sanotac instrument China with a UV detector and a YMC C_{18} column (250 × 20 mm, 5 μM). Column chromatographic separations were carried out with silica gel (200-300 mesh, Qingdao Marine Chemical Group Corporation, Qingdao, China), ODS (50 μM, YMC, Kyoto, Japan). TLC was conducted with glass precoated with silica gel GF254 (Yantai Chemical Industrial Institute, Yantai, China). Chromatographic grade methanol and acetonitrile were purchased from Fisher. All other solvents were of chemical grade (Da Mao Chemical Co. Ltd, Tianjin, China).

1.2. Extraction and isolation

*1.2.1. Tuckahoacid A (**1**)*

White amorphous powder (MeOH); $[\alpha]_D^{20}$ -22.00 (c 0.1, MeOH); UV (MeOH) λ_{max} (log ε) = 205 (0.70), 250 (1.12) nm; CD (c 1.1 × 10^{-3} M, MeOH) λ_{max} ($\Delta\varepsilon$) = 255 (3.46), 280 (-0.71) nm; ^{13}C NMR (C_5D_5N, 150 MHz) data, see **Table 1**; ^{1}H NMR (C_5D_5N, 600 MHz) data, see **Table 2**; HRESIMS m/z 519.3083 $[M + Na]^+$ (calcd for $C_{31}H_{44}O_5Na$, 519.3086).

*1.2.2. Tuckahoacid B (**2**)*

White amorphous powder (MeOH); $[\alpha]_D^{20}$ +2.91 (c 0.3, MeOH); UV (MeOH) λ_{max} (log ε) = 222 (2.52), 270 (0.58) nm; CD (c 1.1 × 10^{-3} M, MeOH) λ_{max} ($\Delta\varepsilon$) = 263 (2.27) nm; ^{13}C NMR (C_5D_5N, 150 MHz) data, see **Table 1**; ^{1}H NMR (C_5D_5N, 600 MHz) data, see **Table 2**; HRESIMS m/z 513.3229 $[M - H]^-$ (calcd for $C_{31}H_{45}O_6$, 513.3216).

*1.2.3. Tuckahoacid C (**3**)*

White amorphous powder (MeOH); $[\alpha]_D^{20}$ -11.20 (c 0.1, MeOH); UV (MeOH) λ_{max} (log ε) = 228 (2.75), 268 (0.58) nm; CD (c 1.1 × 10^{-3} M, MeOH) λ_{max} ($\Delta\varepsilon$) = 272 (6.87) nm; ^{13}C NMR (C_5D_5N, 150 MHz) data, see **Table 1**; ^{1}H NMR (C_5D_5N, 600 MHz) data, see **Table 2**; HRESIMS *m/z* 513.3230 $[M - H]^-$ (calcd for $C_{31}H_{45}O_6$, 513.3216).

*1.2.4. Tuckahoacid D (**4**)*

White amorphous powder (MeOH); $[\alpha]_D^{20}$ -11.33 (c 0.2, MeOH); UV (MeOH) λ_{max} (log ε) = 211 (1.49), 252 (2.03) nm; CD (c 1.1 × 10^{-3} M, MeOH) λ_{max} ($\Delta\varepsilon$) = 201 (20.93), 253 (-20.61) nm; ^{13}C NMR (C_5D_5N, 150 MHz) data, see **Table 1**; ^{1}H NMR (C_5D_5N, 600 MHz) data, see **Table 2**; HRESIMS *m/z* 515.3385 $[M - H]^-$ (calcd for $C_{31}H_{47}O_6$, 515.3373).

*1.2.5. Tuckahoacid E (**5**)*

White amorphous powder (MeOH); $[\alpha]_D^{20}$ -2.67 (c 0.2, MeOH); UV (MeOH) λ_{max} (log ε) = 197 (0.07), 251 (0.28) nm; CD (c 1.1 × 10^{-3} M, MeOH) λ_{max} ($\Delta\varepsilon$) = 198 (8.06), 251 (-10.40) nm; ^{13}C NMR (C_5D_5N, 150 MHz) data, see δ_C 21.4 (3-CH_3CO), 170.8 (3-CH_3CO) and **Table 1**; ^{1}H NMR (C_5D_5N, 600 MHz) data, see δ_H 2.04 (3H, s, 3-CH_3CO) and **Table 2**; HRESIMS *m/z* 581.3451 $[M + Na]^+$ (calcd for $C_{33}H_{50}O_7Na$, 581.3454).

*1.2.6. Tuckahoacid F (**6**)*

White amorphous powder (MeOH); $[\alpha]_D^{20}$ +1.5 (c 0.2, MeOH); UV (MeOH) λ_{max} (log ε) = 218 (2.66), 270 (2.00) nm; CD (*c* 1.1 × 10^{-3} M, MeOH) λ_{max} ($\Delta\varepsilon$) = 269 (1.55) nm; ^{13}C NMR (C_5D_5N, 150 MHz) data, see **Table 1**; ^{1}H NMR (C_5D_5N, 600 MHz) data, see **Table 2**; HRESIMS *m/z* 499.3072 $[M - H]^-$ (calcd for $C_{30}H_{43}O_6$, 499.3060).

*1.2.7. Tuckahoacid G (**7**)*

White amorphous powder (MeOH); $[\alpha]_D^{20}$ -10.29 (c 0.2, MeOH); UV (MeOH) λ_{max} (log ε) = 197 (0.08), 245 (0.40) nm; CD (*c* 1.1 × 10^{-3} M, MeOH) λ_{max} ($\Delta\varepsilon$) = 202 (11.87), 245 (-4.34) nm; ^{13}C NMR (C_5D_5N, 150 MHz) data, see δ_C 55.7 (12-OCH_3) and **Table 1**; ^{1}H NMR (C_5D_5N, 600 MHz) data, see δ_H 3.49 (3H, s, 12-OCH_3) and **Table 2**; HRESIMS m/z 515.3384 $[M - H]^-$ (calcd for $C_{31}H_{47}O_6$, 515.3373).

*1.2.8. Tuckahoacid H (**8**)*

White amorphous powder (MeOH); $[\alpha]_D^{20}$ -10.7 (c 0.2, MeOH); UV (MeOH) λ_{max} (log ε) = 211 (0.86), 245 (1.23) nm; CD (*c* 1.1 × 10^{-3} M, MeOH) λ_{max} ($\Delta\varepsilon$) = 202 (11.07), 246 (-8.13) nm; ^{13}C NMR (C_5D_5N, 150 MHz) data, see δ_C 55.7 (12-OCH_3) and **Table 1**; ^{1}H NMR (C_5D_5N, 600 MHz) data, see δ_H 3.54 (3H, s, 12-OCH_3) and **Table 2**; HRESIMS *m/z* 517.3544 $[M - H]^-$ (calcd for $C_{31}H_{49}O_6$, 517.3529).

*1.2.9. Tuckahoacid I (**9**)*

White amorphous powder (MeOH); $[\alpha]_D^{20}$ -11.00 (c 0.1, MeOH); UV (MeOH) λ_{max} (log ε) = 198 (0.22), 244 (2.68) nm; CD (*c* 1.1 × 10^{-3} M, MeOH) λ_{max} ($\Delta\varepsilon$) = 202 (15.29), 240 (-8.94) nm; ^{13}C NMR (C_5D_5N, 150 MHz) data, see δ_C 55.7 (12-OCH_3) and **Table 1**; ^{1}H NMR (C_5D_5N, 600 MHz) data, see δ_H 3.51 (3H, s, 12-OCH_3) and **Table 2**; HRESIMS m/z 517.3540 $[M - H]^-$ (calcd for $C_{31}H_{49}O_6$, 517.3529).

*1.2.10. Tuckahoacid J (**10**)*

White amorphous powder (MeOH); $[\alpha]_D^{20}$ +11.00 (c 0.2, MeOH); UV (MeOH) λ_{max} (log ε) = 216 (2.22), 240 (0.37) nm; CD (*c* 1.1 × 10^{-3} M, MeOH) λ_{max} ($\Delta\varepsilon$) = 240 (7.48) nm; ^{13}C NMR (C_5D_5N, 150 MHz) data, see δ_C 51.7 (3-$COOCH_3$), 50.5 (25-OCH_3) and **Table 1**; ^{1}H NMR (C_5D_5N, 600 MHz) data, see δ_H 3.62 (3H, s, 3-$COOCH_3$), δ_H 3.04 (3H, s, 25-OCH_3) and **Table 3**; HRESIMS *m/z* 565.3508 $[M + Na]^+$ (calcd for $C_{33}H_{50}O_6Na$, 565.3505).

*1.2.11. Tuckahoacid K (**11**)*

White amorphous powder (MeOH); $[\alpha]_D^{20}$ +6.29 (c 0.2, MeOH); UV (MeOH) λ_{max} (log ε) = 196 (0.08), 242 (0.26) nm; CD (*c* 1.1 × 10^{-3} M, MeOH) λ_{max} ($\Delta\varepsilon$) = 240 (4.51) nm; ^{13}C NMR (C_5D_5N, 150 MHz) data, see δ_C 51.8 (3-$COOCH_3$) and **Table 1**; ^{1}H NMR (C_5D_5N, 600 MHz) data, see δ_H 3.63 (3H, s, 3-$COOCH_3$) and **Table 3**; HRESIMS *m/z* 511.3434 $[M - H]^-$ (calcd for $C_{32}H_{47}O_5$, 511.3423).

*1.2.12. Tuckahoacid L (**12**)*

White amorphous powder (MeOH); $[\alpha]_D^{20}$ -33.00 (c 0.1, MeOH); UV (MeOH) λ_{max} (log ε) = 202 (0.25), 242 (0.72) nm; CD (*c* 1.1 × 10^{-3} M, MeOH) λ_{max} ($\Delta\varepsilon$) = 241 (4.08) nm; ^{13}C NMR (C_5D_5N, 150 MHz) data, see δ_C 51.8 (3-$COOCH_3$) and **Table 1**; ^{1}H NMR (C_5D_5N, 600 MHz) data, see δ_H 3.62 (3H, s, 3-$COOCH_3$) and **Table 3**; HRESIMS m/z 543.3337 $[M - H]^-$ (calcd for $C_{32}H_{47}O_7$, 543.3322).

*1.2.13. Tuckahoacid M (**13**)*

White amorphous powder (MeOH); $[\alpha]_D^{20}$ -28.00 (c 0.1, MeOH); UV (MeOH) λ_{max} (log ε) = 205 (0.51), 242 (1.13) nm; CD (*c* 1.1 × 10^{-3} M, MeOH) λ_{max} ($\Delta\varepsilon$) = 241 (9.68) nm; ^{13}C NMR (C_5D_5N, 150 MHz) data, see δ_C 51.7 (3-$COOCH_3$) and **Table 1**; ^{1}H NMR (C_5D_5N, 600 MHz) data, see δ_H 3.62 (3H, s, 3-COOCH$_3$) and **Table 3**; HRESIMS *m/z* 543.3334 [M - H]$^-$ (calcd for $C_{32}H_{47}O_7$, 543.3322).

*1.2.14. Tuckahoacid N (**14**)*

White amorphous powder (MeOH); $[\alpha]_D^{20}$ +10.00 (c 0.1, MeOH); UV (MeOH) λ_{max} (log ε) = 242 (1.44), 288 (0.87) nm; CD (*c* 1.1 × 10^{-3} M, MeOH) λ_{max} ($\Delta\varepsilon$) = 222 (4.21), 250 (-0.54), 290 (6.70) nm; ^{13}C NMR (C_5D_5N, 150 MHz) data, see δ_C 51.8 (3-COOCH$_3$) and **Table 1**; ^{1}H NMR (C_5D_5N, 600 MHz) data, see δ_H 3.62 (3H, s, 3-COOCH$_3$) and **Table 3**; HRESIMS *m/z* 545.3487 [M - H]$^-$ (calcd for $C_{32}H_{49}O_7$, 545.3478).

*1.2.15. Tuckahoacid O (**15**)*

White amorphous powder (MeOH); $[\alpha]_D^{20}$ +9.6 (c 0.1, MeOH); UV (MeOH) λ_{max} (log ε) = 242 (0.47), 289 (0.30) nm; CD (*c* 1.1 × 10^{-3} M, MeOH) λ_{max} ($\Delta\varepsilon$) = 220 (3.98), 243 (-2.03), 292 (6.50) nm; ^{13}C NMR (C_5D_5N, 150 MHz) data, see δ_C 51.8 (3-COOCH$_3$) and **Table 1**; ^{1}H NMR (C_5D_5N, 600 MHz) data, see δ_H 3.63 (3H, s, 3-COOCH$_3$) and **Table 3**; HRESIMS *m/z* 561.3438 [M - H]$^-$ (calcd for $C_{32}H_{49}O_8$, 561.3427).

*1.2.16. Tuckahoacid P (**16**)*

White amorphous powder (MeOH); $[\alpha]_D^{20}$ +2.67 (c 0.1, MeOH); UV (MeOH) λ_{max} (log ε) = 242 (0.63), 290 (0.39) nm; CD (*c* 1.1 × 10^{-3} M, MeOH) λ_{max} ($\Delta\varepsilon$) = 221 (5.00), 251 (-0.60), 289 (6.48) nm; ^{13}C NMR (C_5D_5N, 150 MHz) data, see δ_C 51.8 (3-COOCH$_3$) and **Table 1**; ^{1}H NMR (C_5D_5N, 600 MHz) data, see δ_H 3.63 (3H, s, 3-COOCH$_3$) and **Table 3**; HRESIMS *m/z* 585.3396 [M + Na]$^+$ (calcd for $C_{32}H_{50}O_8Na$, 585.3403).

*1.2.17. Tuckahoacid Q (**17**)*

White amorphous powder (MeOH); $[\alpha]_D^{20}$ +4.67 (c 0.2, MeOH); UV (MeOH) λ_{max} (log ε) = 214 (2.17), 267 (0.19) nm; CD (*c* 1.1 × 10^{-3} M, MeOH) λ_{max} ($\Delta\varepsilon$) = 200 (-5.08), 207 (0.98), 214 (-4.17), 227 (2.09) nm; ^{13}C NMR (C_5D_5N, 150 MHz) data, see **Table 1**; ^{1}H NMR (C_5D_5N, 600 MHz) data, see **Table 3**; HRESIMS m/z 497.3278 [M - H]$^-$ (calcd for $C_{31}H_{45}O_5$, 497.3267).

1.3. Cell culture

RAW264.7 murine macrophages were obtained from the Chinese Academy of Sciences (Shanghai, China) and cultured in Dulbecco's Modified Eagle Medium (DMEM, Gibco, USA) with 4.5 g/L glucose, 10% fetal bovine serum (FBS, Gibco, USA), and 1% penicillin/streptomycin (Gibco, USA) in a cell incubator (37 °C and 5% CO_2).

1.4. Cell viability assay

Briefly, RAW264.7 cells (10000 cells/well) were seeded into a 96-well plate and incubated overnight at 37 °C. The tested compounds were added to the cells, dimethyl sulfoxide (DMSO) was used as the vehicle control. Following incubation for 24 h, 20 μL of 3-(4,5-dimethylthiazol-2-yl)-2,5-diphenyltetrazolium bromide (MTT, Sigma-Aldrich, USA) agent was added to cells, and then incubated for 4 h at 37 °C. Next, the absorbance at 570 nm was recorded using a microplate reader (Thermo Fisher, Waltham, USA).

1.5. Detection of NO, PGE$_2$

In brief, RAW264.7 cells were seeded into a 96-well plate at a density of 10000 cells/well, and then incubated overnight. Next, cells were pre-treated with the tested compounds at the indicated concentrations for 1 h and followed by stimulation of LPS (200 ng/mL, isolated from *Escherichia coli* 055: B5, Sigma, Shanghai, China) for another 24 h. Subsequently, the culture medium was collected, and centrifuged for 5 min at 4 °C (1,000 rpm). The supernatants were used to measure the NO levels using Griess reagent (Beyotime, Shanghai, China). On the other hand, the level of PGE_2 in the supernatants was then assessed using ELISA kits according to the manufacturer's protocols (R&D Systems, Minneapolis, MN, USA).

1.6. Immunofluorescent

RAW264.7 cells were seeded into a 24-well plate at a density of 2.5×10^5 cells/well, and incubated overnight. Then, cells were pre-treated with the tested compounds for 1 h and followed stimulation of LPS (200 ng/mL) for another 1 h. Cells were washed with PBS, fixed with 4% paraformaldehyde (PFA) for 10 min, and permeabilized with 0.5% Triton X-100 for 20 min at RT. Next, cells were blocked with 1% bovine serum albumin (BSA) for 30 min at RT and incubated with primary antibody (1:100) overnight at 4°C. After washing with PBS thrice, cells were incubated with FITC fluorescent secondary antibody (1:1000) for 1 h in the darkroom at RT. The nucleuses were then stained with Hoechst 33258 (DAPI, 0.5 μg/mL, Beyotime, Shanghai, China) for 15 min in the darkroom at RT. Finally, the subcellular localizations of NF-κB and Nrf2 were observed using the Fluorescent inverted microscope (Olympus, Japan).

1.7. qRT-PCR

In brief, RAW264.7 cells were seeded into a 24-well plate at a density of 2.5×10^5 cells/mL and then incubated overnight. Next, cells were pre-treated with the tested compounds at the indicated concentrations for 1 h and followed by stimulation of LPS (200 ng/mL) for another 4 h. Total RNA was extracted with TRIzol kit (Invitrogen, USA). According to the instructions, 2 μg RNA as template was added into HiScript II Q RT Supermix (Nanjing Nuowizan Biological Technology, China) for qPCR reverse transcription to obtain cDNA. The cDNA samples were amplified by Transstart Top Green qPCR Supermix (Beijing Quansi Gold Biotechnology, China) at a final volume of 20 μL. qRT-PCR was performed using Thermo Scientific Pikoreal (Thermo Fisher Scientific, MA, USA). Real-time PCR primers were designed and synthesized by Shanghai Sangon Co., Ltd. The sequences of the primers were listed in Table S3.

1.8. Western blotting

Following treatment with the tested compounds, RAW264.7 cells were washed with phosphate buffered solution (PBS) and then lysed with pre-cold radio-immunoprecipitation assay (RIPA) buffer containing 1% protease and phosphatase inhibitors (ApexBio, USA). After centrifuging for 5 min at 4 °C (12,000 rpm), the supernatants were collected, mixed with loading buffer, and then boiled at 100 °C for 5 min. Next, the cell lysates were subjected to sodium dodecyl sulfate polyacrylamide gel (SDS-PAGE) electrophoresis. The proteins were then transferred to the polyvinylidene difluoride (PVDF) membranes (Millipore, Bedford, USA). The membranes were blocked with tris-buffered saline with tween 20 (TBST) buffer containing 5% non-fat milk powder and incubated with specific primary antibodies (1:1000) overnight at 4 °C. After washing with TBST buffer 3 times, the membranes were incubated with horseradish peroxidase (HRP)-labeled secondary antibody for 1 h at room temperature (RT). Next, the membranes were washed with TBST buffer thrice, and the immunoblot signals were detected in the Gel DOC™ XR+system using a chemiluminescence agent (Beyotime, Shanghai, China). The antibodies used in this experiment were as follows: Primary antibody against iNOS was purchased from Abcam (USA), Primary antibody against COX2, JNK, and LaminB were from ProteinTech Group (USA), the remaining antibodies were purchased from Santa Cruz (Shanghai, China).

1.9. Statistical analysis

All results were representative of three independent experiments. Data were expressed as mean values ± standard deviation (SD). Statistical analyses were performed with GraphPad Prism 5.0 software (La Jolla, CA, USA), and compared by One-way ANOVA. The differences were considered statistically significant when $p < 0.05$.

1.10. ECD calculation

In general, conformational analyses were carried out via random searching in the Sybyl-X 2.0 using the MMFF94S force field with an energy cutoff of 5 kcal/mol.[1] The results showed five lowest energy conformers for both compounds. Subsequently, geometry optimizations and frequency analyses were implemented at the B3LYP-D3(BJ)/6-31G* level in PCM methanol using ORCA4.2.1[2,3] All conformers used for property calculations in this work were characterized to be a stable point on potential energy surface (PES) with no imaginary frequencies. The excitation energies, oscillator strengths, and rotational strengths (velocity) of the first 60 excited states were calculated using the TD-DFT methodology at the PBE0/def2-TZVP level in methanol. The ECD spectra were simulated by the overlapping Gaussian function (half the bandwidth at 1/e peak height, sigma = 0.30 for all).[4] Gibbs free energies for conformers were determined by using thermal correction at B3LYP-D3(BJ)/6-31G* level and electronic energies evaluated at the wB97M-V/def2-TZVP level in PCM methanol using ORCA4.2.1[2,3] To get the final spectra, the simulated spectra of the conformers were averaged according to the boltzmann distribution theory and their relative Gibbs free energy (ΔG). By comparing the experimental spectra with the calculated model molecules, the absolute configuration of the only chiral center was determined to be.

References

(1) Sybyl Software, version X 2.0; Tripos Associates Inc.: St. Louis, MO, **2013**.
(2) Neese, F. The ORCA program system, Wiley Interdiscip. Rev.: *Comput. Mol. Sci*., **2012**, *2*, 73-78.
(3) Neese, F. Software update: the ORCA program system, version 4.0, Wiley Interdiscip. Rev.: *Comput. Mol. Sci*. **2017**, *8*, e1327.
(4) Stephens, P. J.; Harada, N. ECD cotton effect approximated by the Gaussian curve and other methods. *Chirality* **2010**, *22*, 229–233.

1.11. The crystallization condition

5 mg of compound and 500 μL of MeOH were added into the vitric autosampler bottle and dissolved completely. The saturation of the compound was beneficial, sometimes we could add some drops of water. Parafilm was used to seal the bottle. We poked two eyelets at the parafilm with the needle. The vitric autosampler bottle should be put in low temperature environment and the solvent should volatilize slowly.

Table S1. Cell viability of the EtOH extract and solvent-partitioned fractions in RAW264.7 macrophages.

Samples	Concentration (μg/mL)	RAW264.7 cell viability (of % control)
EtOH extract	50	100.5
	25	102.5
	12.5	105.4
PE	50	95.7
	25	96.1
	12.5	97.1
MC	50	94.4
	25	96.5
	12.5	107.0
EA	50	103.9
	25	108.5
	12.5	109.9
BuOH	50	96.1
	25	101.6
	12.5	102.2

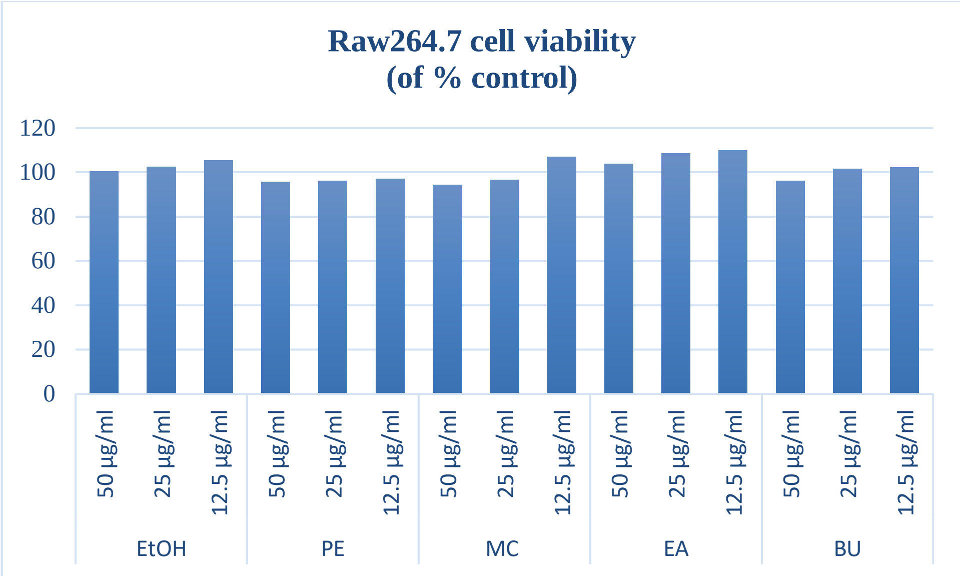

Figure S1. Cell viability of the EtOH extract and solvent-partitioned fractions in RAW264.7 macrophages.

Table S2. Inhibitory effects of the EtOH extract and solvent-partitioned fractions on NO production in LPS-activated RAW264.7 macrophages.

Samples	Concentration (μg/mL)	NO production (of % LPS)
LPS	0.2	100
	50	80.3
EtOH extract	25	96.5
	12.5	97.8
	50	79.6
PE	25	81.7
	12.5	83.6
	50	21.1
MC	25	51.8
	12.5	73.9
	50	61.8
EA	25	71.9
	12.5	77.2
	50	91.3
BuOH	25	90.4
	12.5	97.2

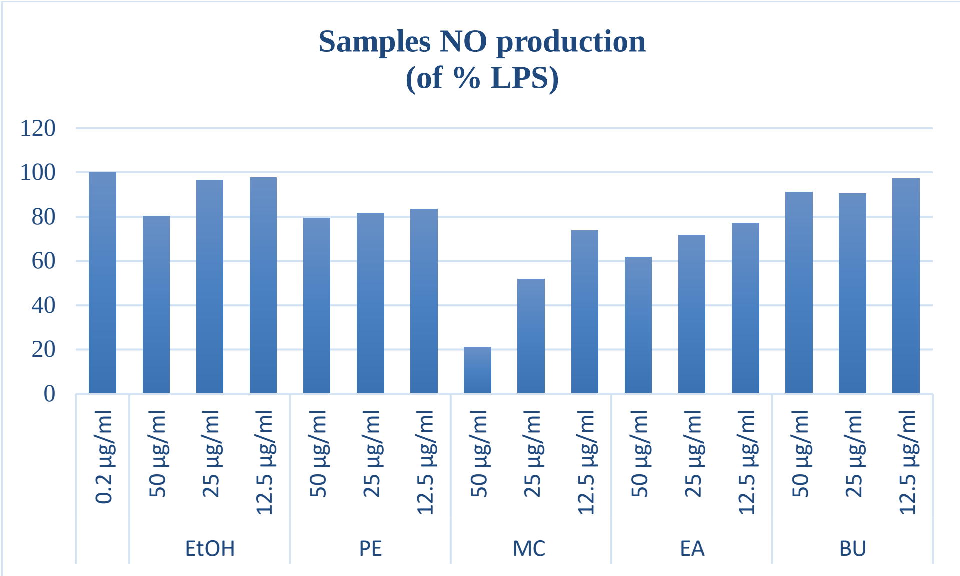

Figure S2. Inhibitory effects of the EtOH extract and solvent-partitioned fractions on NO production in LPS-activated RAW264.7 macrophages.

Table S3. The sequences of the primers.

Gene	Sequence (5′ to 3′)
iNOS	F: AGCCAAGCCCTCACCTACTT R: GCCTCCAATCTCTGCCTATC
COX-2	F: CCAGCACTTCACCCATCAGT R: GGGATACACCTCTCCACCAA
TNF-α	F: CAGACCCTCACACTCAGATCATCTT R: CAGAGCAATGACTCCAAAGTAGACCT
IL-6	F: CACGGCCTTCCCTACTTCAC R: TGCAAGTGCATCATCGTTGT
IL-1β	F: GTTGACGGACCCCAAAAGAT R: CCTCATCCTGGAAGGTCCAC
β-actin	F: ATGTGGATCAGCAAGCAGGA R: AAGGGTGTAAAACGCAGCTCA
Nrf2	F: TCAGCGACAGAAGGACTATGAG R： AGGCATCTTGTTTGGGAATG
Keap1	F: TCTCCAAGGGTCTCCTGAAT R: CAACACCACACCAACATTTACA
HO-1	F: GCCAGCCACACAGCACTAT R： GGCGGTCTTAGCCTCTTCTG
NQO1	F: AGTGGCATCCTGCGTTTCT R： TCTCCTCCCAGACGGTTTC

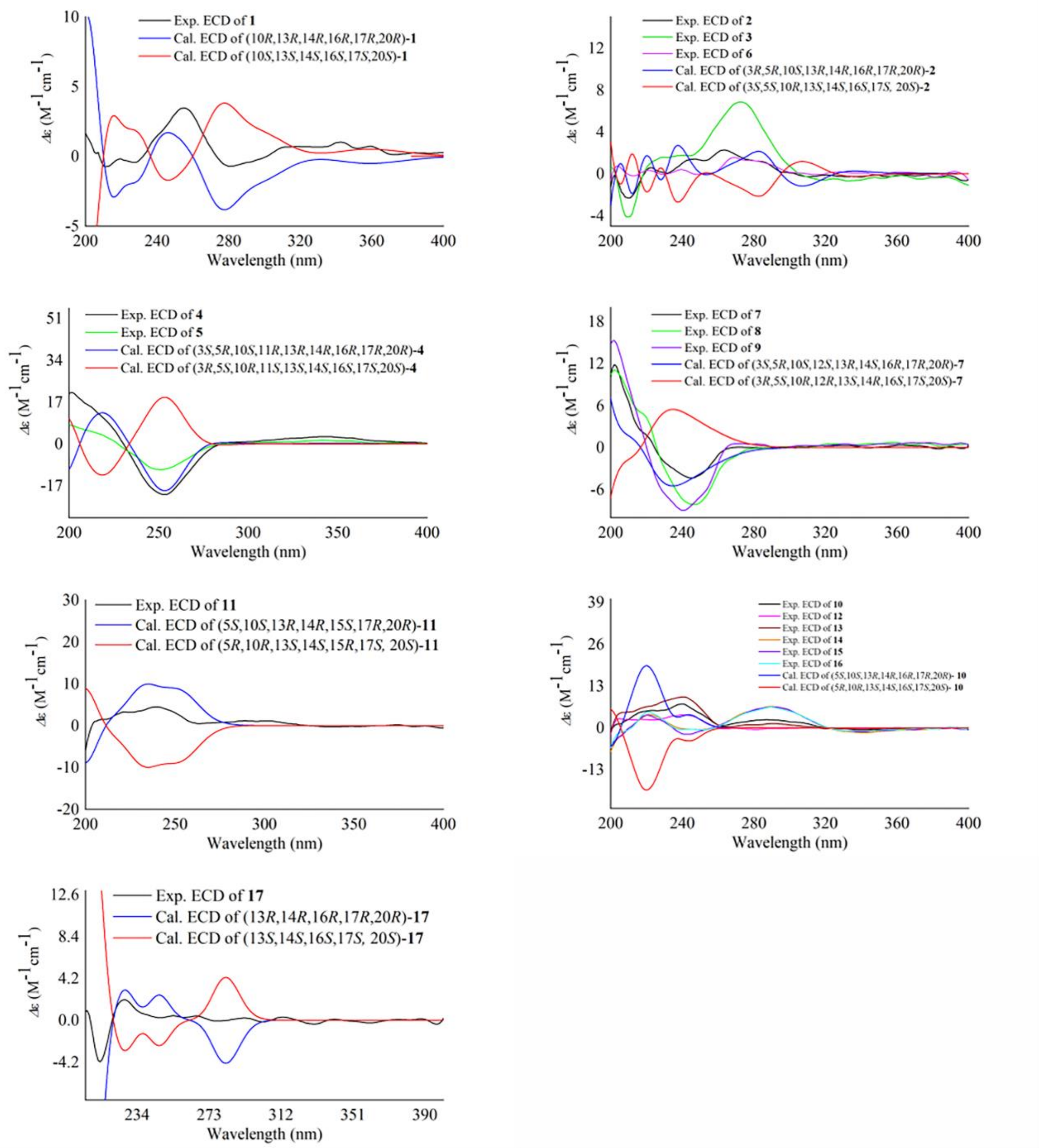

Figure S3. Experimental ECD and calculated ECD spectra of new compounds.

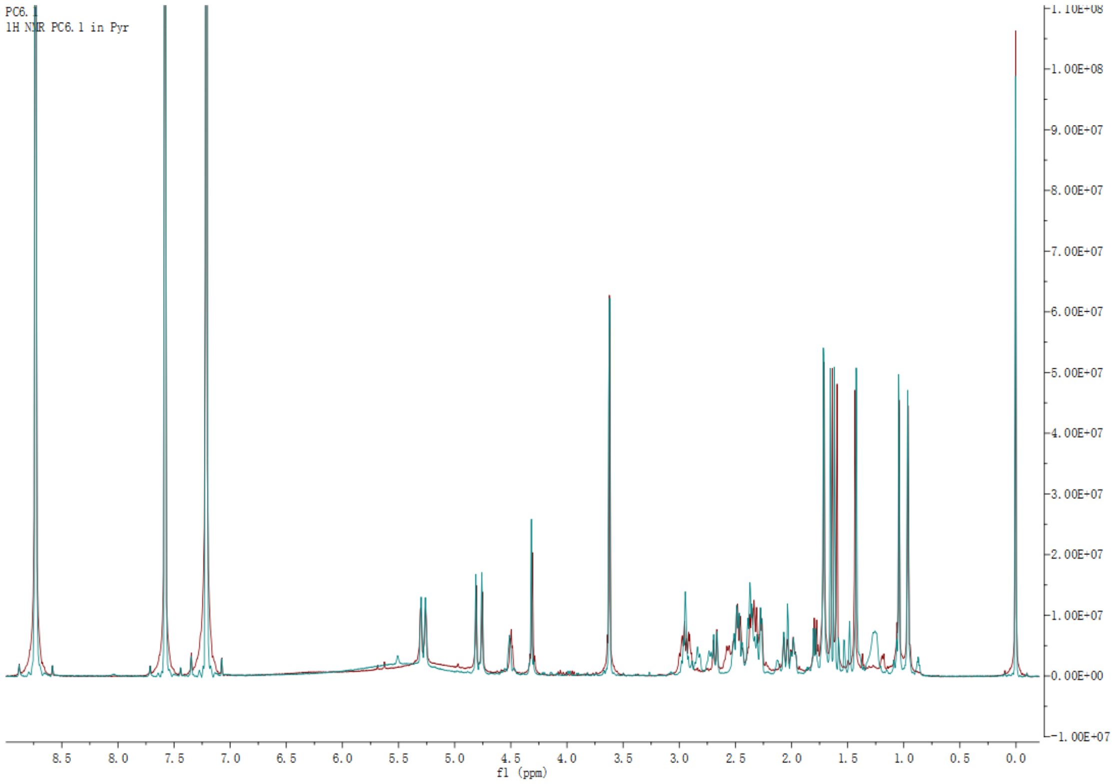

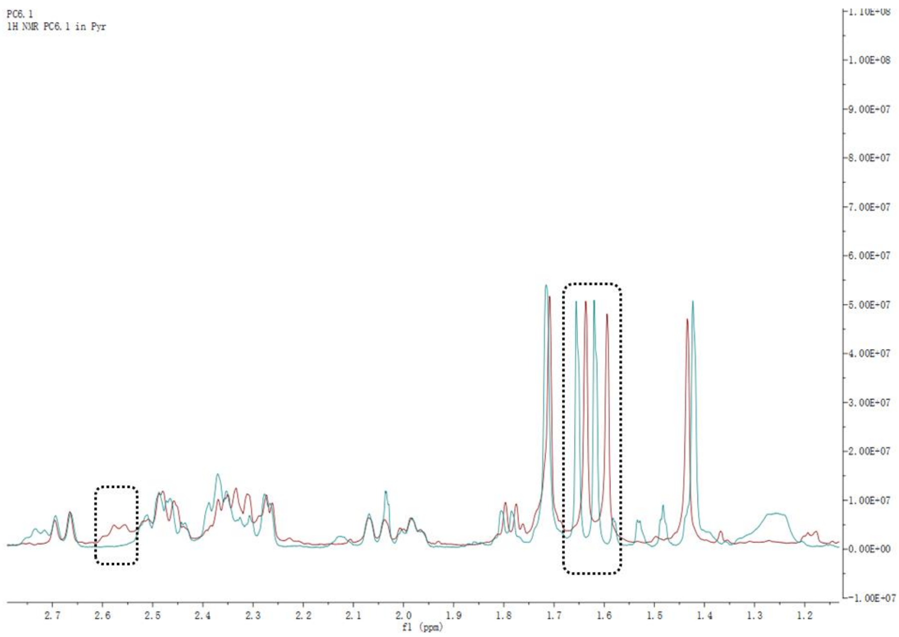

Figure S4. The stack graph of compounds **15** and **16** ^{1}H NMR spectra.

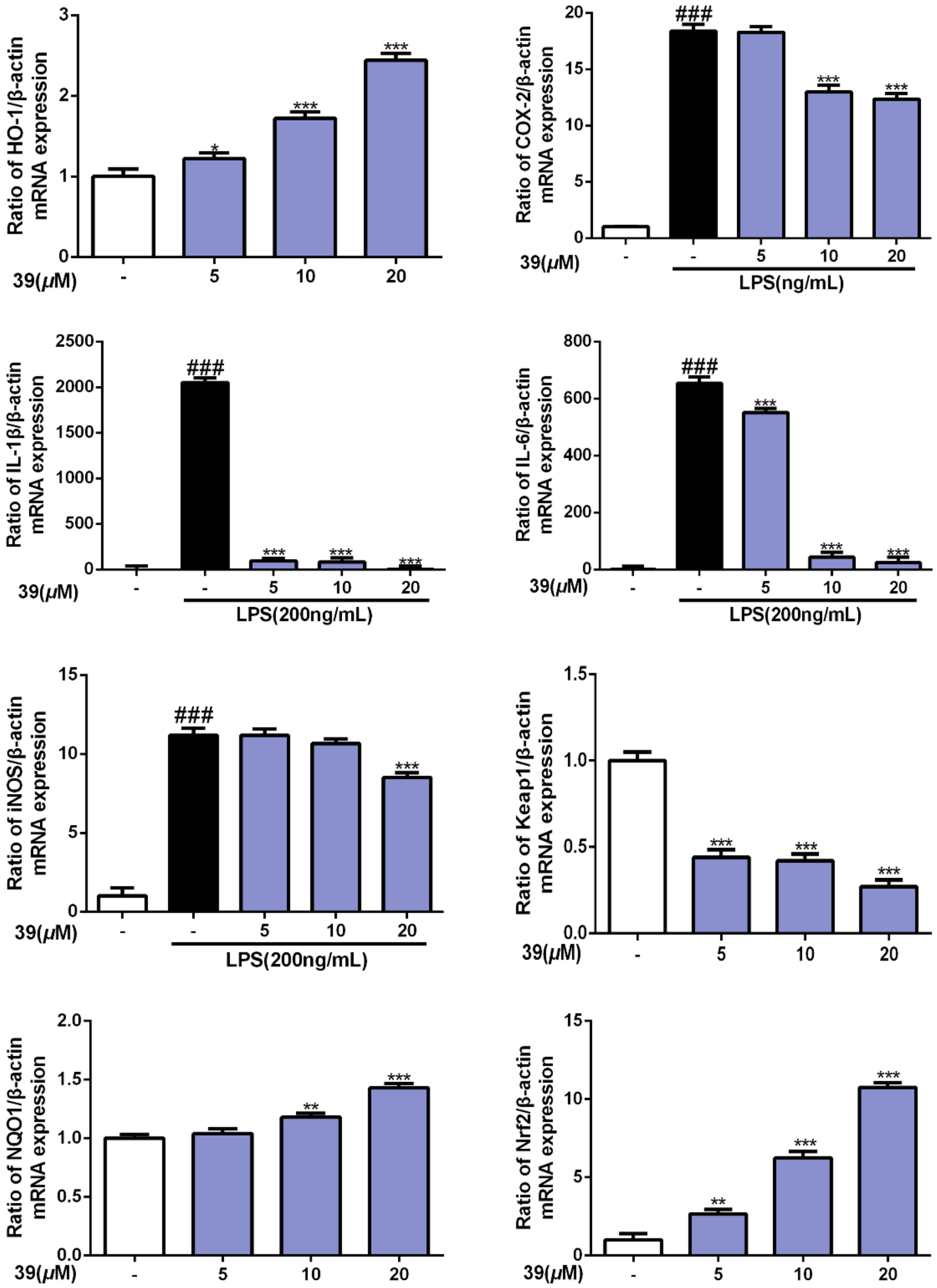

Figure S5. RAW264.7 cells were treated with poricoic acid GM (**39**) from 5 to 20 μM at the indicated dose with stimulated by LPS (200 ng/mL) for 4 h. The mRNA of iNOS, COX-2, TNF-α, IL-1β and IL-6 and β-actin was detected by RT-PCR with specific primers. The amplified DNA fragment was analyzed by 1% agarose gel and visualized by ethidium bromide staining. Effects of poricoic acid GM (**39**) on Nrf2, HO-1, Keap1 and NQO1 gene expressions in RAW264.7 cells. The cells were treated with poricoic acid GM (**39**) (5, 10 and 20 μM) for 4 h. Data shown are the means ± SD from three independent experiments, *p < 0.05, **p < 0.01, ***p < 0.001 vs LPS-treated group and ###p < 0.001 vs control group.

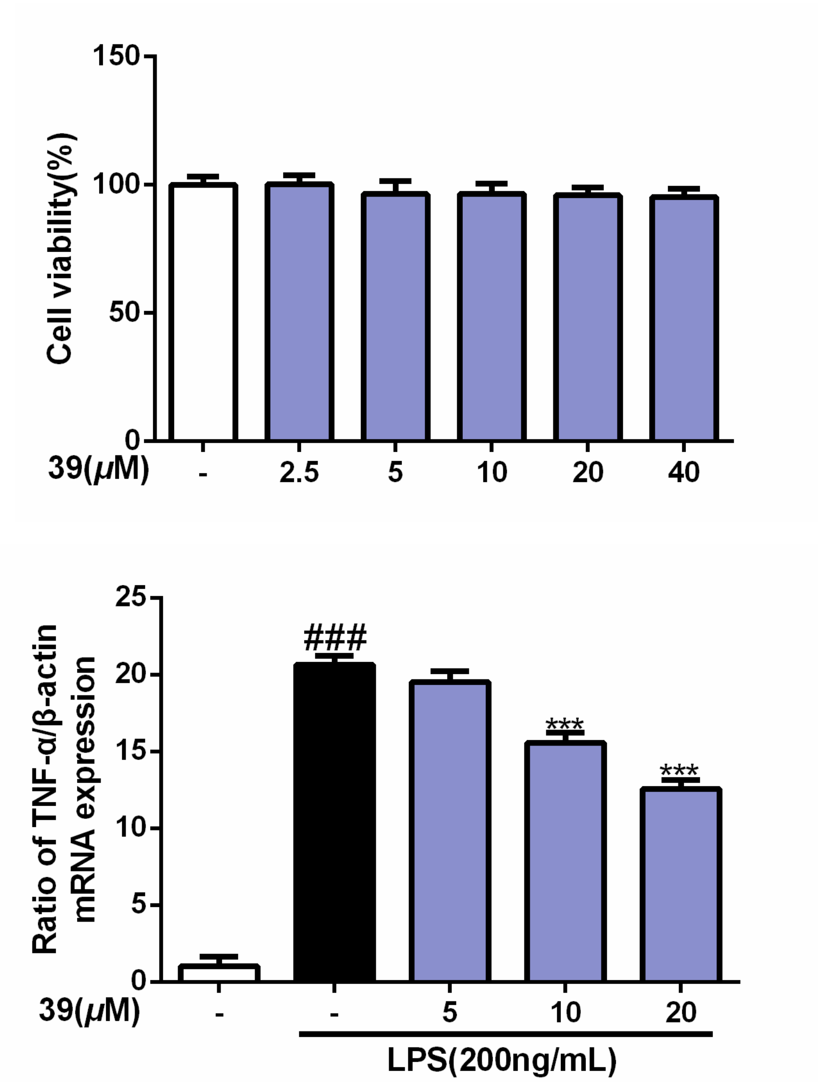

Figure S6. RAW264.7 cells were seeded on 96 well plates and treated with different concentrations of poricoic acid GM (**39**) (2.5, 5, 10, 20, 40 μM) for 24 h. MTT was added to detect the cell survival rate. RAW264.7 cells were treated with poricoic acid GM (**39**) from 5 to 20 μM at the indicated dose with stimulated by LPS (200 ng/mL) for 4 h. The mRNA of TNF-α and β-actin was detected by RT-PCR with specific primers. The amplified DNA fragment was analyzed by 1% agarose gel and visualized by ethidium bromide staining. Data shown are the means ± SD from three independent experiments, *p < 0.05, **p < 0.01, ***p < 0.001 vs LPS-treated group and ###p < 0.001 vs control group.

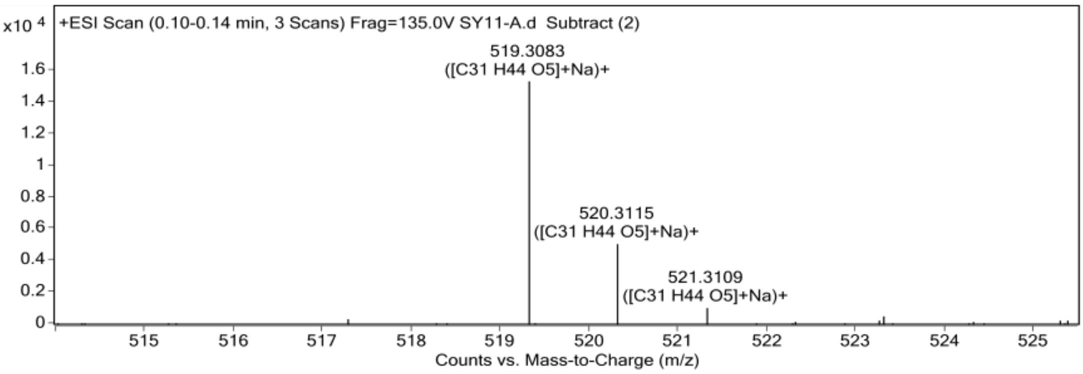

Figure S7. HRESIMS spectrum of compound **1**

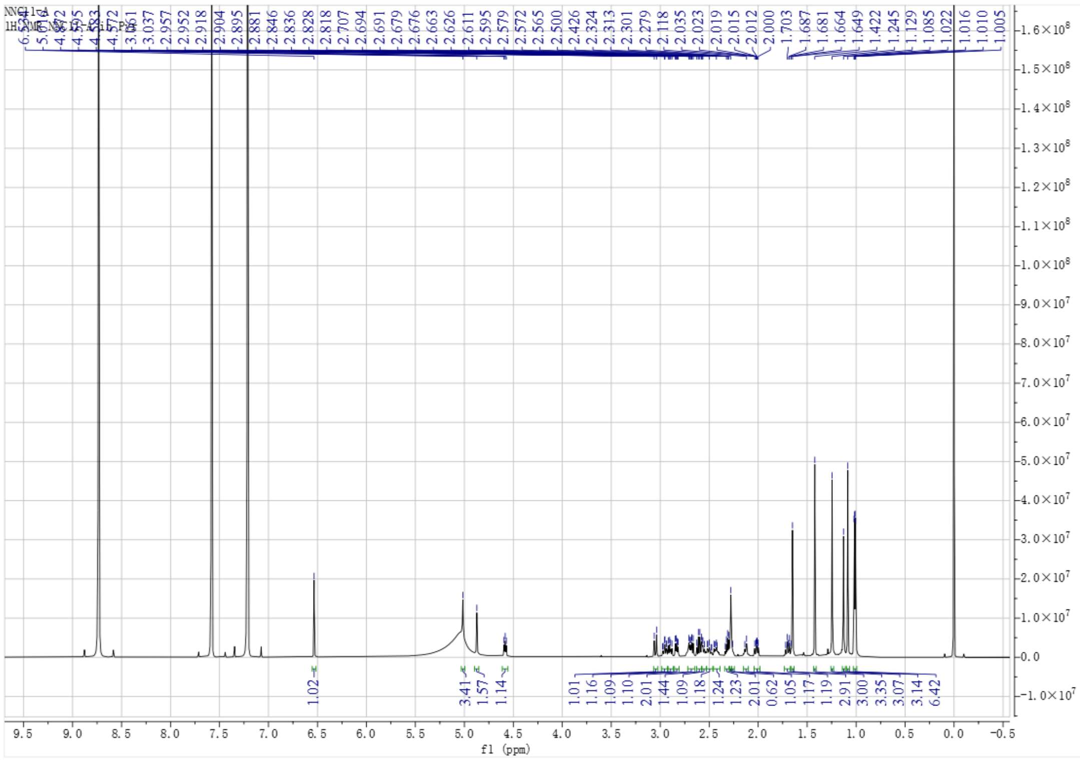

Figure S8. ^{1}H NMR spectrum (600 MHz, C_5D_5N) of compound **1**

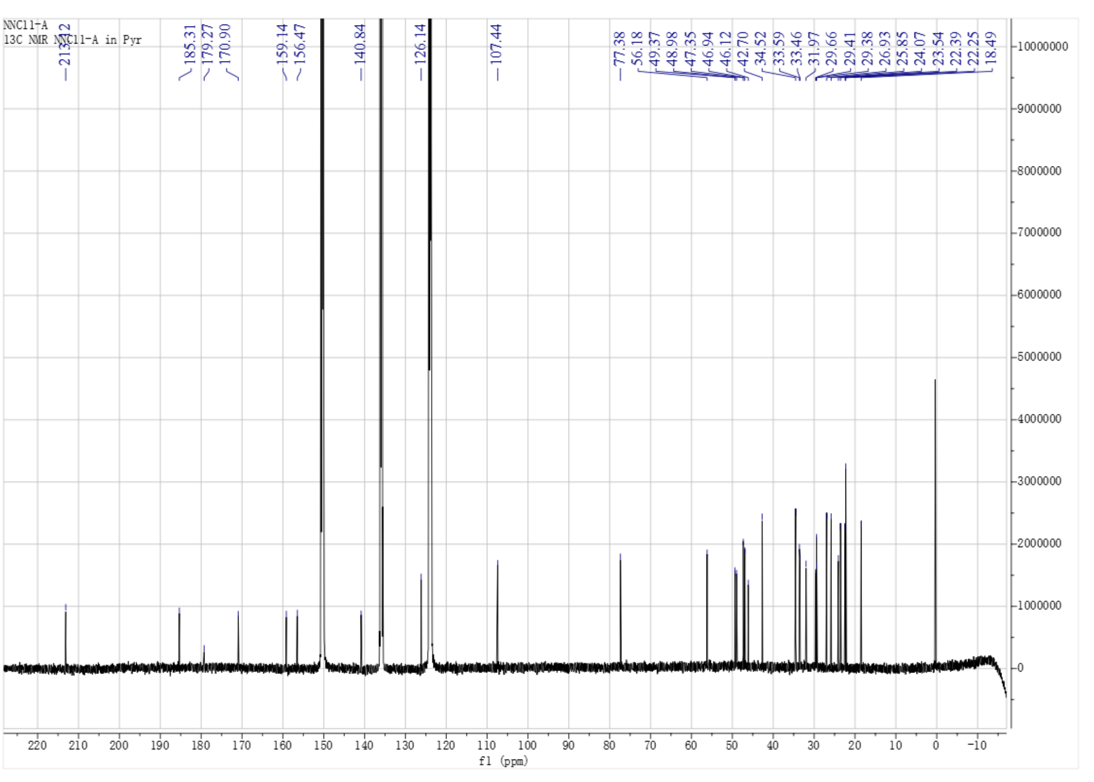

Figure S9. ^{13}C NMR spectrum (150 MHz, C_5D_5N) of compound **1**

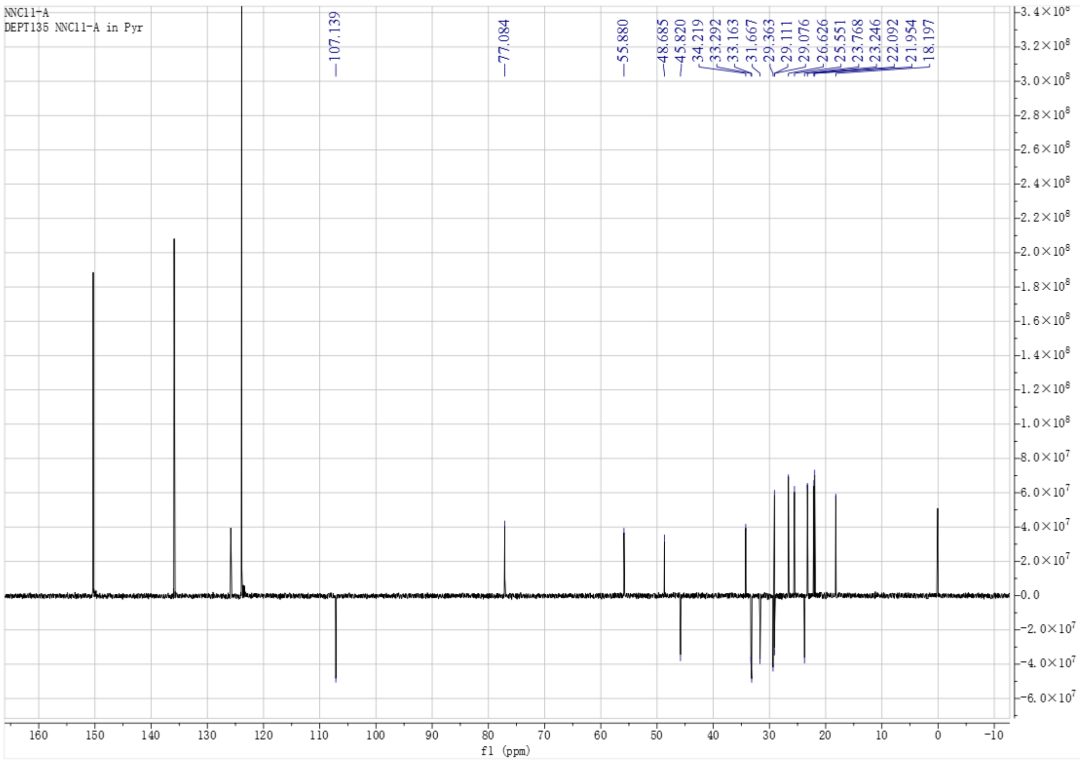

Figure S10. DEPT 135° spectrum (150 MHz, C_5D_5N) of compound **1**

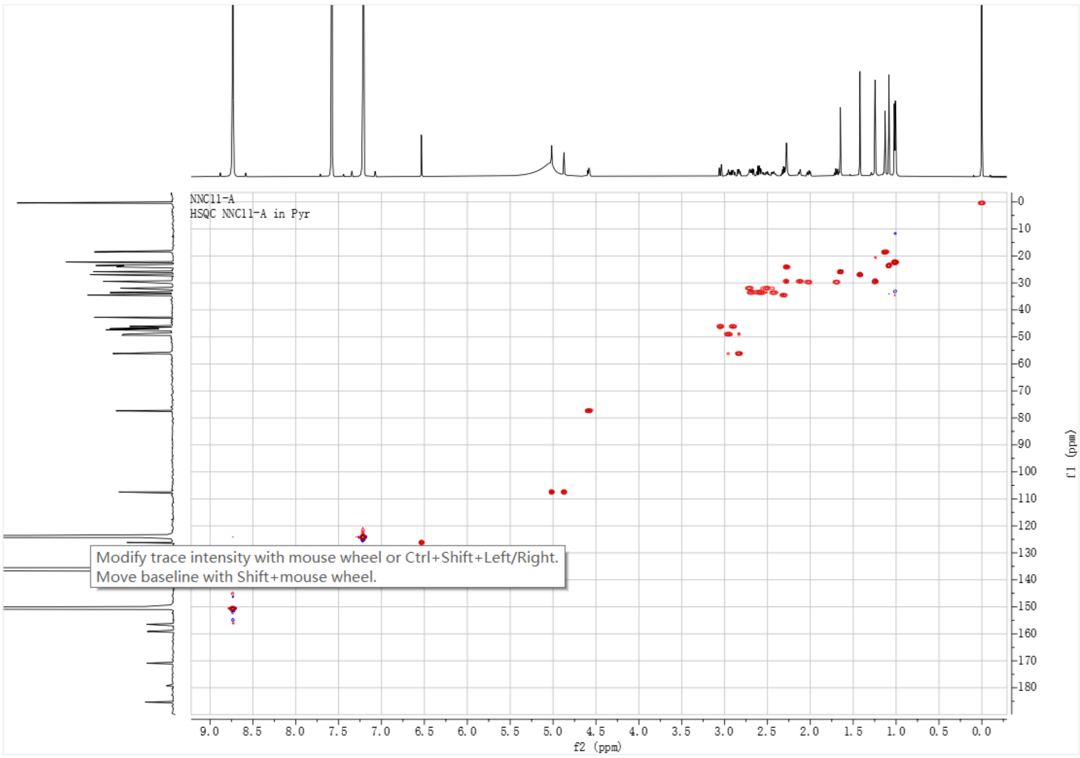

Figure S11. HSQC spectrum (600 MHz, C_5D_5N) of compound **1**

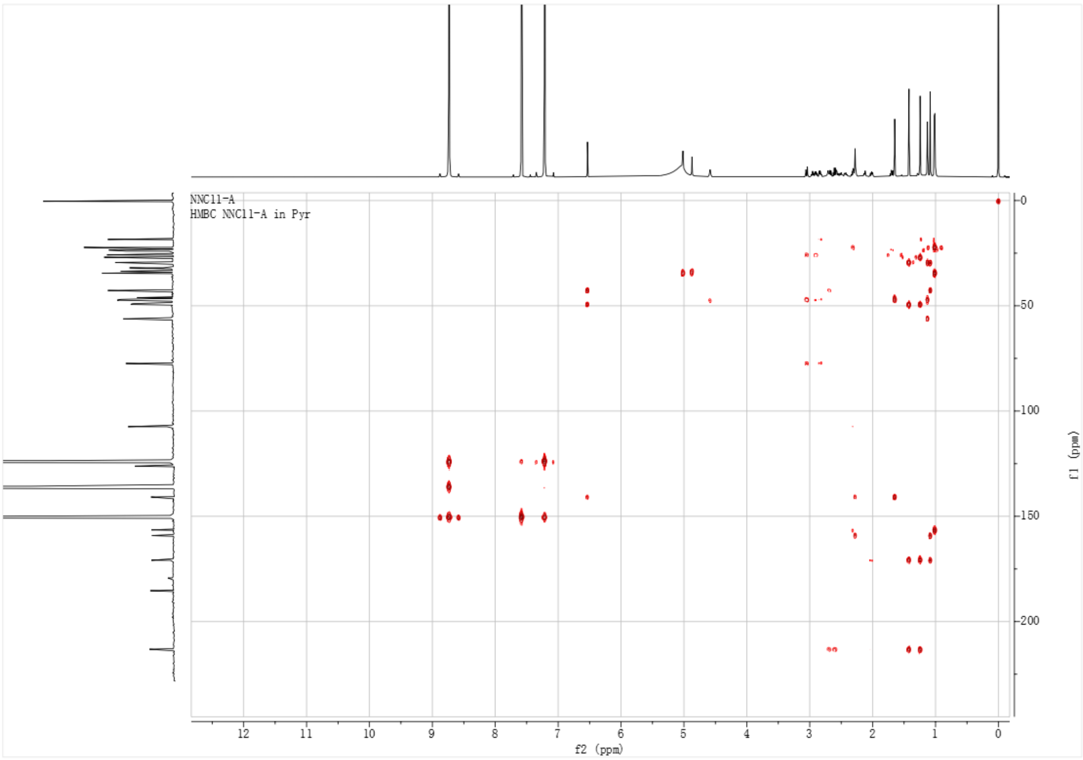

Figure S12. HMBC spectrum (600 MHz, C_5D_5N) of compound **1**

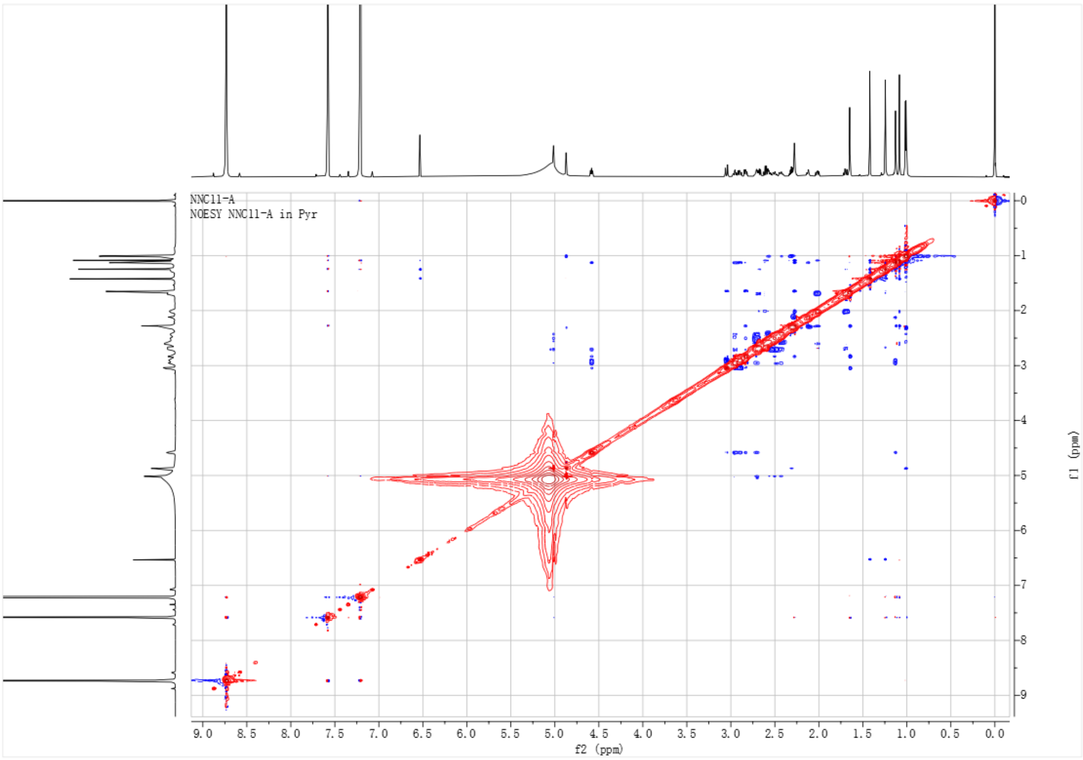

Figure S13. NOESY spectrum (600 MHz, C_5D_5N) of compound **1**

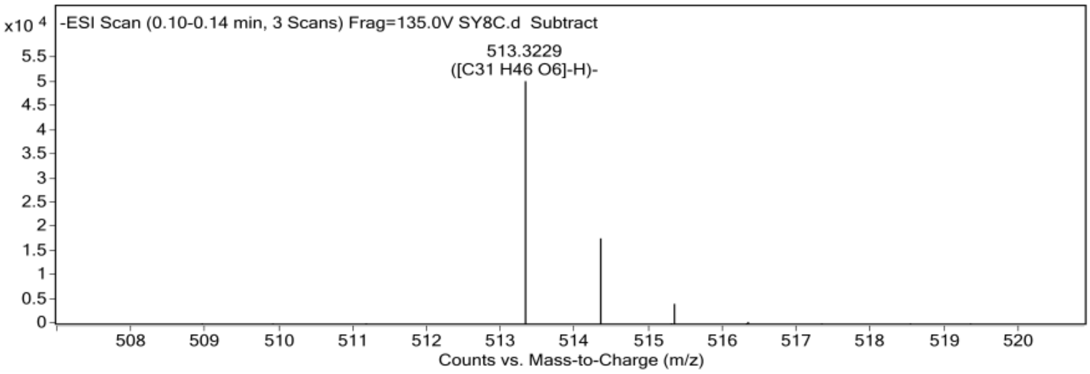

Figure S14. HRESIMS spectrum of compound **2**

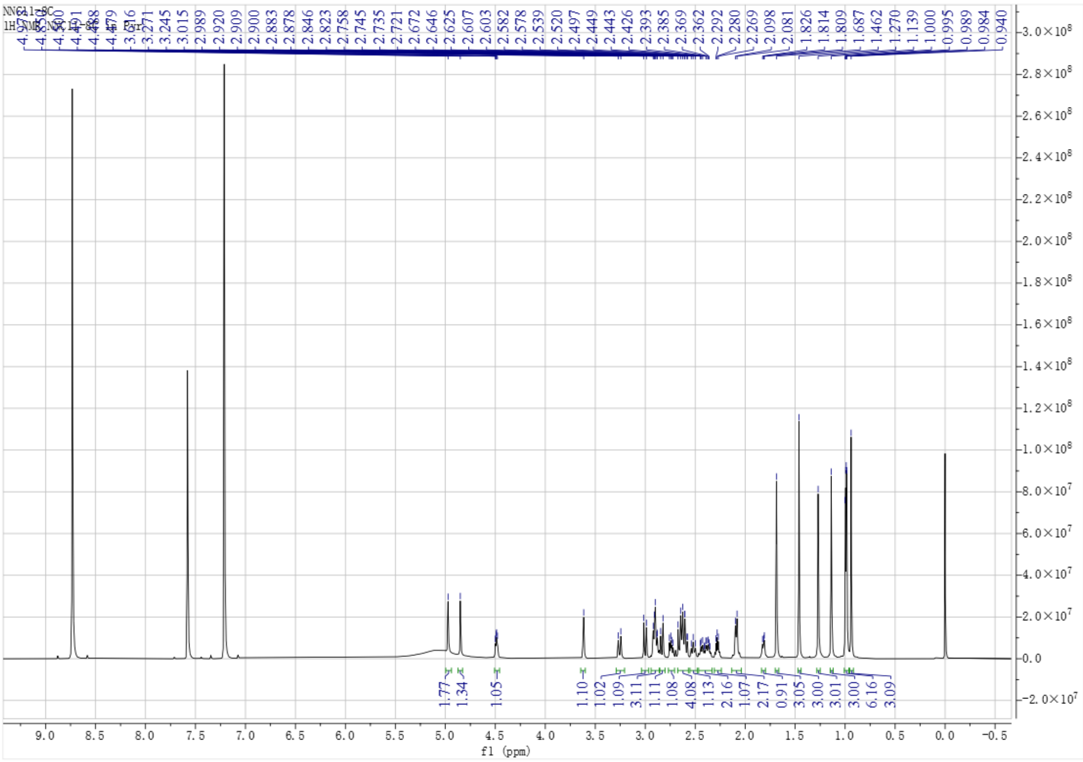

Figure S15. ^{1}H NMR spectrum (600 MHz, C_5D_5N) of compound **2**

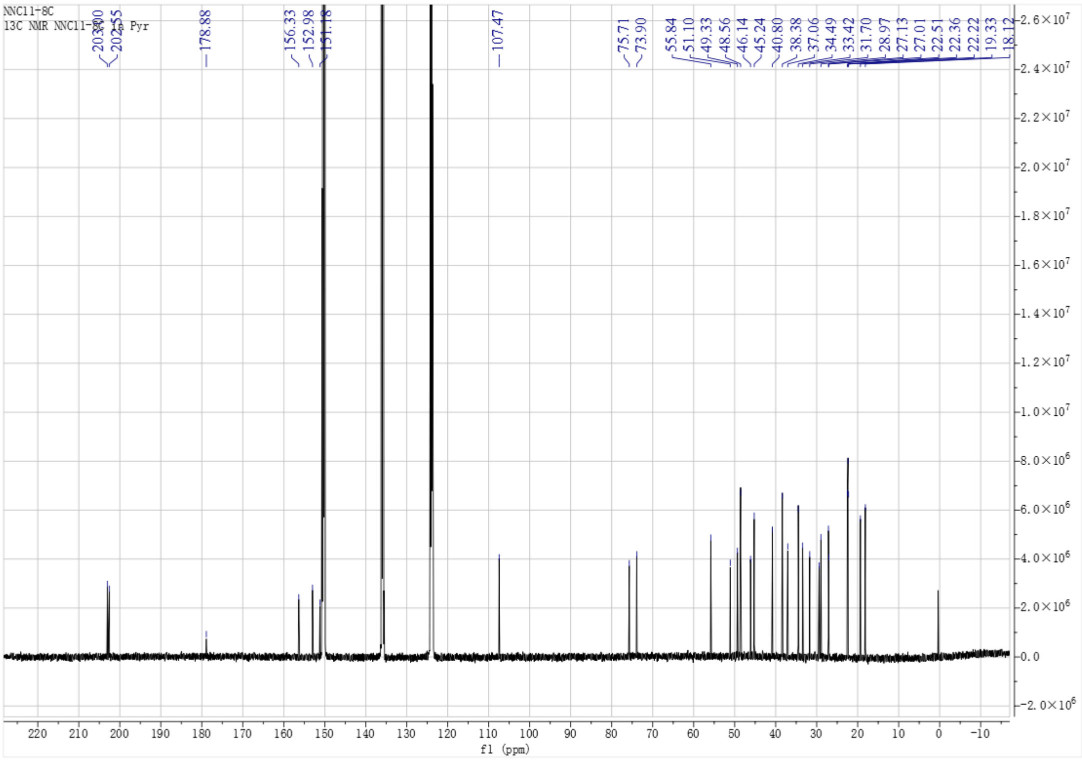

Figure S16. ^{13}C NMR spectrum (150 MHz, C_5D_5N) of compound **2**

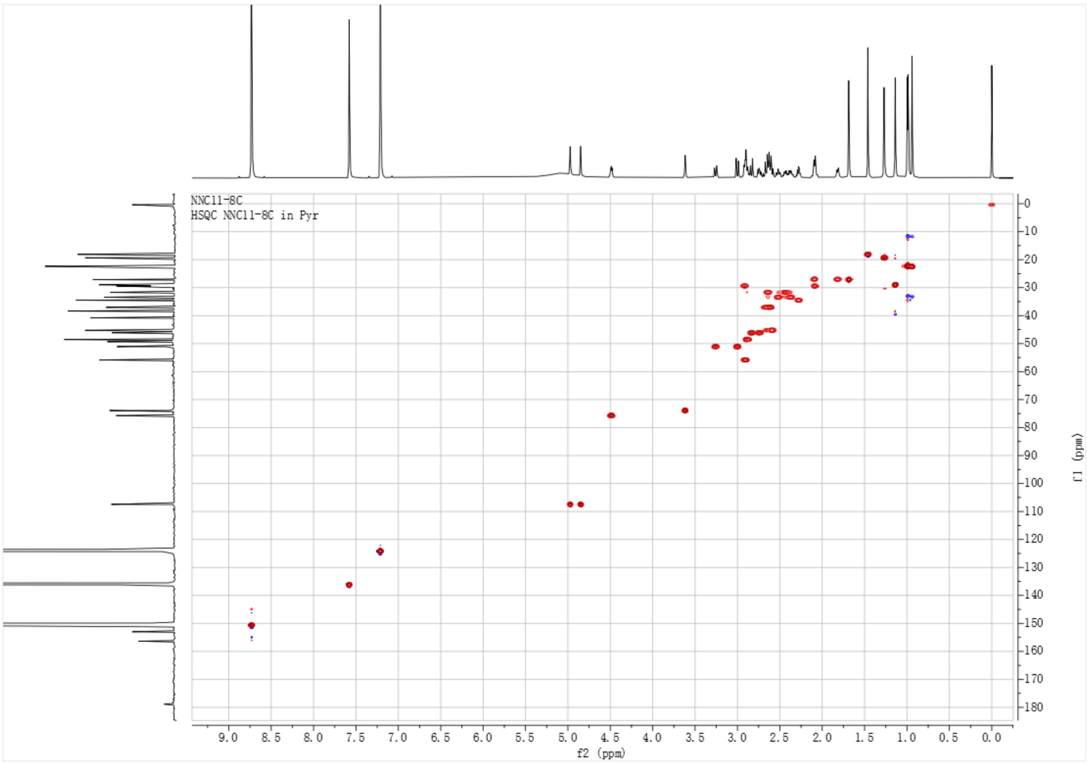

Figure S17. HSQC spectrum (600 MHz, C_5D_5N) of compound **2**

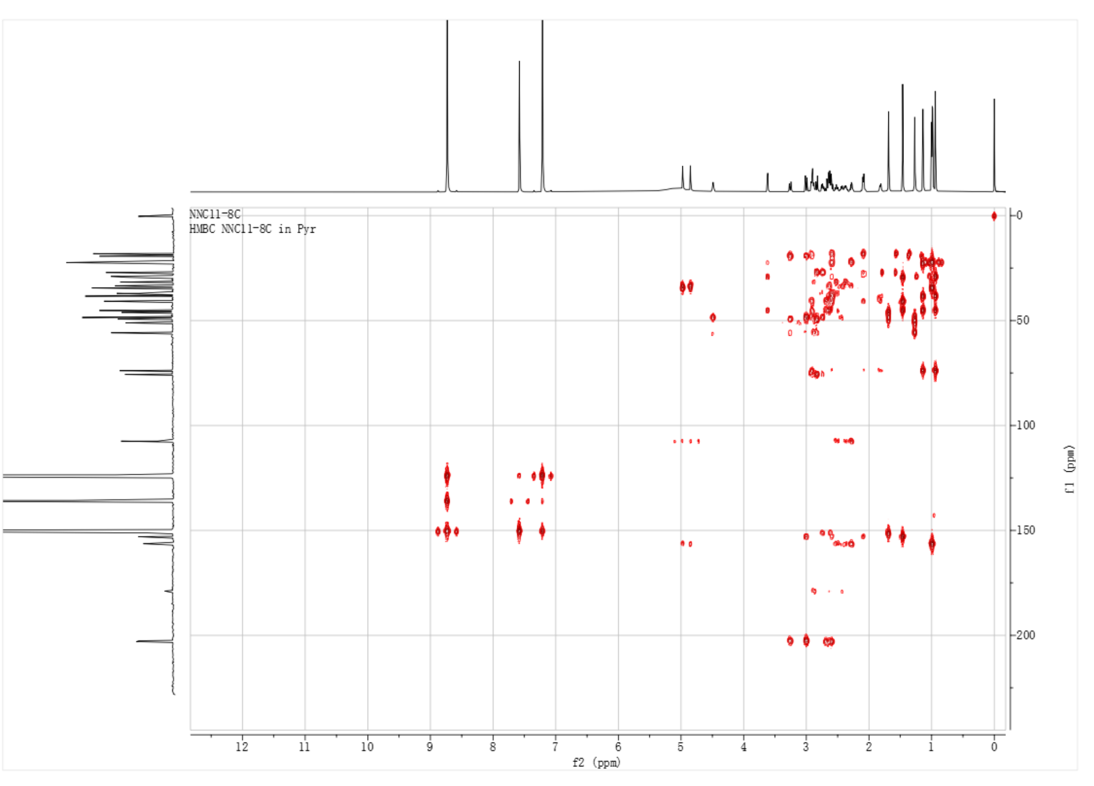

Figure S18. HMBC spectrum (600 MHz, C_5D_5N) of compound **2**

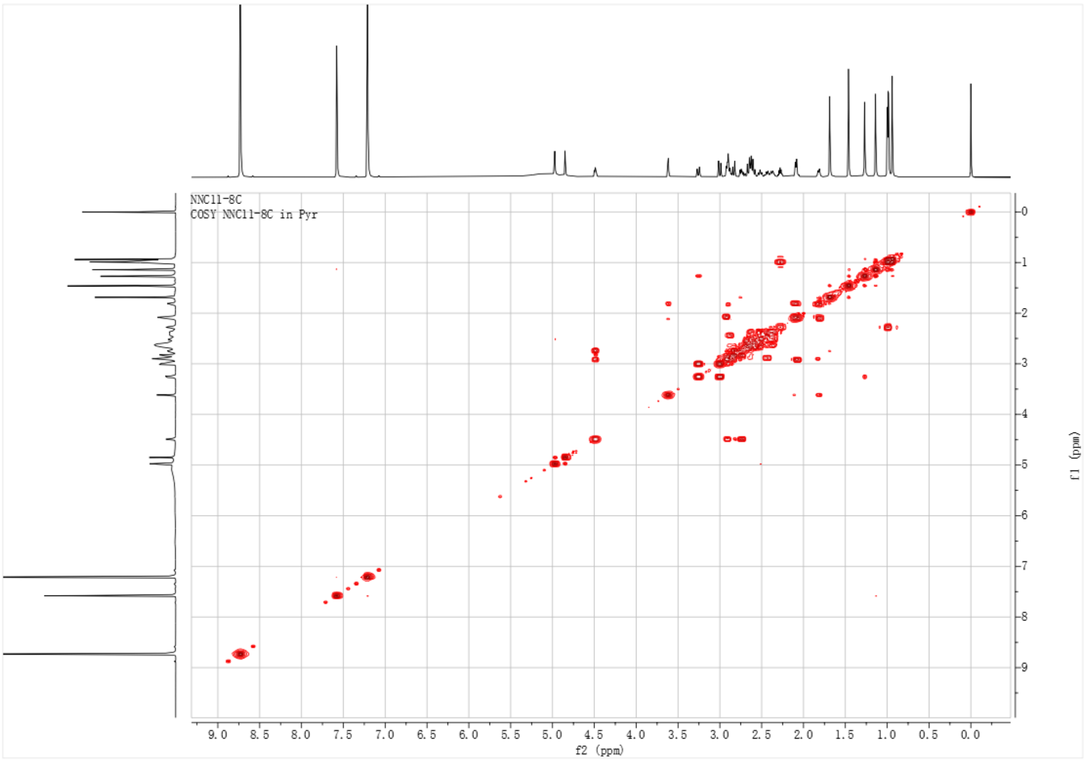

Figure S19. ^{1}H-^{1}H COSY spectrum (600 MHz, C_5D_5N) of compound **2**

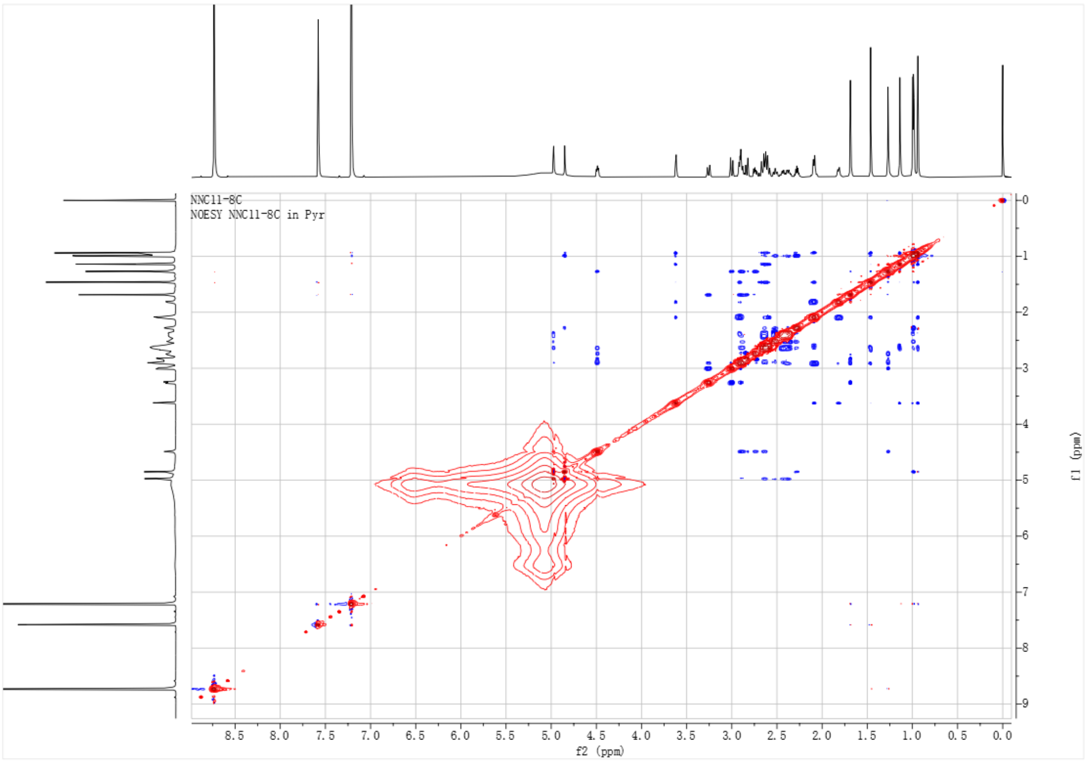

Figure S20. NOESY spectrum (600 MHz, C_5D_5N) of compound **2**

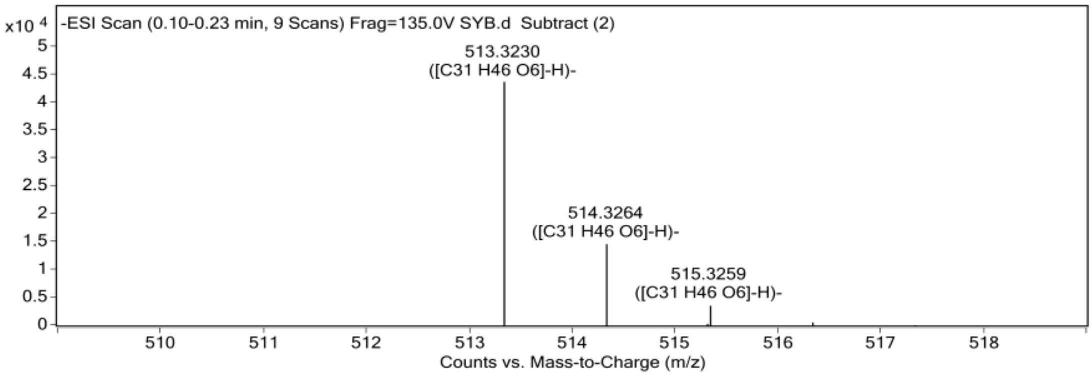

Figure S21. HRESIMS spectrum of compound **3**

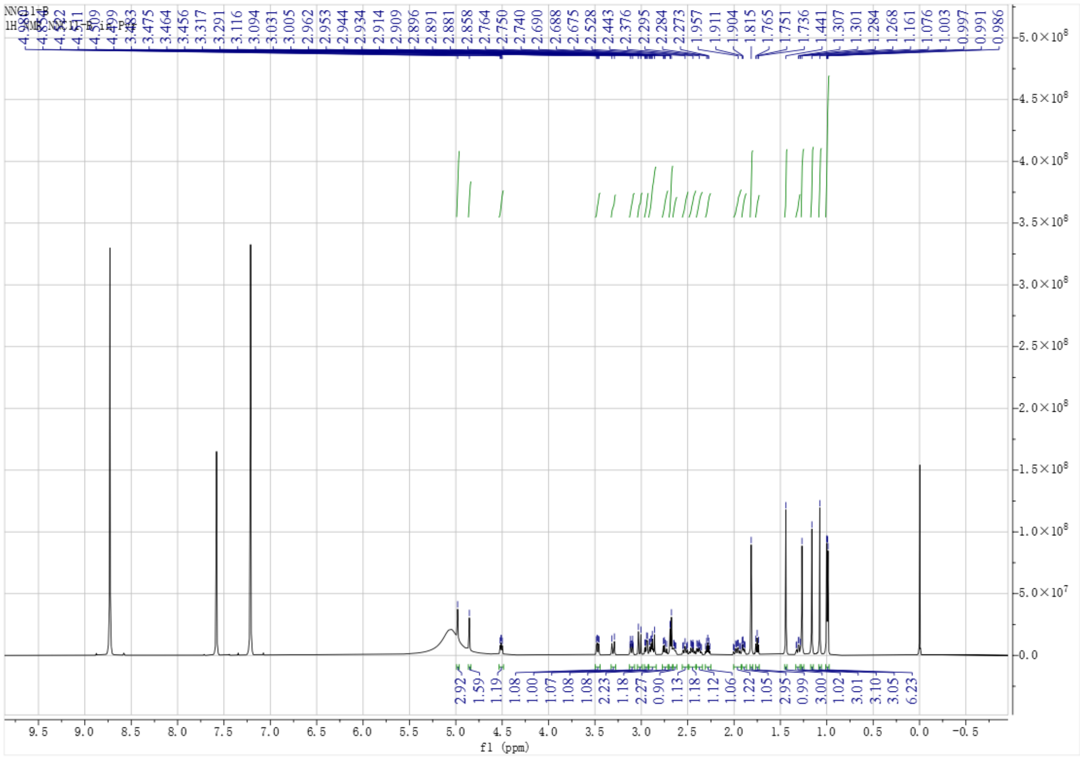

Figure S22. ^{1}H NMR spectrum (600 MHz, C_5D_5N) of compound **3**

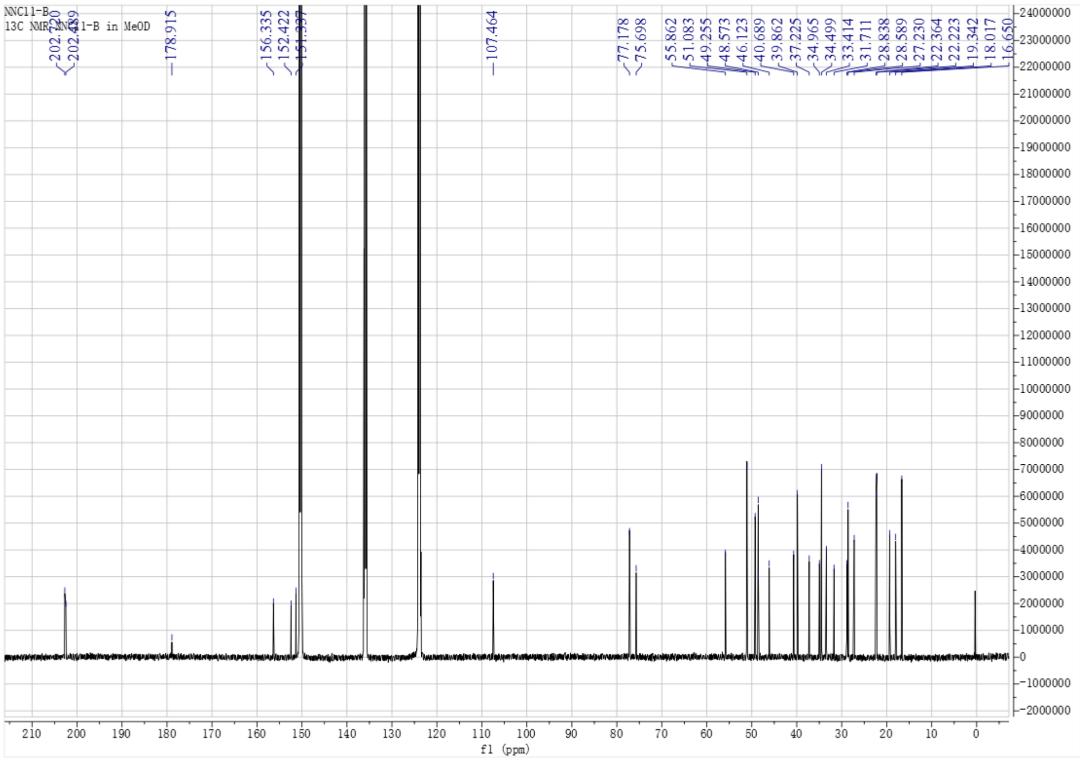

Figure S23. ^{13}C NMR spectrum (150 MHz, C_5D_5N) of compound **3**

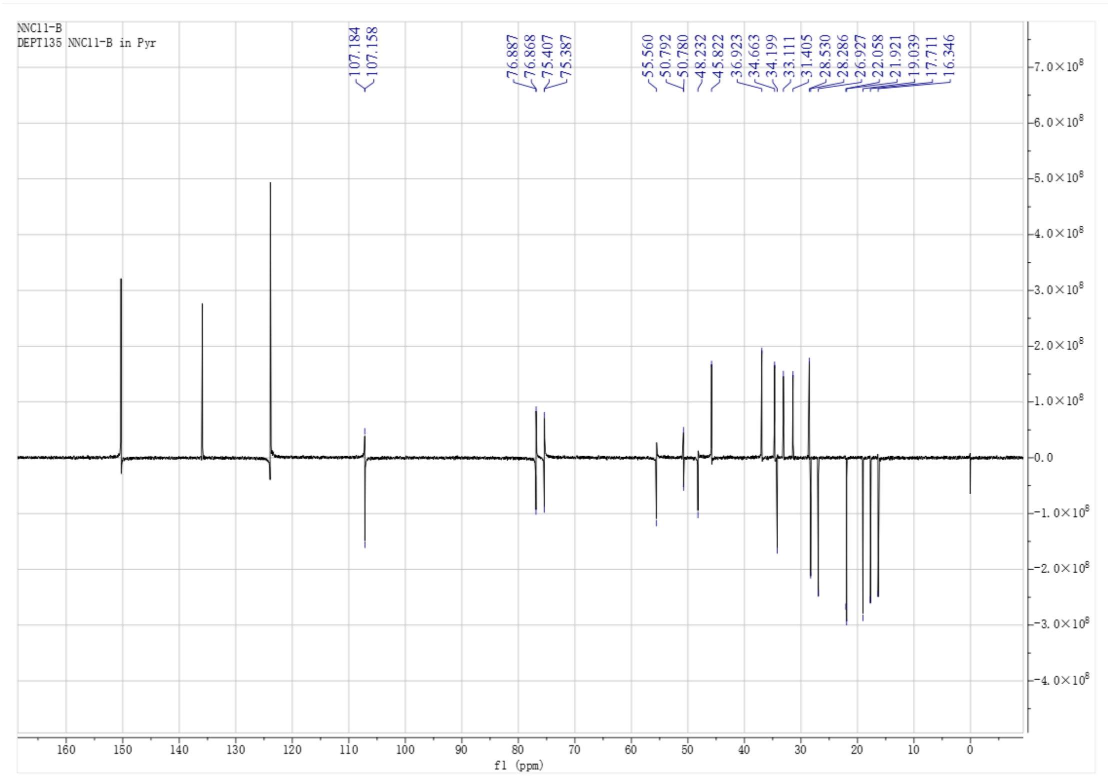

Figure S24. DEPT 135° spectrum (150 MHz, C_5D_5N) of compound **3**

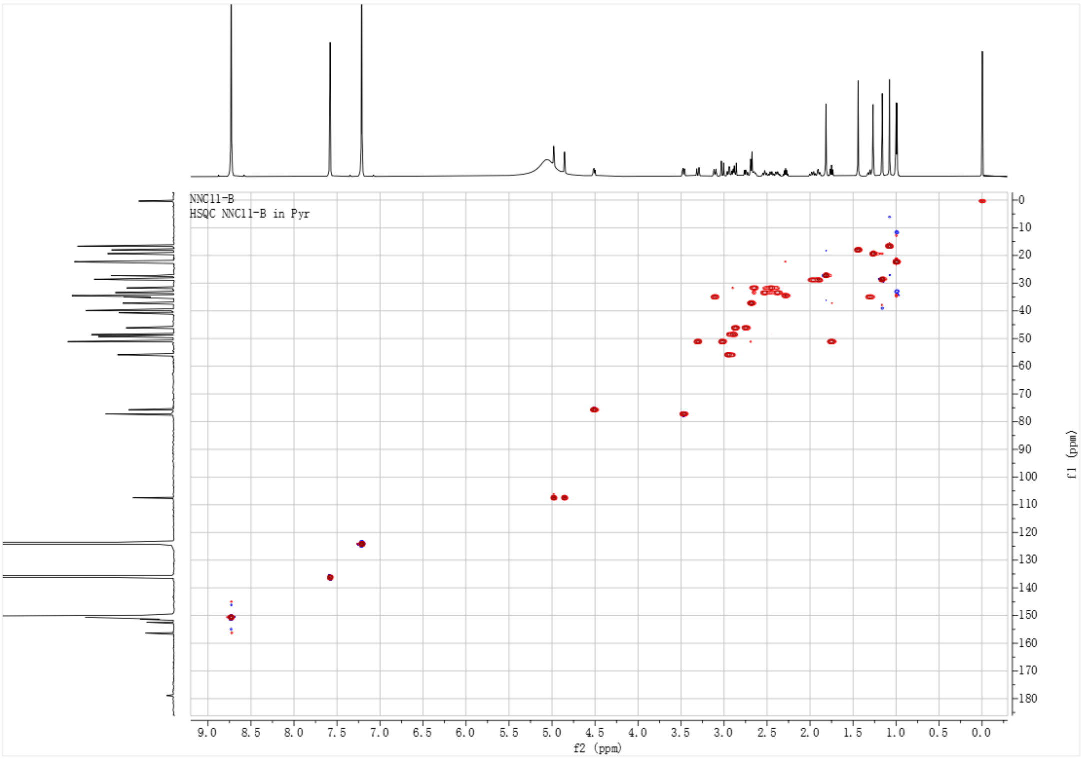

Figure S25. HSQC spectrum (600 MHz, C_5D_5N) of compound **3**

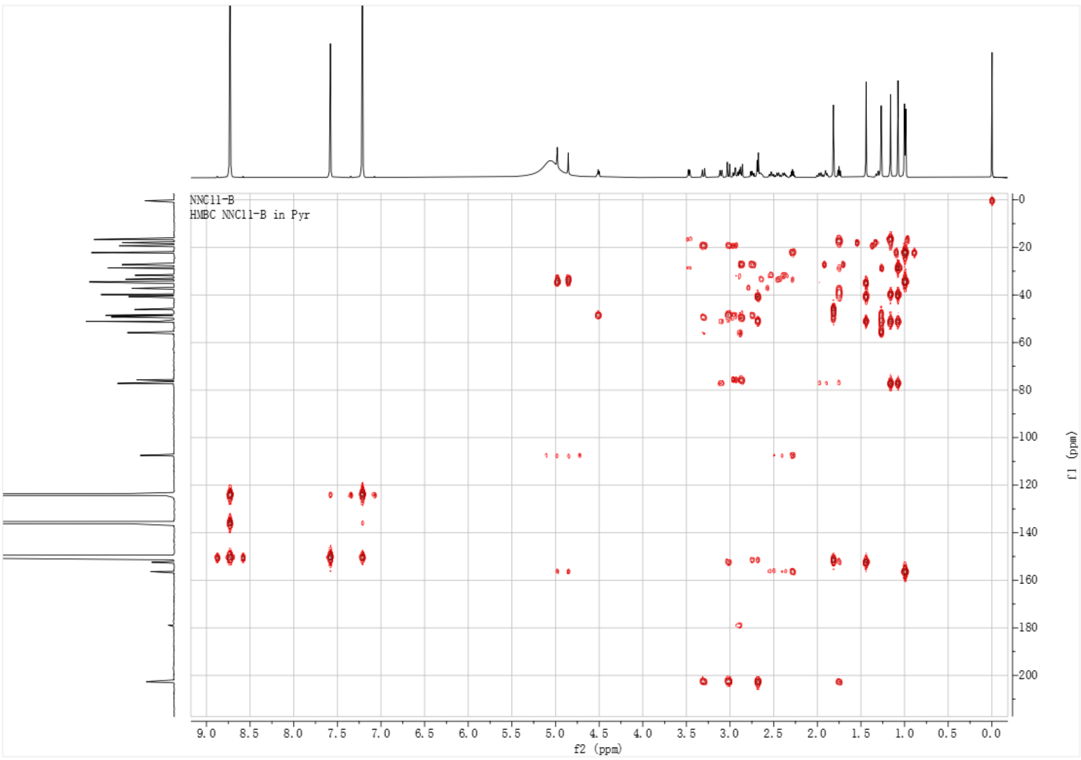

Figure S26. HMBC spectrum (600 MHz, C_5D_5N) of compound **3**

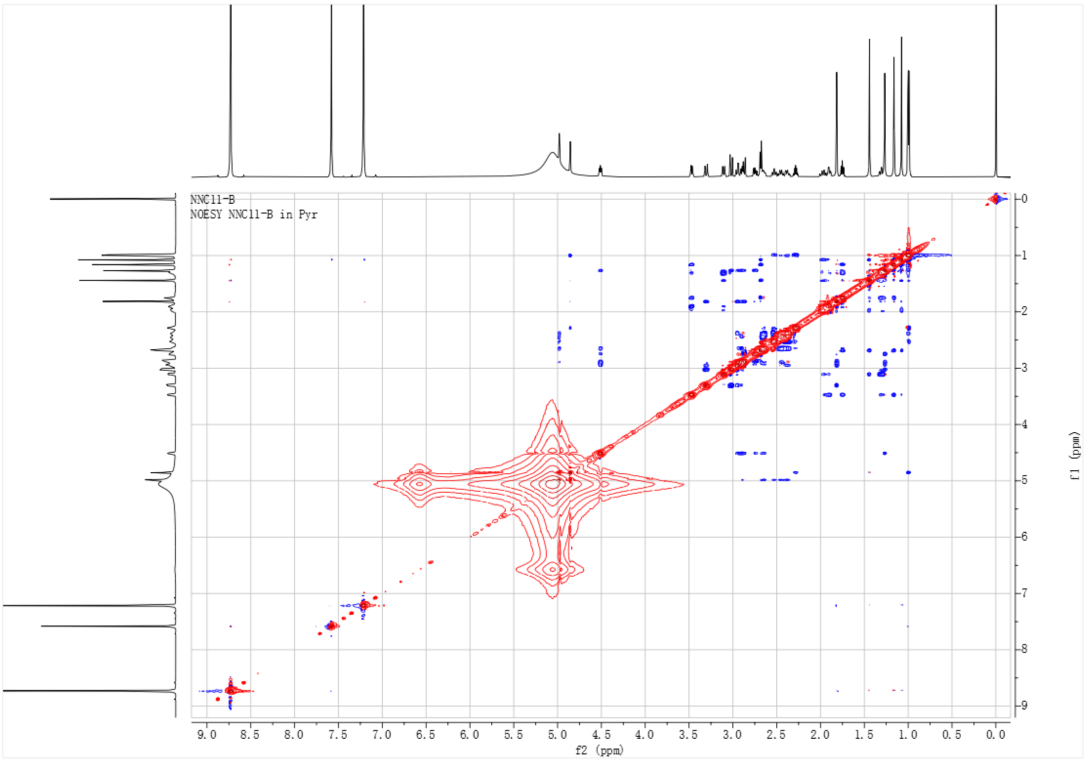

Figure S27. NOESY spectrum (600 MHz, C_5D_5N) of compound **3**

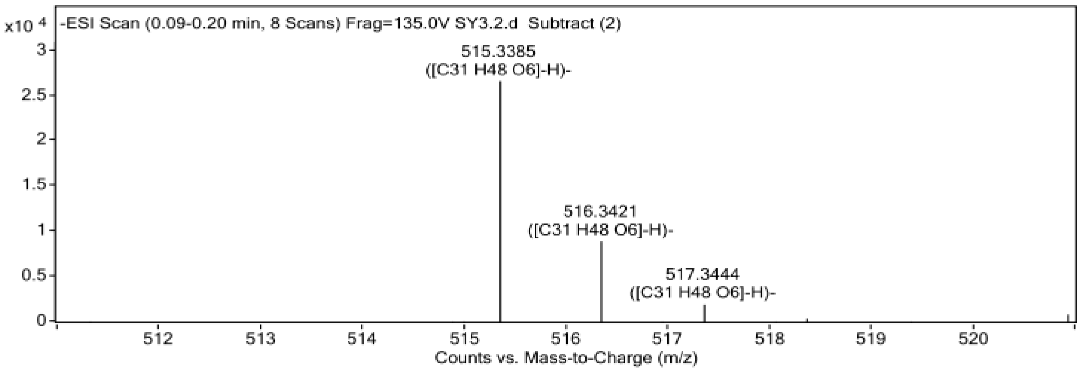

Figure S28. HRESIMS spectrum of compound **4**

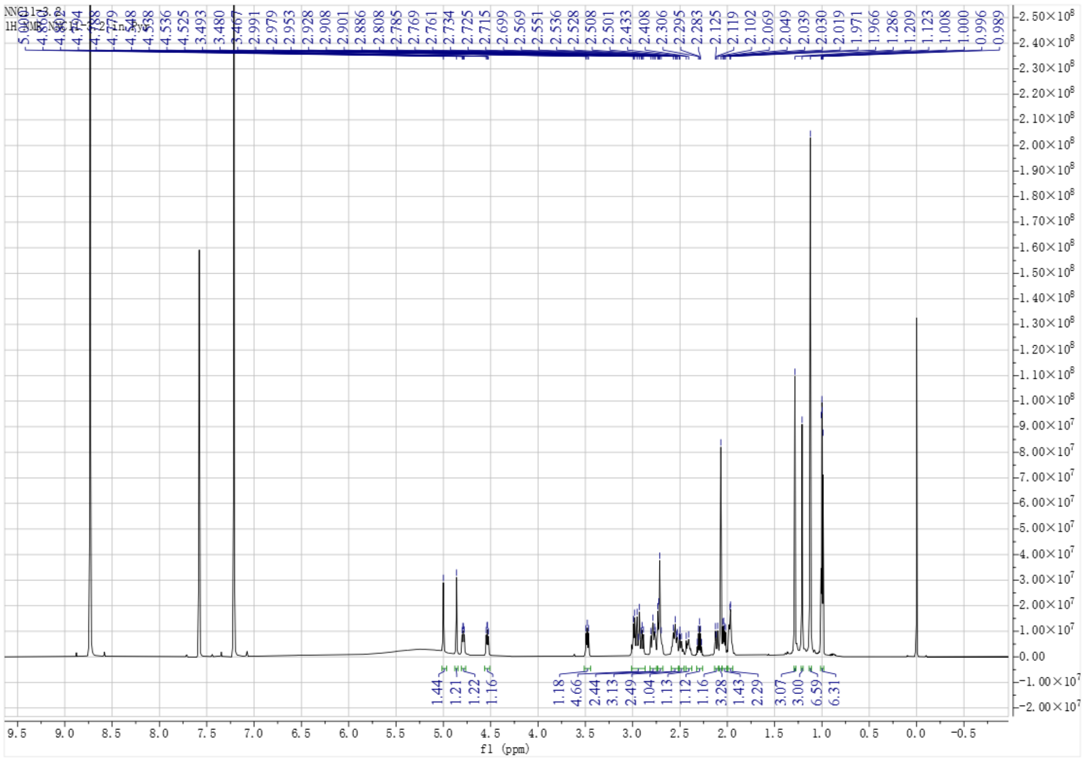

Figure S29. ^{1}H NMR spectrum (600 MHz, C_5D_5N) of compound **4**

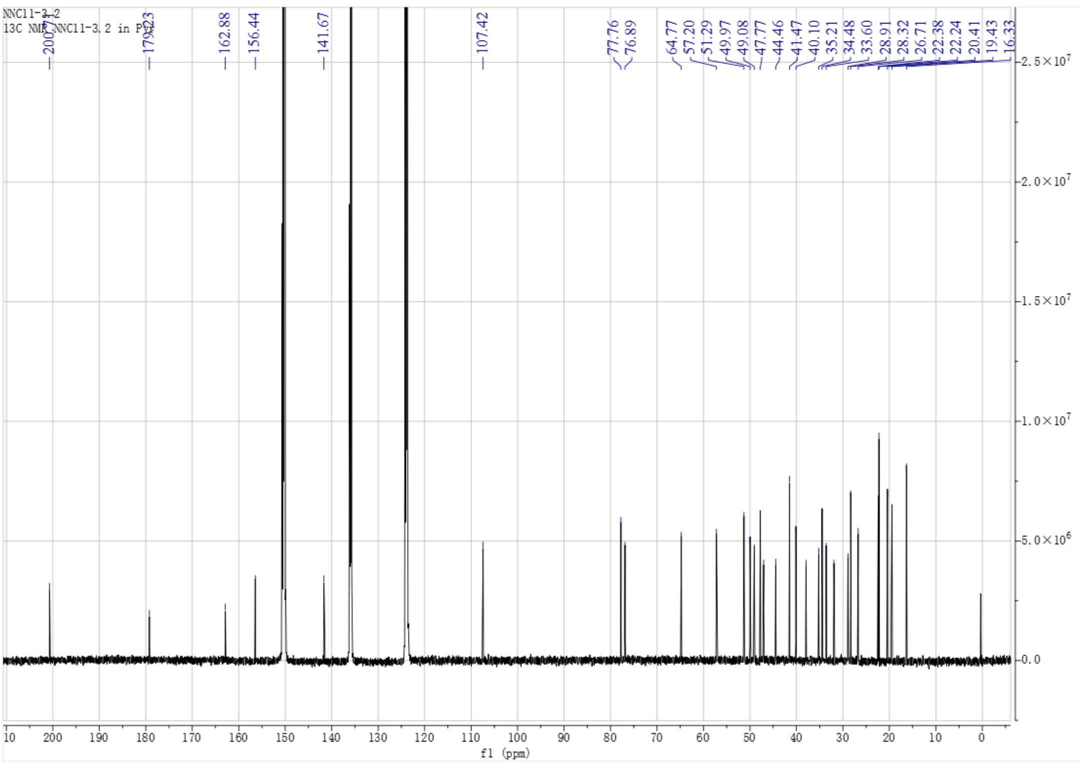

Figure S30. ^{13}C NMR spectrum (150 MHz, C_5D_5N) of compound **4**

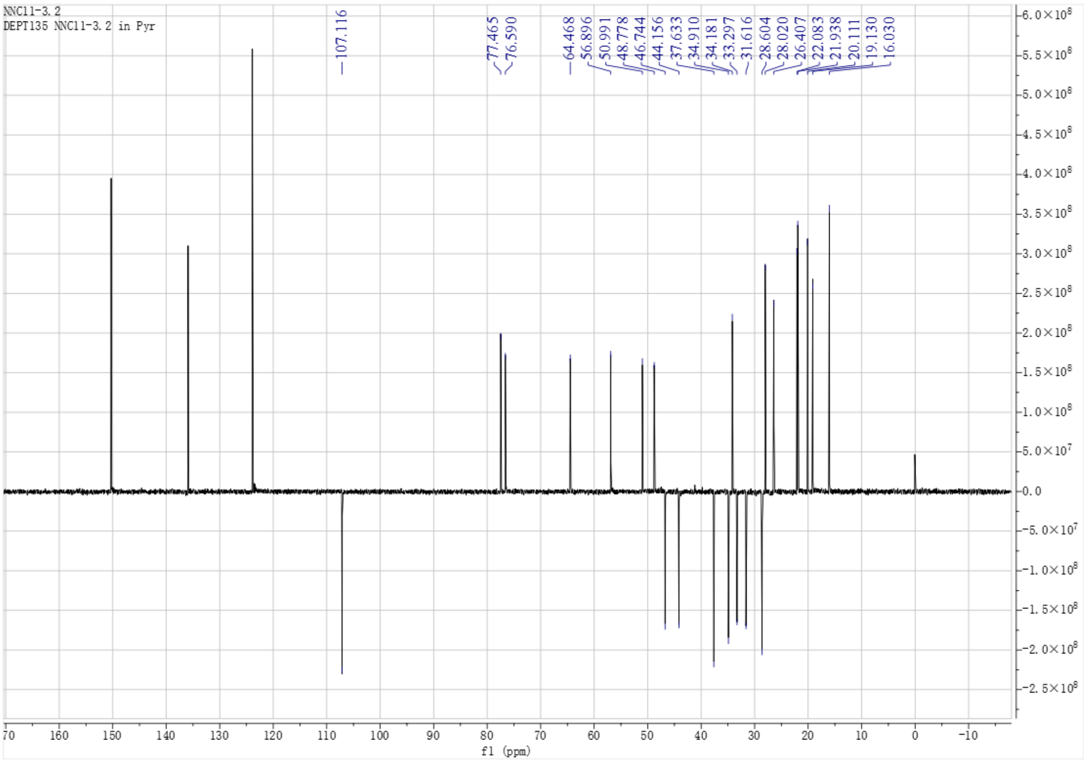

Figure S31. DEPT 135° spectrum (150 MHz, C_5D_5N) of compound **4**

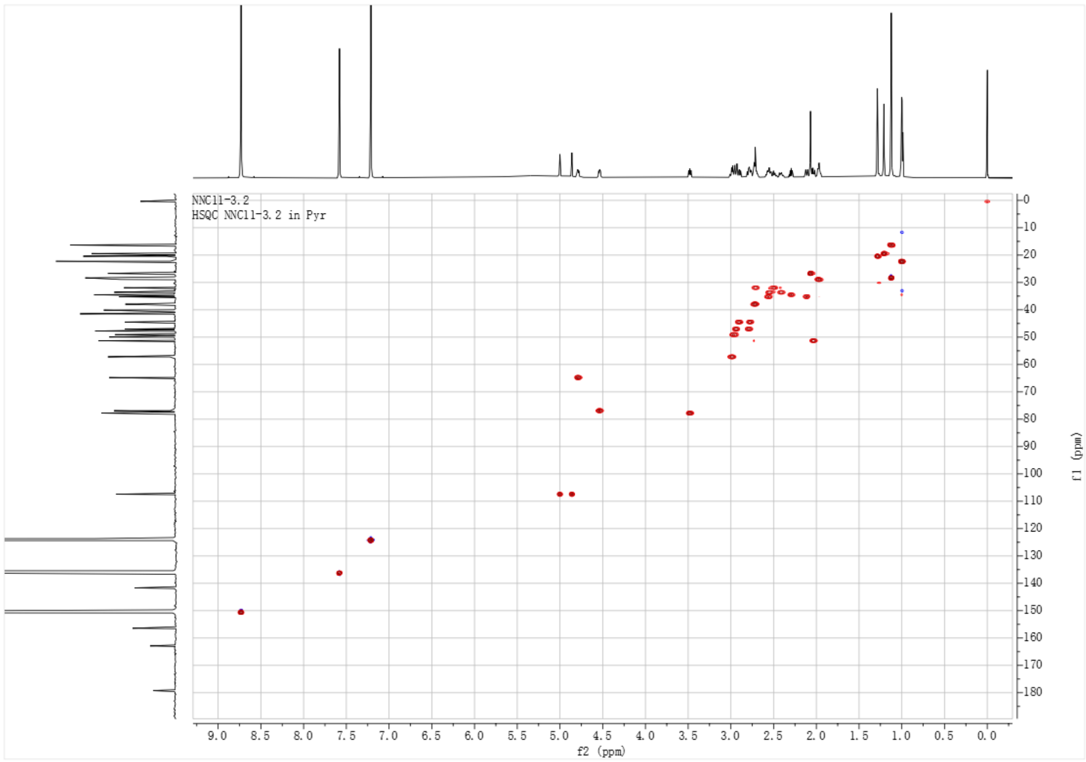

Figure S32. HSQC spectrum (600 MHz, C_5D_5N) of compound **4**

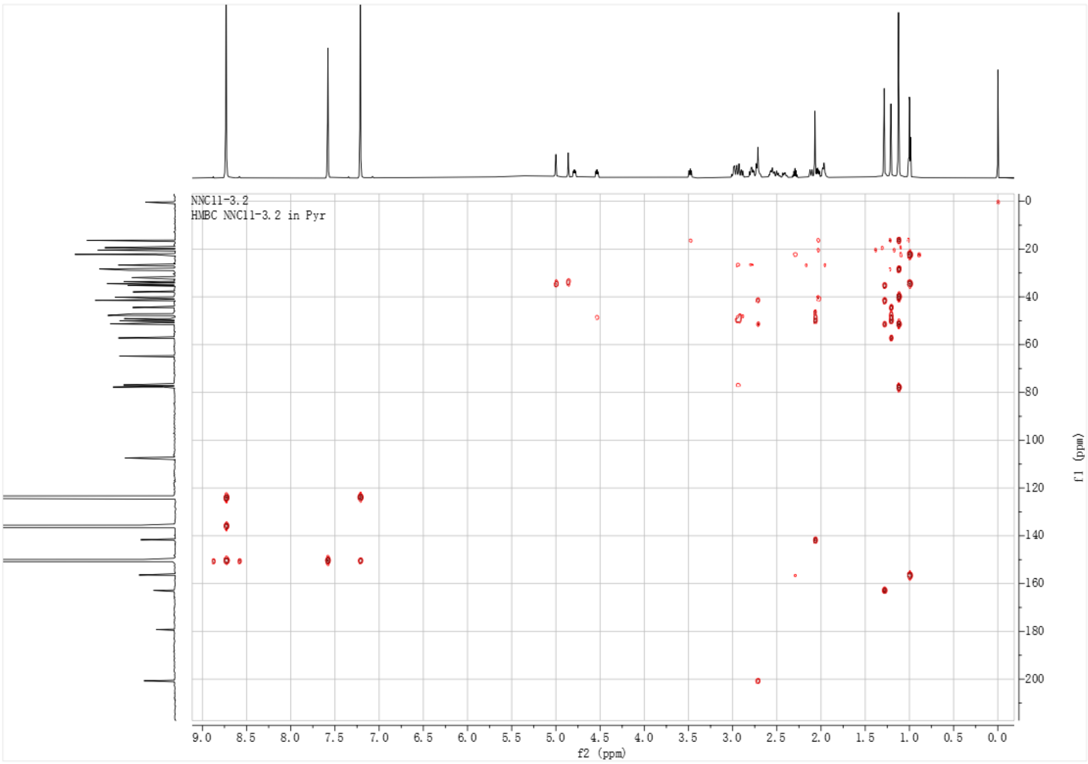

Figure S33. HMBC spectrum (600 MHz, C_5D_5N) of compound **4**

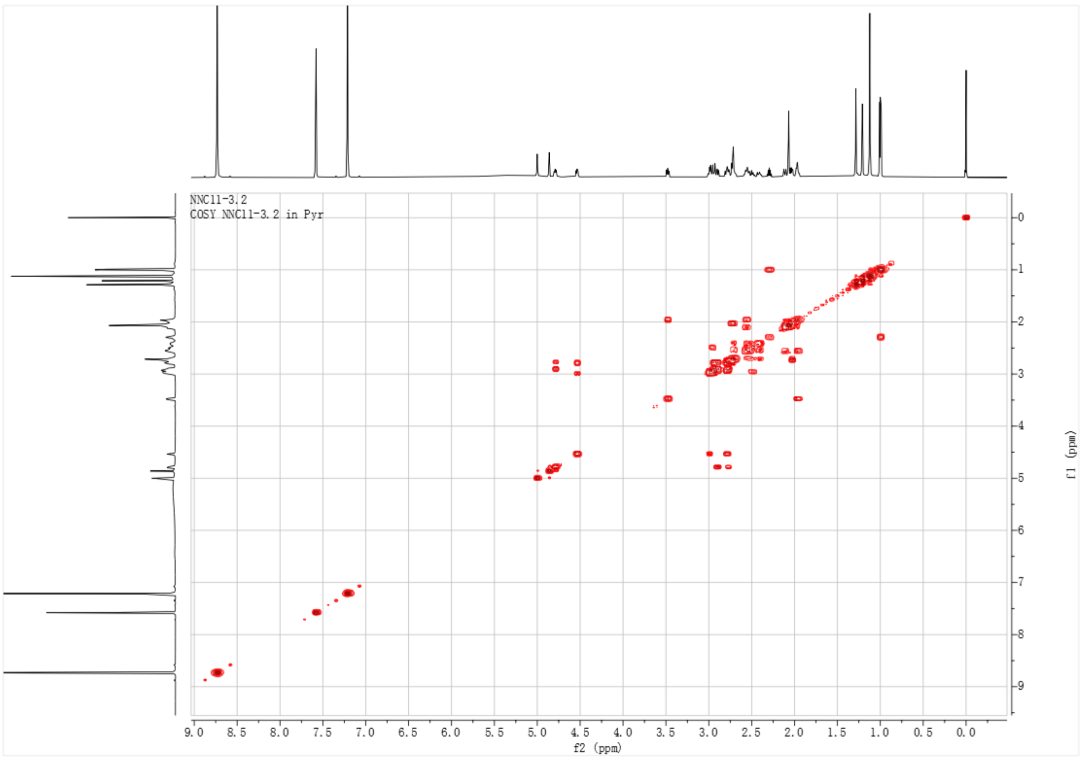

Figure S34. ^1H-^1H COSY spectrum (600 MHz, C_5D_5N) of compound **4**

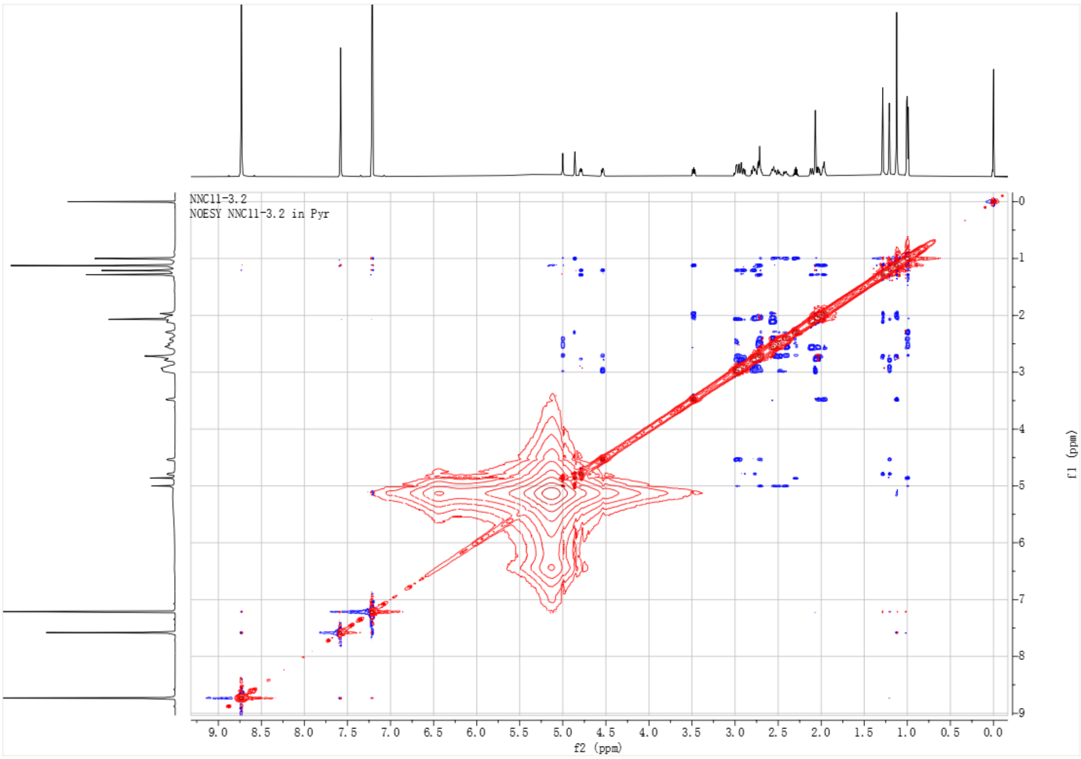

Figure S35. NOESY spectrum (600 MHz, C_5D_5N) of compound **4**

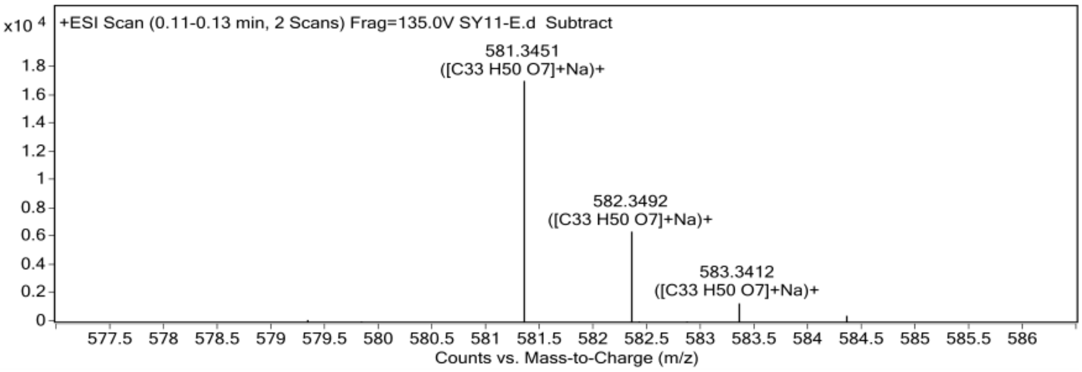

Figure S36. HRESIMS spectrum of compound **5**

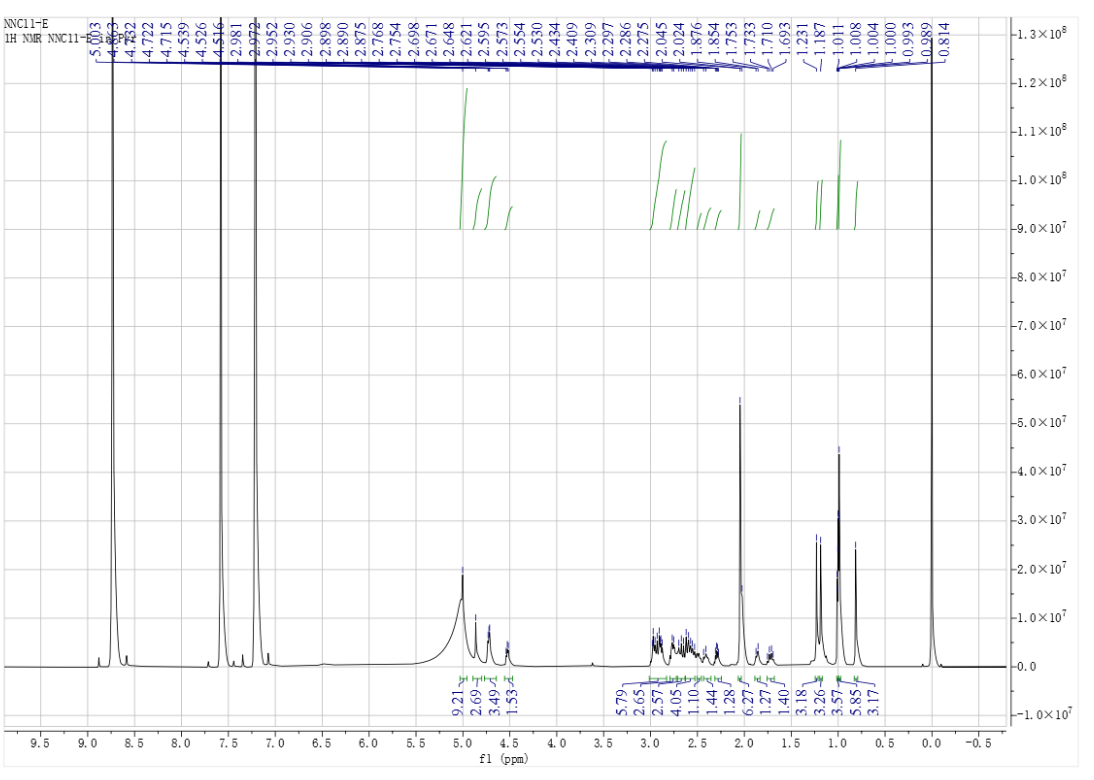

Figure S37. ^{1}H NMR spectrum (600 MHz, C_5D_5N) of compound **5**

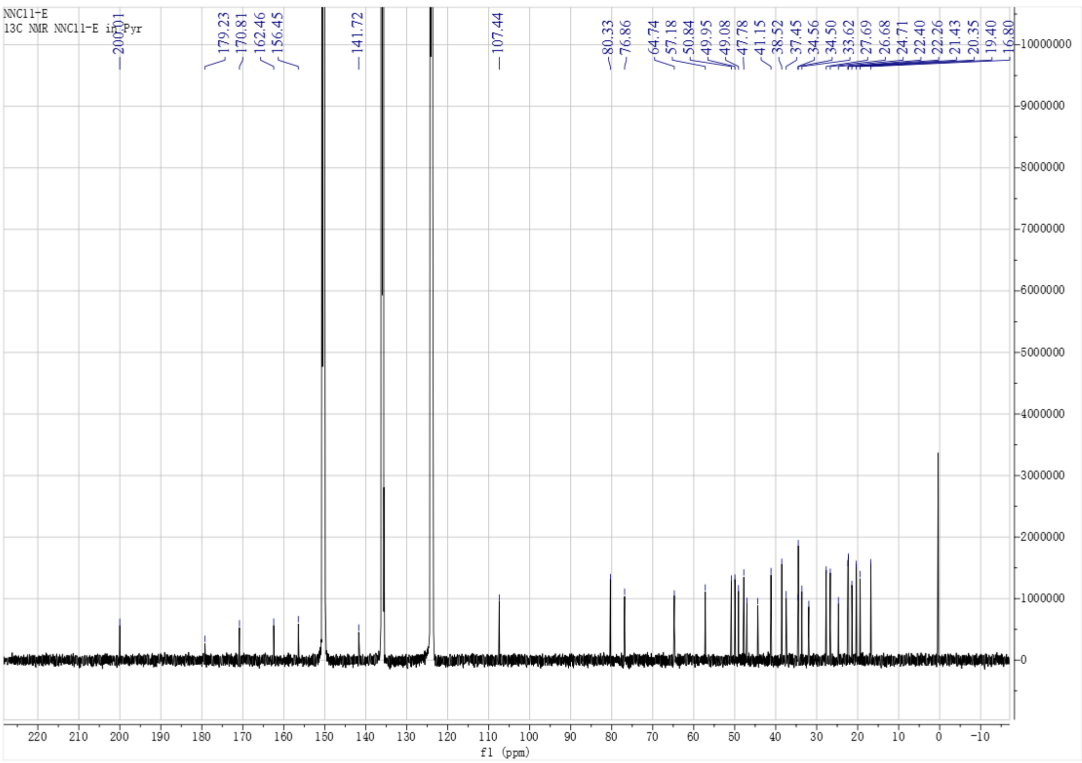

Figure S38. ^{13}C NMR spectrum (150 MHz, C_5D_5N) of compound **5**

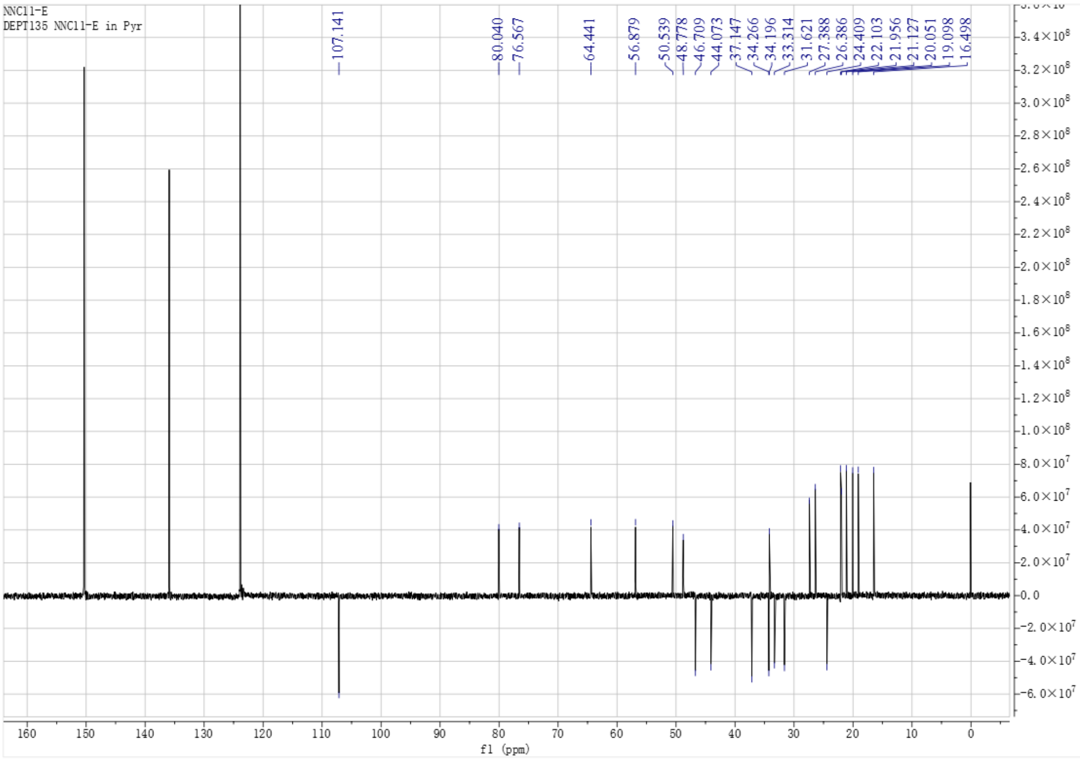

Figure S39. DEPT 135° spectrum (150 MHz, C_5D_5N) of compound **5**

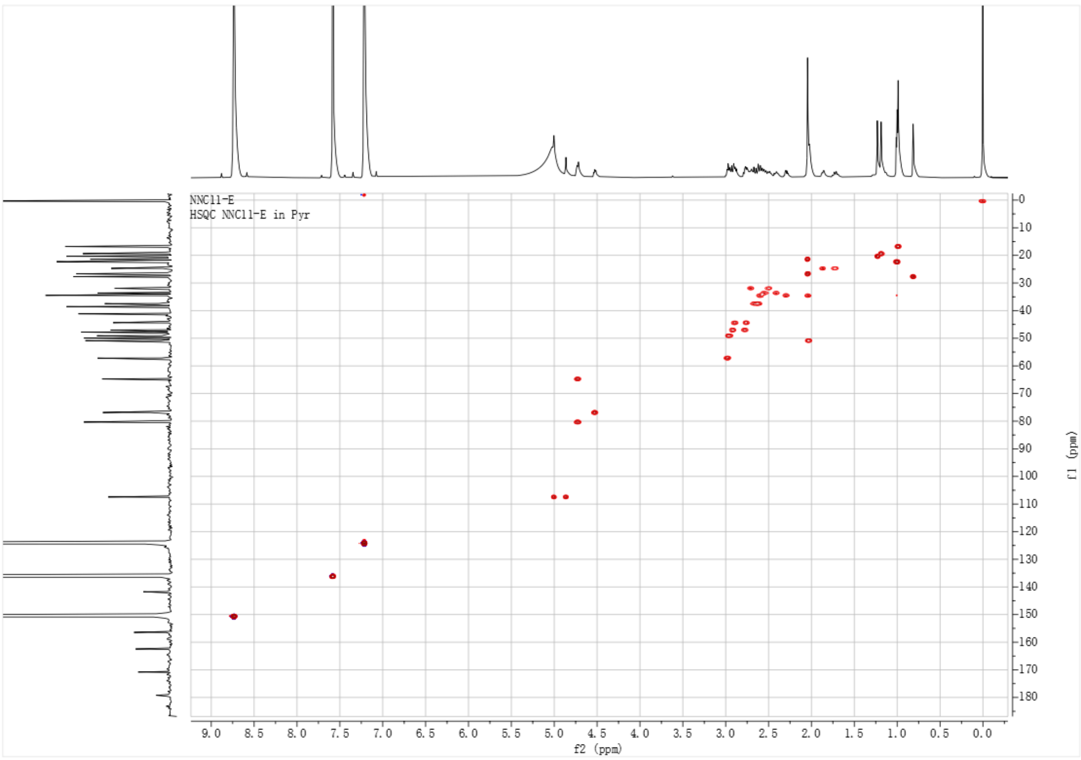

Figure S40. HSQC spectrum (600 MHz, C_5D_5N) of compound **5**

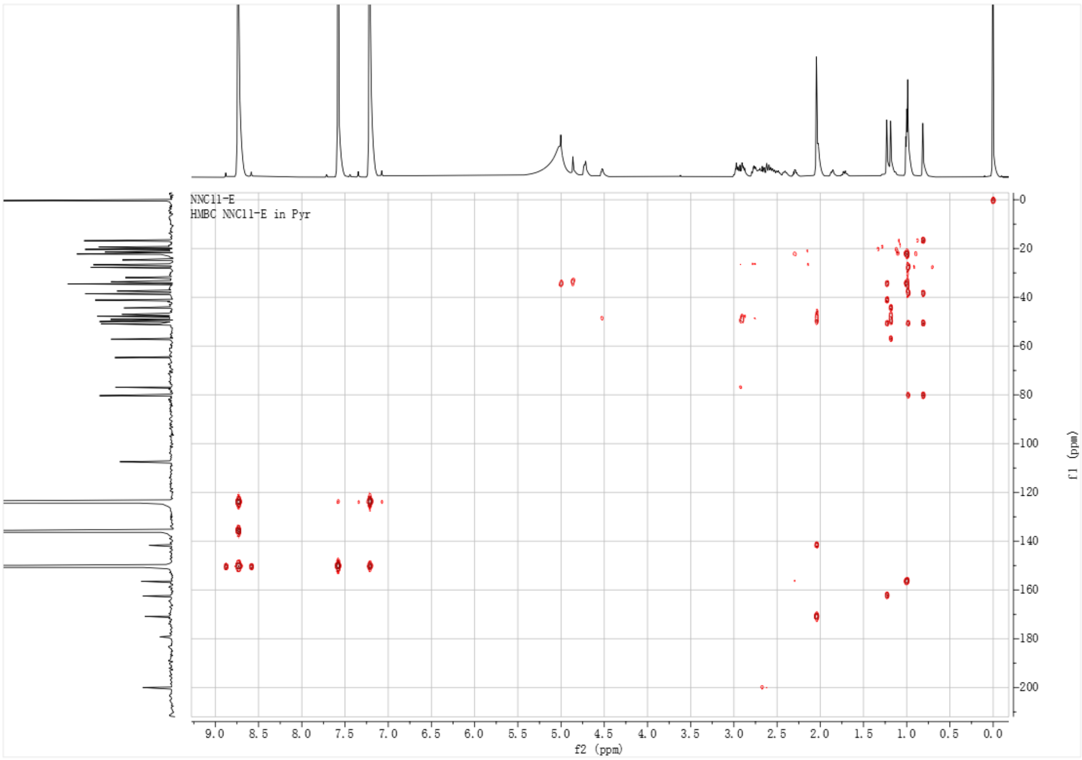

Figure S41. HMBC spectrum (600 MHz, C_5D_5N) of compound **5**

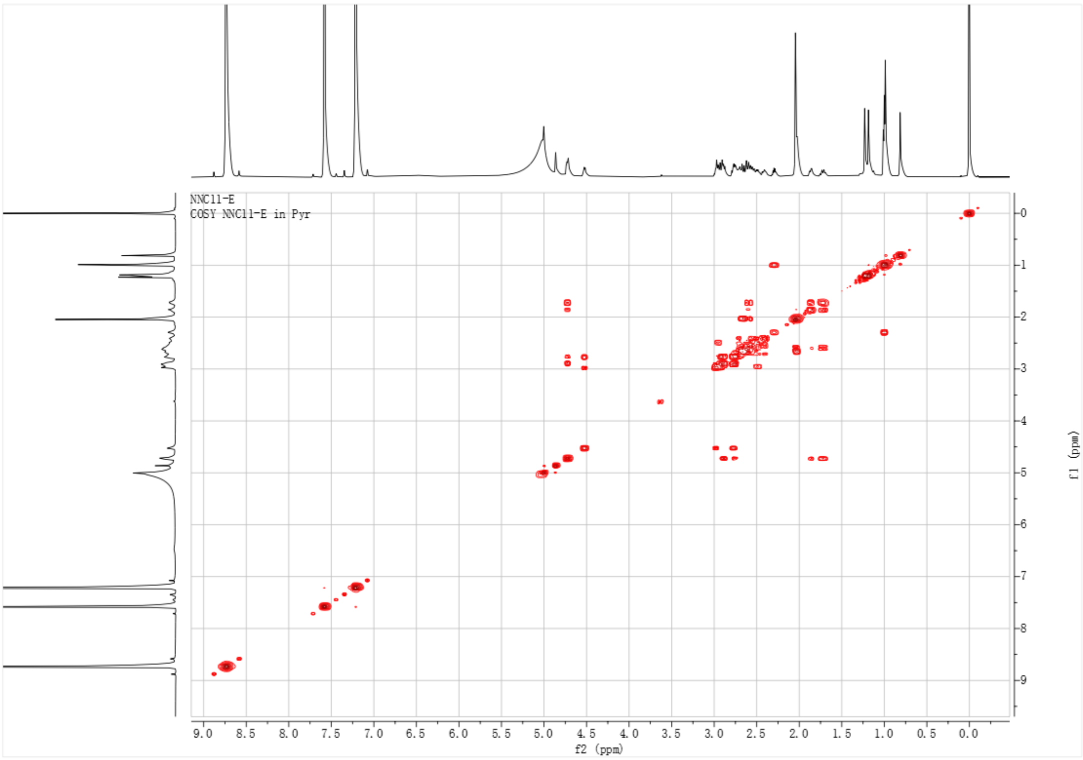

Figure S42. ^{1}H-^{1}H COSY spectrum (600 MHz, C_5D_5N) of compound **5**

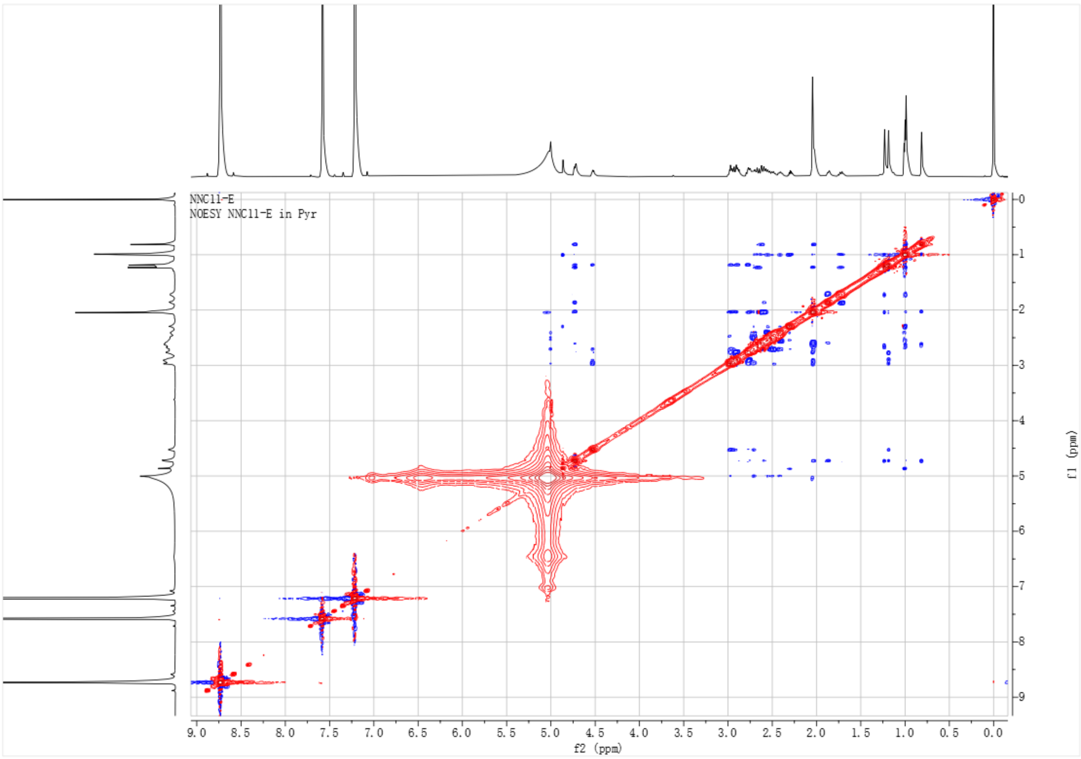

Figure S43. NOESY spectrum (600 MHz, C_5D_5N) of compound **5**

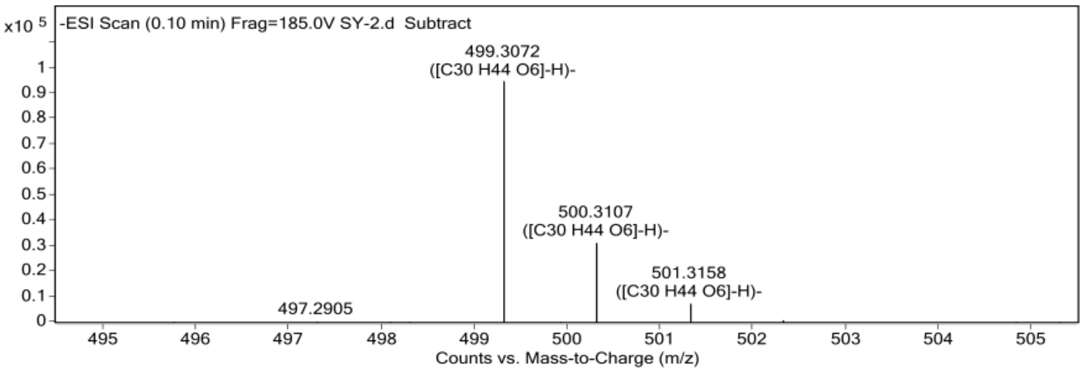

Figure S44. HRESIMS spectrum of compound **6**

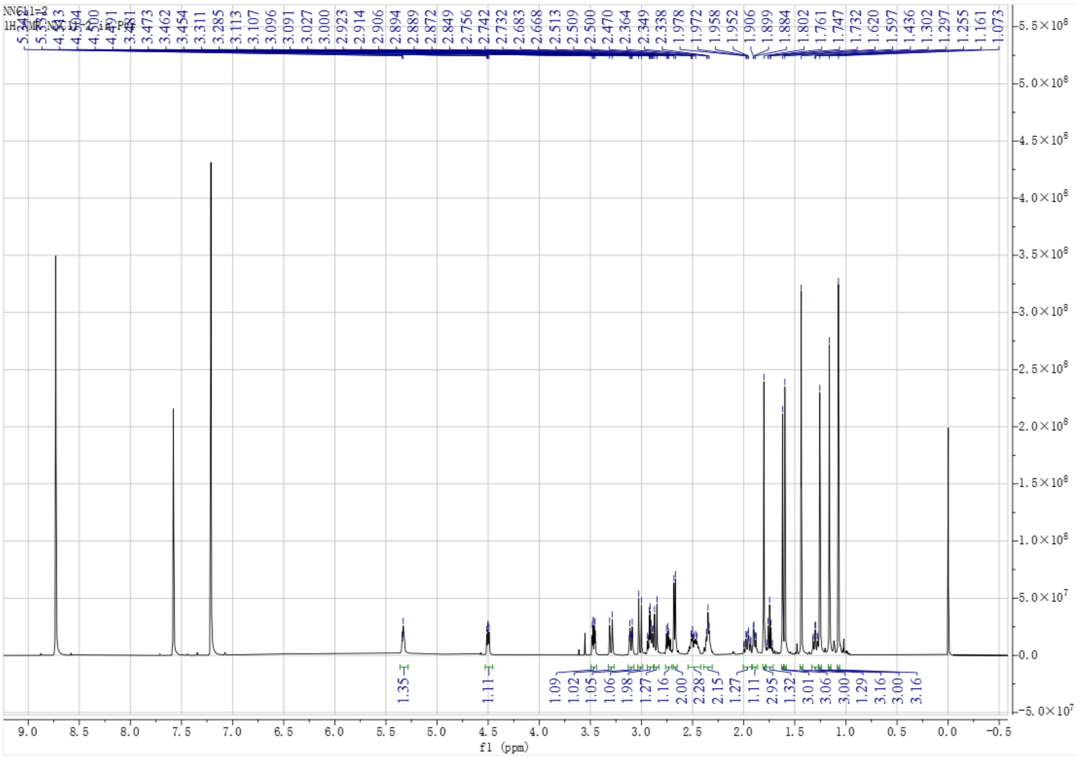

Figure S45. ^{1}H NMR spectrum (600 MHz, C_5D_5N) of compound **6**

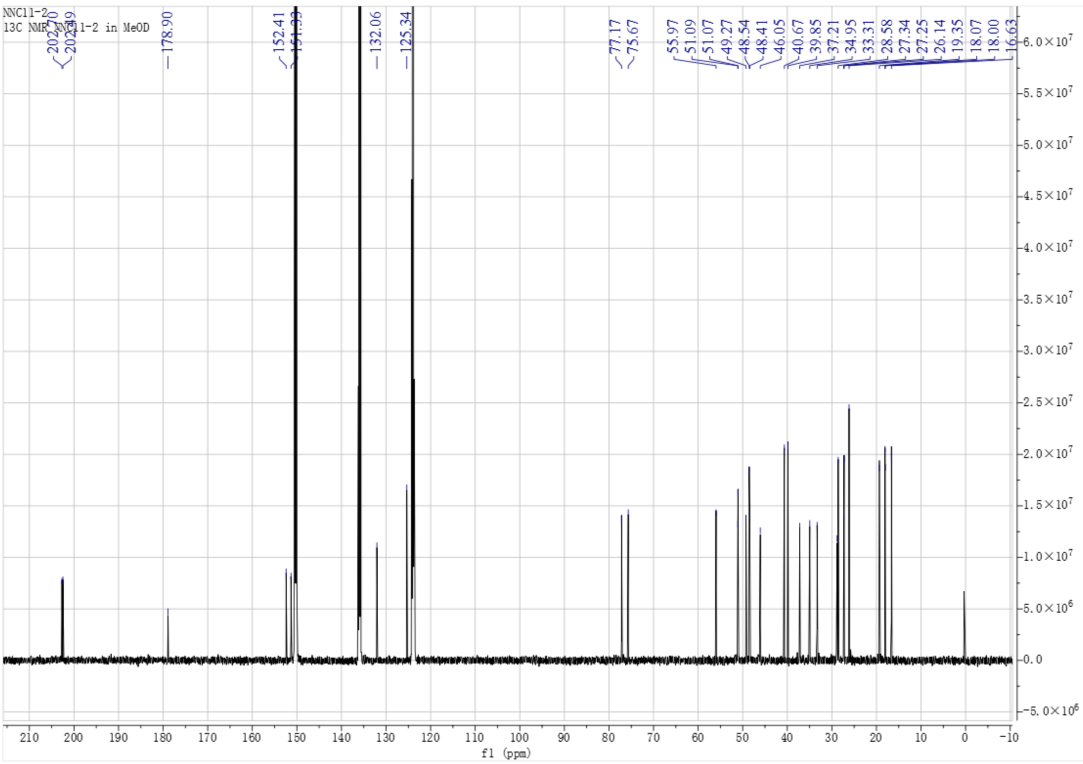

Figure S46. ^{13}C NMR spectrum (150 MHz, C_5D_5N) of compound **6**

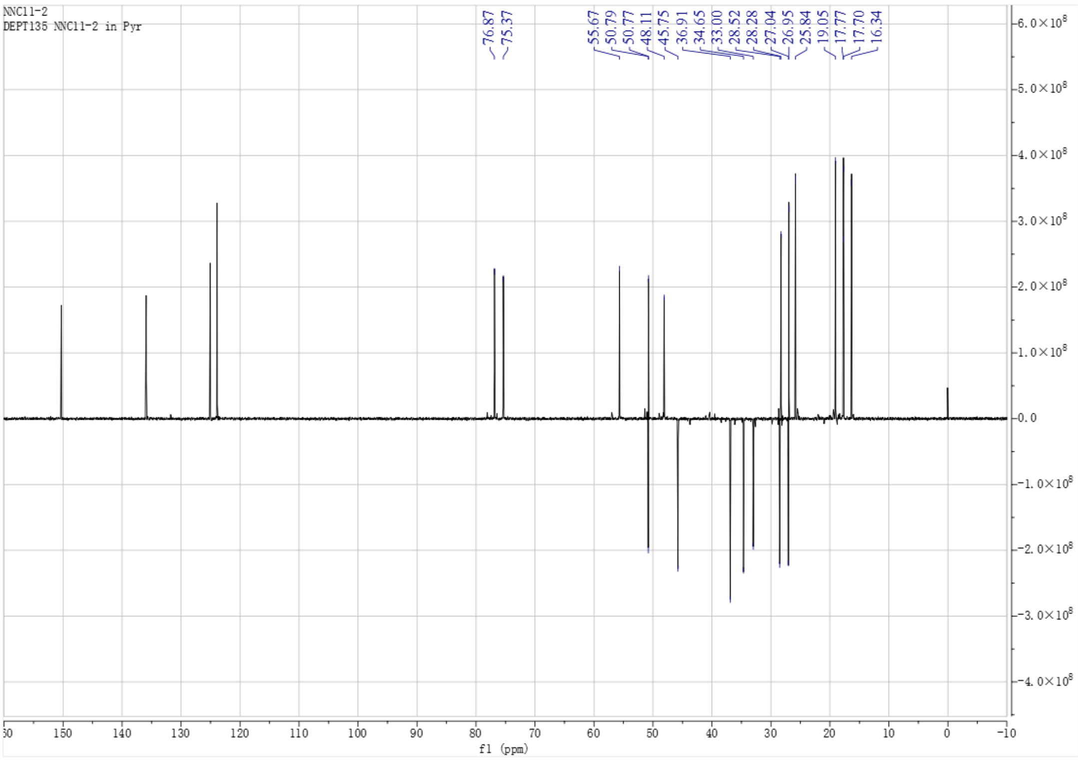

Figure S47. DEPT 135° spectrum (150 MHz, C_5D_5N) of compound **6**

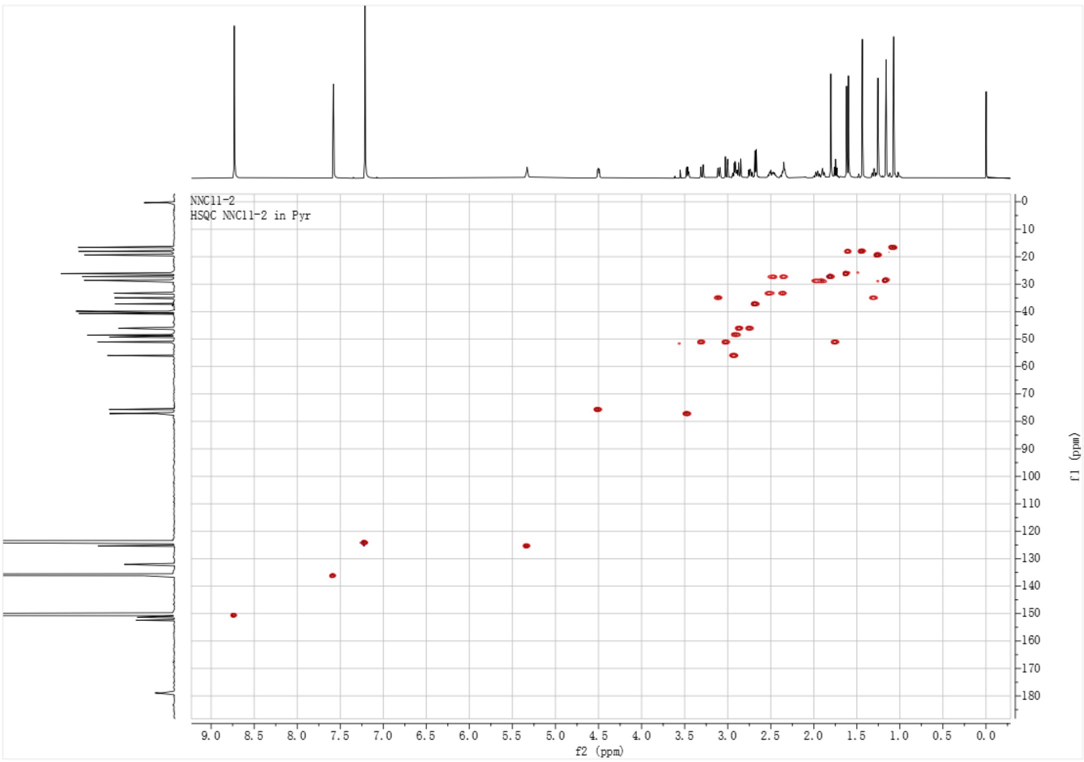

Figure S48. HSQC spectrum (600 MHz, C_5D_5N) of compound **6**

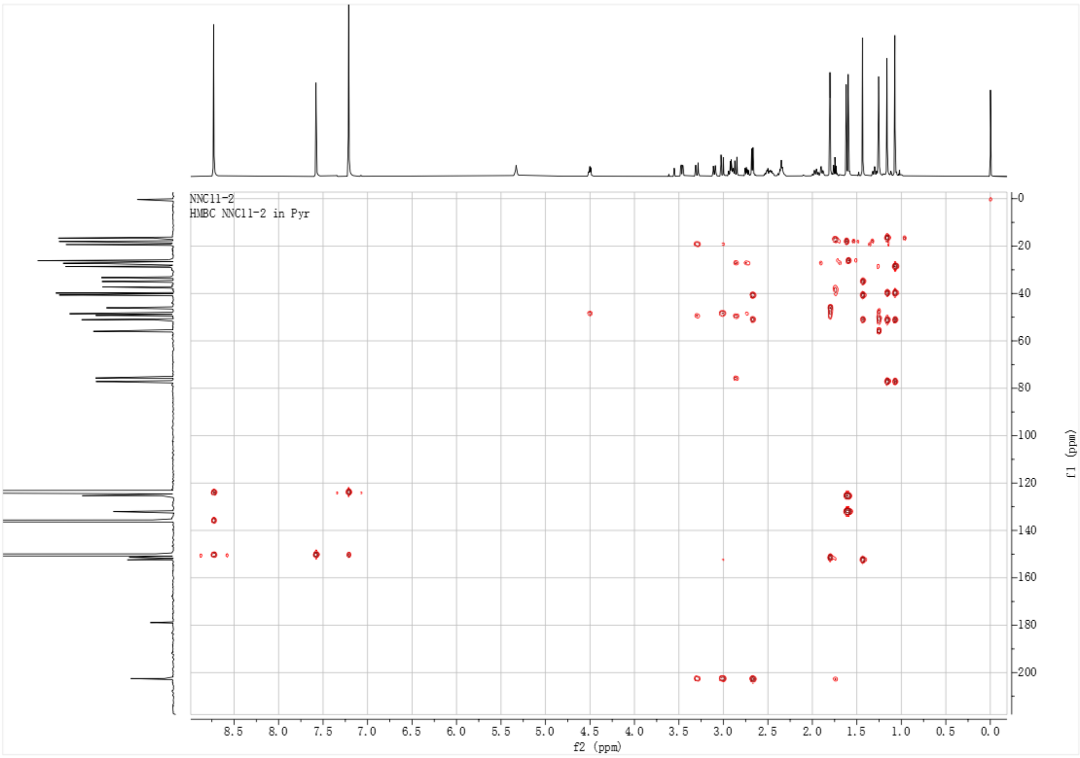

Figure S49. HMBC spectrum (600 MHz, C_5D_5N) of compound **6**

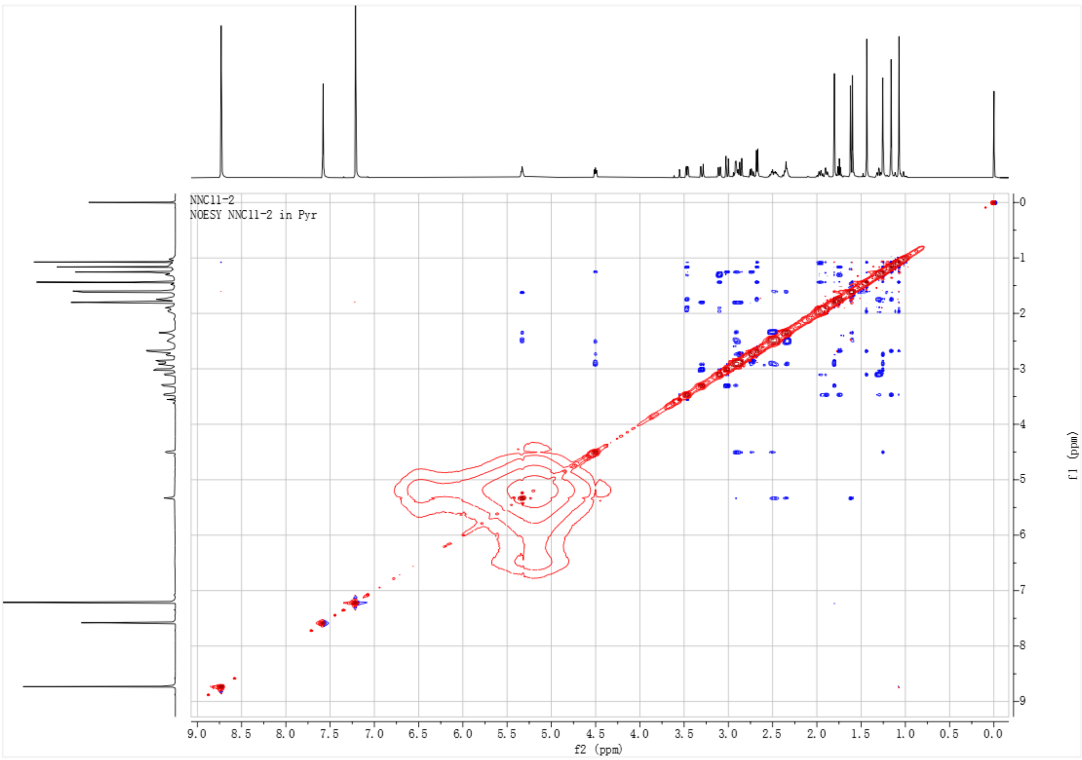

Figure S50. NOESY spectrum (600 MHz, C_5D_5N) of compound **6**

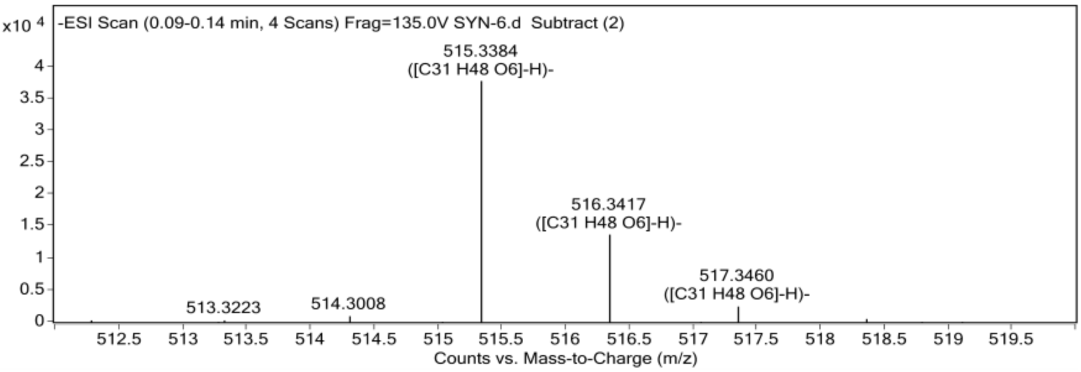

Figure S51. HRESIMS spectrum of compound **7**

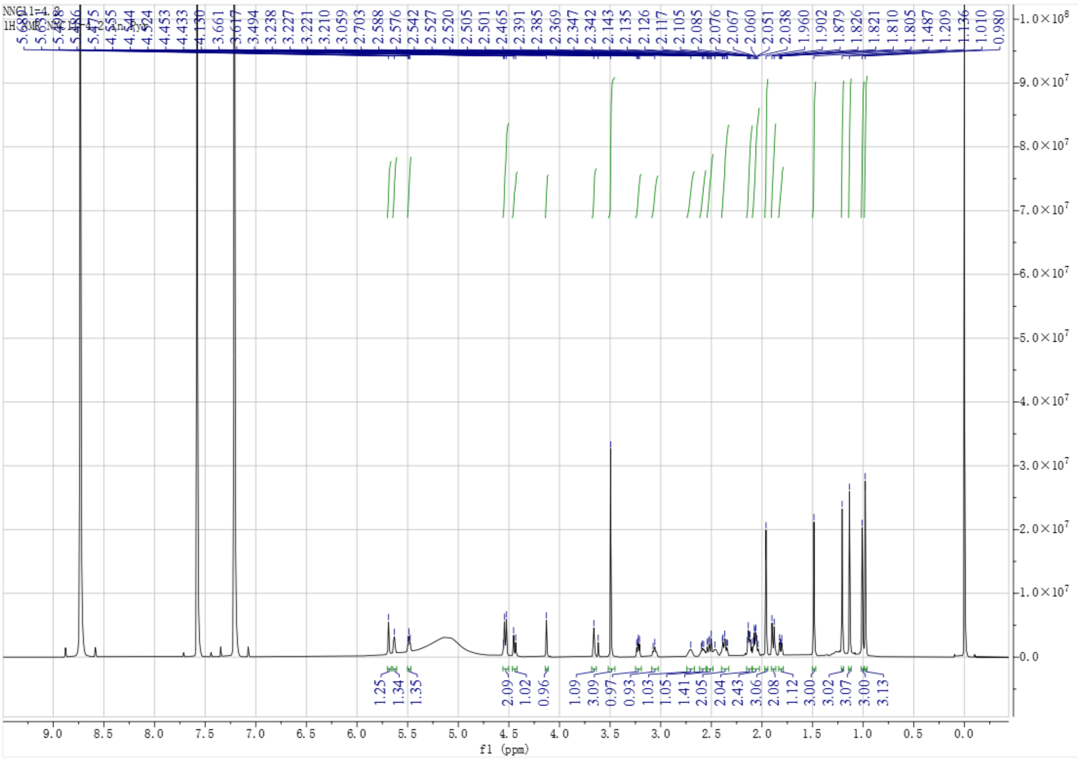

Figure S52. ^{1}H NMR spectrum (600 MHz, C_5D_5N) of compound **7**

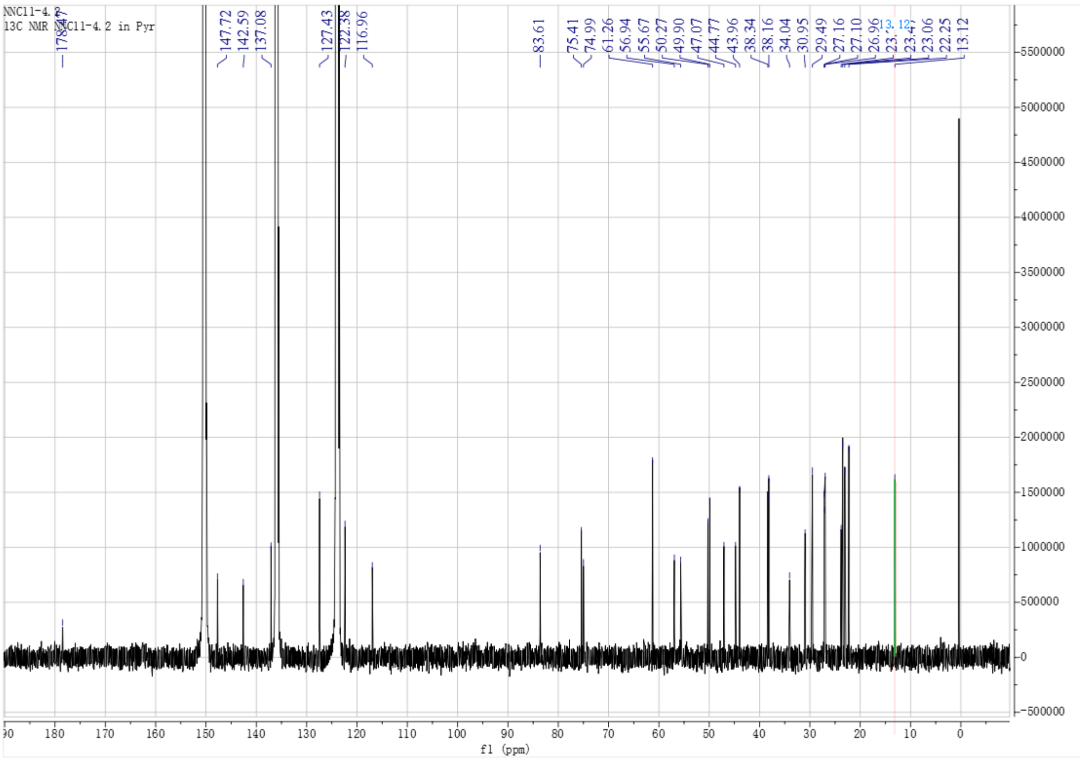

Figure S53. ^{13}C NMR spectrum (150 MHz, C_5D_5N) of compound **7**

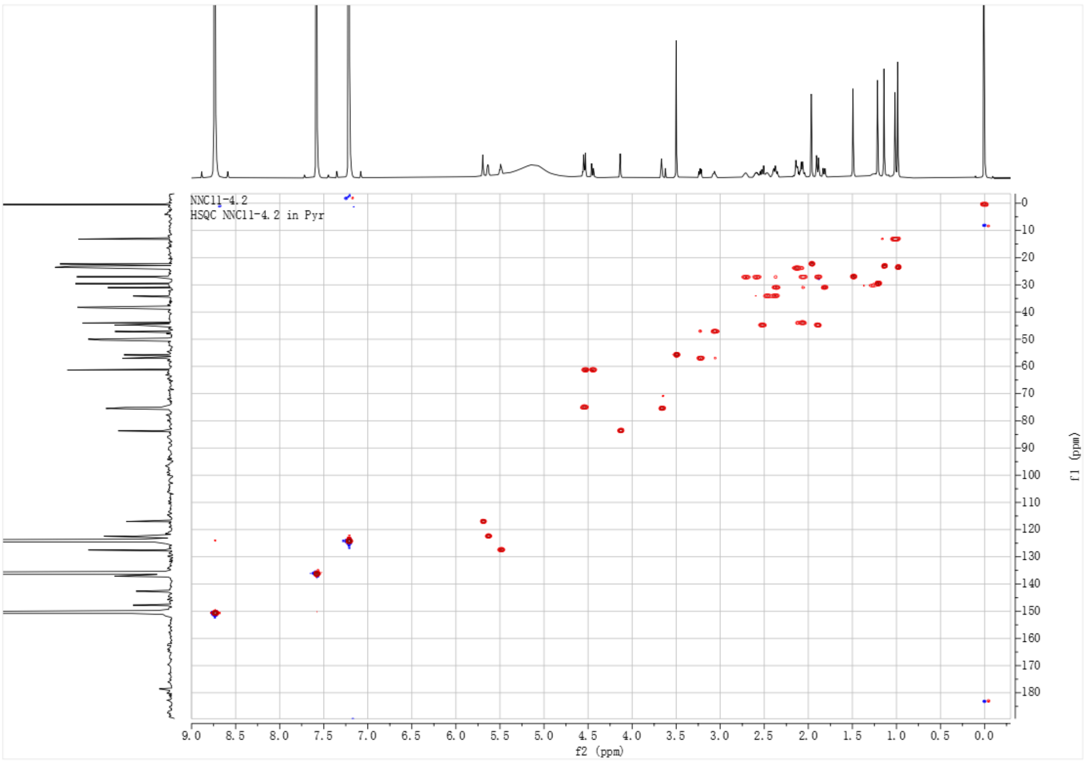

Figure S54. HSQC spectrum (600 MHz, C_5D_5N) of compound **7**

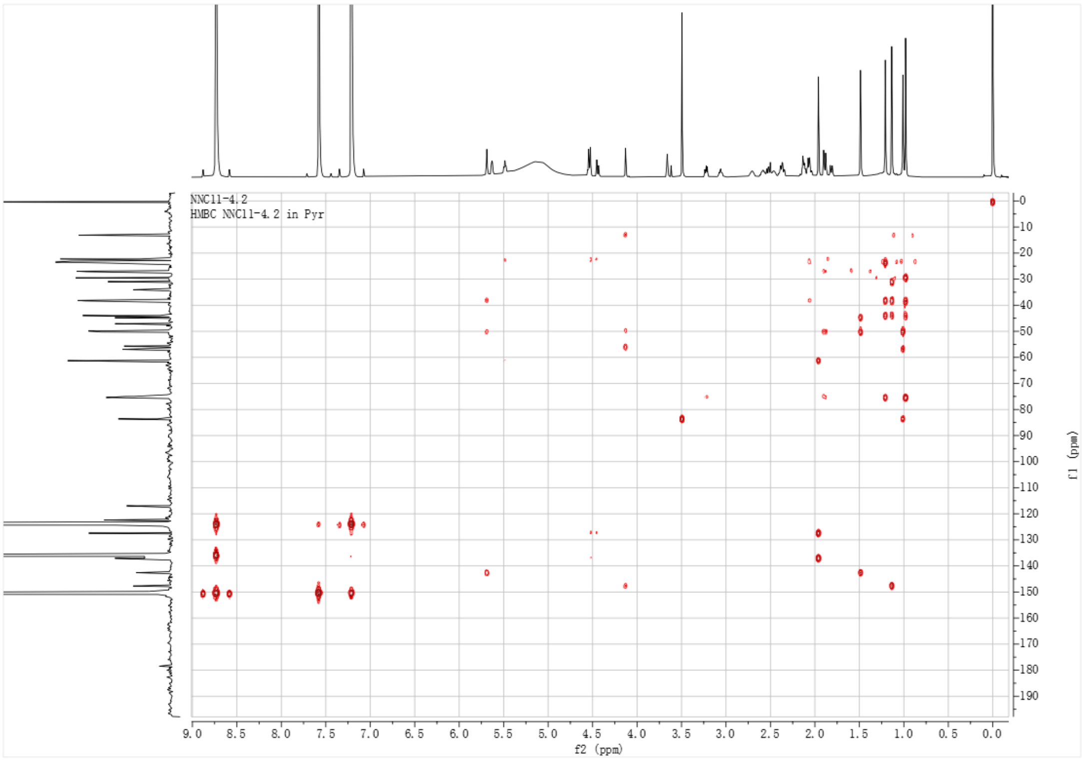

Figure S55. HMBC spectrum (600 MHz, C_5D_5N) of compound **7**

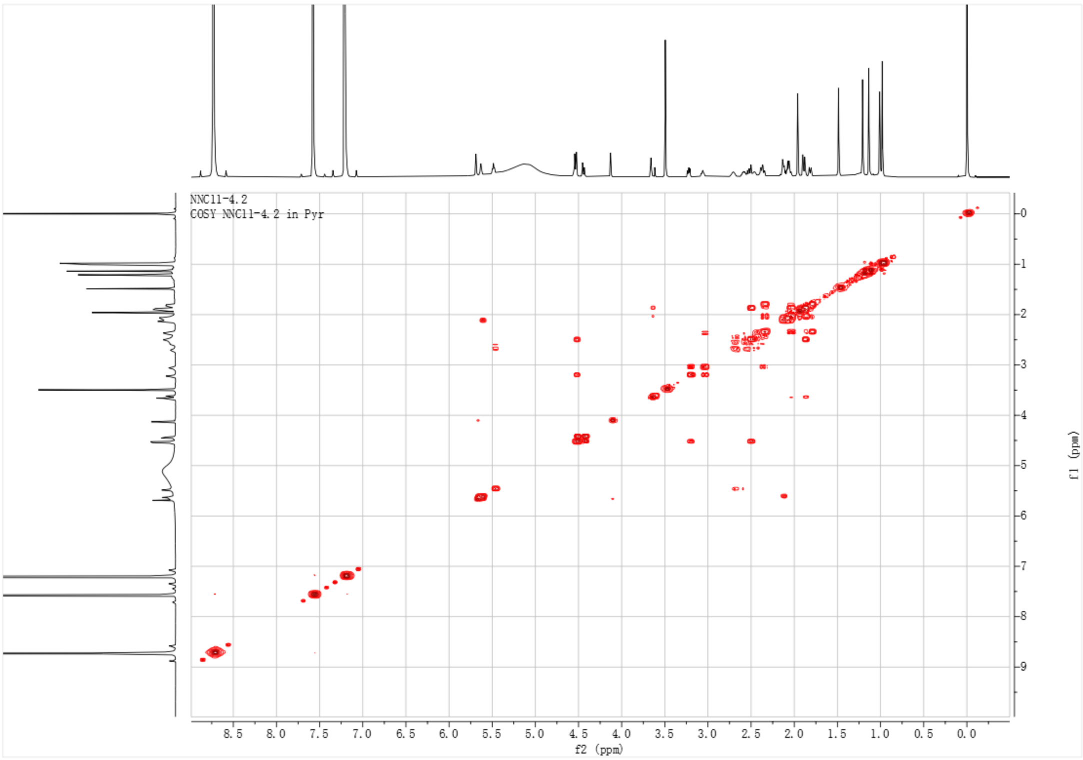

Figure S56. ^1H-^1H COSY spectrum (600 MHz, C_5D_5N) of compound **7**

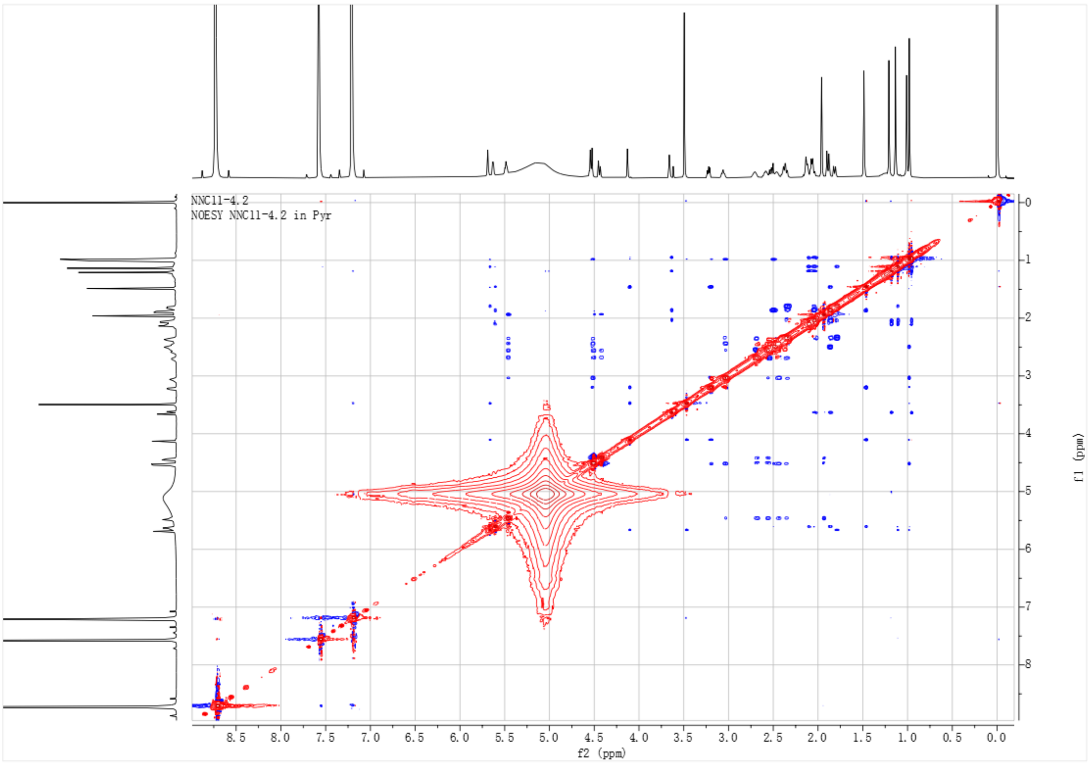

Figure S57. NOESY spectrum (600 MHz, C_5D_5N) of compound **7**

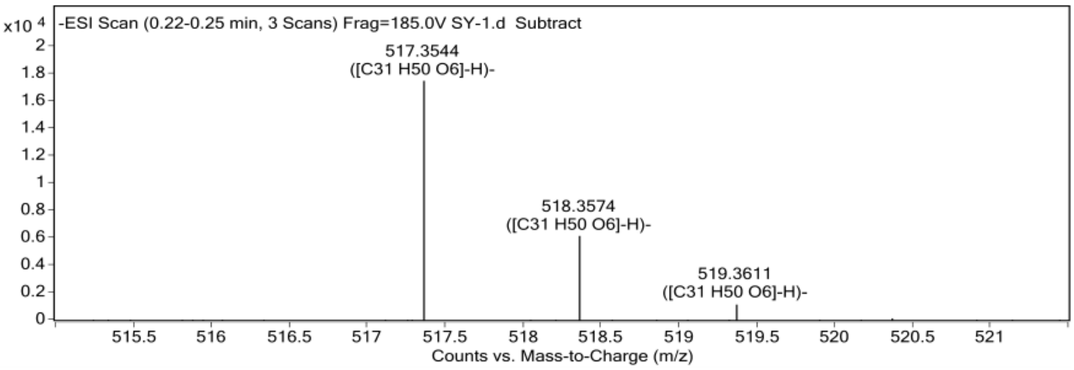

Figure S58. HRESIMS spectrum of compound **8**

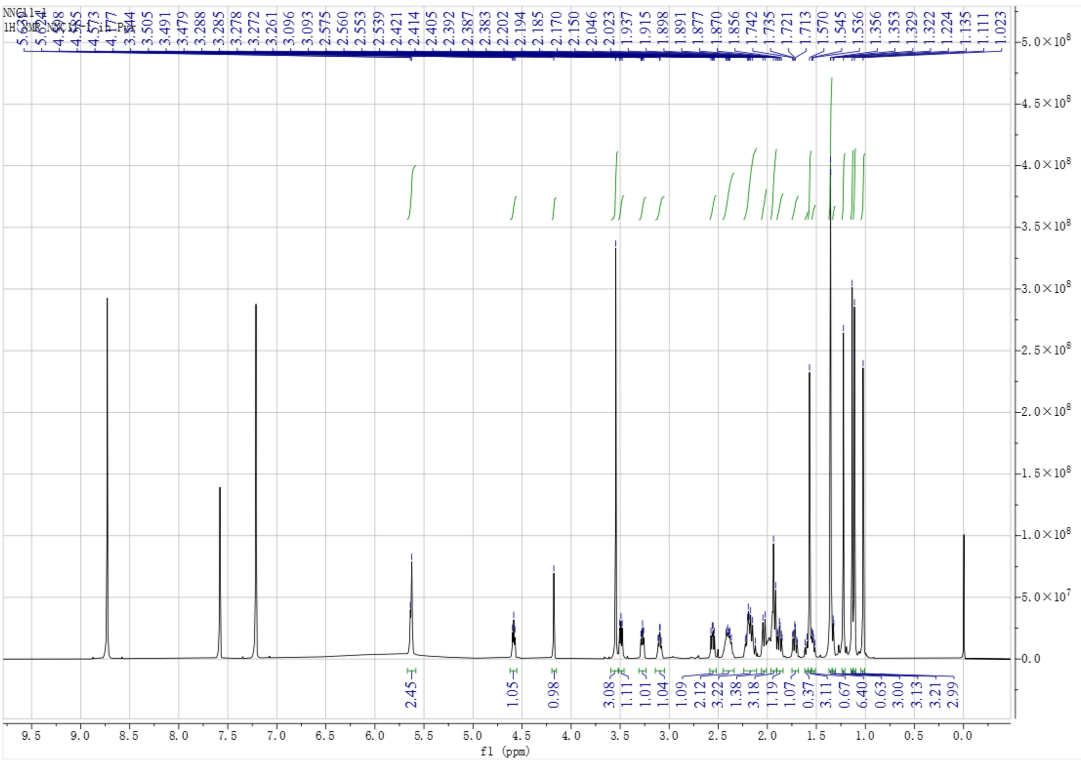

Figure S59. ^{1}H NMR spectrum (600 MHz, C_5D_5N) of compound **8**

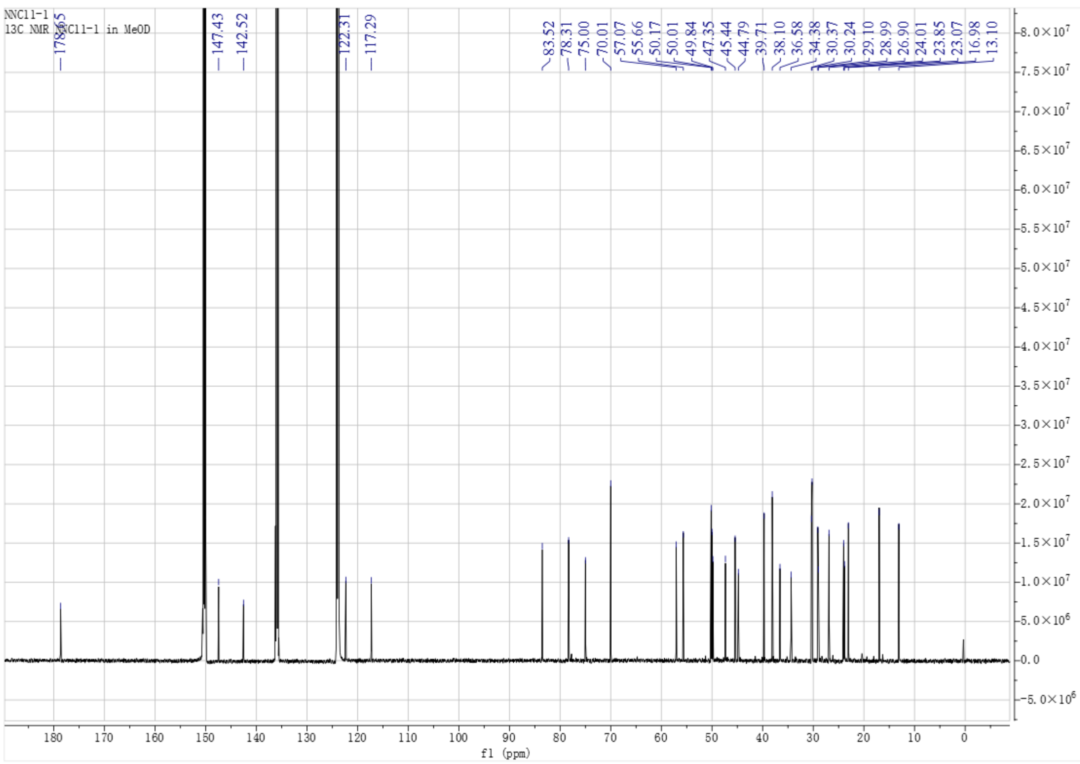

Figure S60. ^{13}C NMR spectrum (150 MHz, C_5D_5N) of compound **8**

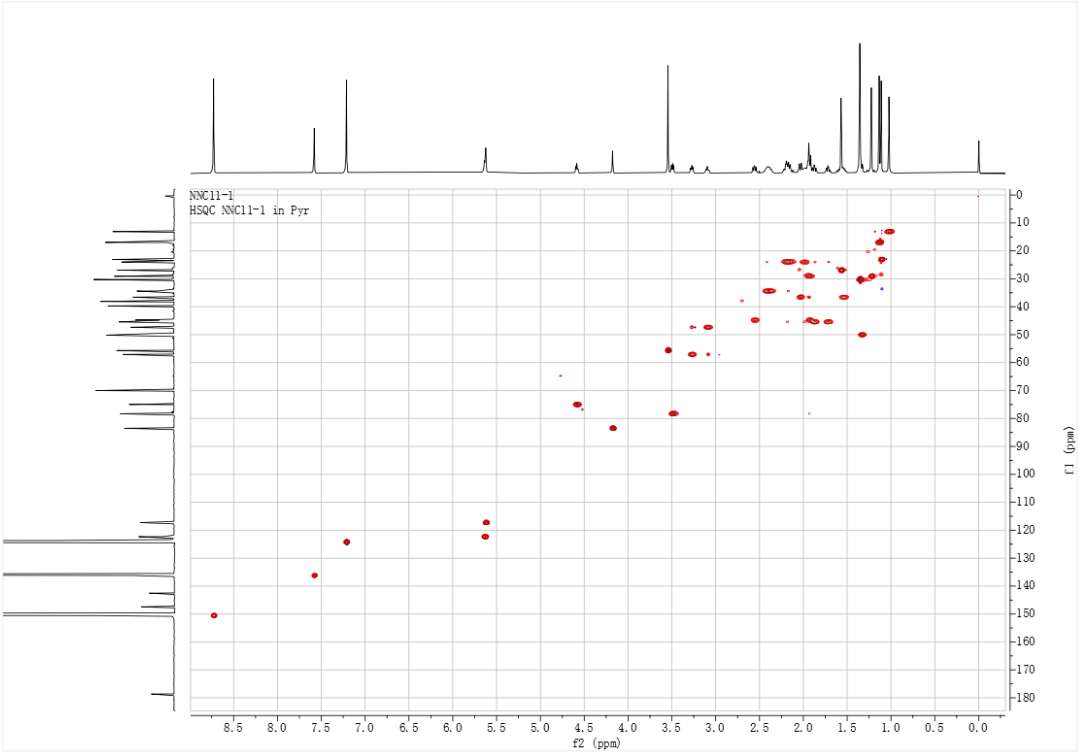

Figure S61. HSQC spectrum (600 MHz, C_5D_5N) of compound **8**

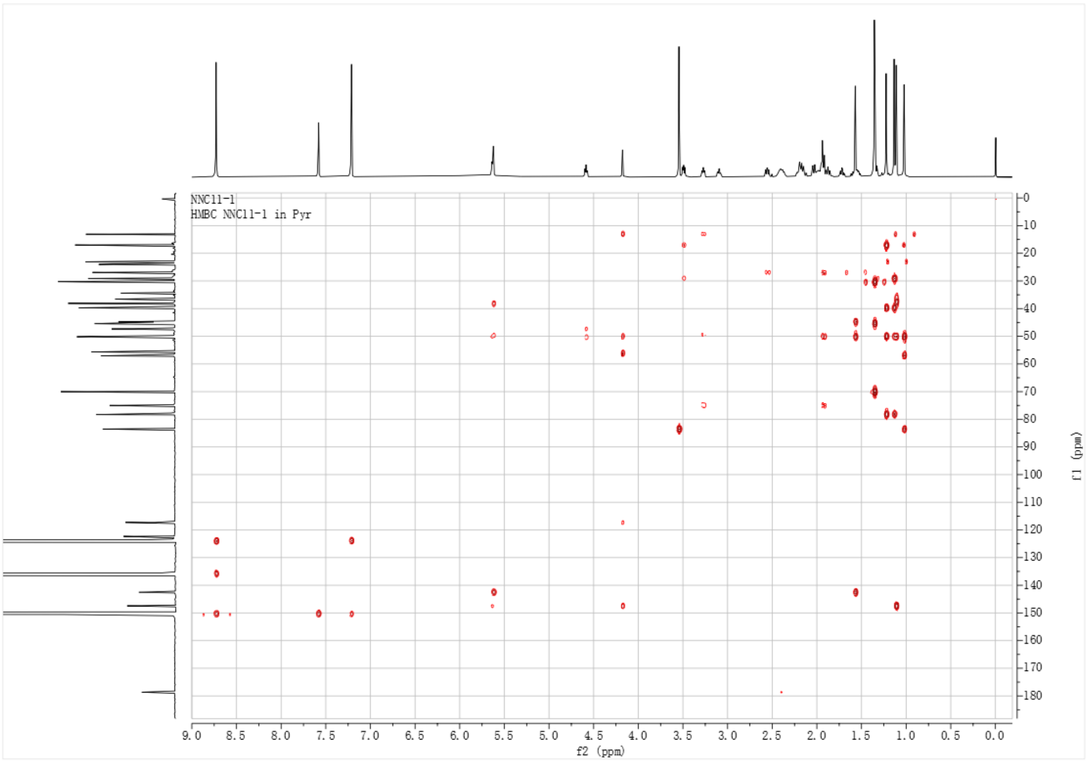

Figure S62. HMBC spectrum (600 MHz, C_5D_5N) of compound **8**

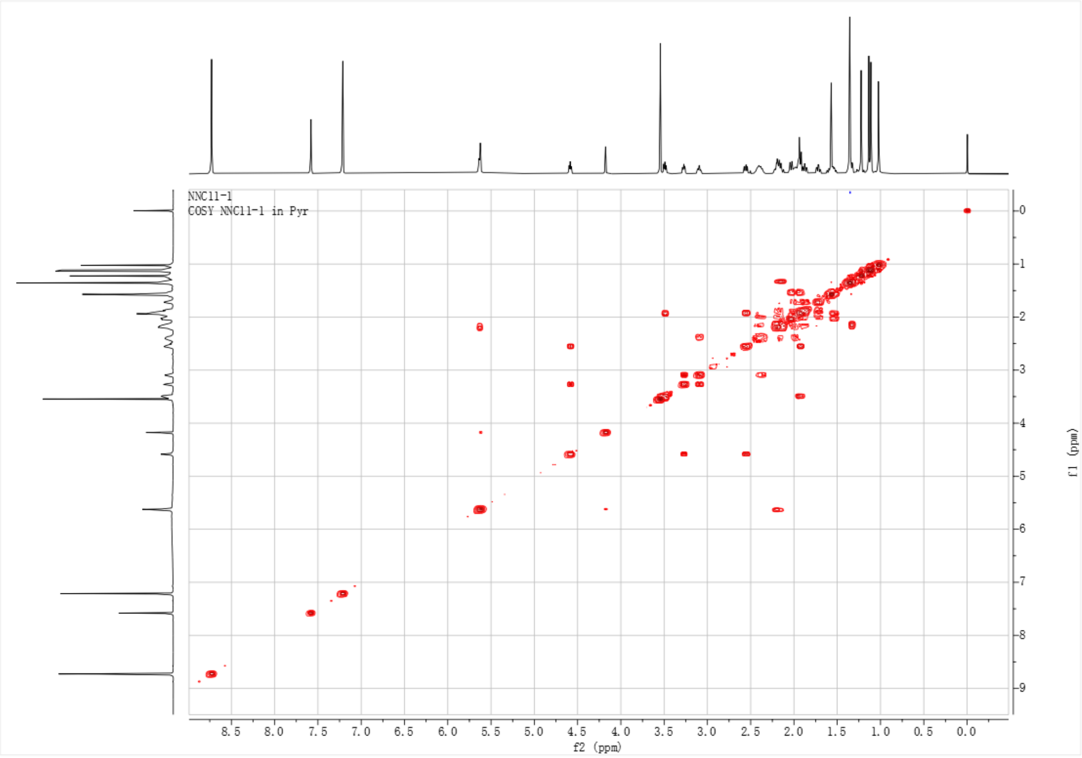

Figure S63. ^{1}H-^{1}H COSY spectrum (600 MHz, C_5D_5N) of compound **8**

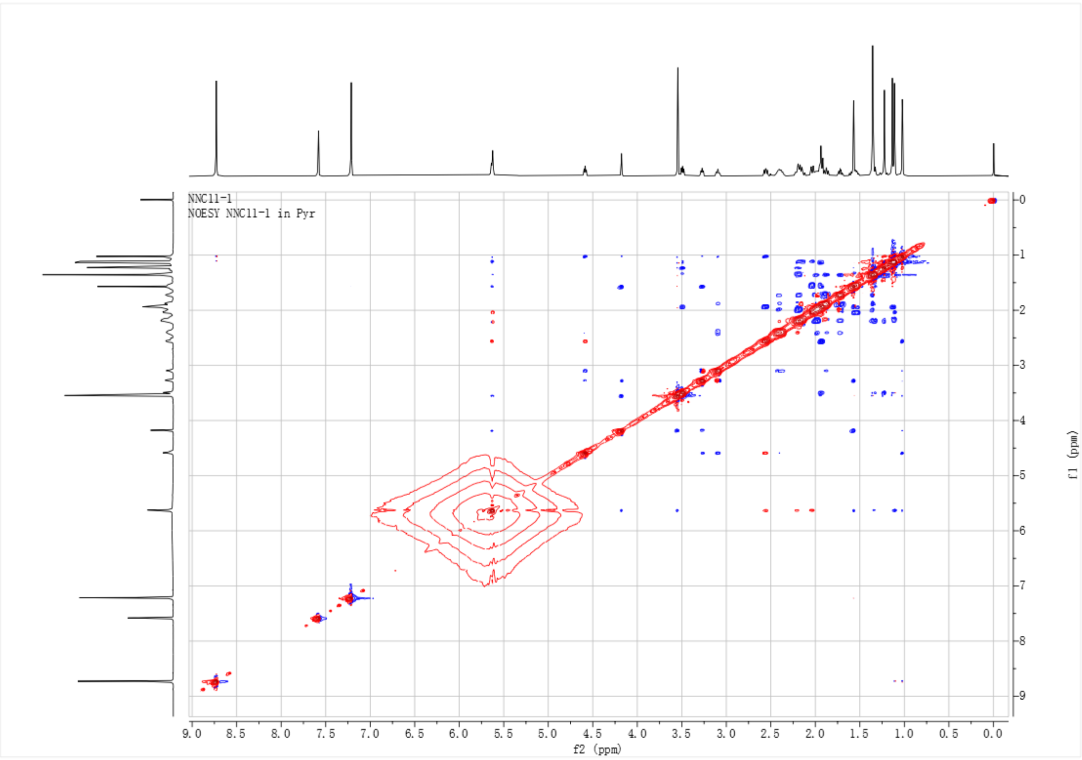

Figure S64. NOESY spectrum (600 MHz, C_5D_5N) of compound **8**

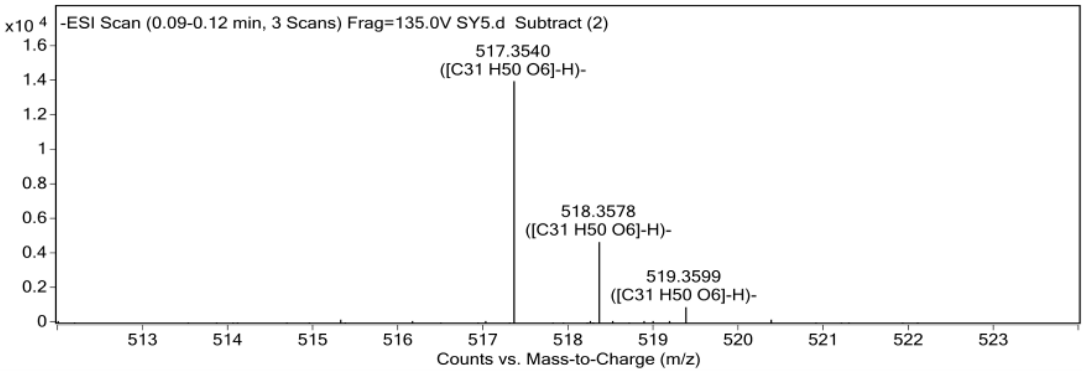

Figure S65. HRESIMS spectrum of compound **9**

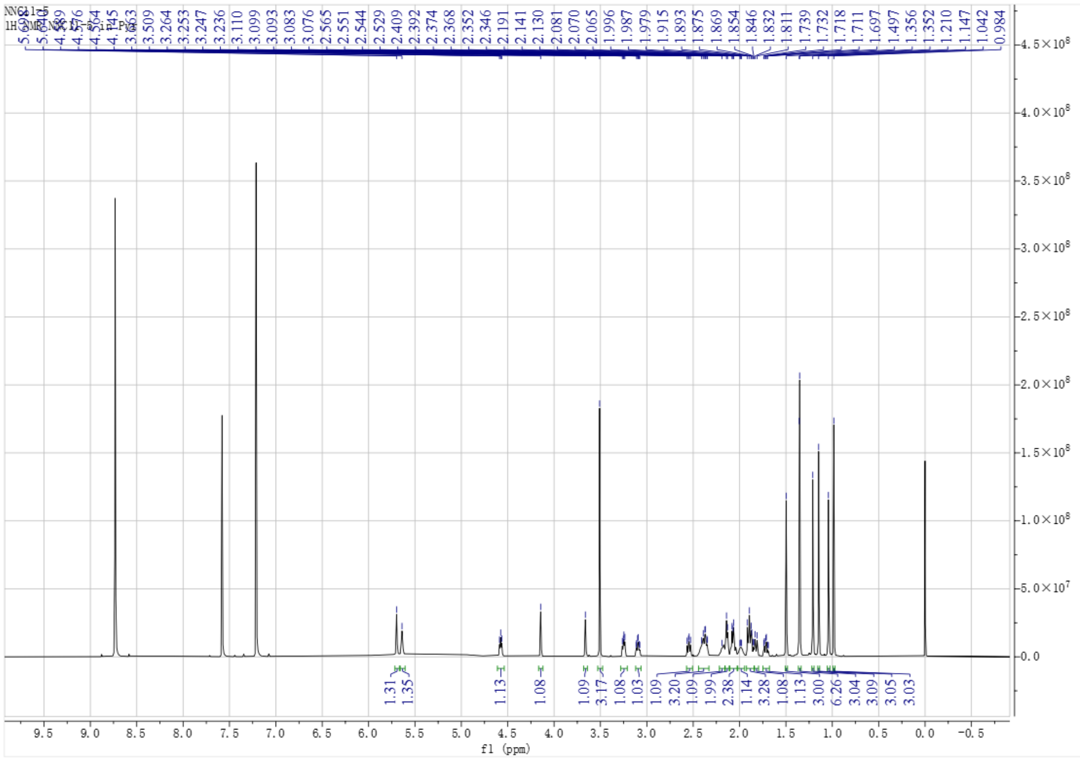

Figure S66. ^{1}H NMR spectrum (600 MHz, C_5D_5N) of compound **9**

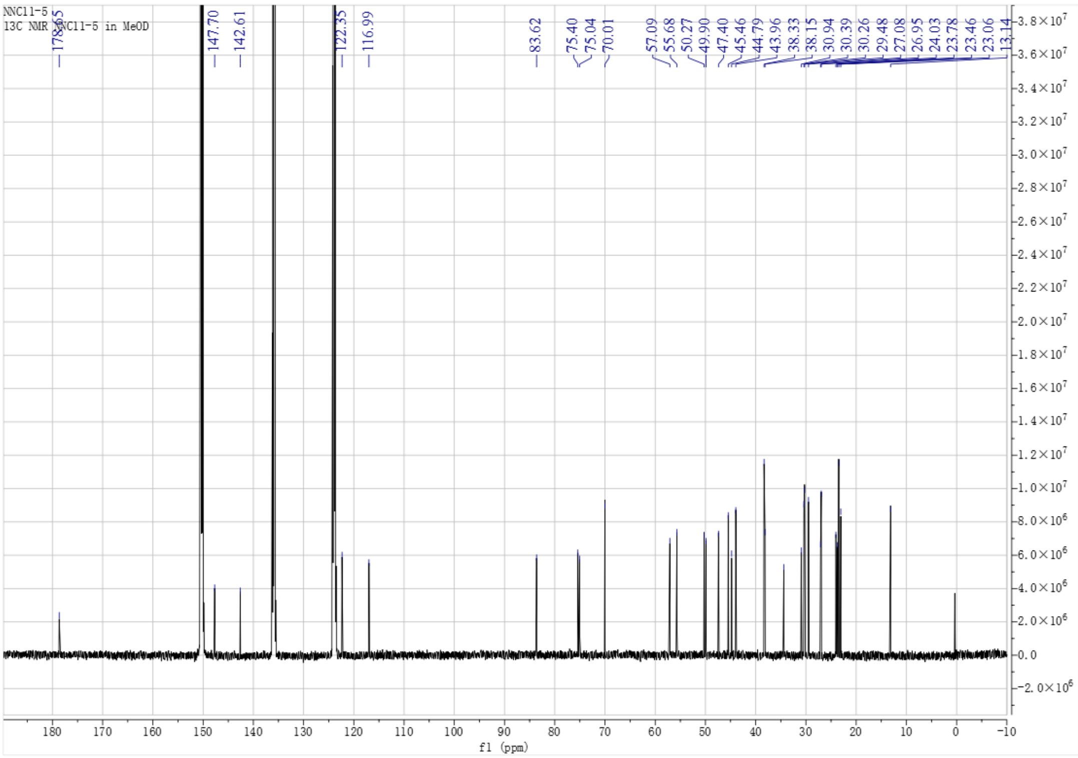

Figure S67. ^{13}C NMR spectrum (150 MHz, C_5D_5N) of compound **9**

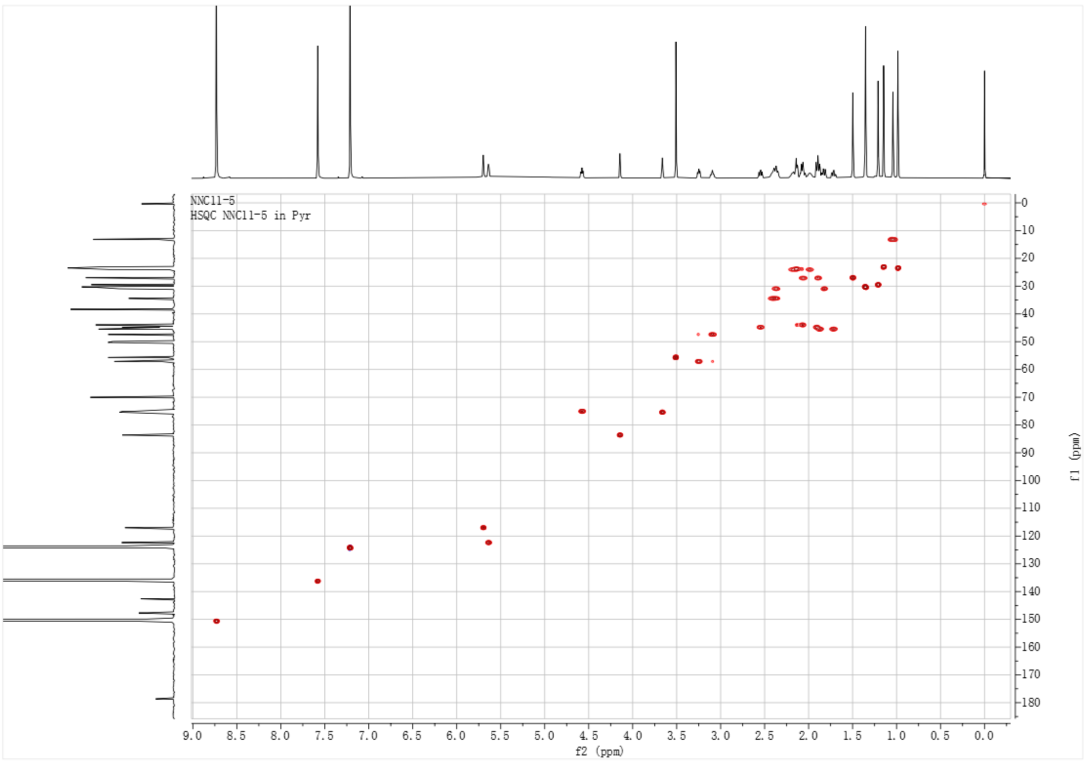

Figure S68. HSQC spectrum (600 MHz, C_5D_5N) of compound **9**

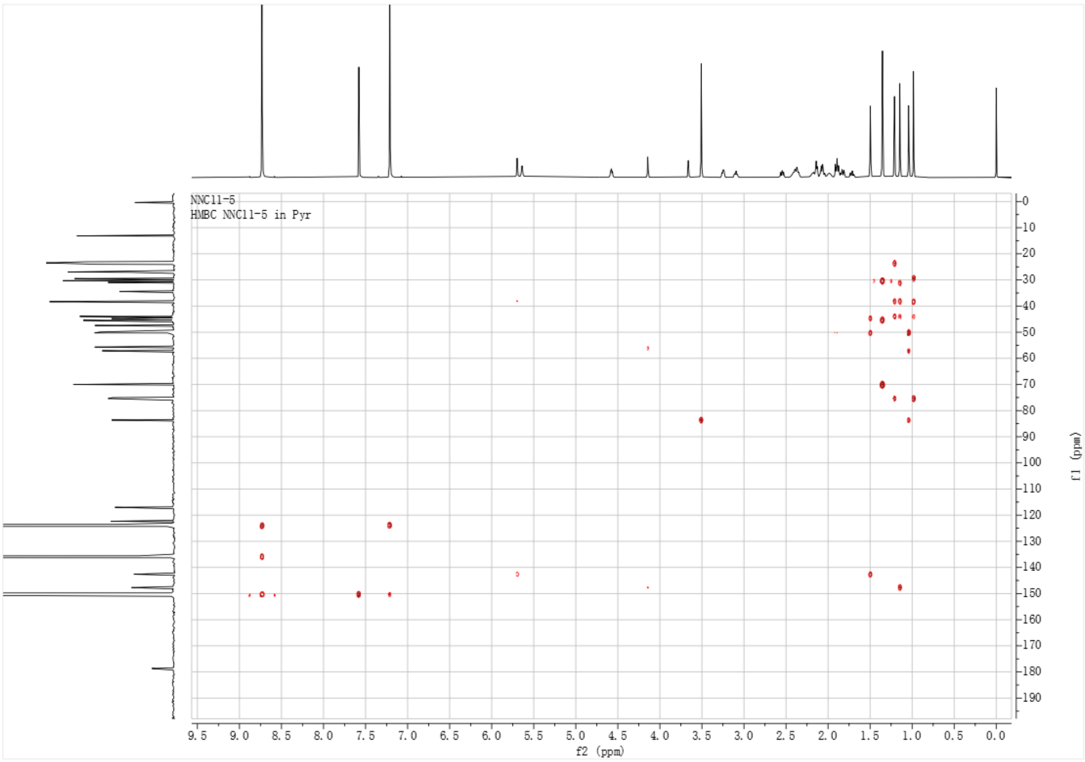

Figure S69. HMBC spectrum (600 MHz, C_5D_5N) of compound **9**

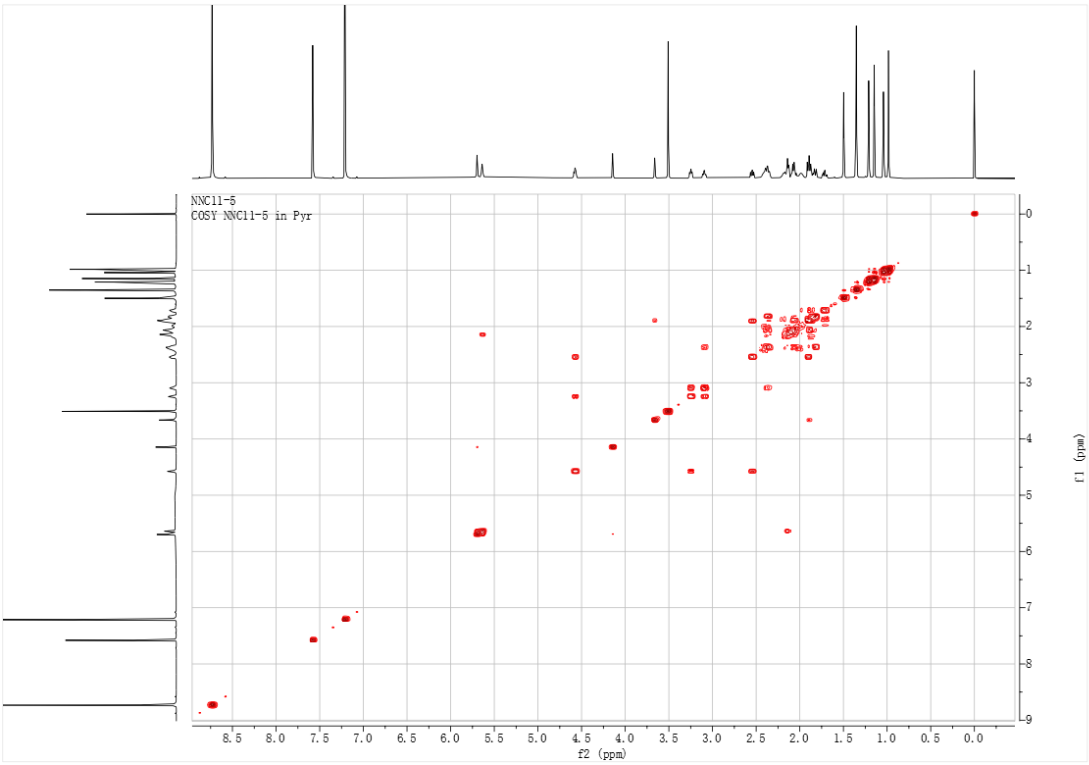

Figure S70. ^1H-^1H COSY spectrum (600 MHz, C_5D_5N) of compound **9**

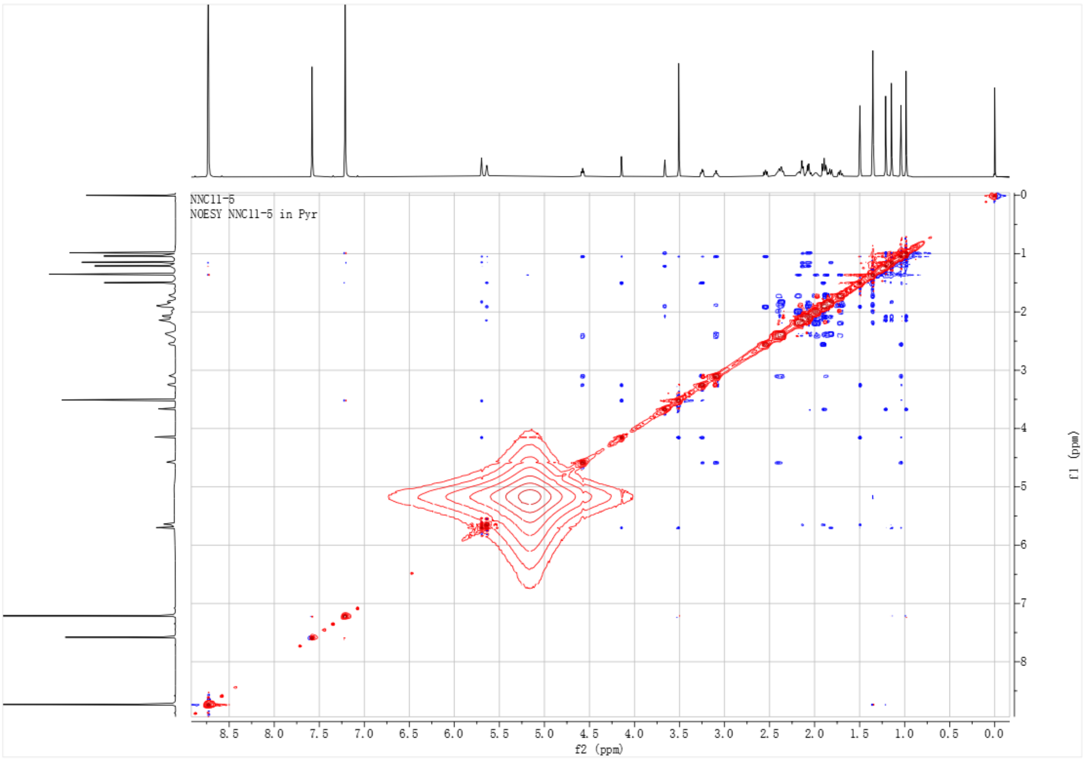

Figure S71. NOESY spectrum (600 MHz, C_5D_5N) of compound **9**

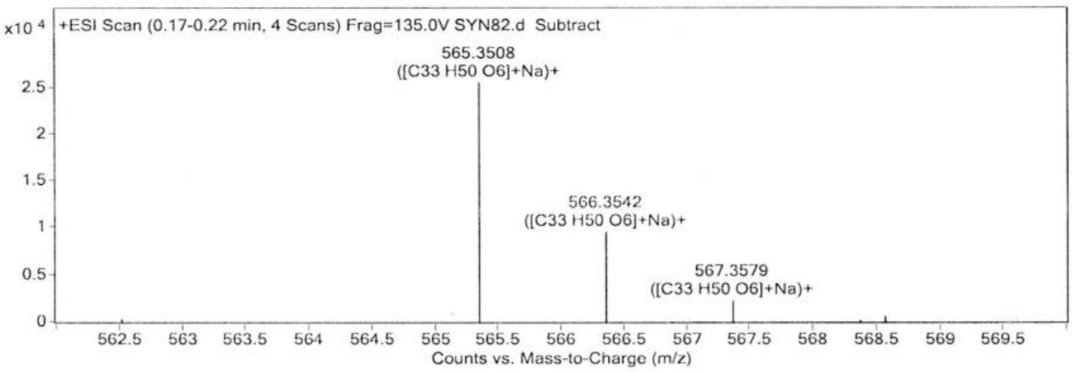

Figure S72. HRESIMS spectrum of compound **10**

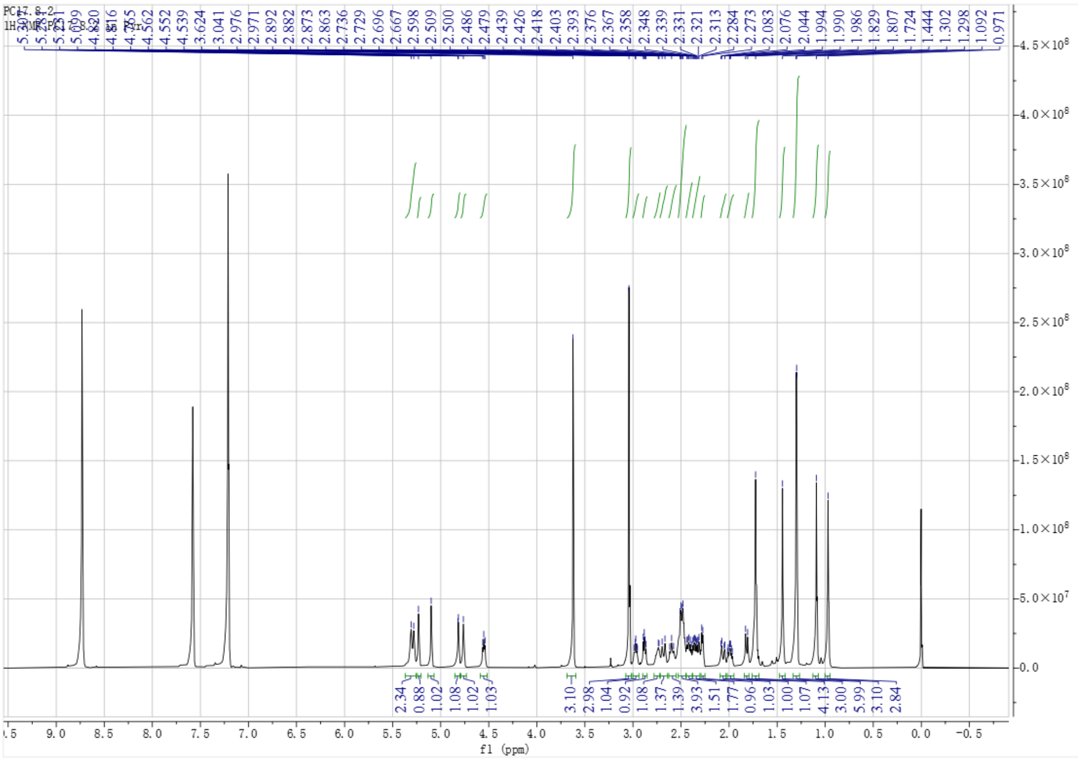

Figure S73. ^{1}H NMR spectrum (600 MHz, C_5D_5N) of compound **10**

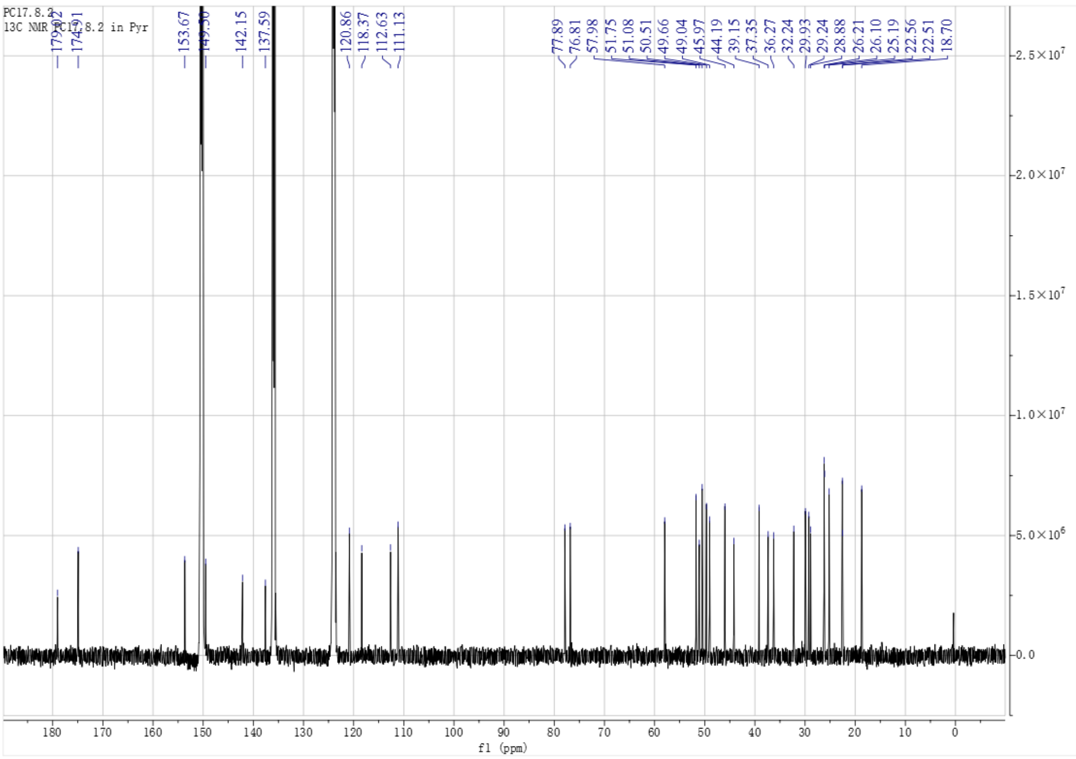

Figure S74. ^{13}C NMR spectrum (150 MHz, C_5D_5N) of compound **10**

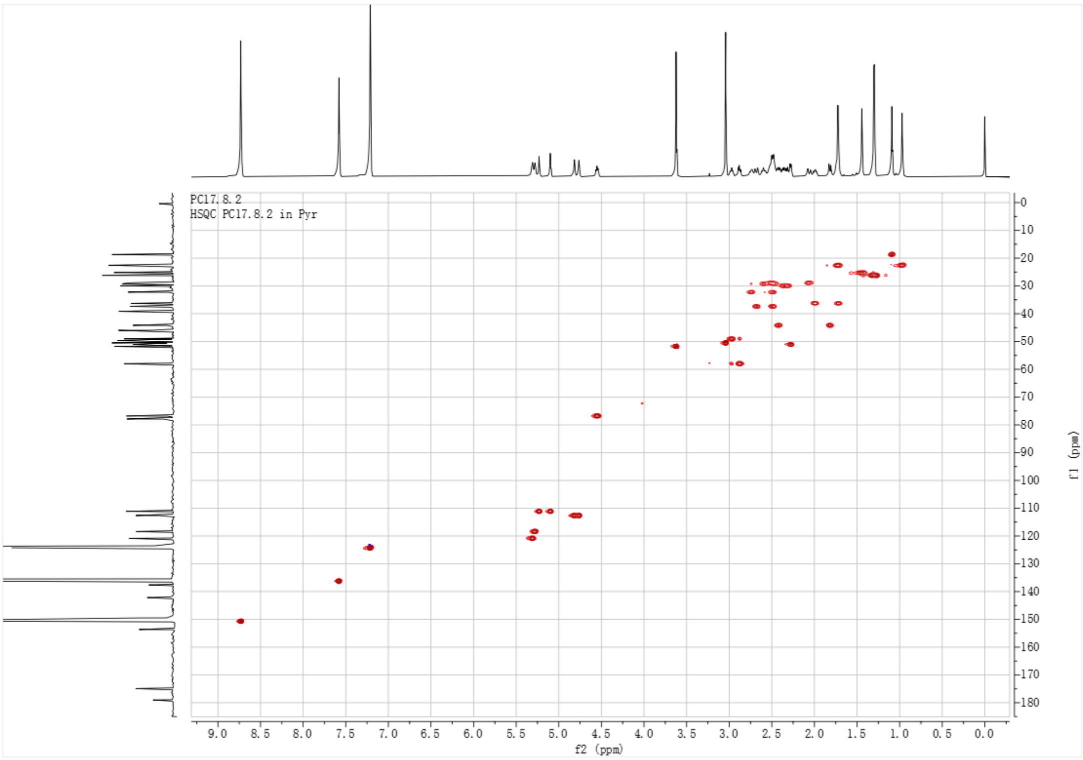

Figure S75. HSQC spectrum (600 MHz, C_5D_5N) of compound **10**

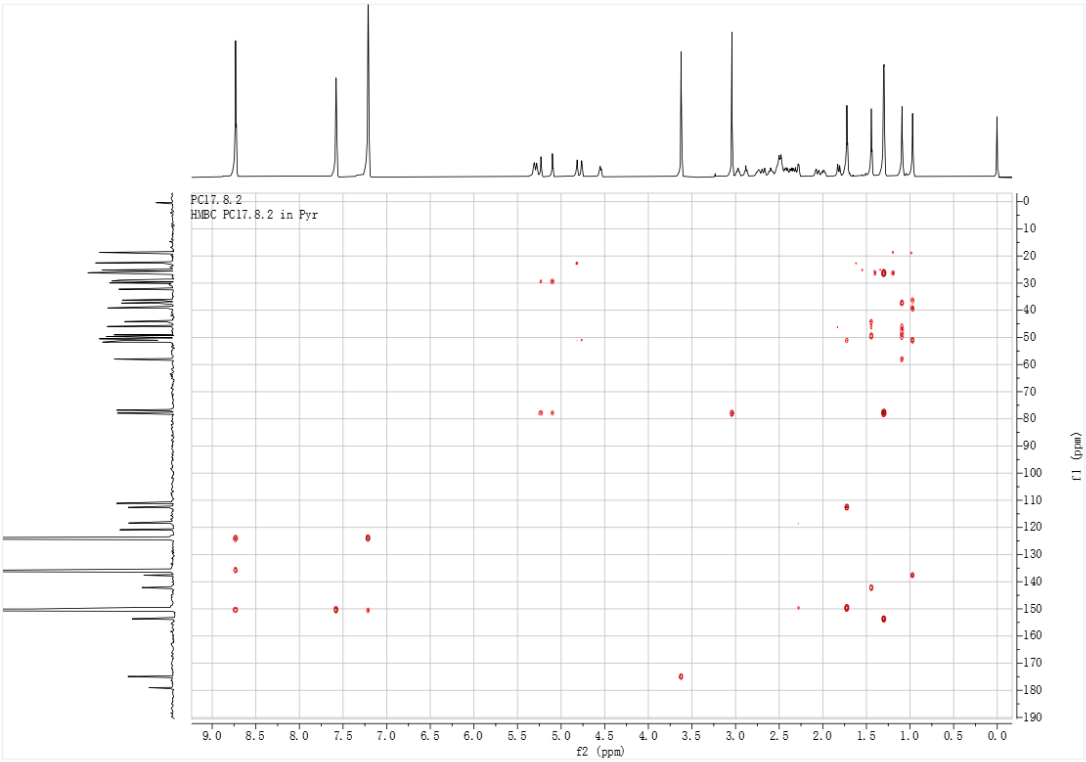

Figure S76. HMBC spectrum (600 MHz, C_5D_5N) of compound **10**

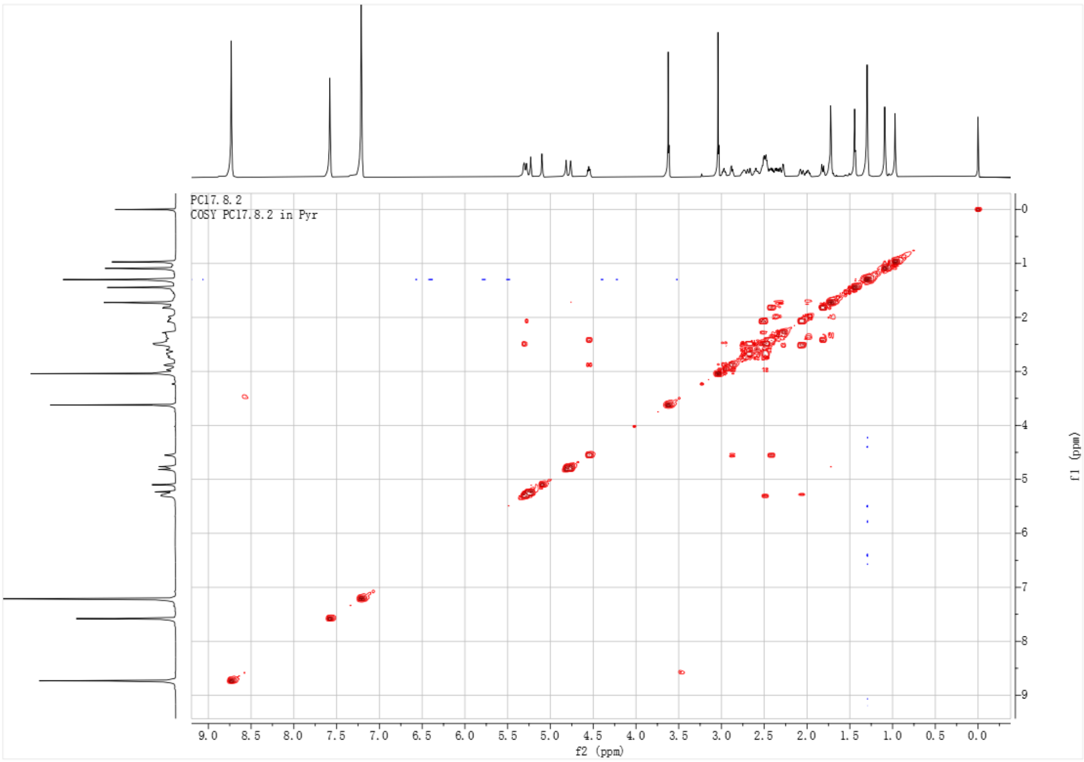

Figure S77. ^{1}H-^{1}H COSY spectrum (600 MHz, C_5D_5N) of compound **10**

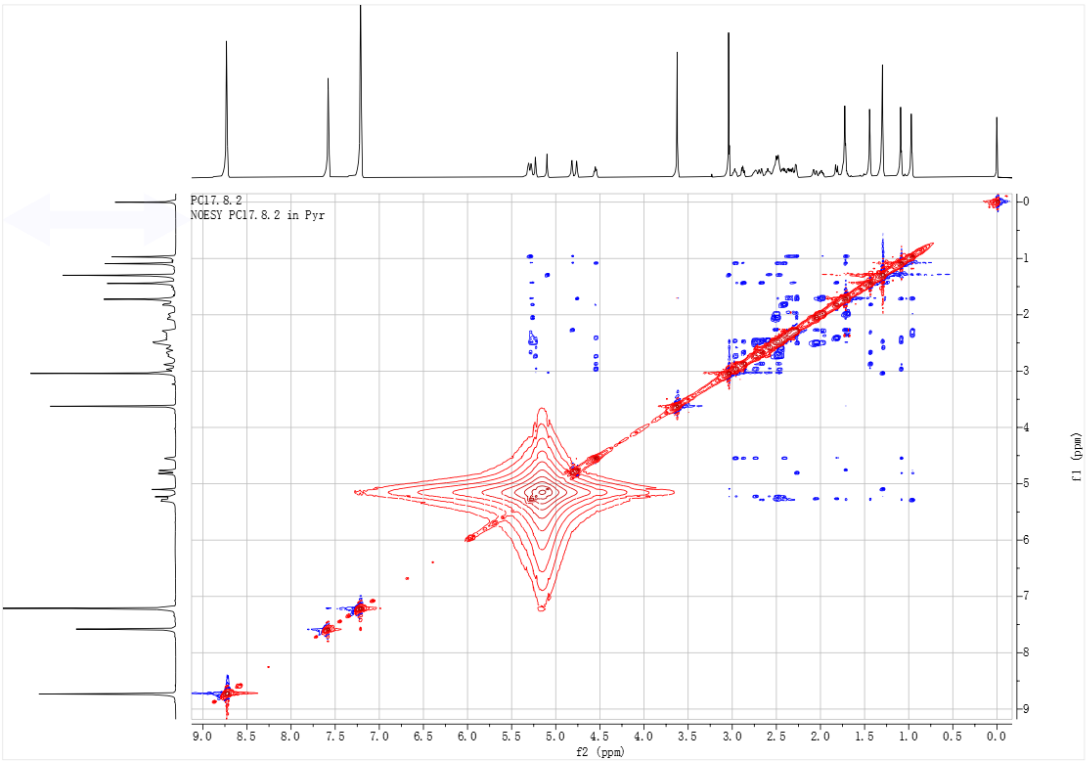

Figure S78. NOESY spectrum (600 MHz, C_5D_5N) of compound **10**

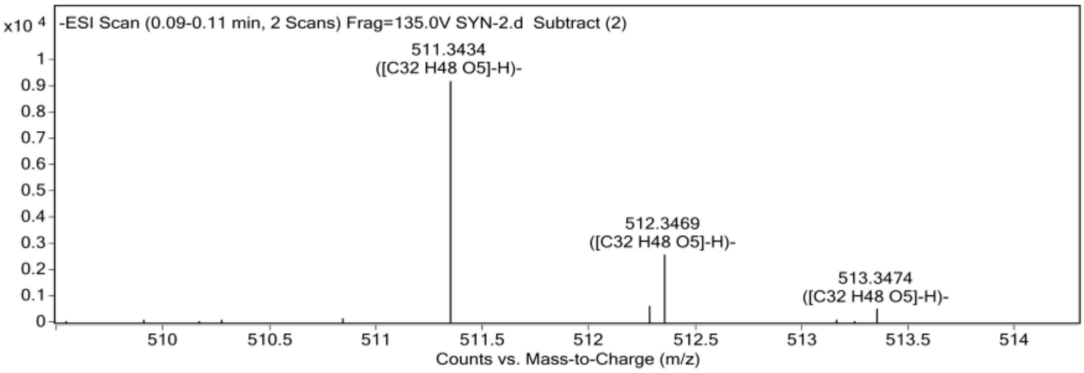

Figure S79. HRESIMS spectrum of compound **11**

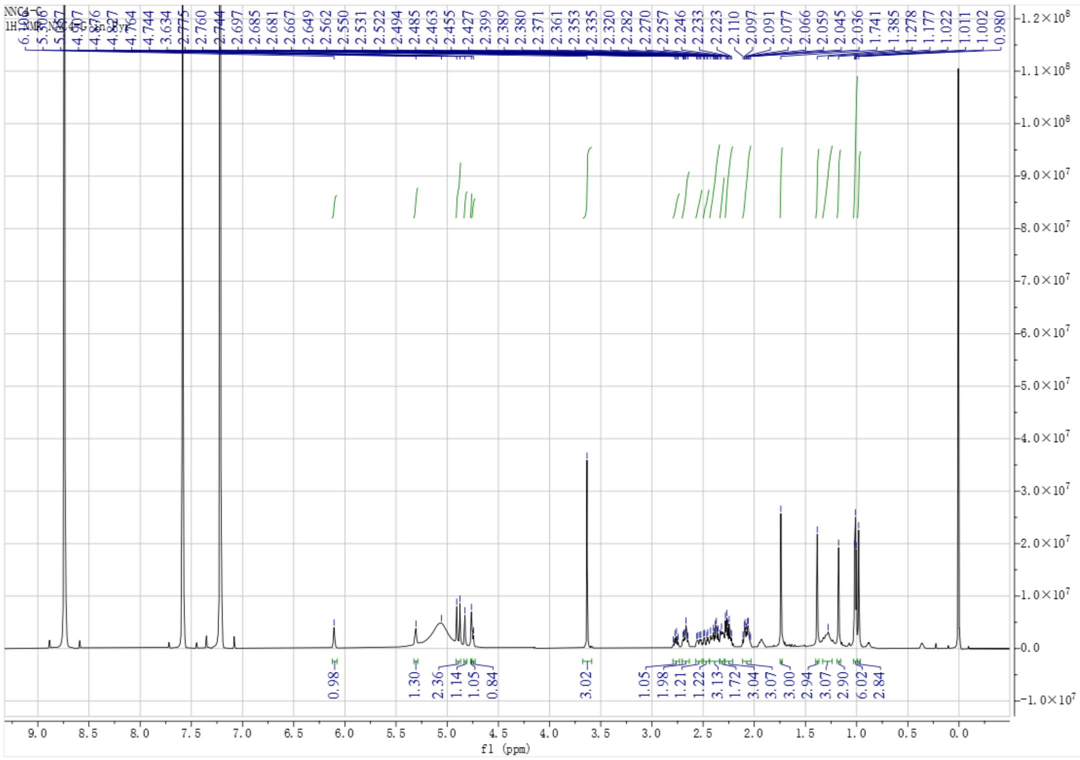

Figure S80. ^{1}H NMR spectrum (600 MHz, C_5D_5N) of compound **11**

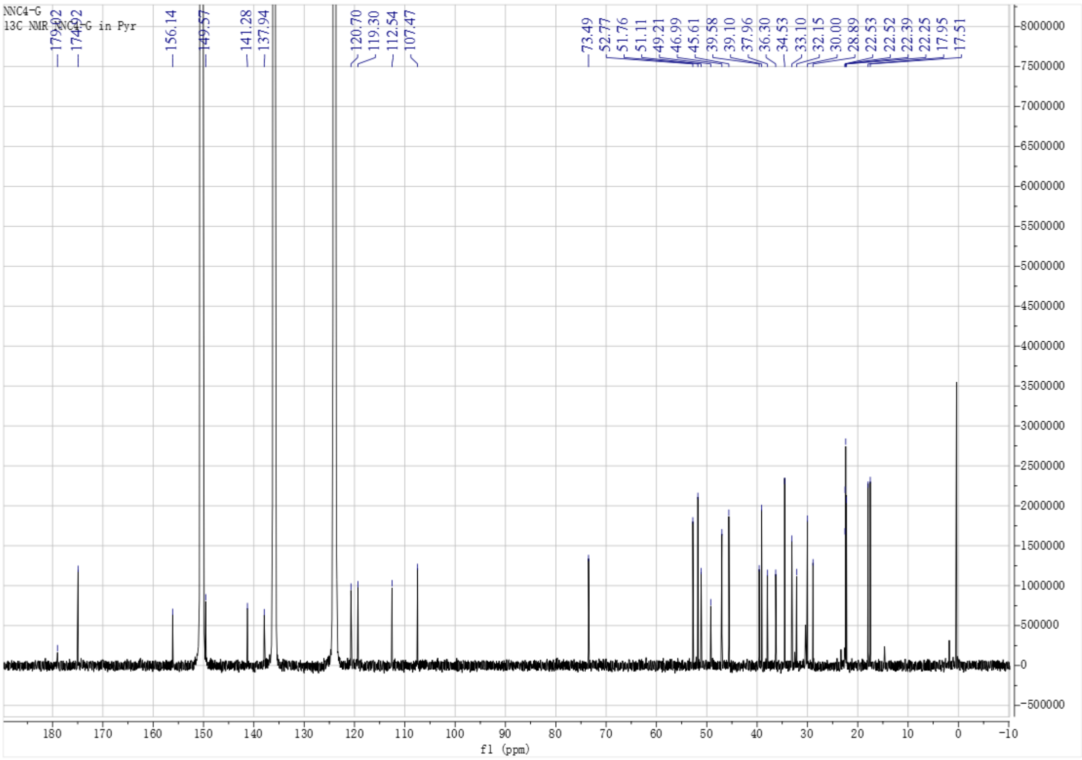

Figure S81. ^{13}C NMR spectrum (150 MHz, C_5D_5N) of compound **11**

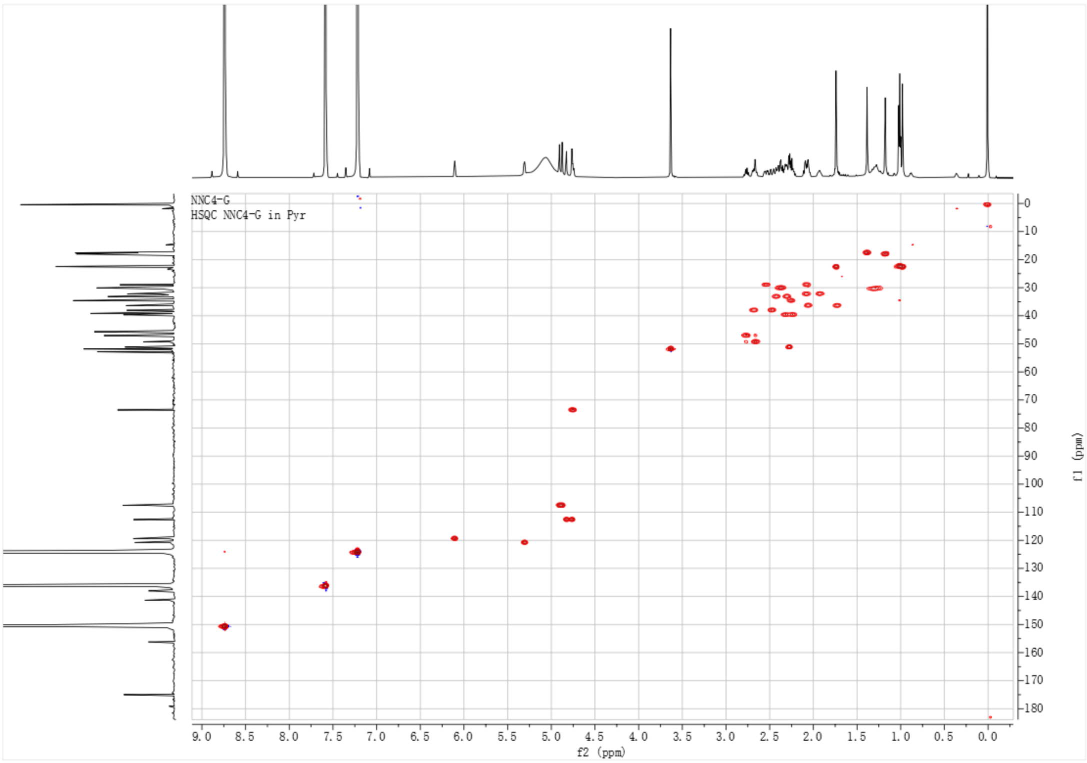

Figure S82. HSQC spectrum (600 MHz, C_5D_5N) of compound **11**

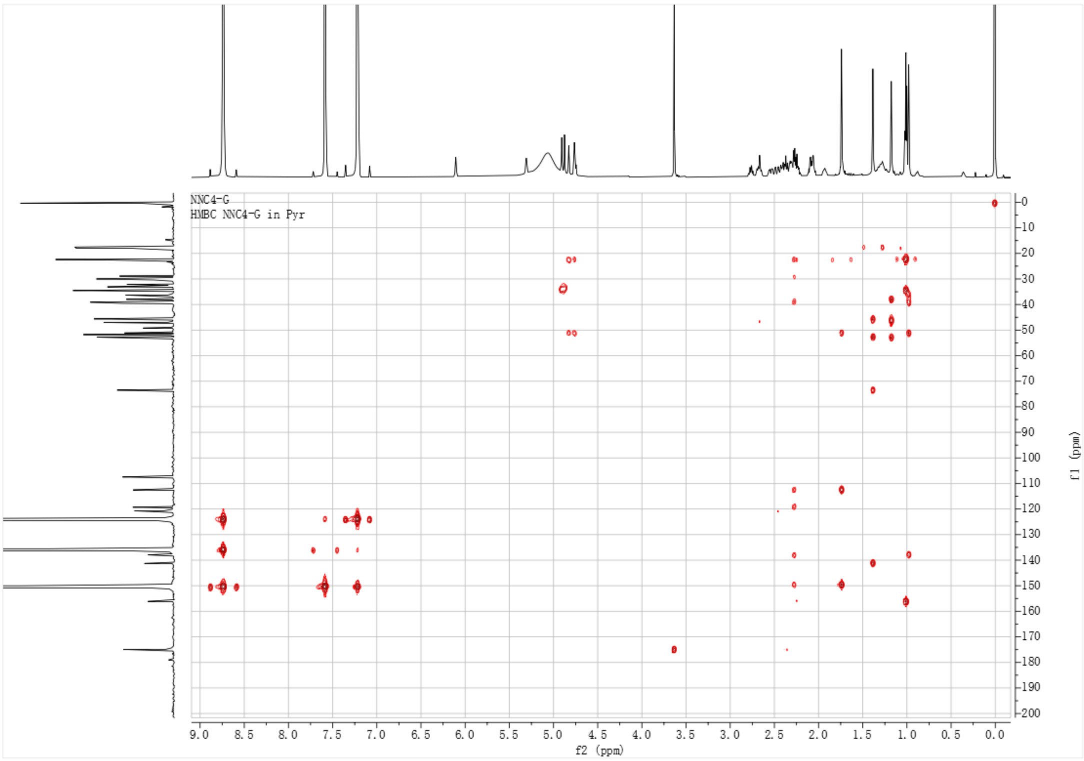

Figure S83. HMBC spectrum (600 MHz, C_5D_5N) of compound **11**

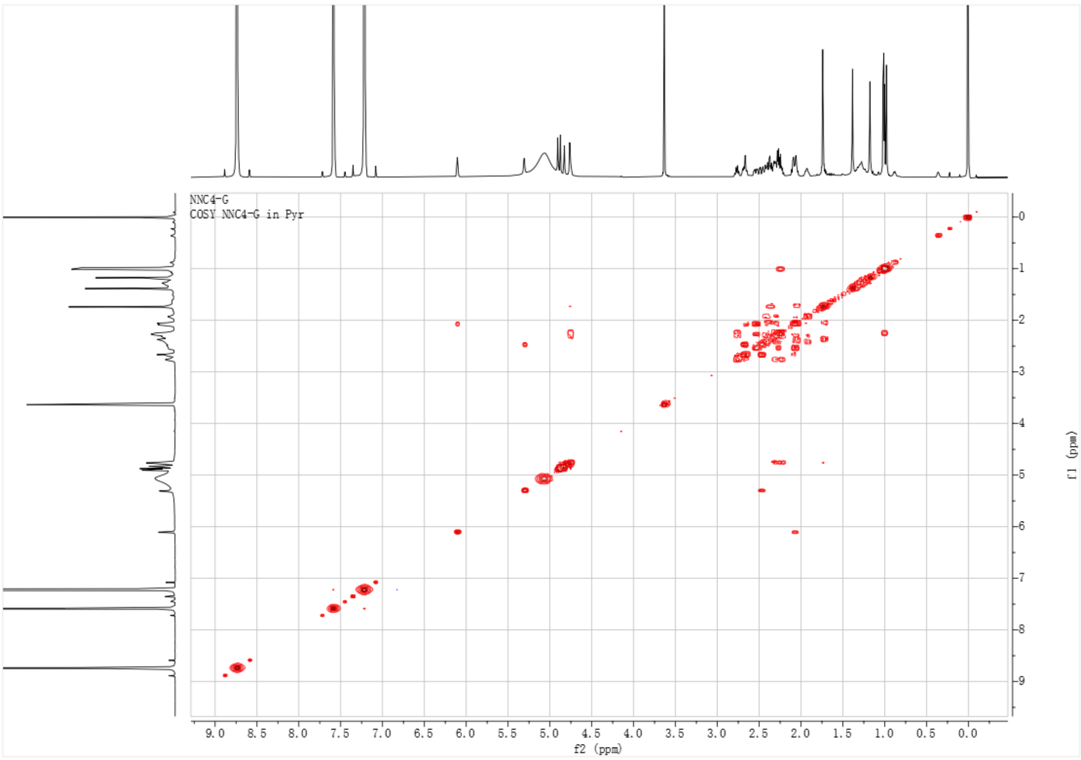

Figure S84. ^1H-^1H COSY spectrum (600 MHz, C_5D_5N) of compound **11**

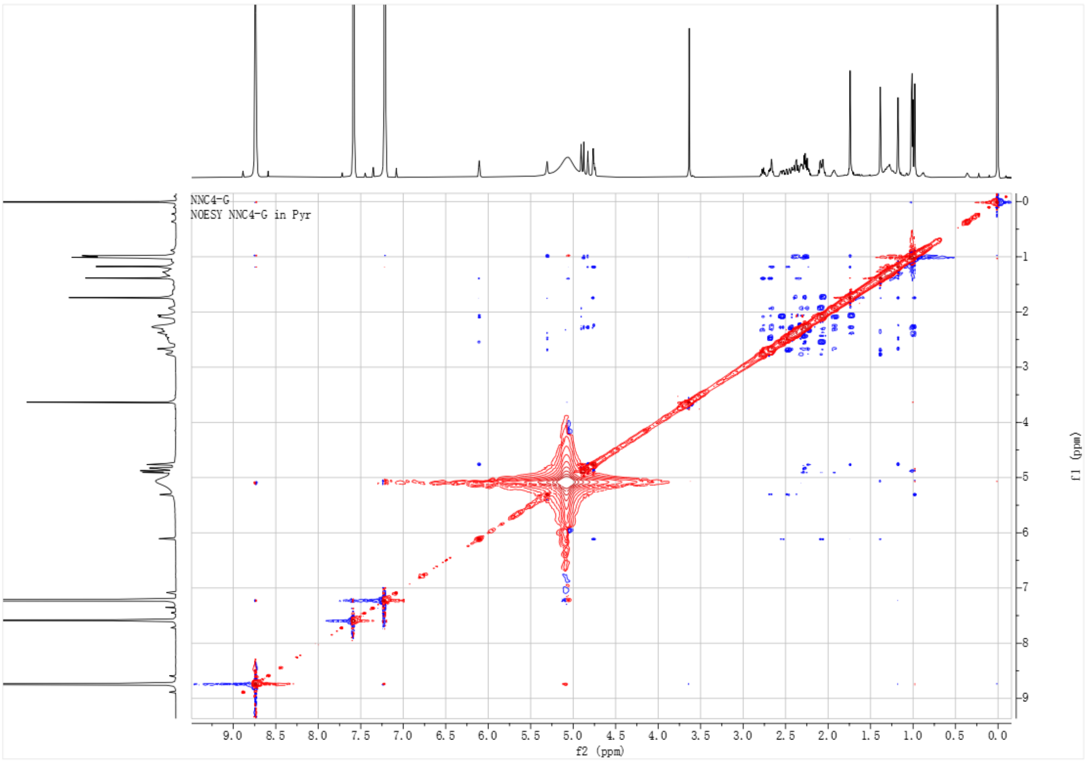

Figure S85. NOESY spectrum (600 MHz, C_5D_5N) of compound **11**

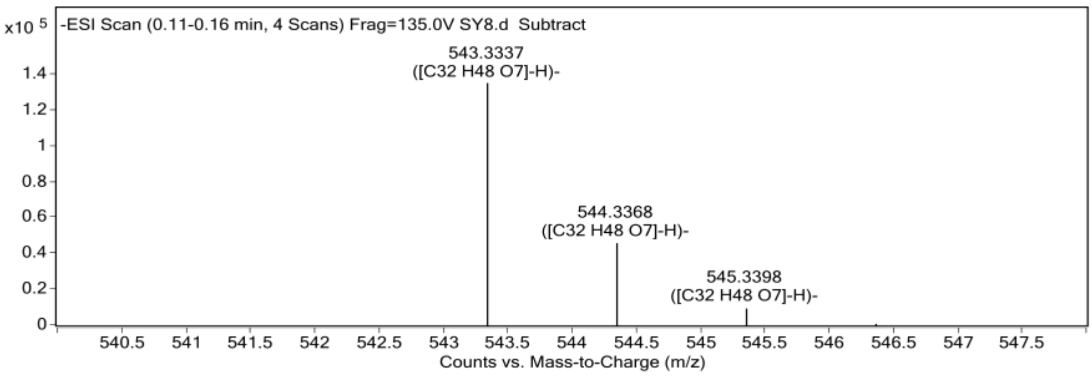

Figure S86. HRESIMS spectrum of compound **12**

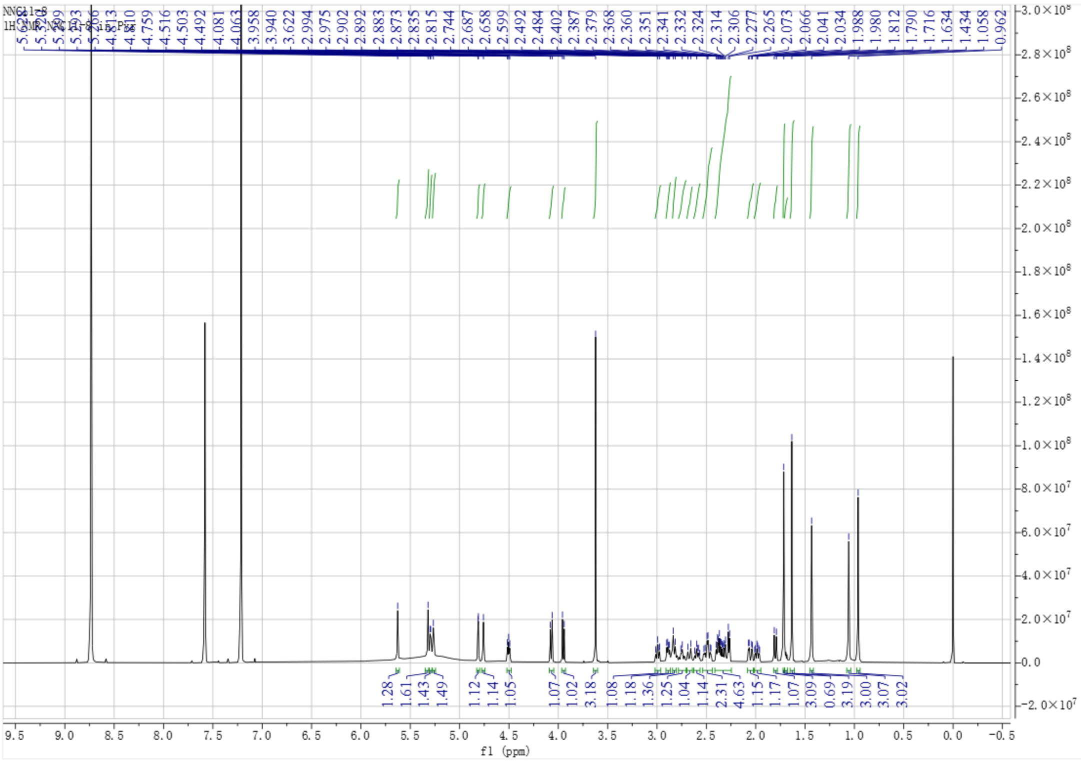

Figure S87. ^{1}H NMR spectrum (600 MHz, C_5D_5N) of compound **12**

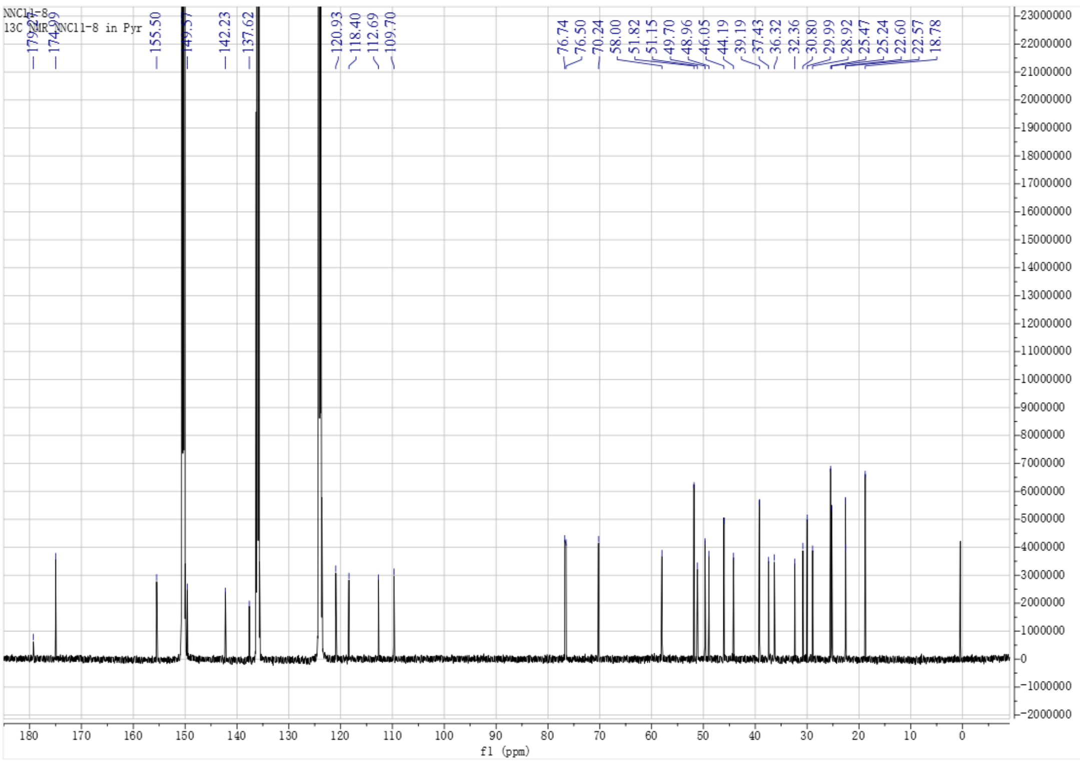

Figure S88. ^{13}C NMR spectrum (150 MHz, C_5D_5N) of compound **12**

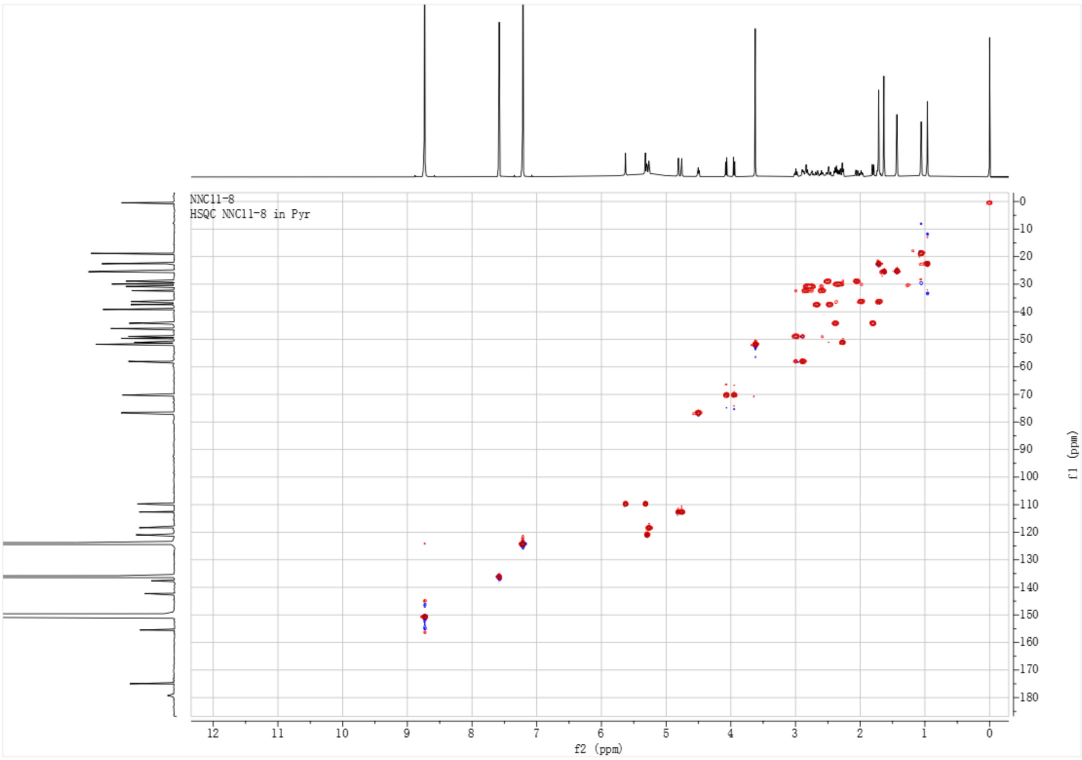

Figure S89. HSQC spectrum (600 MHz, C_5D_5N) of compound **12**

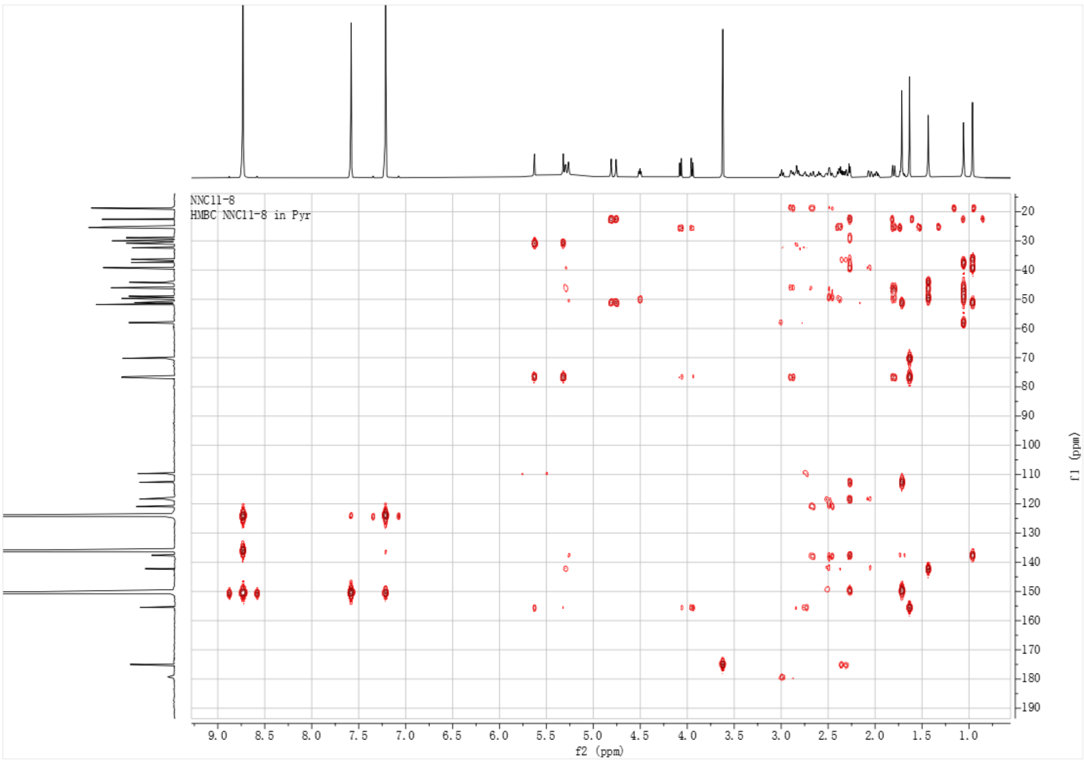

Figure S90. HMBC spectrum (600 MHz, C_5D_5N) of compound **12**

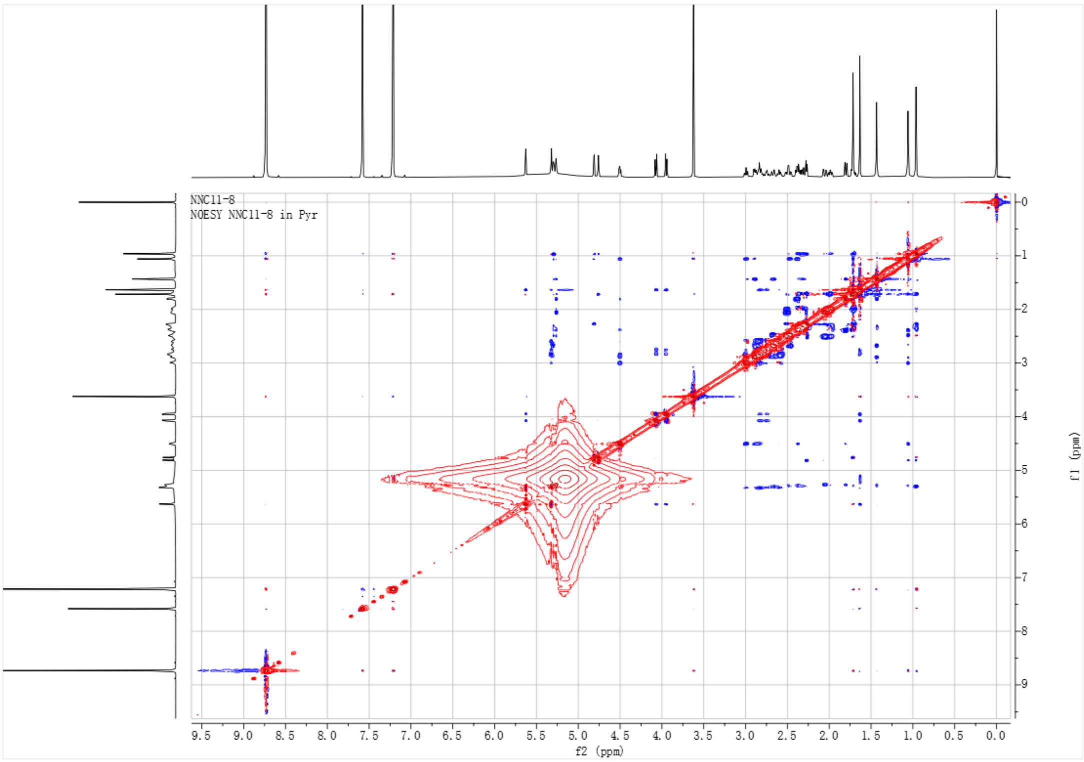

Figure S91. NOESY spectrum (600 MHz, C_5D_5N) of compound **12**

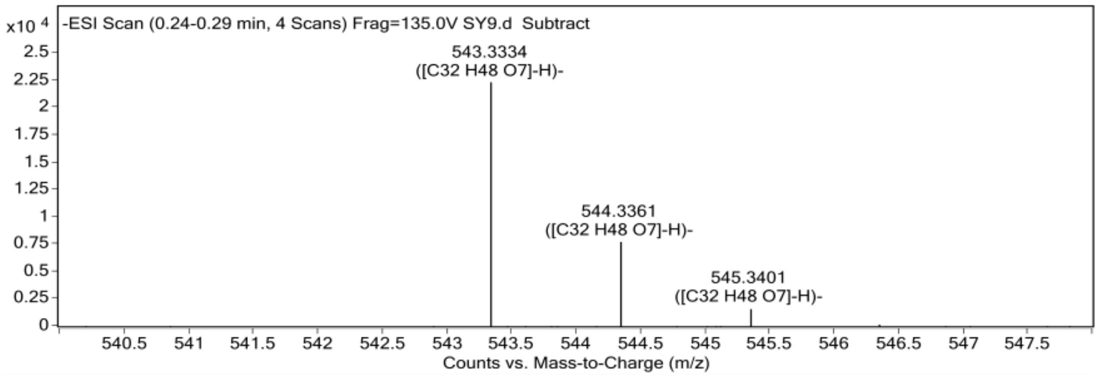

Figure S92. HRESIMS spectrum of compound **13**

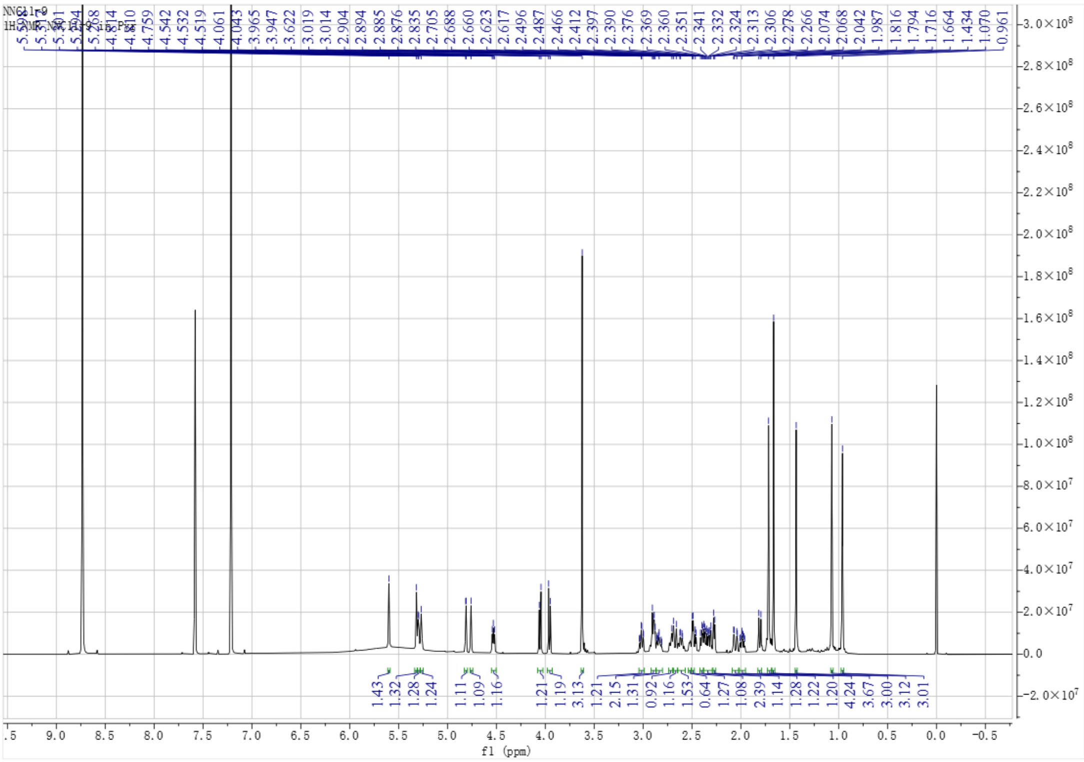

Figure S93. ^{1}H NMR spectrum (600 MHz, C_5D_5N) of compound **13**

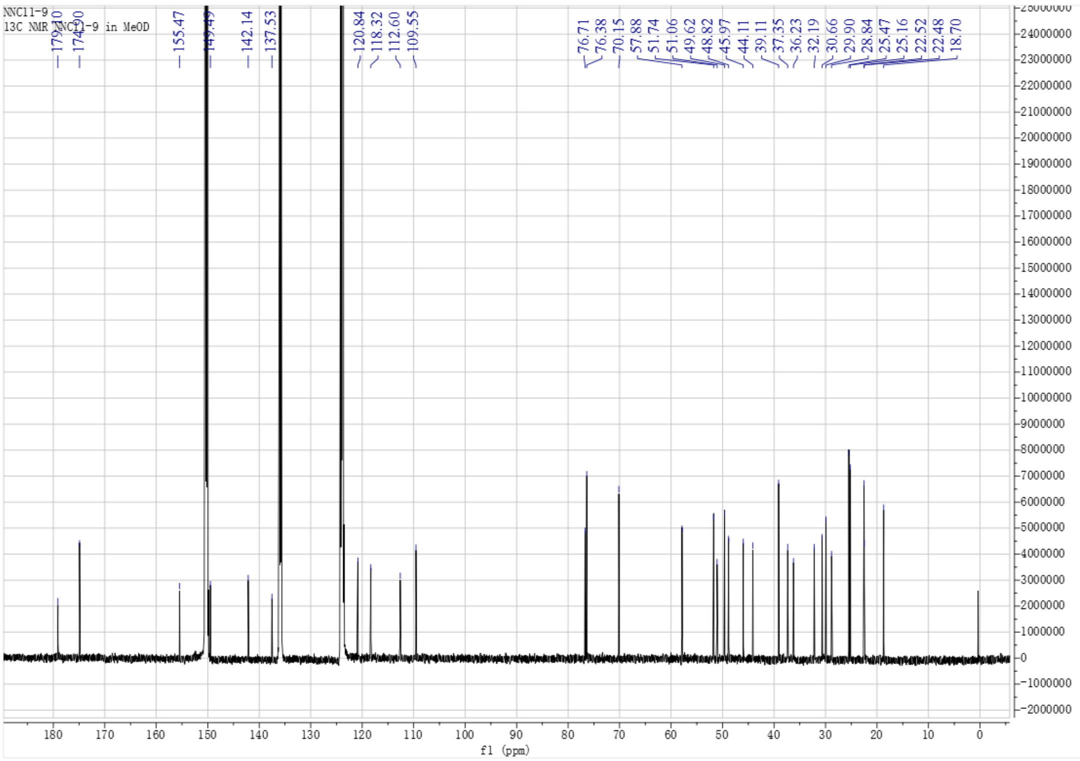

Figure S94. ^{13}C NMR spectrum (150 MHz, C_5D_5N) of compound **13**

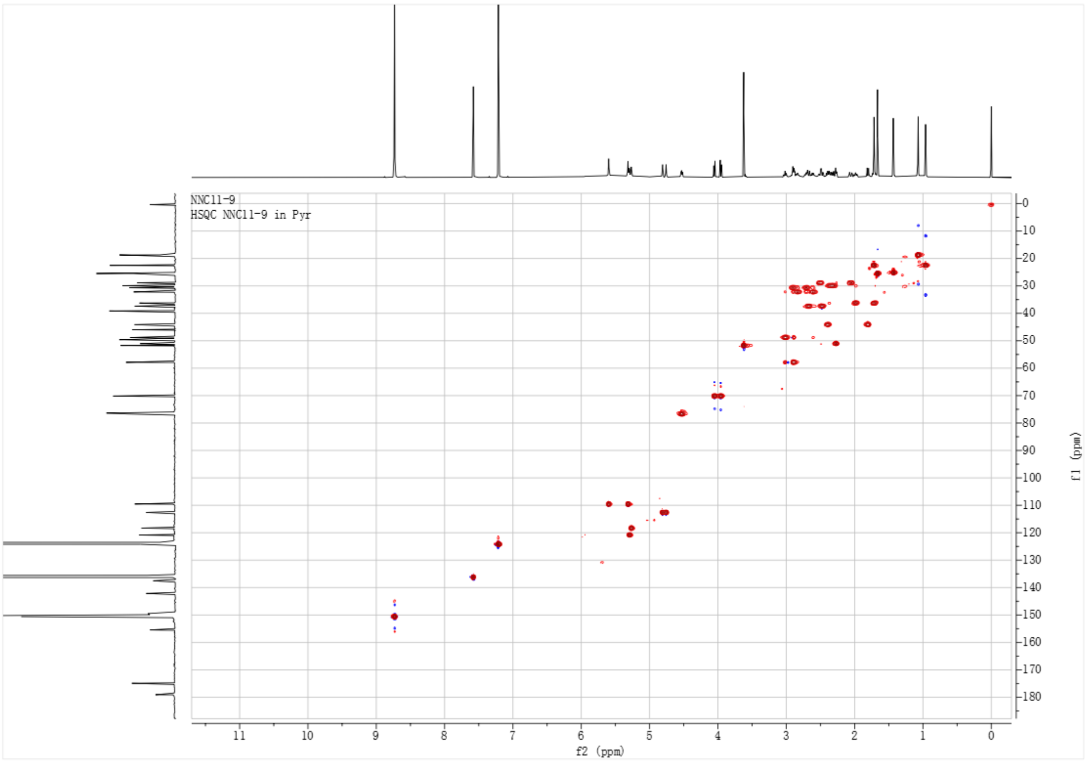

Figure S95. HSQC spectrum (600 MHz, C_5D_5N) of compound **13**

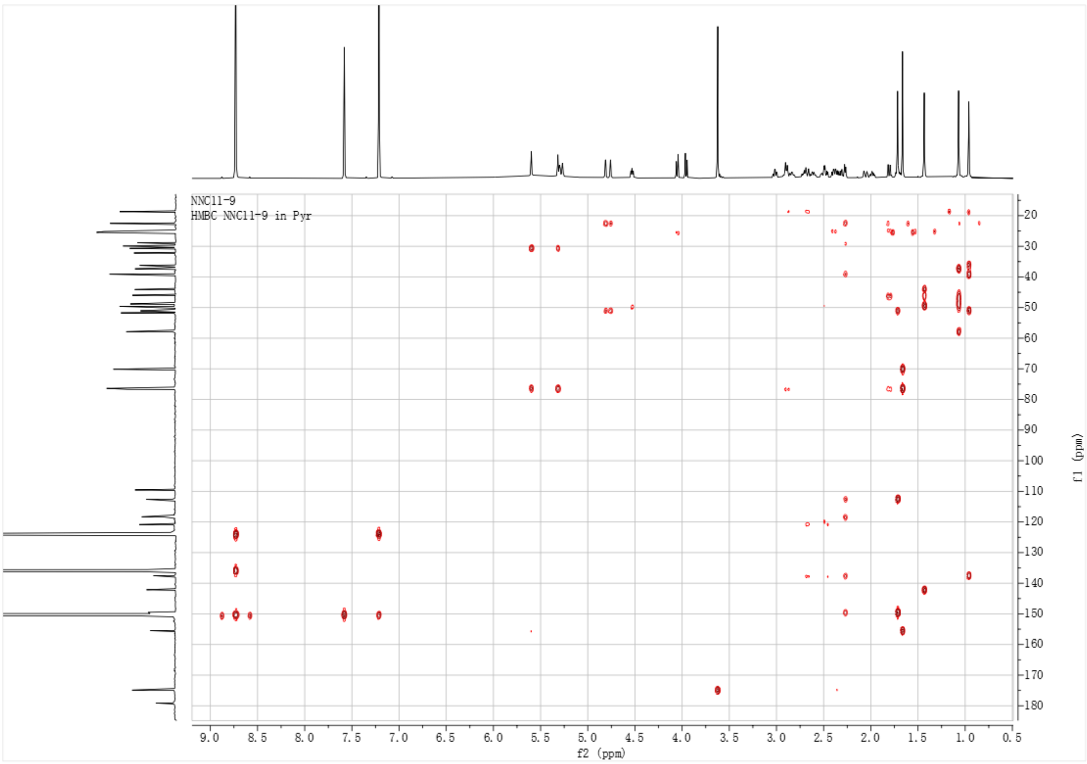

Figure S96. HMBC spectrum (600 MHz, C_5D_5N) of compound **13**

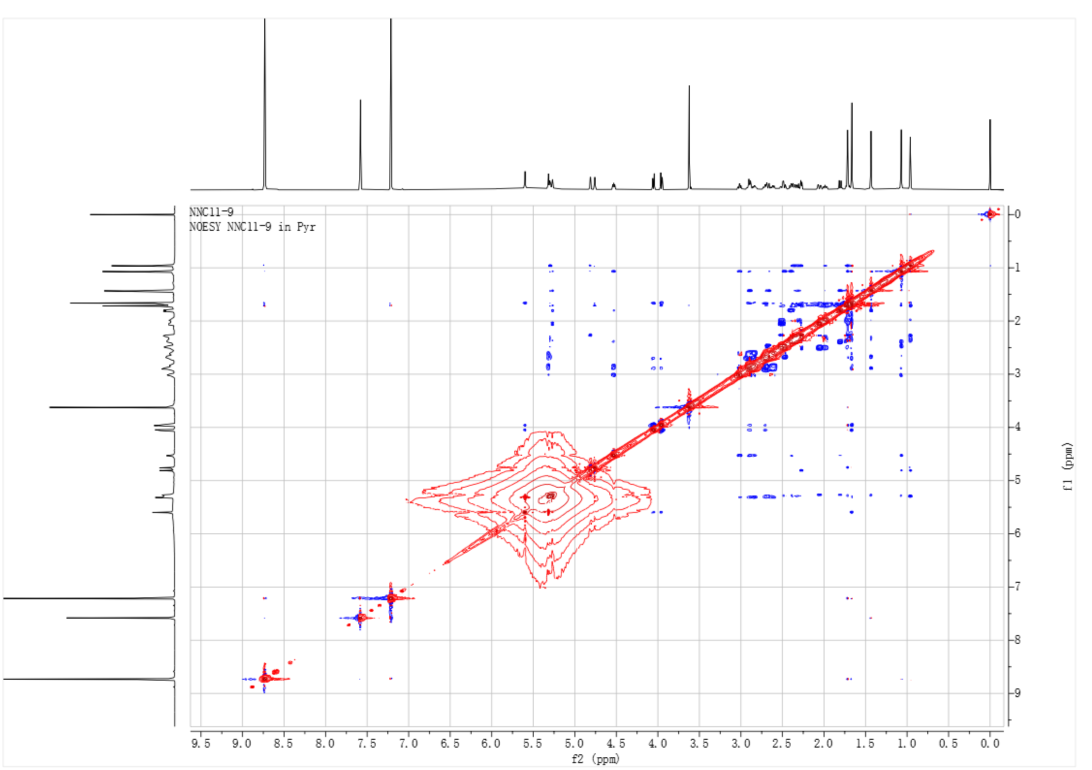

Figure S97. NOESY spectrum (600 MHz, C_5D_5N) of compound **13**

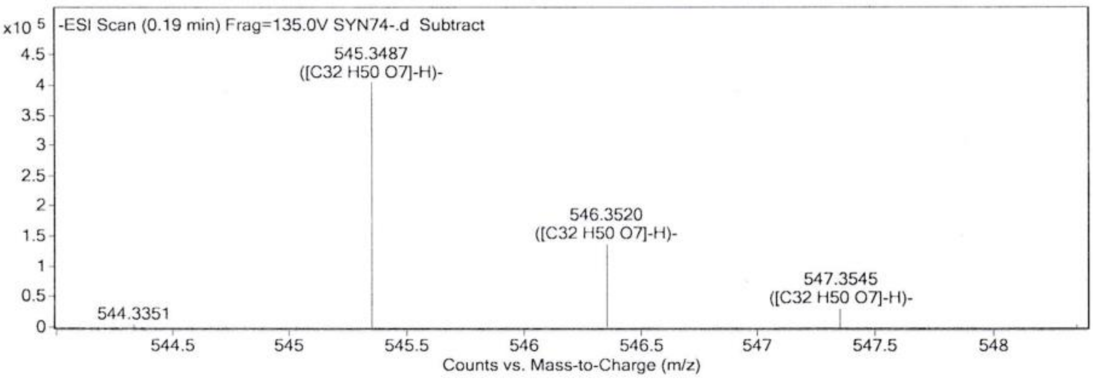

Figure S98. HRESIMS spectrum of compound **14**

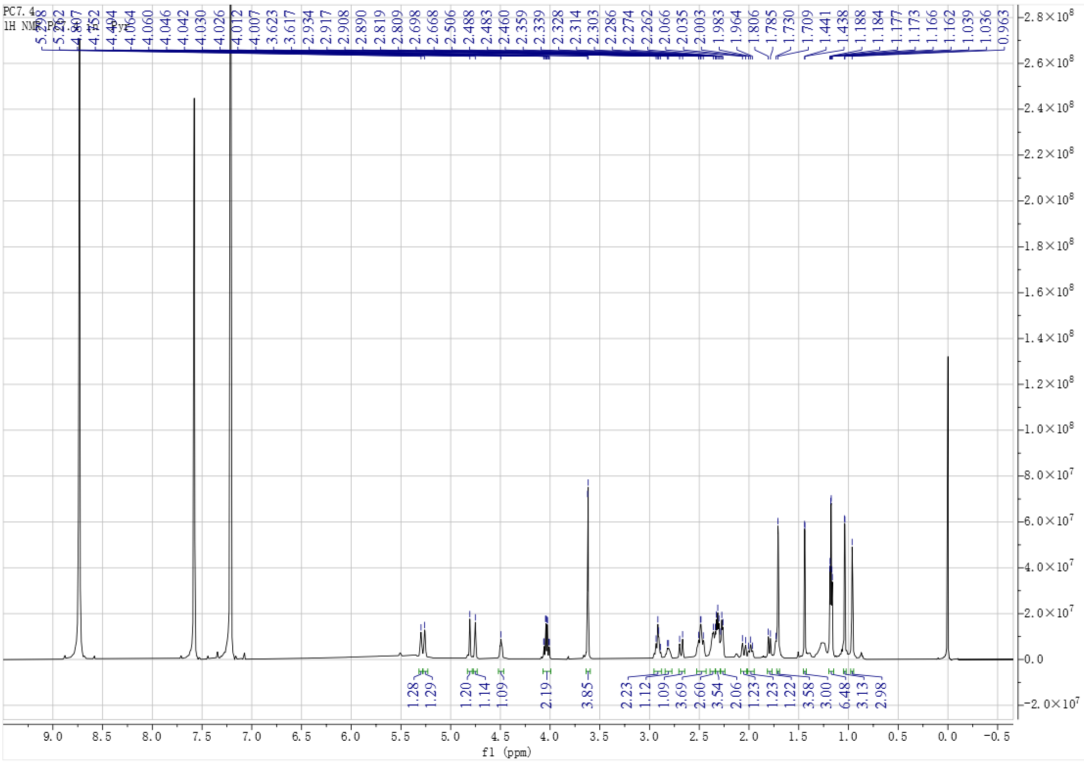

Figure S99. ^{1}H NMR spectrum (600 MHz, C_5D_5N) of compound **14**

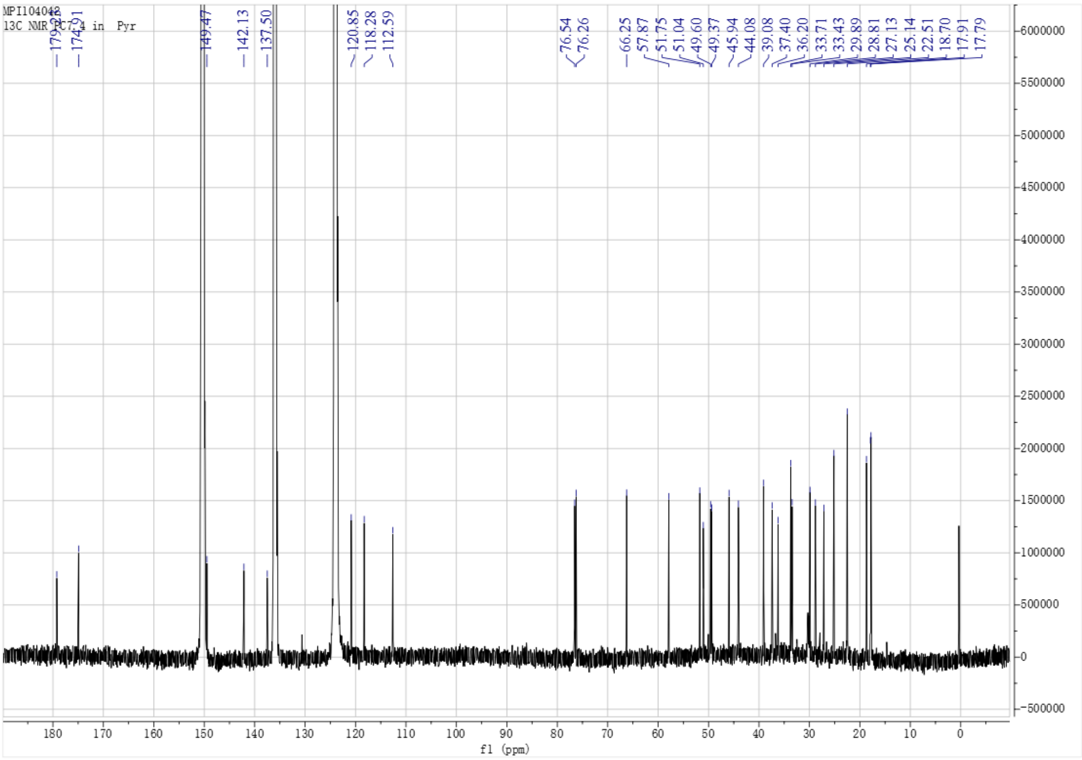

Figure S100. ^{13}C NMR spectrum (150 MHz, C_5D_5N) of compound **14**

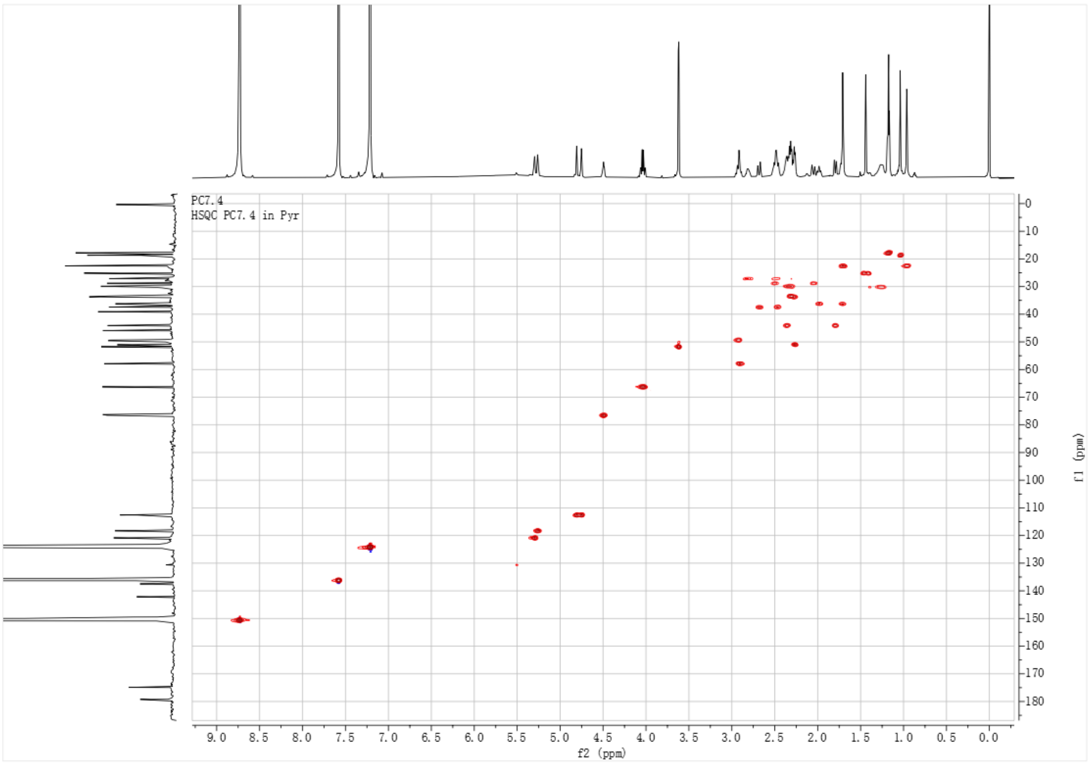

Figure S101. HSQC spectrum (600 MHz, C_5D_5N) of compound **14**

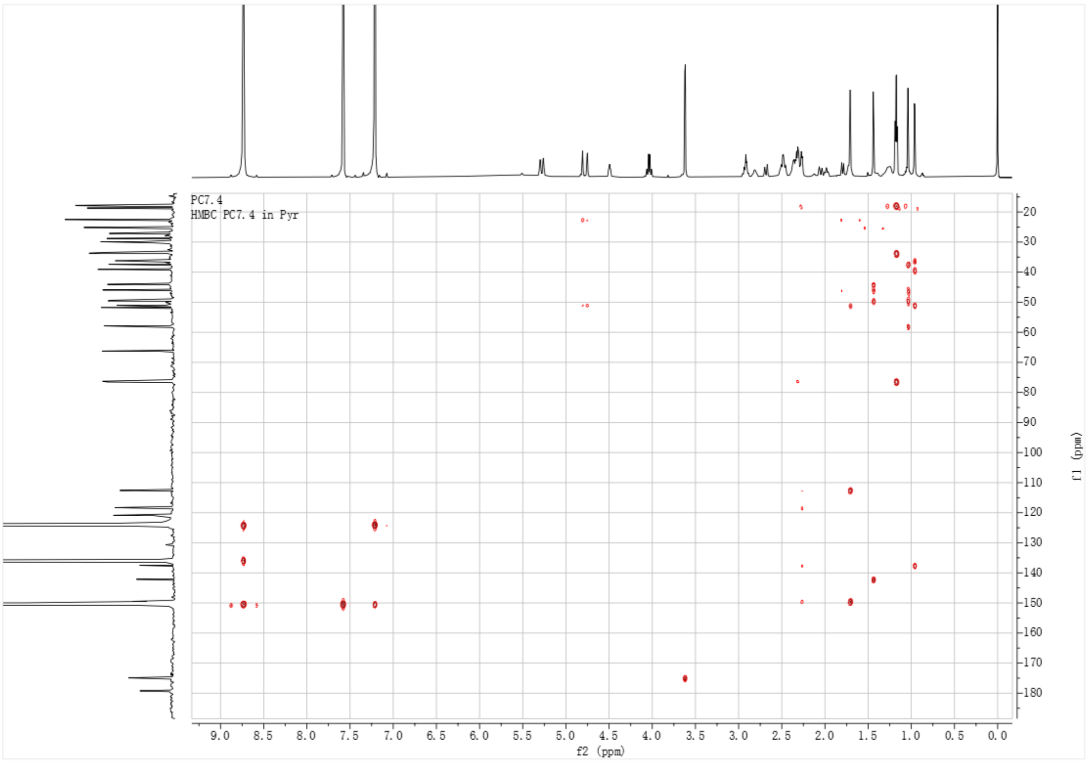

Figure S102. HMBC spectrum (600 MHz, C_5D_5N) of compound **14**

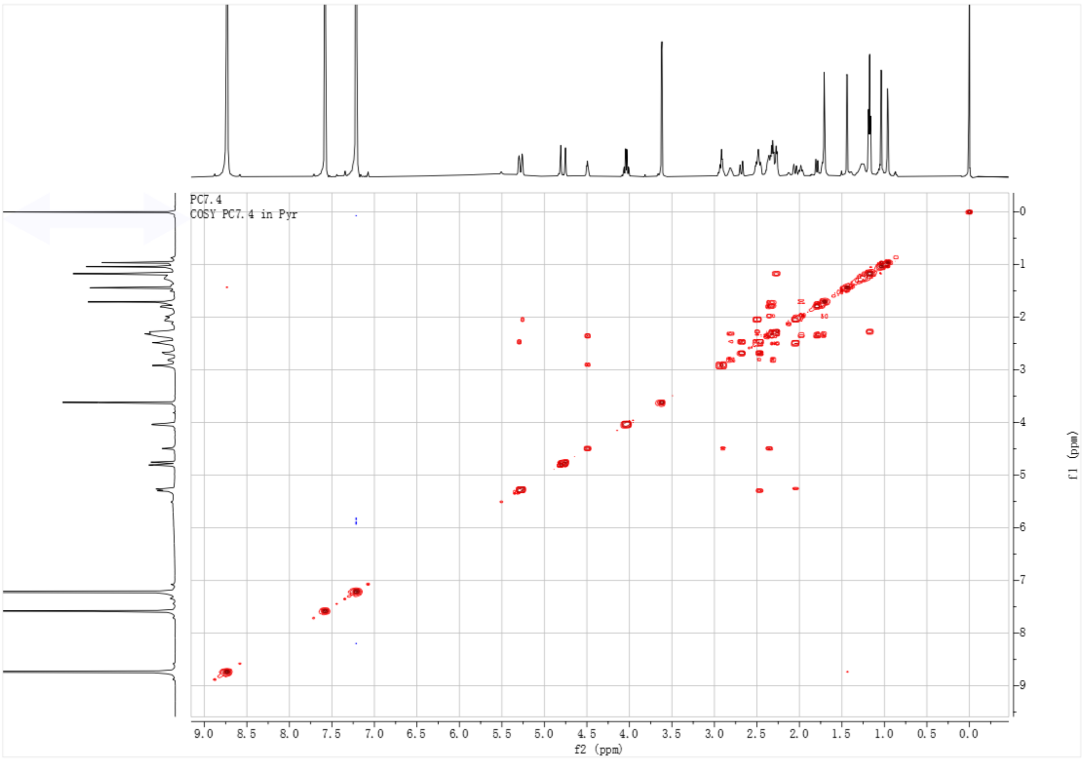

Figure S103. ^{1}H-^{1}H COSY spectrum (600 MHz, C_5D_5N) of compound **14**

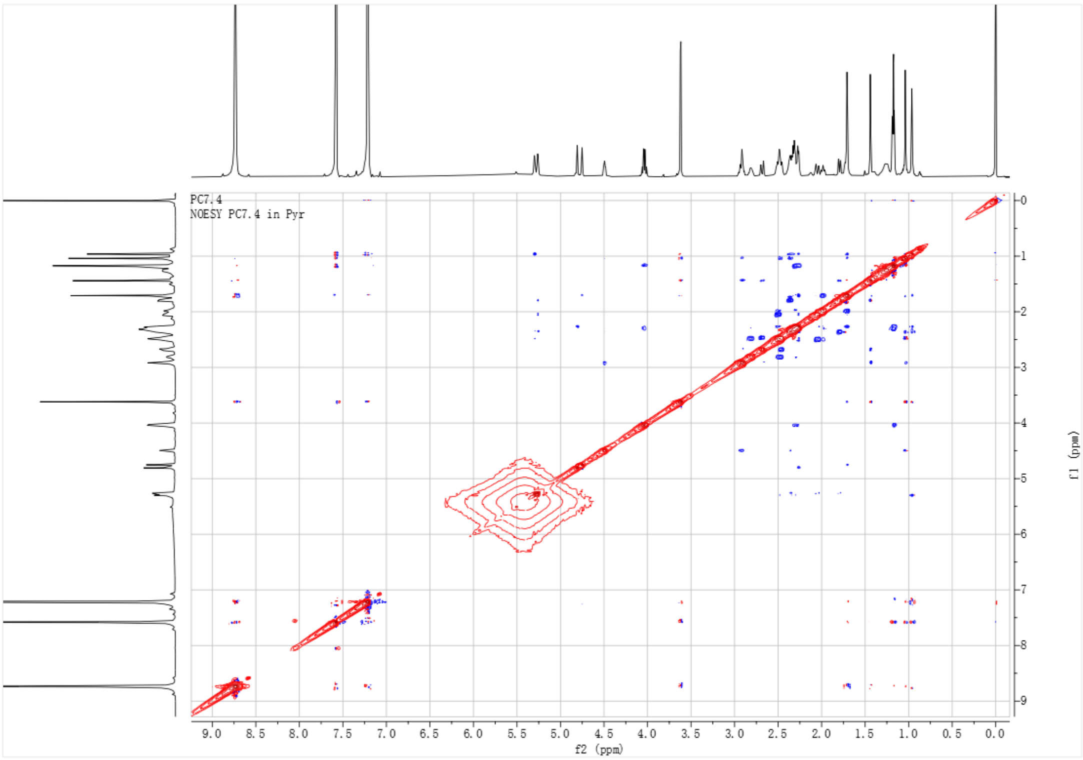

Figure S104. NOESY spectrum (600 MHz, C_5D_5N) of compound **14**

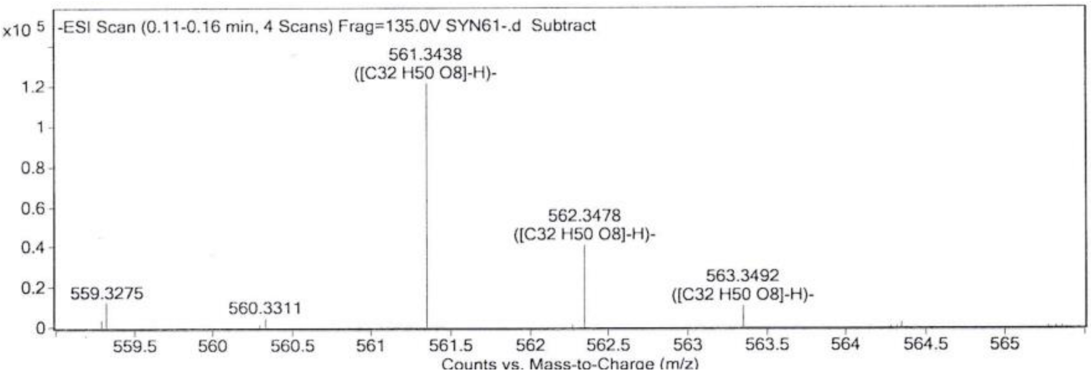

Figure S105. HRESIMS spectrum of compound **15**

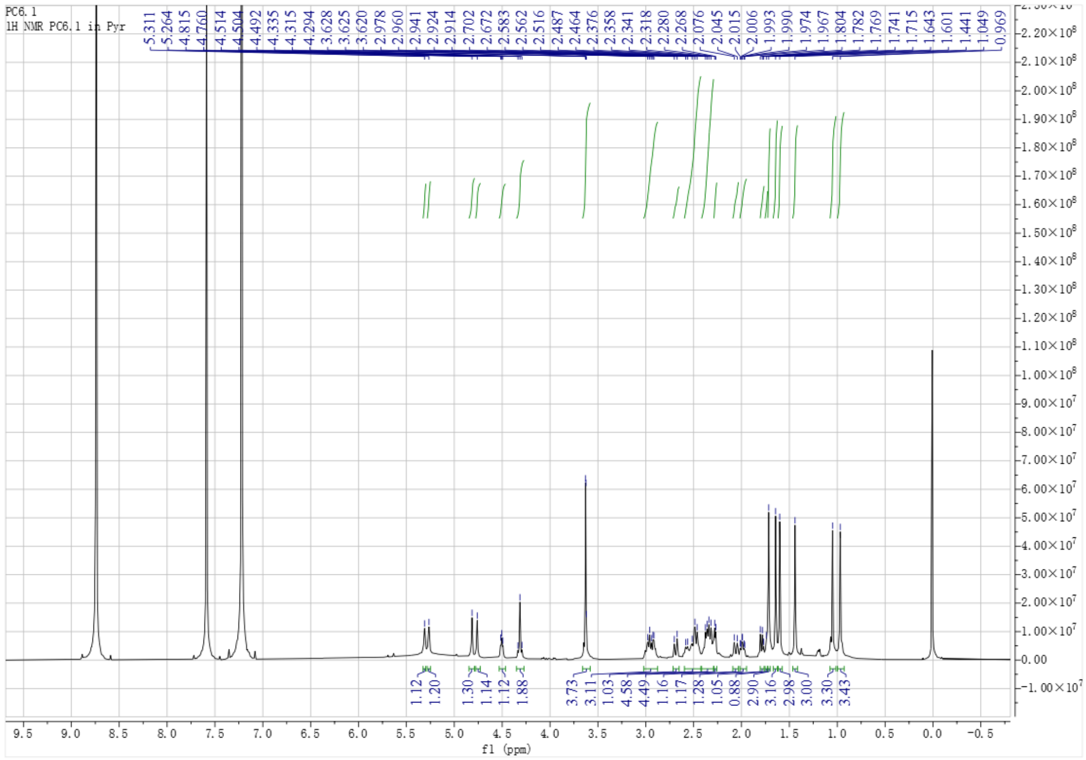

Figure S106. [1]H NMR spectrum (600 MHz, C_5D_5N) of compound **15**

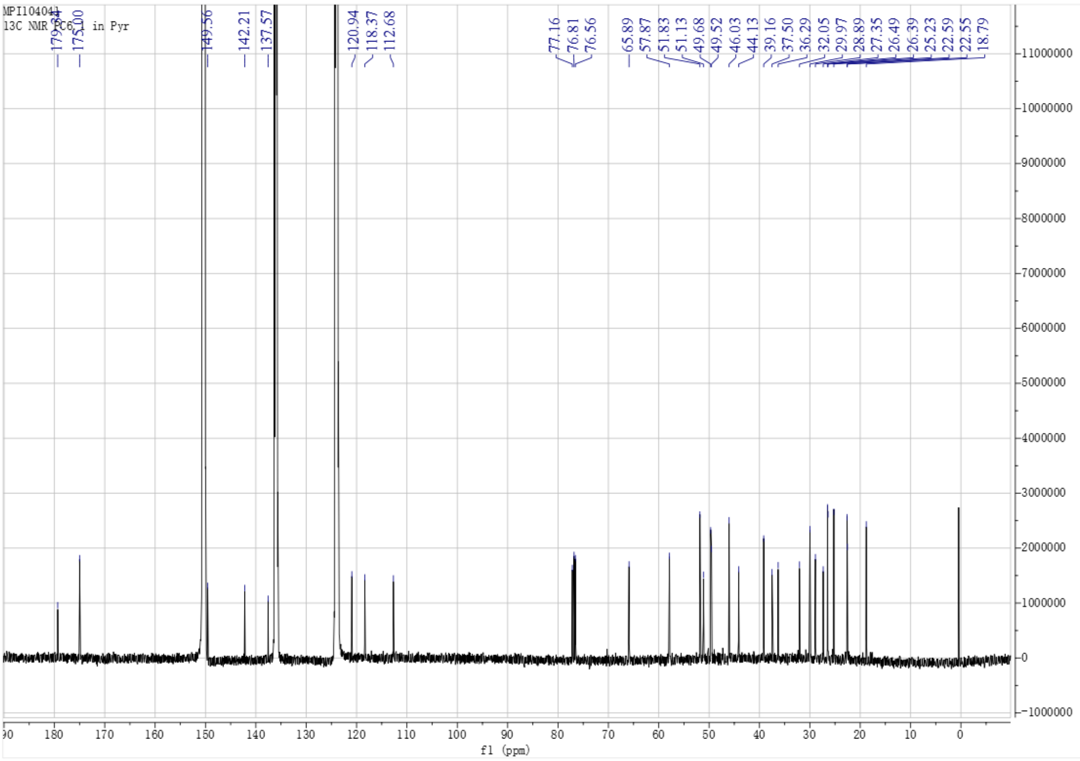

Figure S107. ^{13}C NMR spectrum (150 MHz, C_5D_5N) of compound **15**

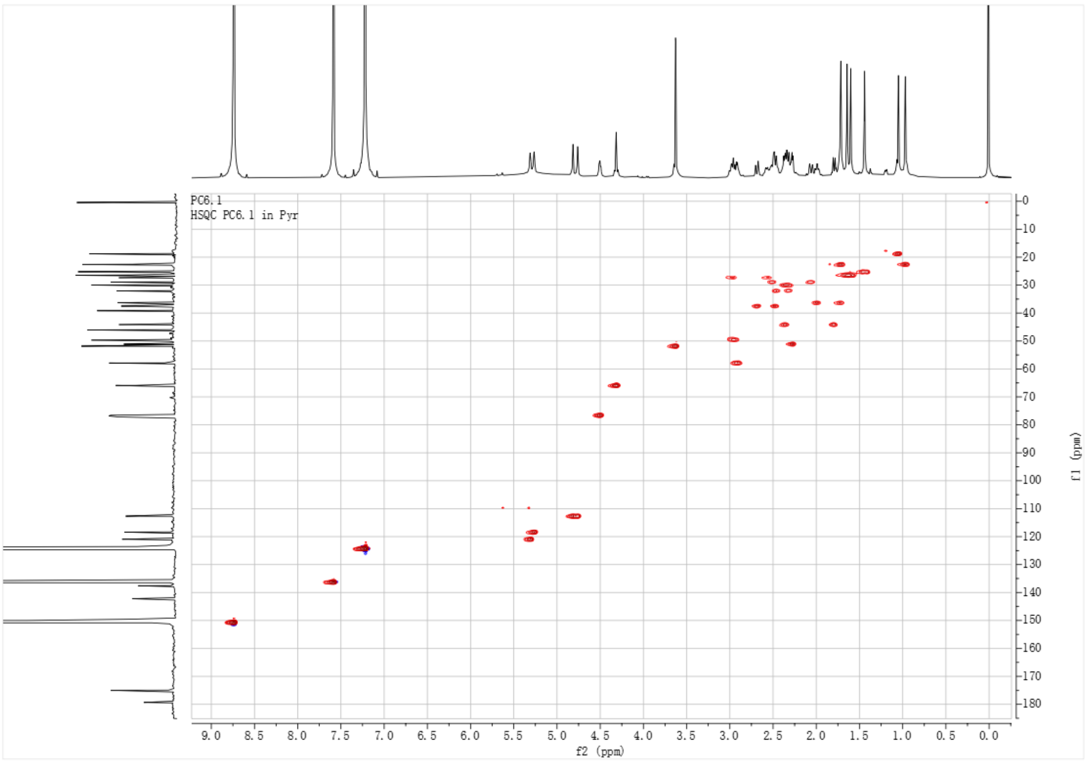

Figure S108. HSQC spectrum (600 MHz, C_5D_5N) of compound **15**

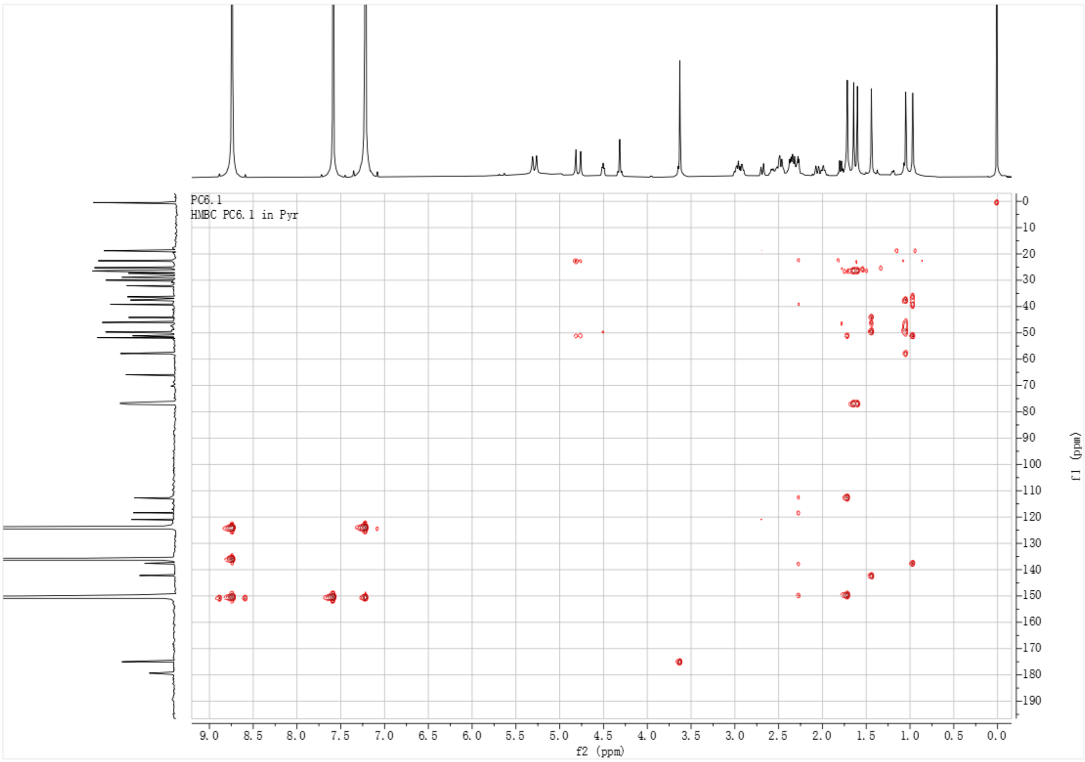

Figure S109. HMBC spectrum (600 MHz, C_5D_5N) of compound **15**

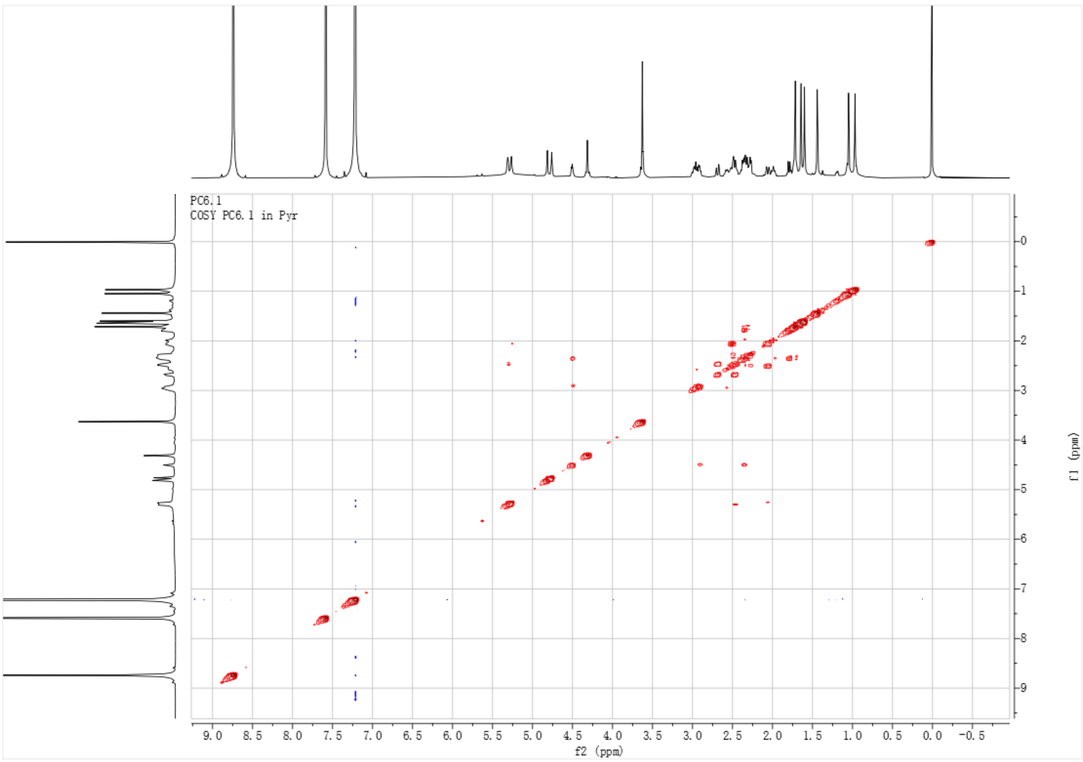

Figure S110. ^1H-^1H COSY spectrum (600 MHz, C_5D_5N) of compound **15**

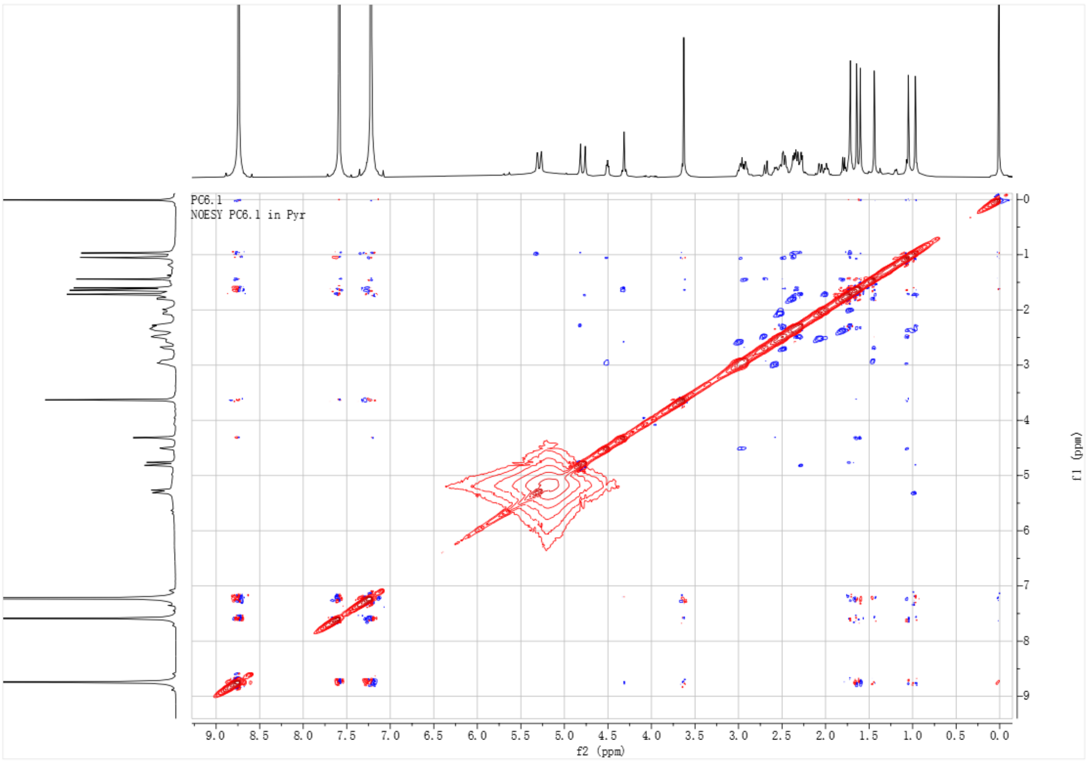

Figure S111. NOESY spectrum (600 MHz, C_5D_5N) of compound **15**

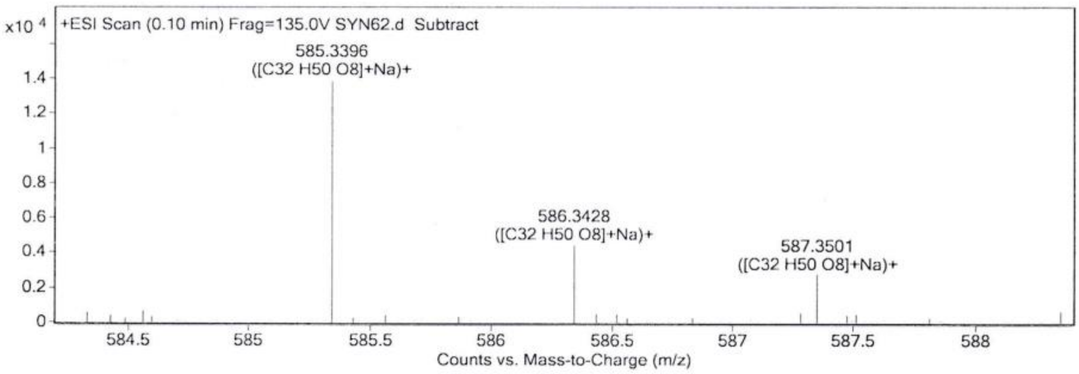

Figure S112. HRESIMS spectrum of compound **16**

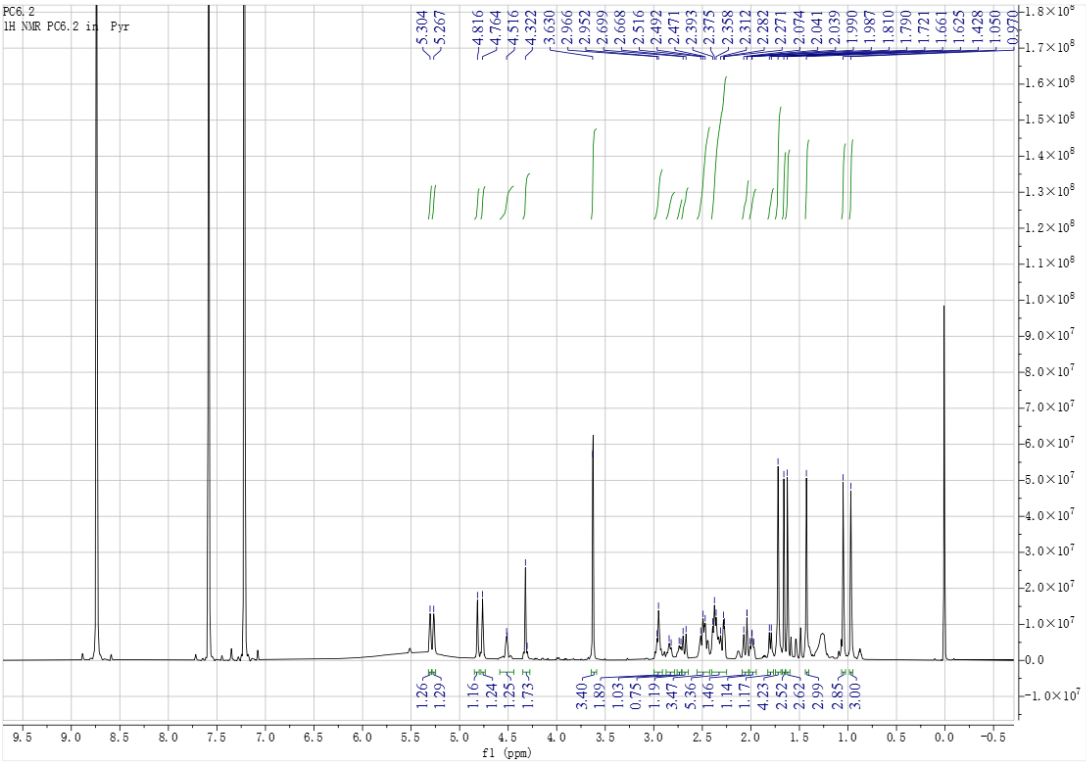

Figure S113. ^{1}H NMR spectrum (600 MHz, C_5D_5N) of compound **16**

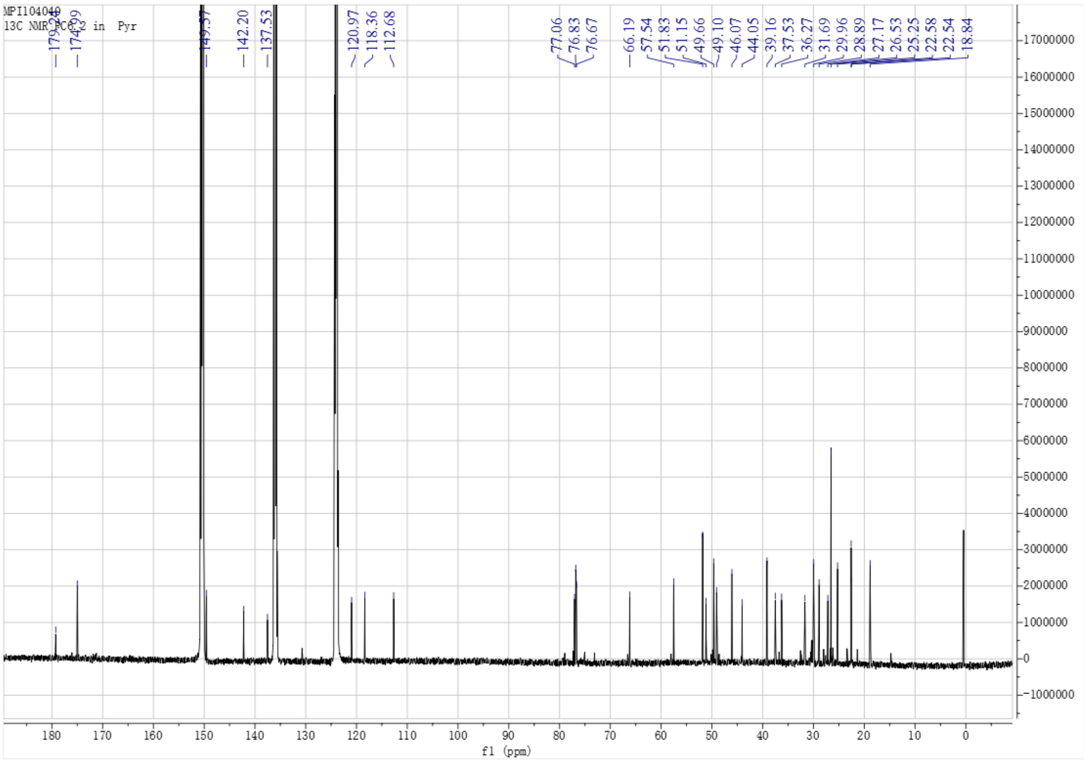

Figure S114. ^{13}C NMR spectrum (150 MHz, C_5D_5N) of compound **16**

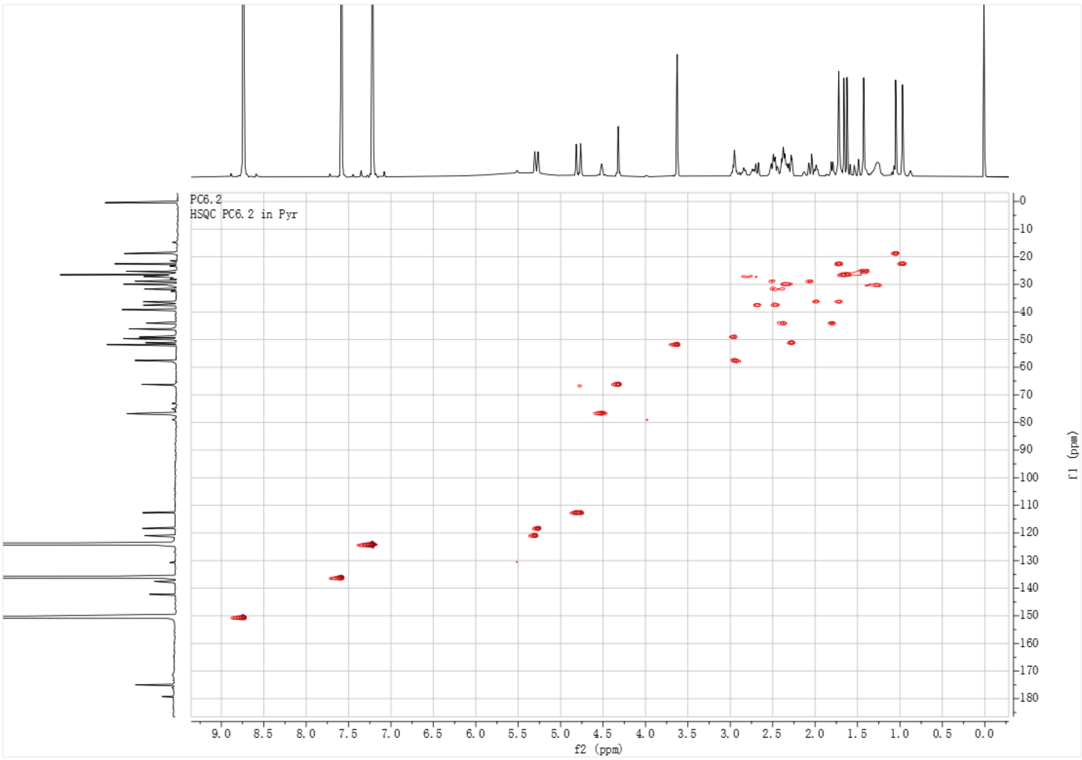

Figure S115. HSQC spectrum (600 MHz, C_5D_5N) of compound **16**

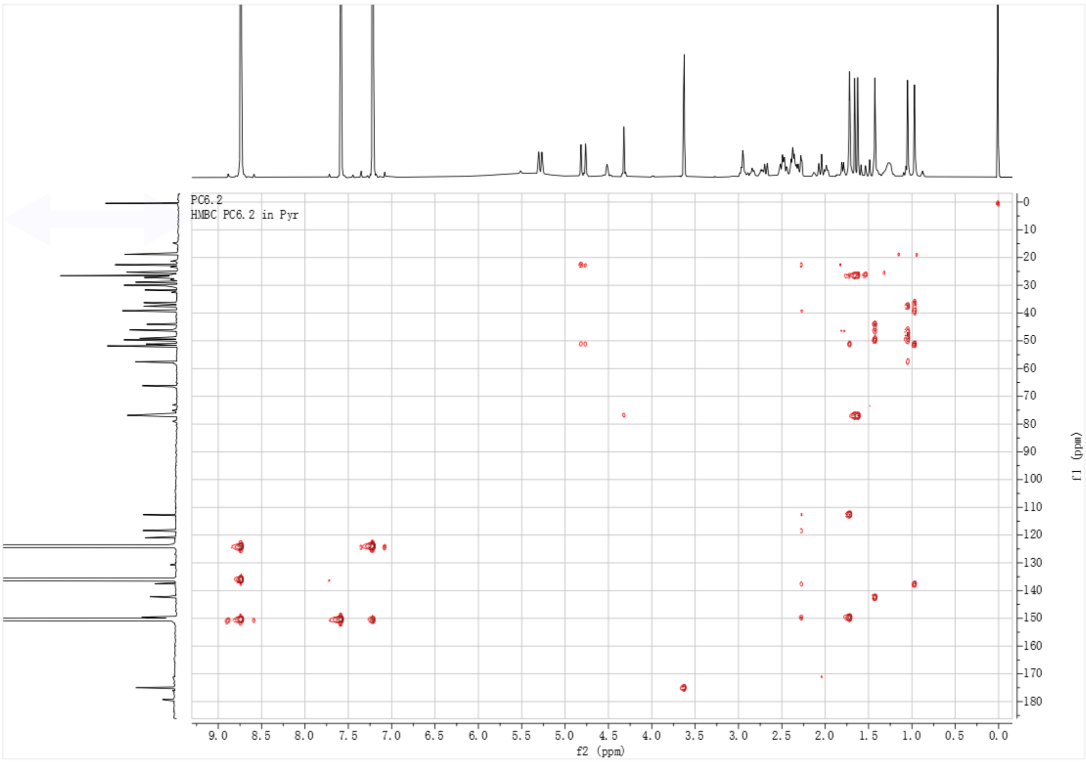

Figure S116. HMBC spectrum (600 MHz, C_5D_5N) of compound **16**

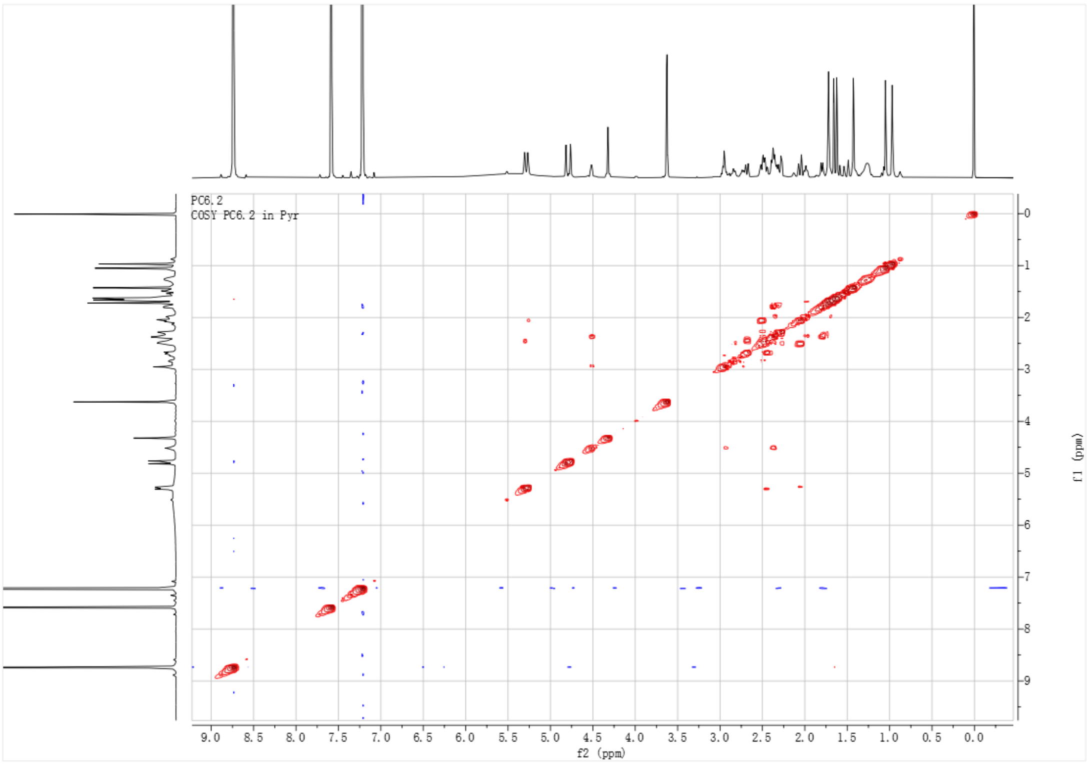

Figure S117. ^{1}H-^{1}H COSY spectrum (600 MHz, C_5D_5N) of compound **16**

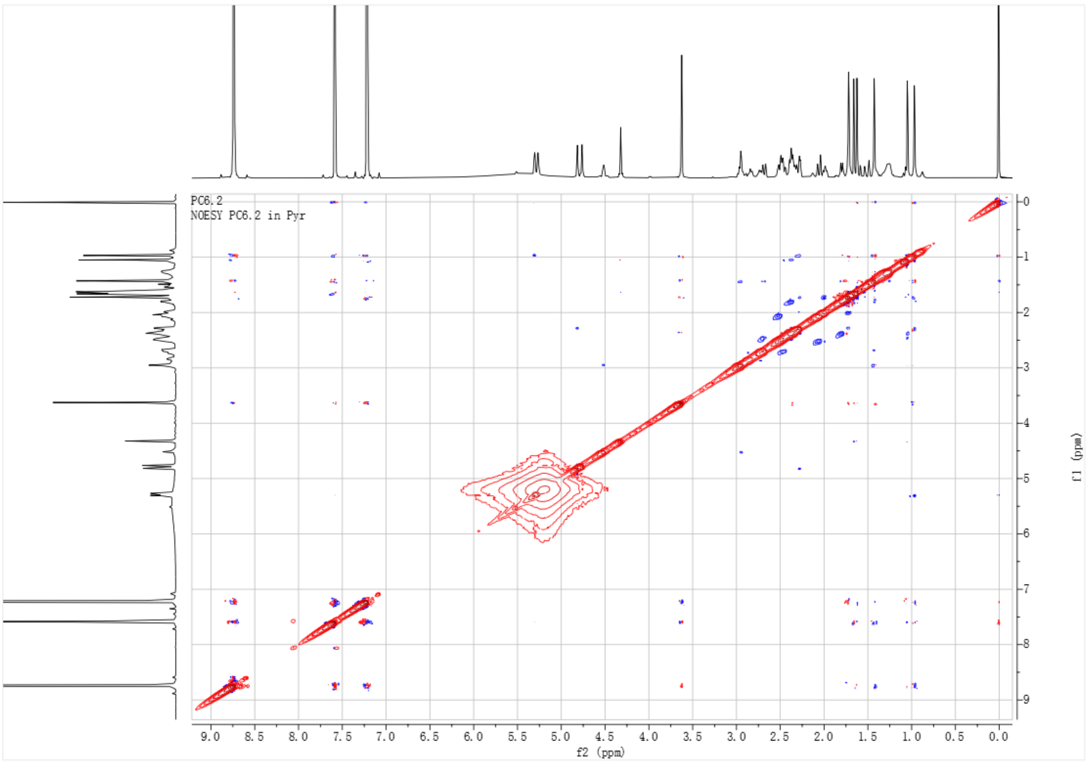

Figure S118. NOESY spectrum (600 MHz, C_5D_5N) of compound **16**

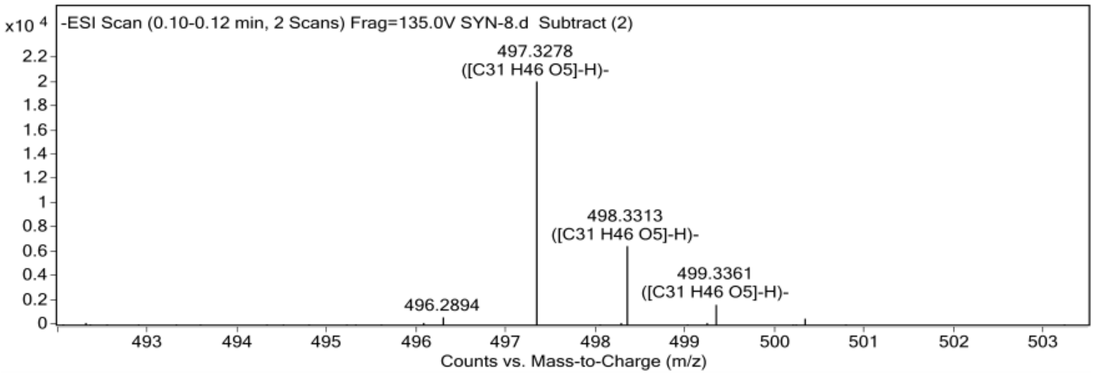

Figure S119. HRESIMS spectrum of compound **17**

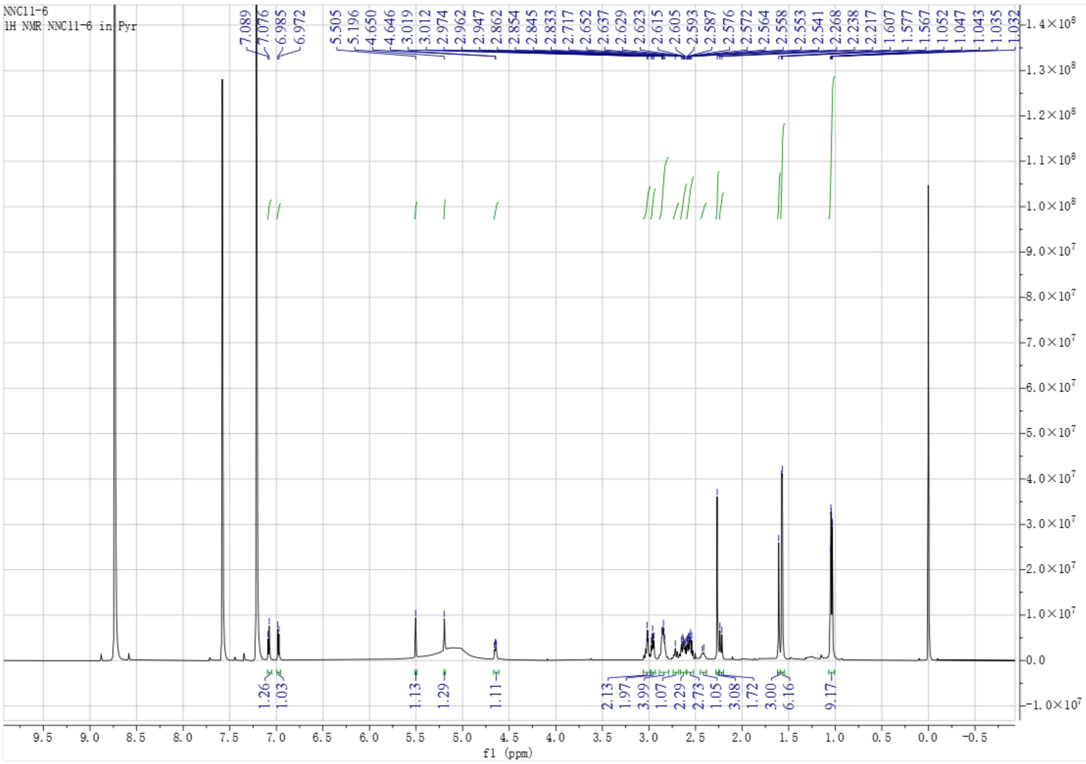

Figure S120. [1]H NMR spectrum (600 MHz, C_5D_5N) of compound **17**

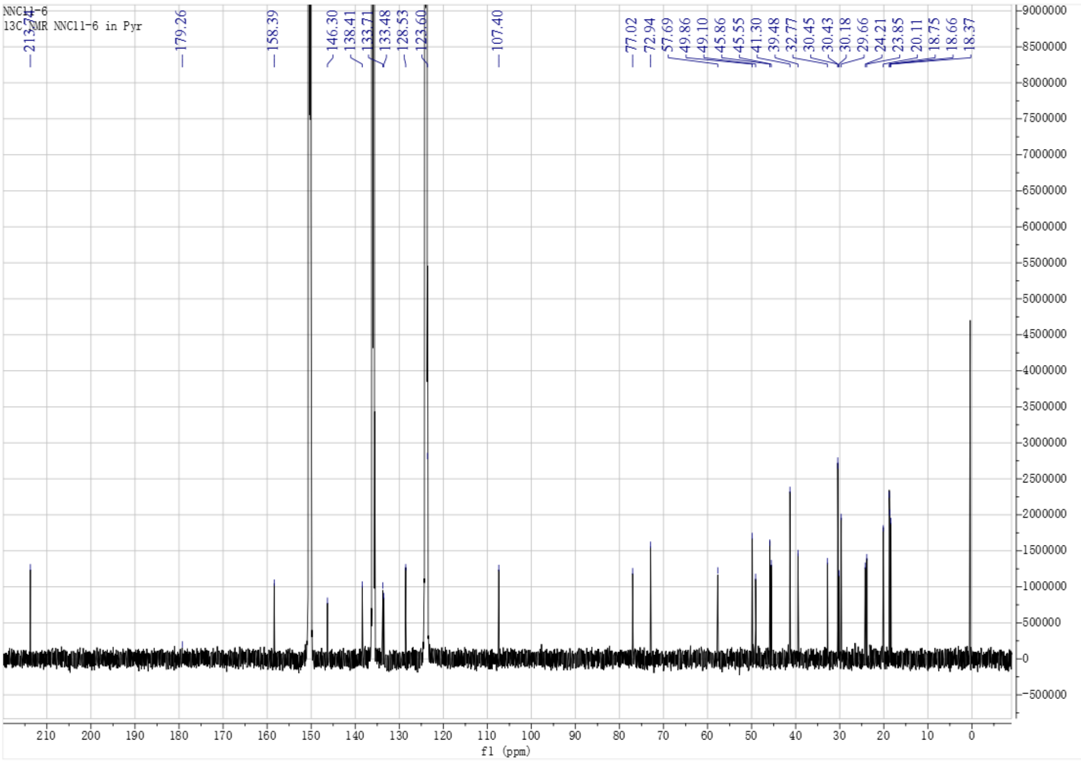

Figure S121. ^{13}C NMR spectrum (150 MHz, C_5D_5N) of compound **17**

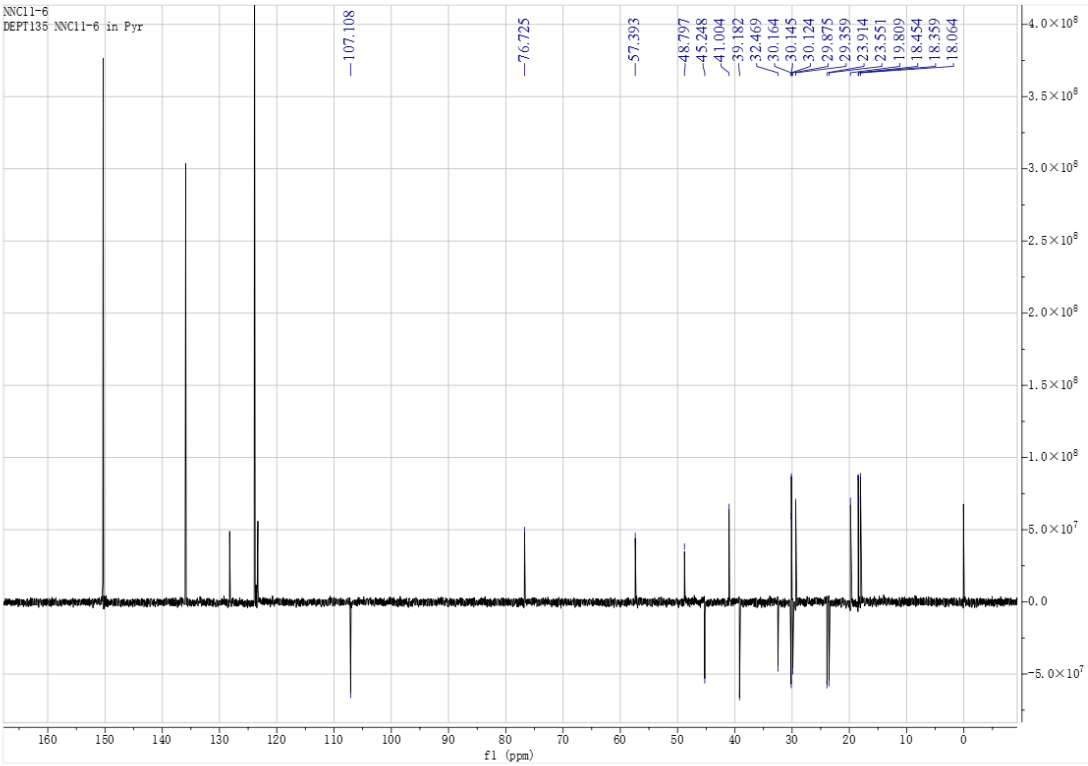

Figure S122. DEPT 135° spectrum (150 MHz, C_5D_5N) of compound **17**

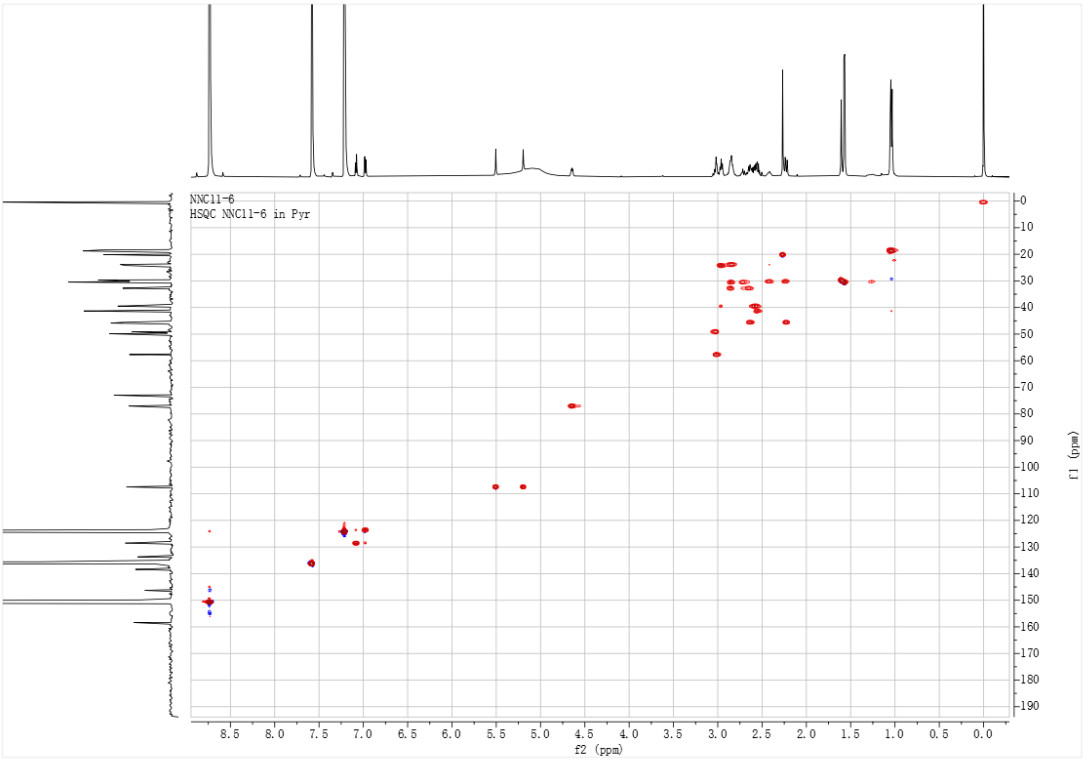

Figure S123. HSQC spectrum (600 MHz, C_5D_5N) of compound **17**

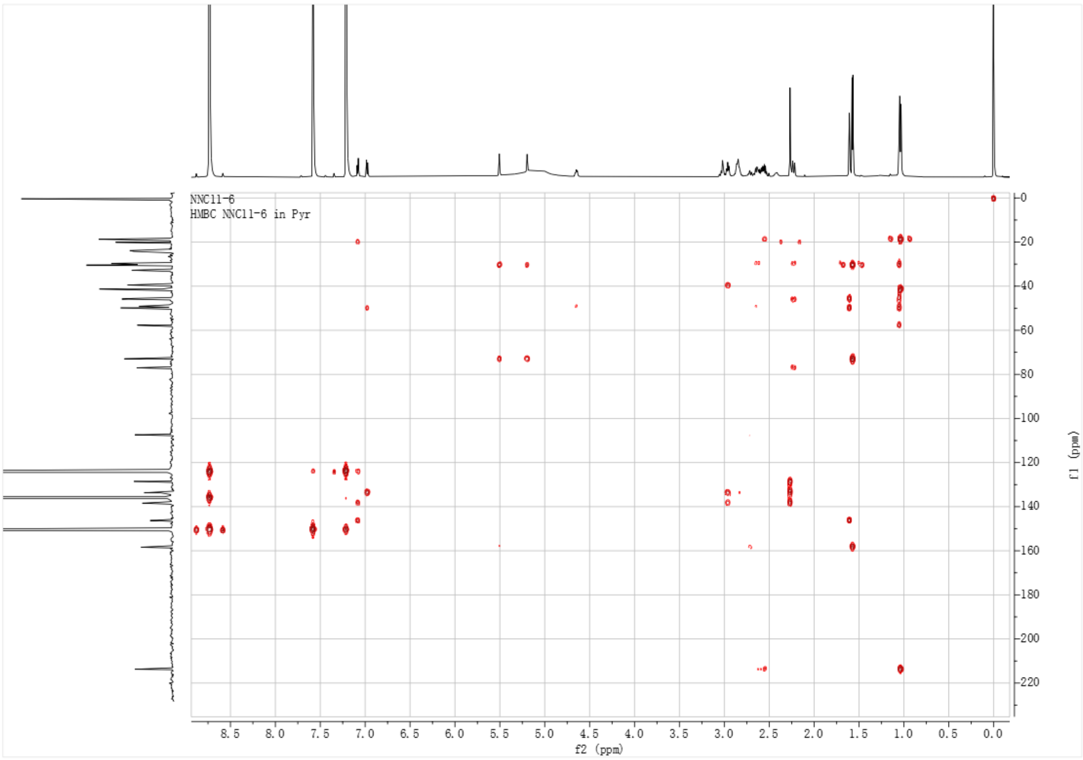

Figure S124. HMBC spectrum (600 MHz, C_5D_5N) of compound **17**

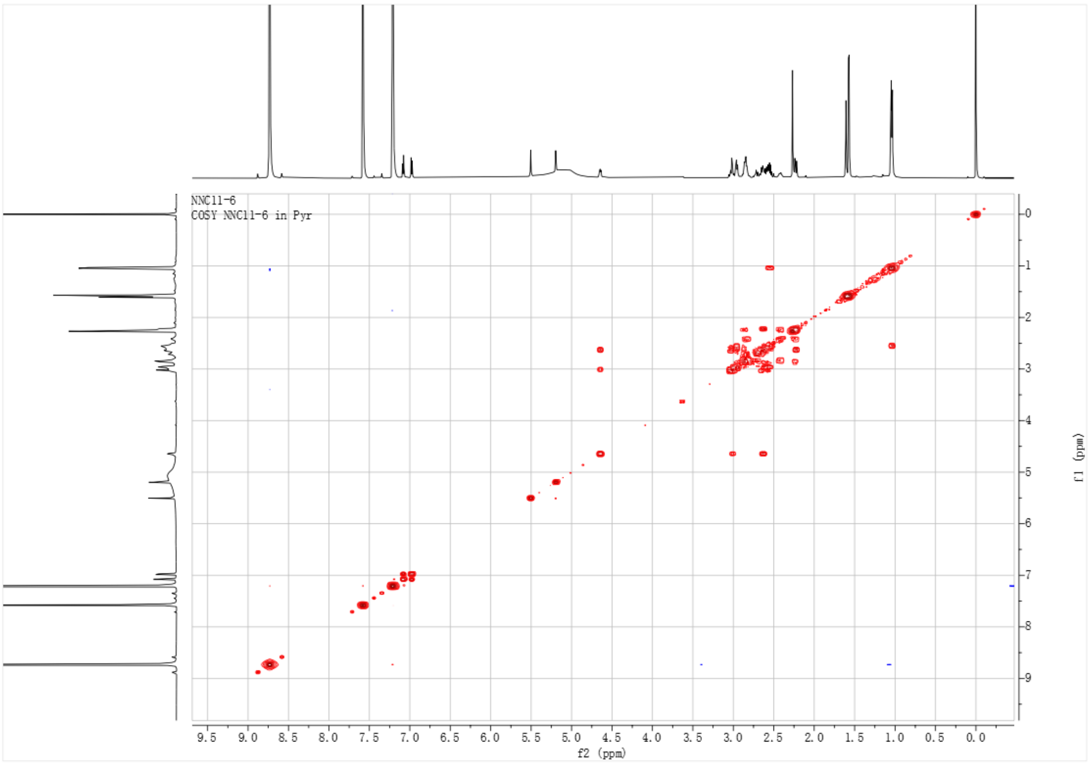

Figure S125. ^1H-^1H COSY spectrum (600 MHz, C_5D_5N) of compound **17**

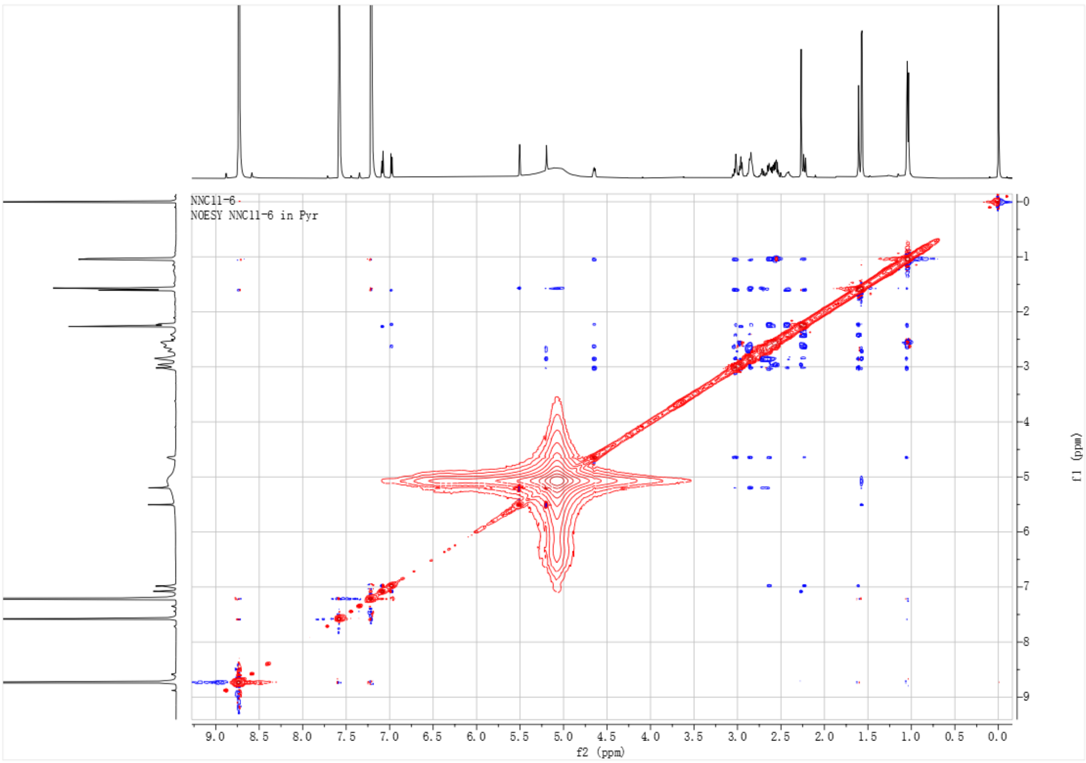

Figure S126. NOESY spectrum (600 MHz, C_5D_5N) of compound **17**

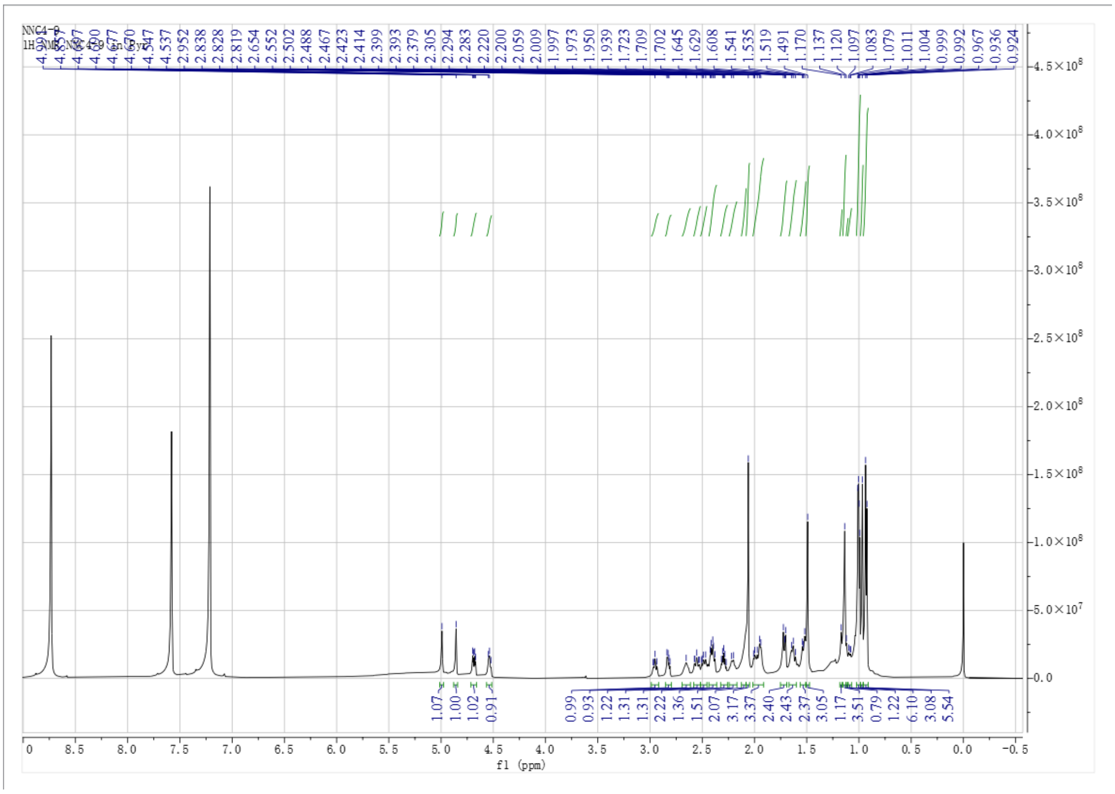

Figure S127. ^{1}H NMR spectrum (600 MHz, C_5D_5N) of compound **18**

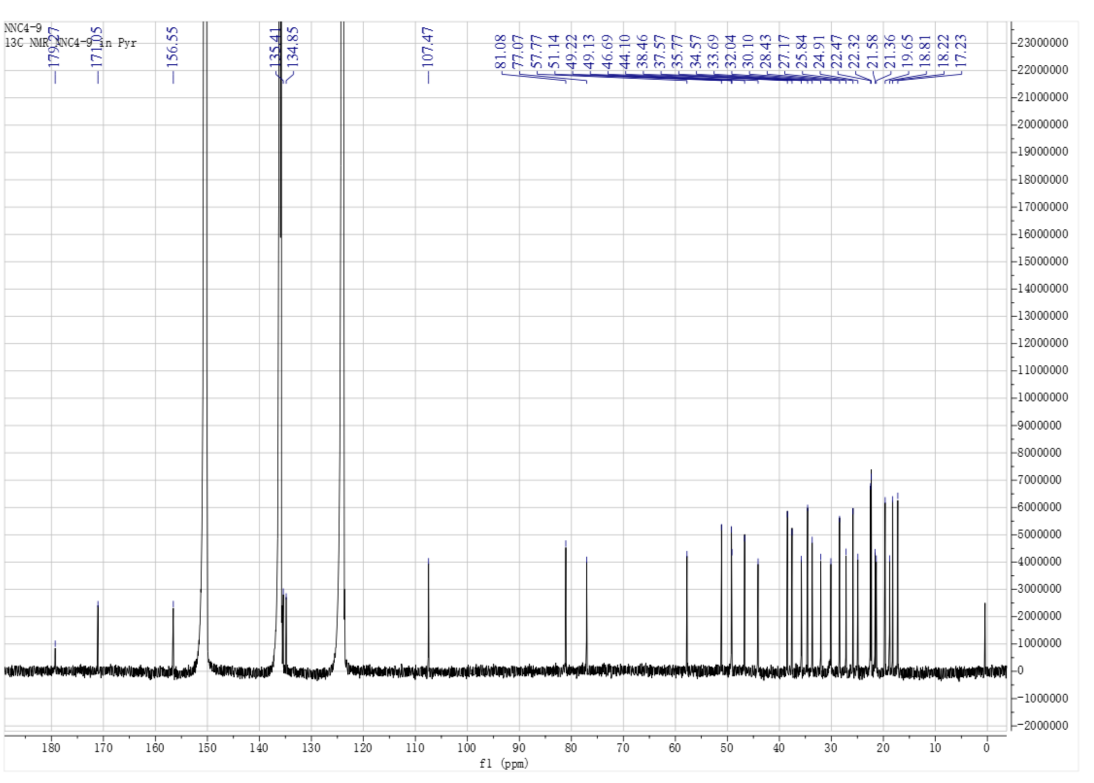

Figure S128. ^{13}C NMR spectrum (150 MHz, C_5D_5N) of compound **18**

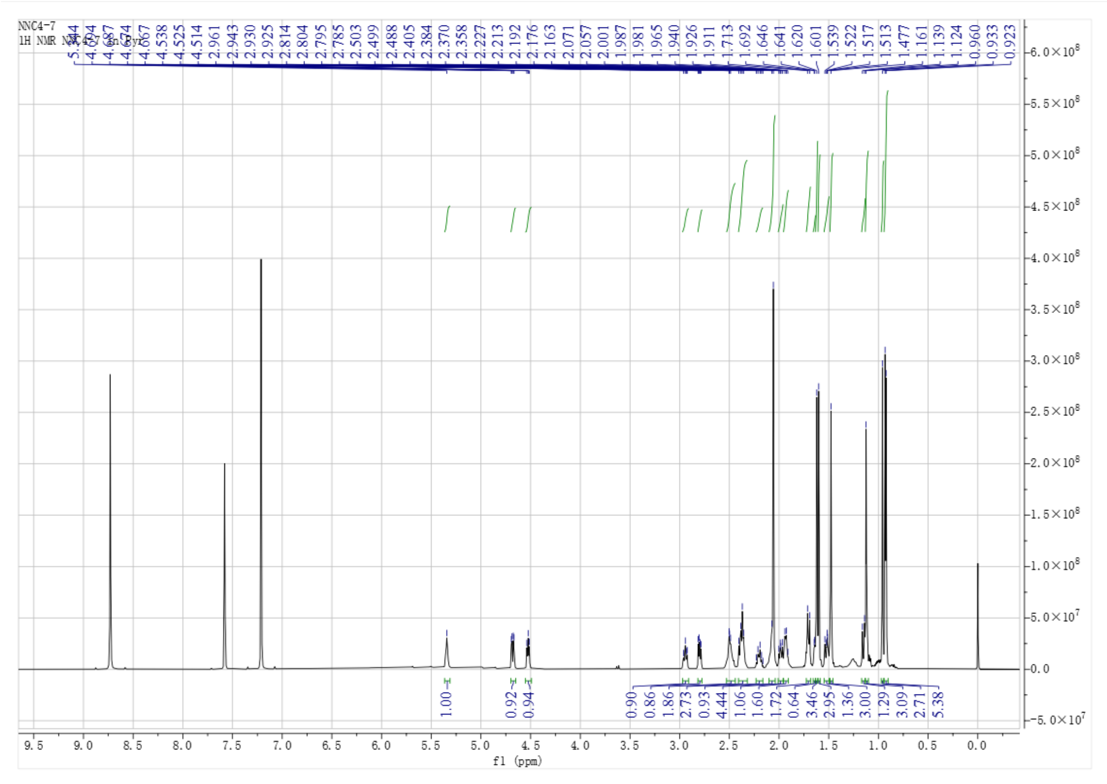

Figure S129. ^{1}H NMR spectrum (600 MHz, C_5D_5N) of compound **19**

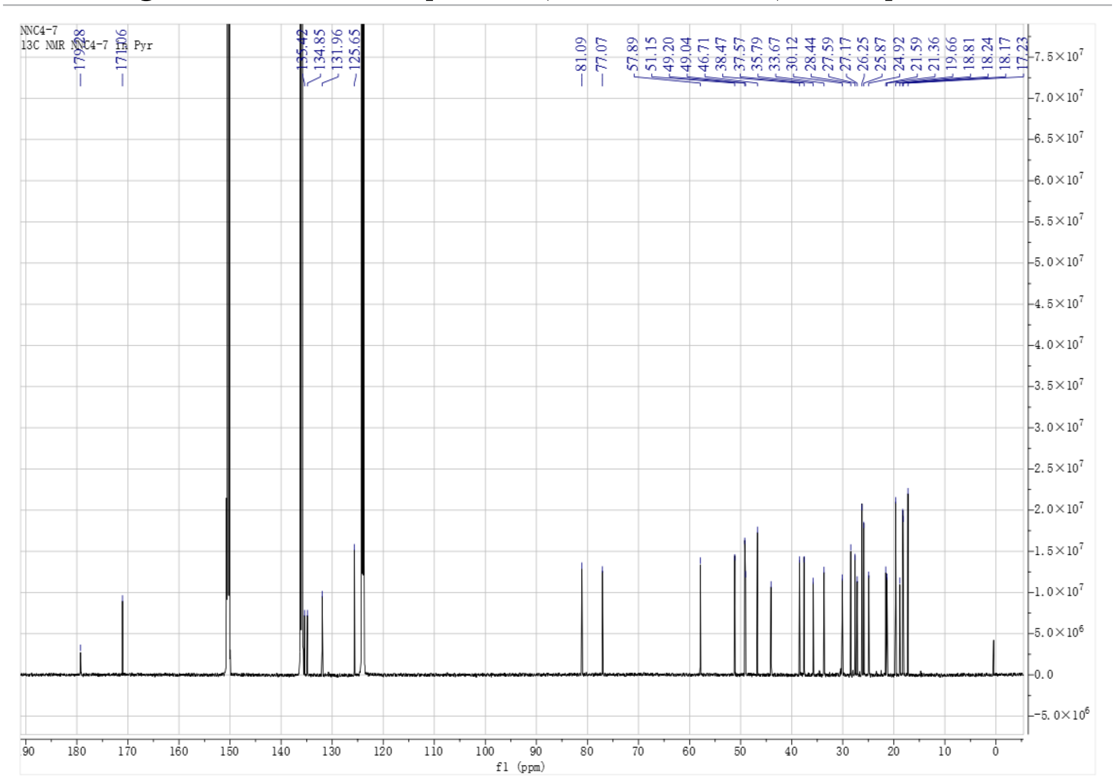

Figure S130. ^{13}C NMR spectrum (150 MHz, C_5D_5N) of compound **19**

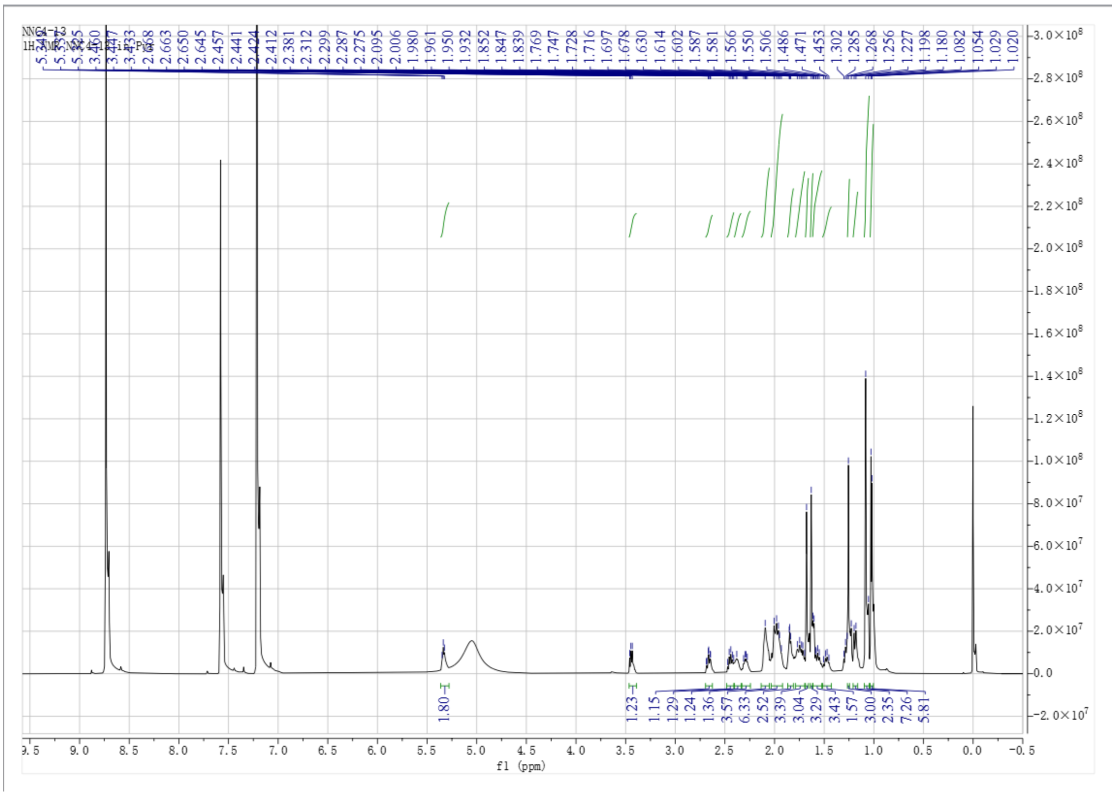

Figure S131. ^{1}H NMR spectrum (600 MHz, C_5D_5N) of compound **20**

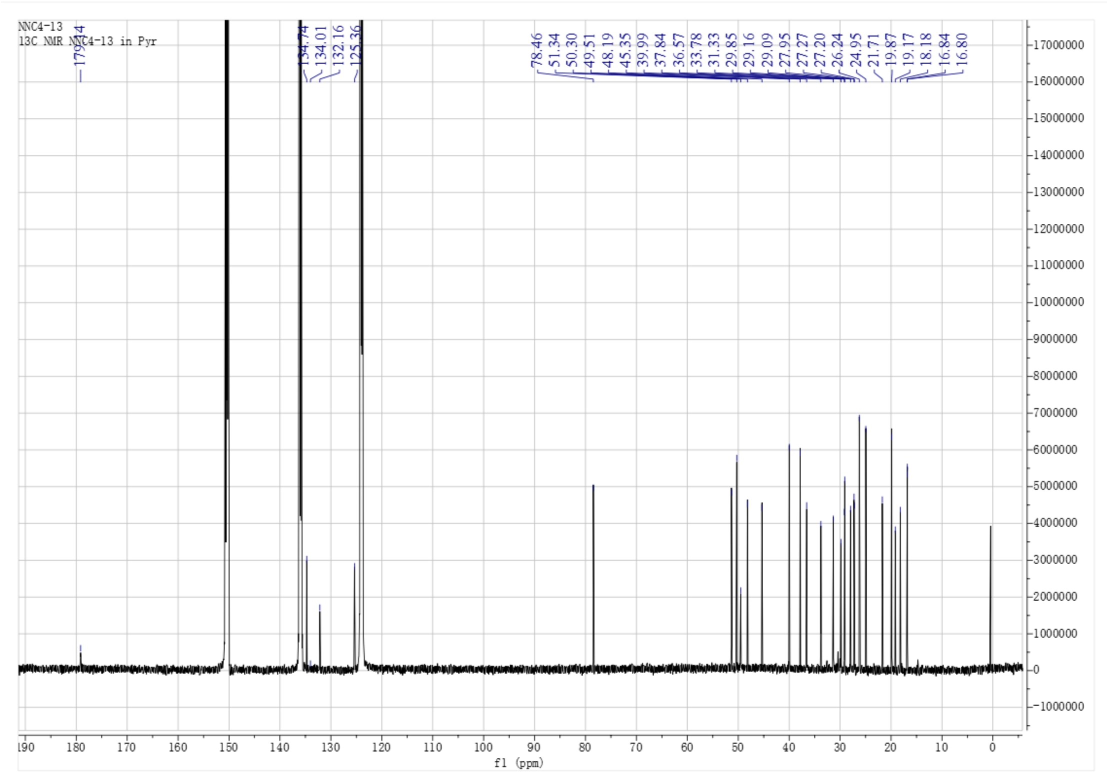

Figure S132. ^{13}C NMR spectrum (150 MHz, C_5D_5N) of compound **20**

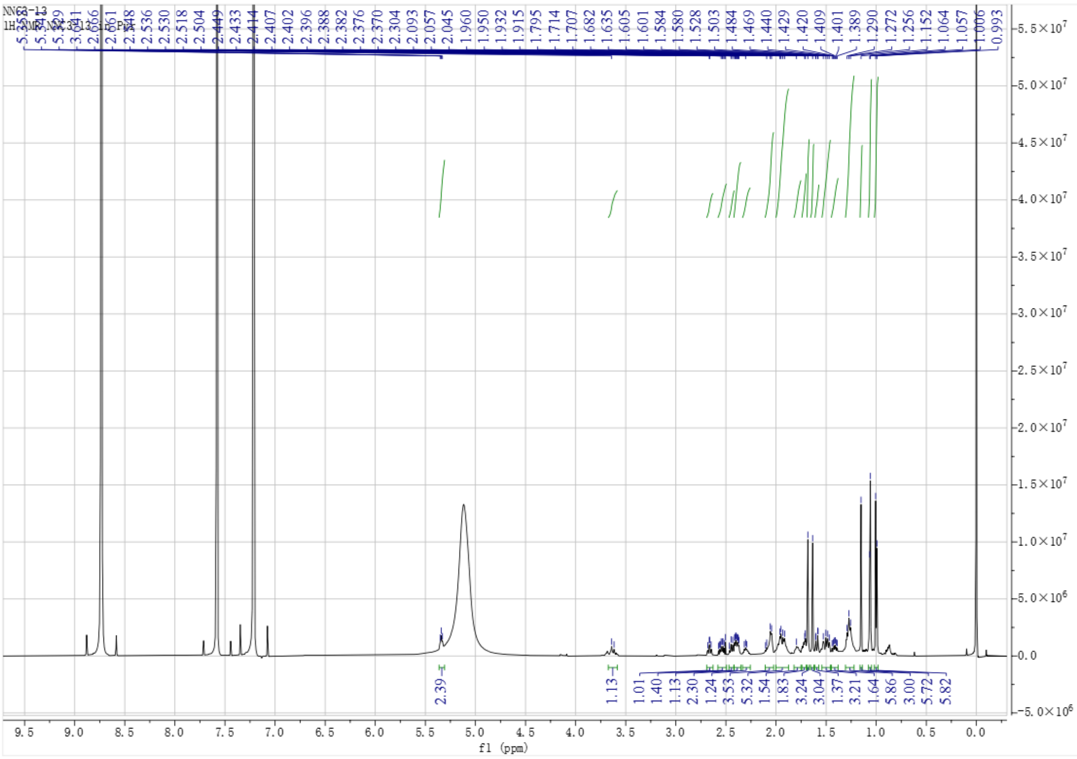

Figure S133. ^{1}H NMR spectrum (600 MHz, C_5D_5N) of compound **21**

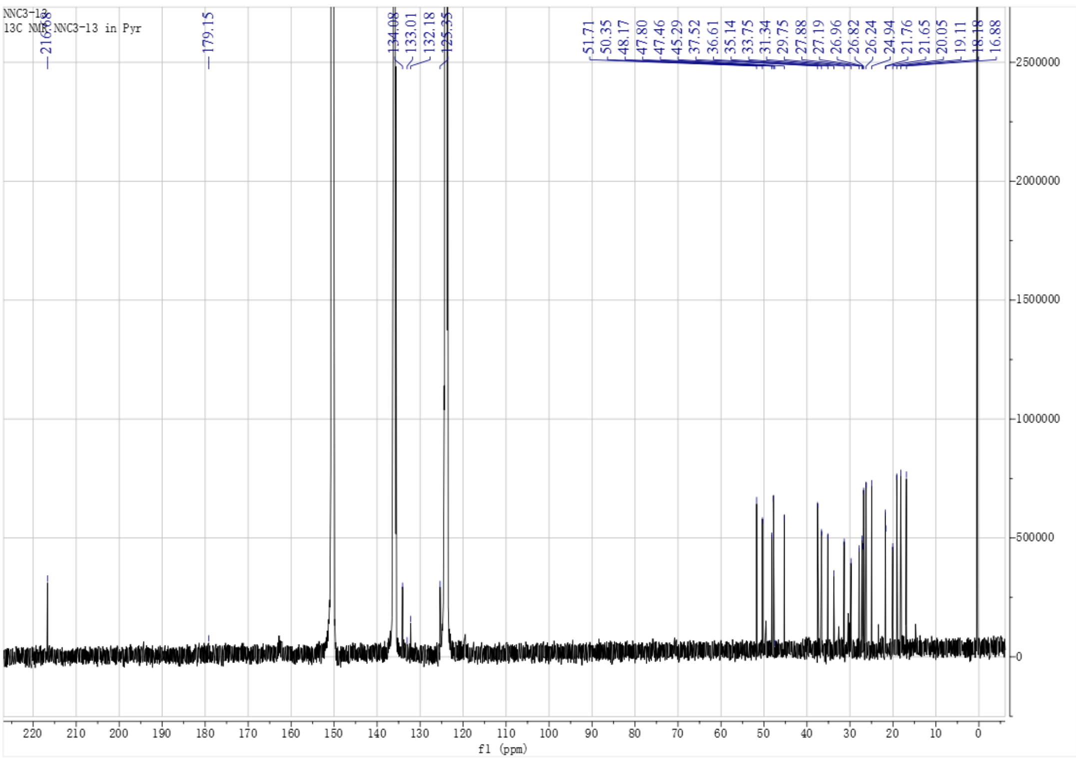

Figure S134. ^{13}C NMR spectrum (150 MHz, C_5D_5N) of compound **21**

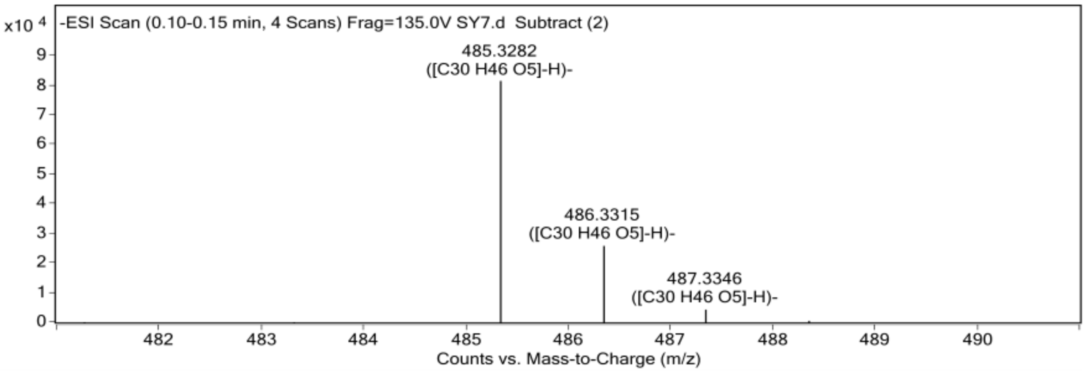

Figure S135. HRESIMS spectrum of compound **22**

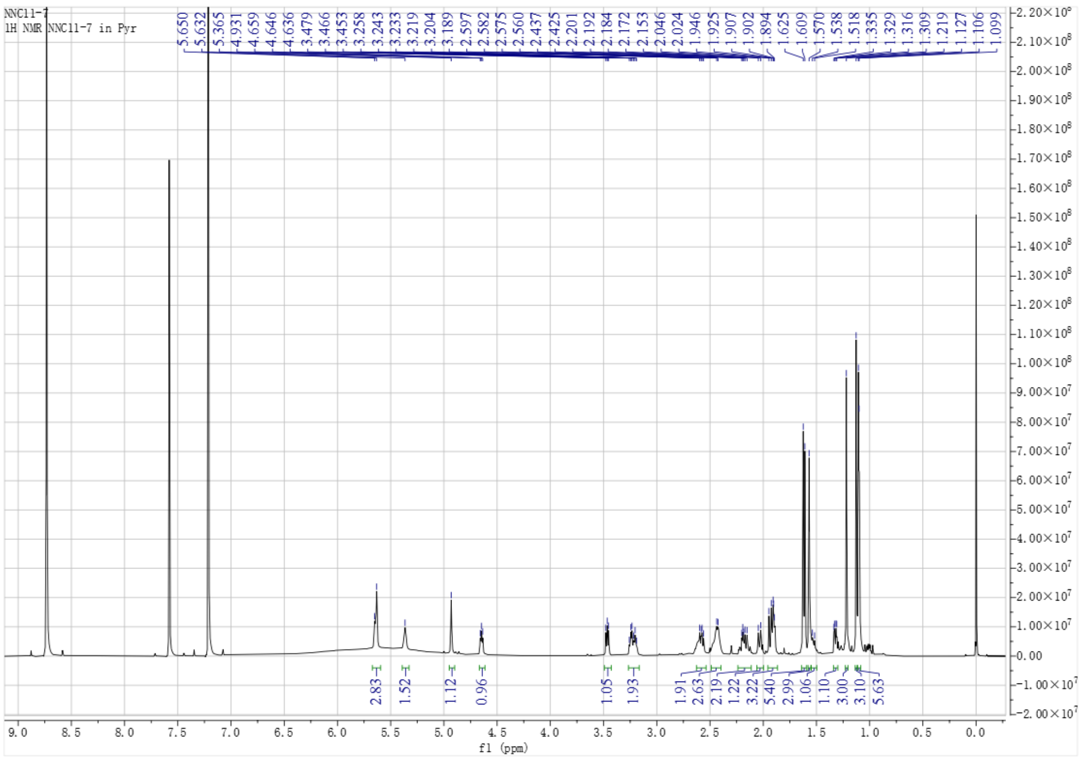

Figure S136. [1]H NMR spectrum (600 MHz, C_5D_5N) of compound **22**

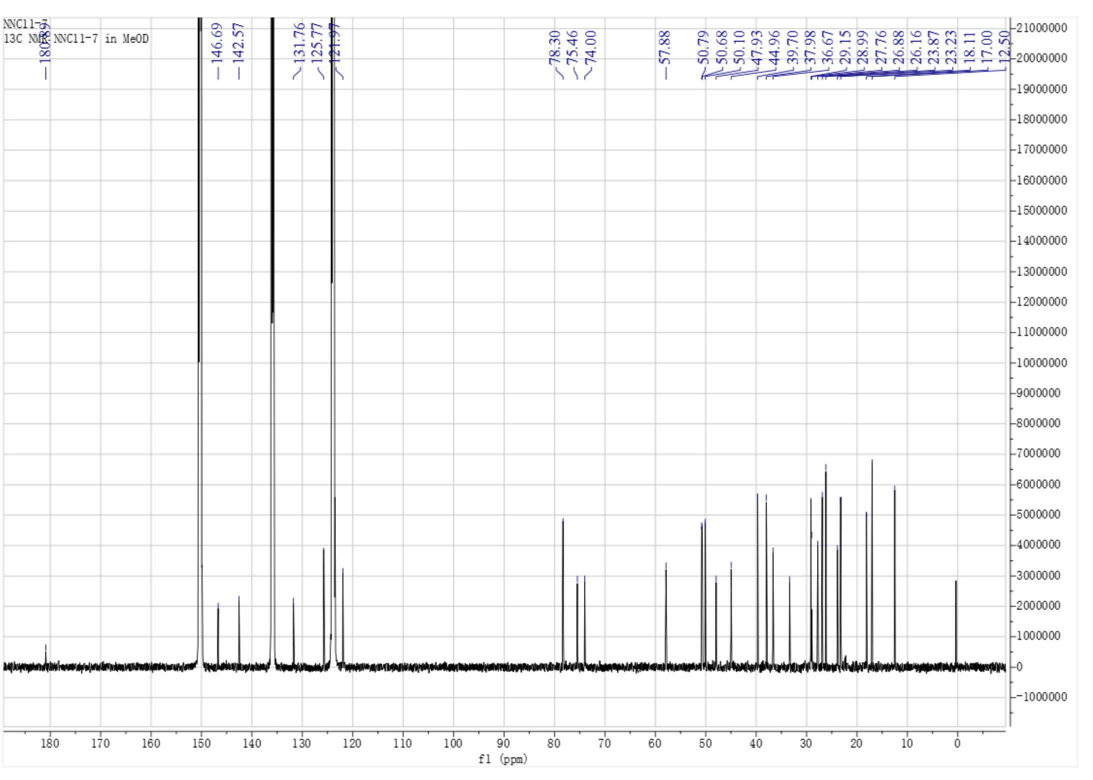

Figure S137. ^{13}C NMR spectrum (150 MHz, C_5D_5N) of compound **22**

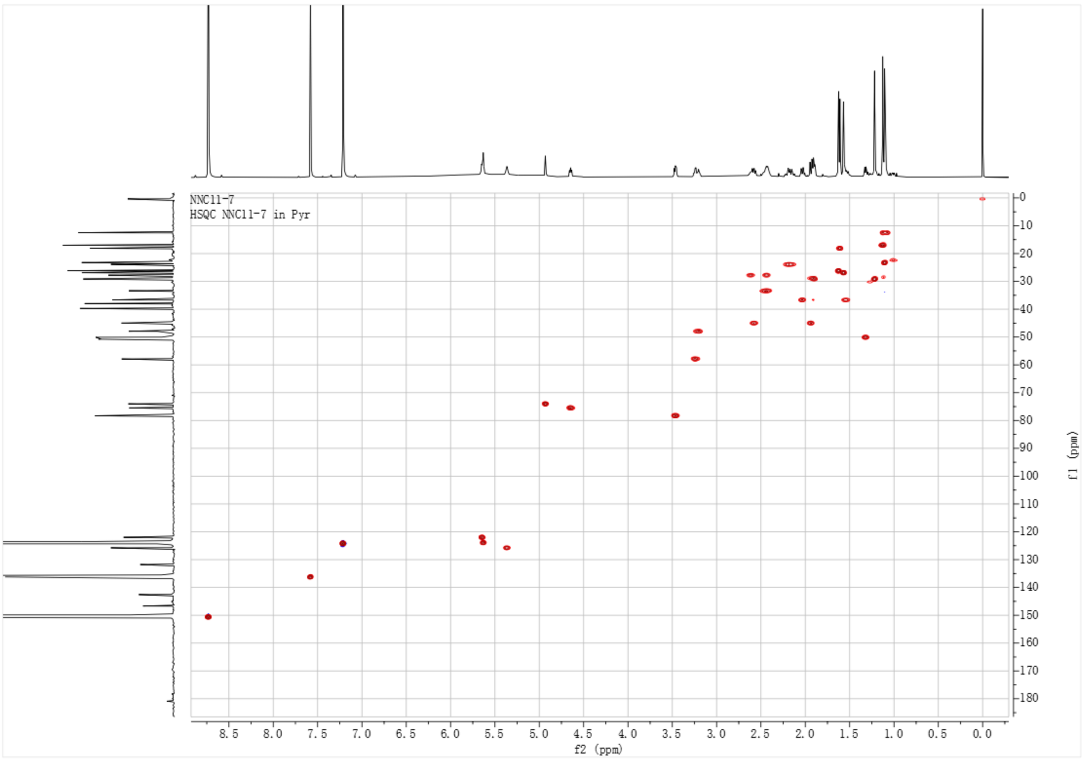

Figure S138. HSQC spectrum (600 MHz, C_5D_5N) of compound **22**

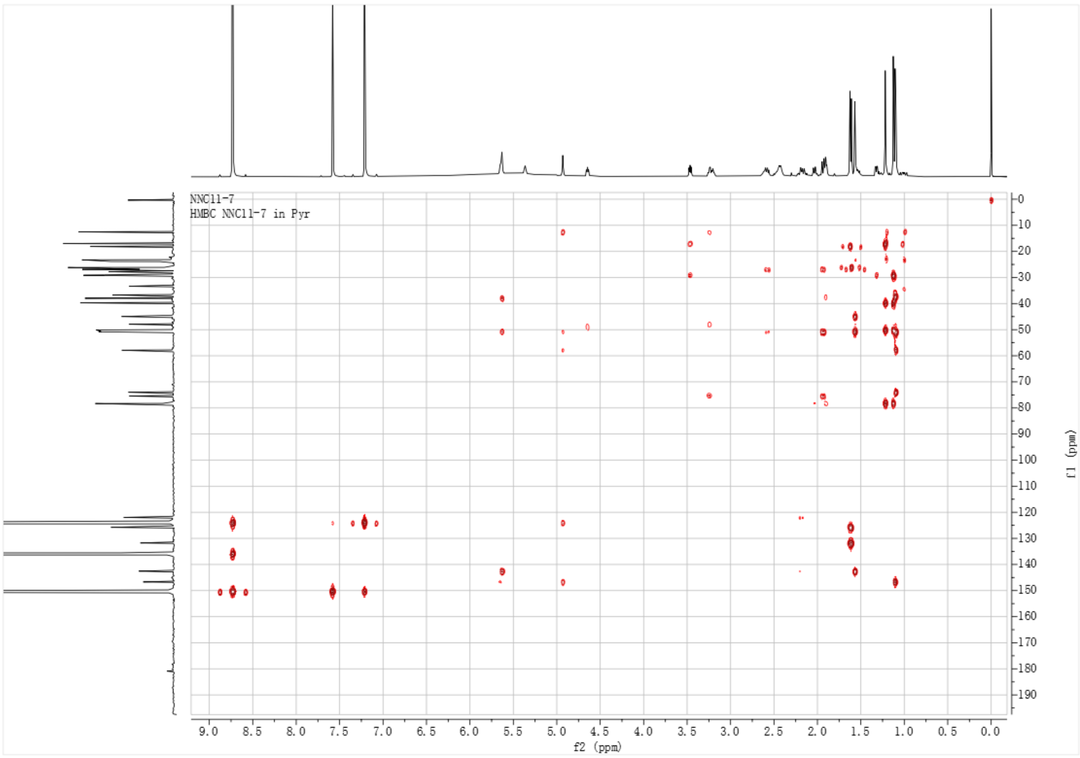

Figure S139. HMBC spectrum (600 MHz, C_5D_5N) of compound **22**

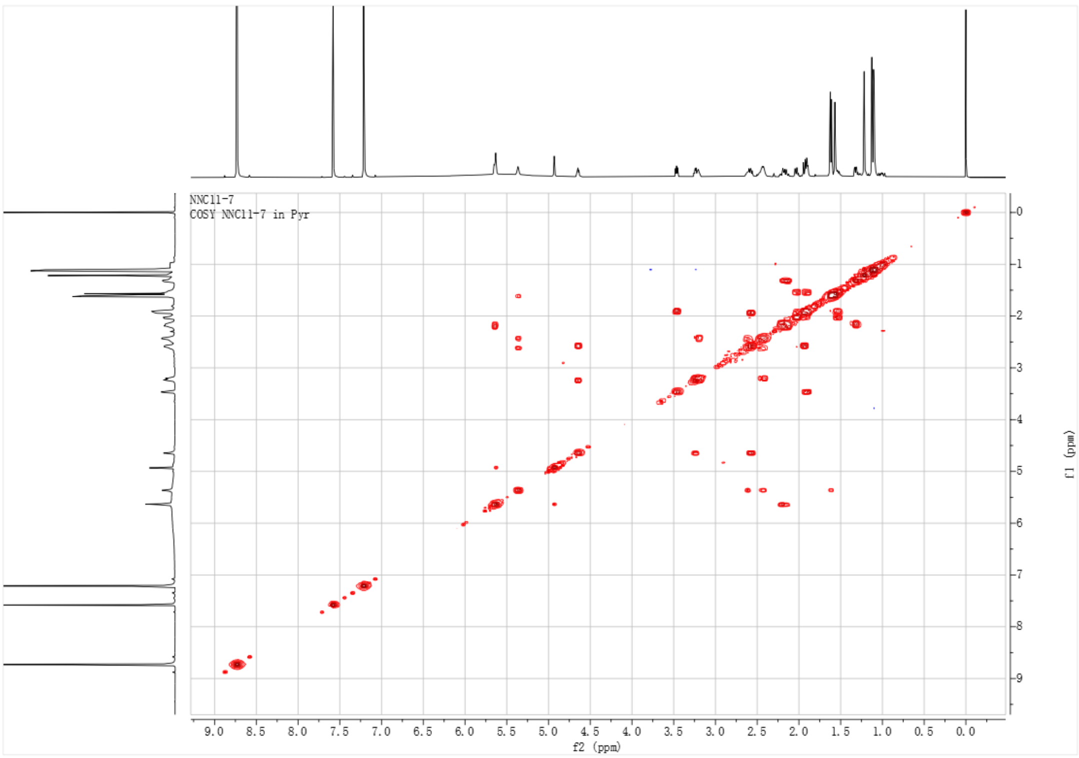

Figure S140. ^{1}H-^{1}H COSY spectrum (600 MHz, C_5D_5N) of compound **22**

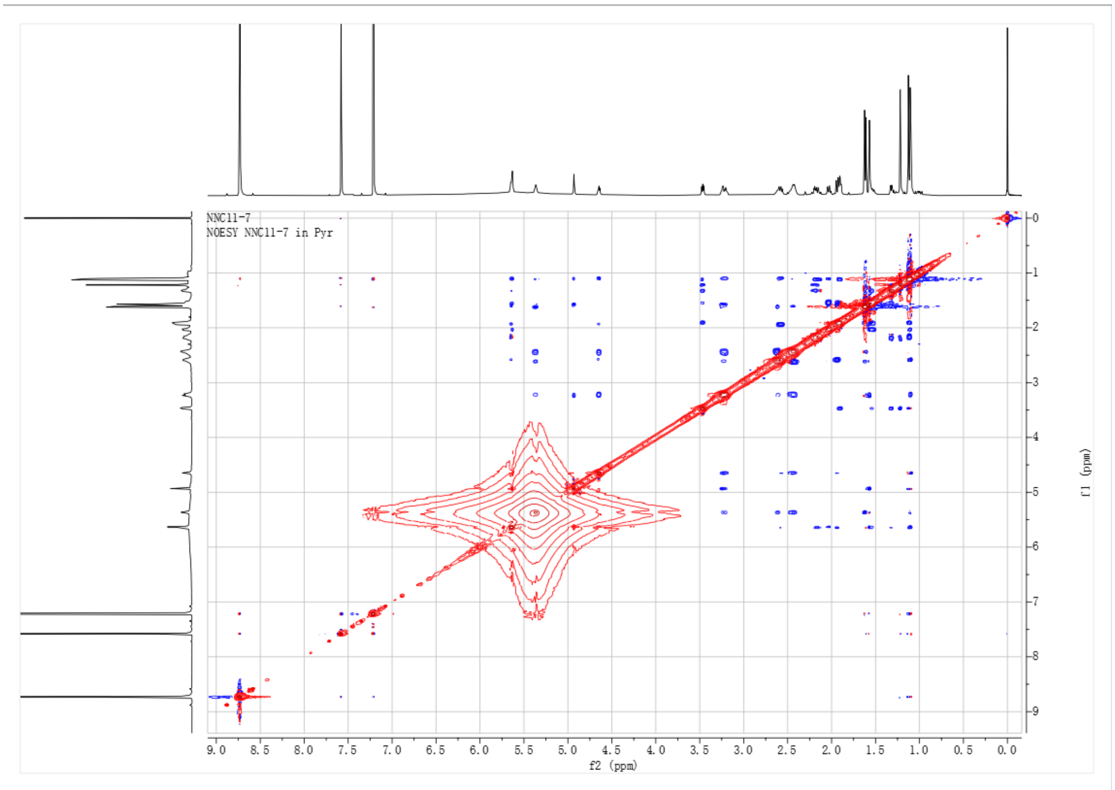

Figure S141. NOESY spectrum (600 MHz, C_5D_5N) of compound **22**

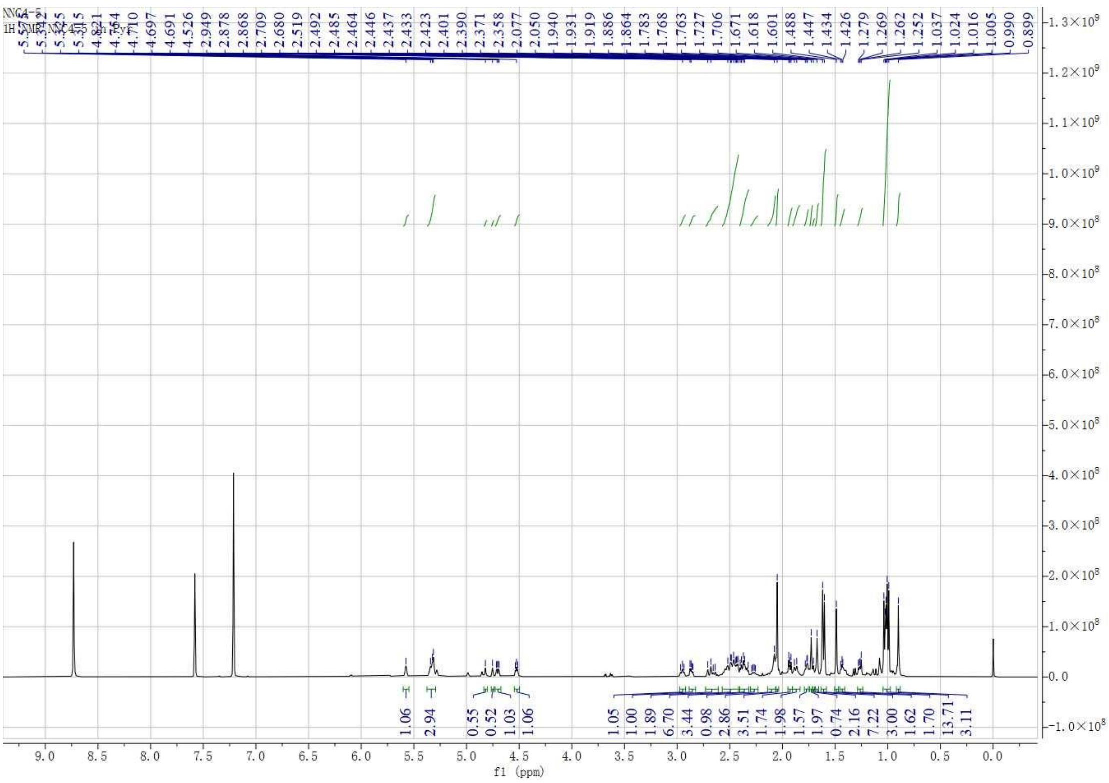

Figure S142. ^1H NMR spectrum (600 MHz, C_5D_5N) of compound **23**

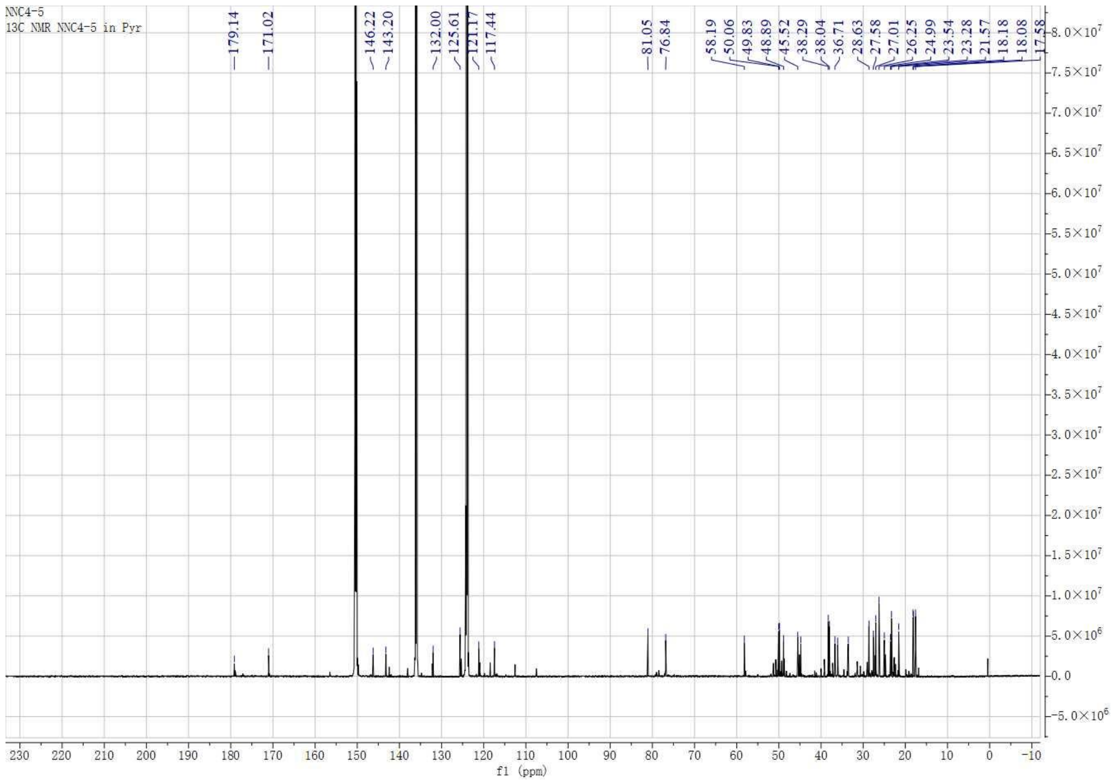

Figure S143. ^{13}C NMR spectrum (150 MHz, C_5D_5N) of compound **23**

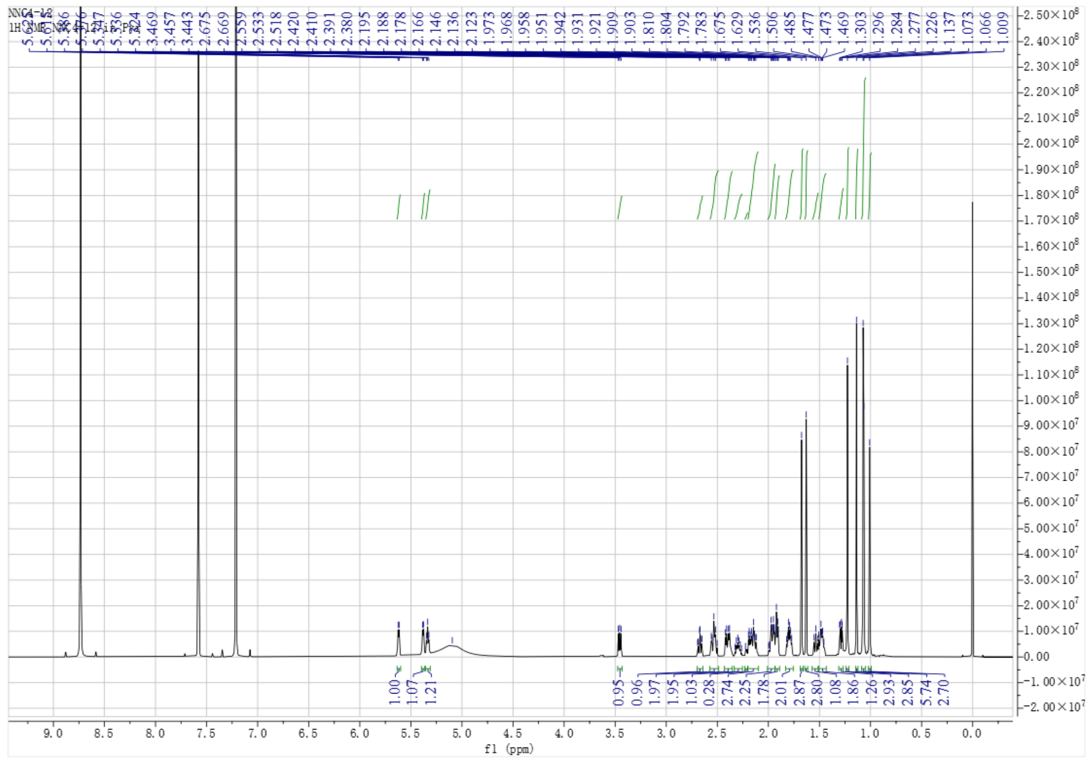

Figure S144. ^{1}H NMR spectrum (600 MHz, C_5D_5N) of compound **24**

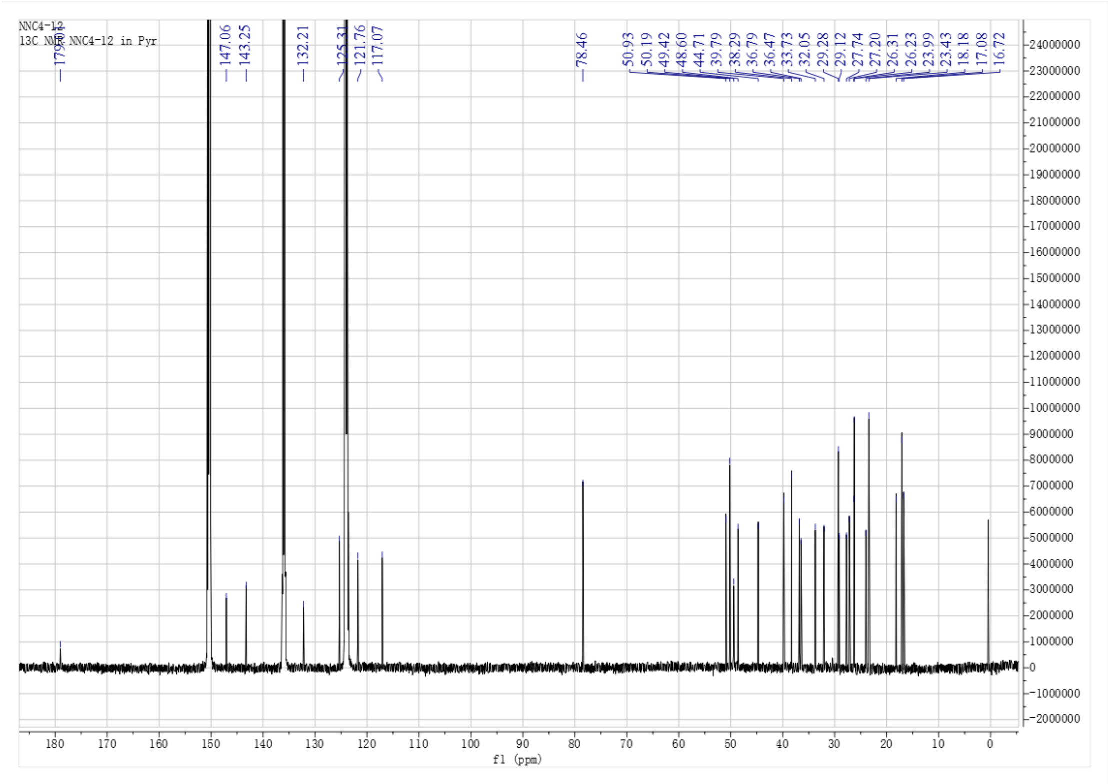

Figure S145. ^{13}C NMR spectrum (150 MHz, C_5D_5N) of compound **24**

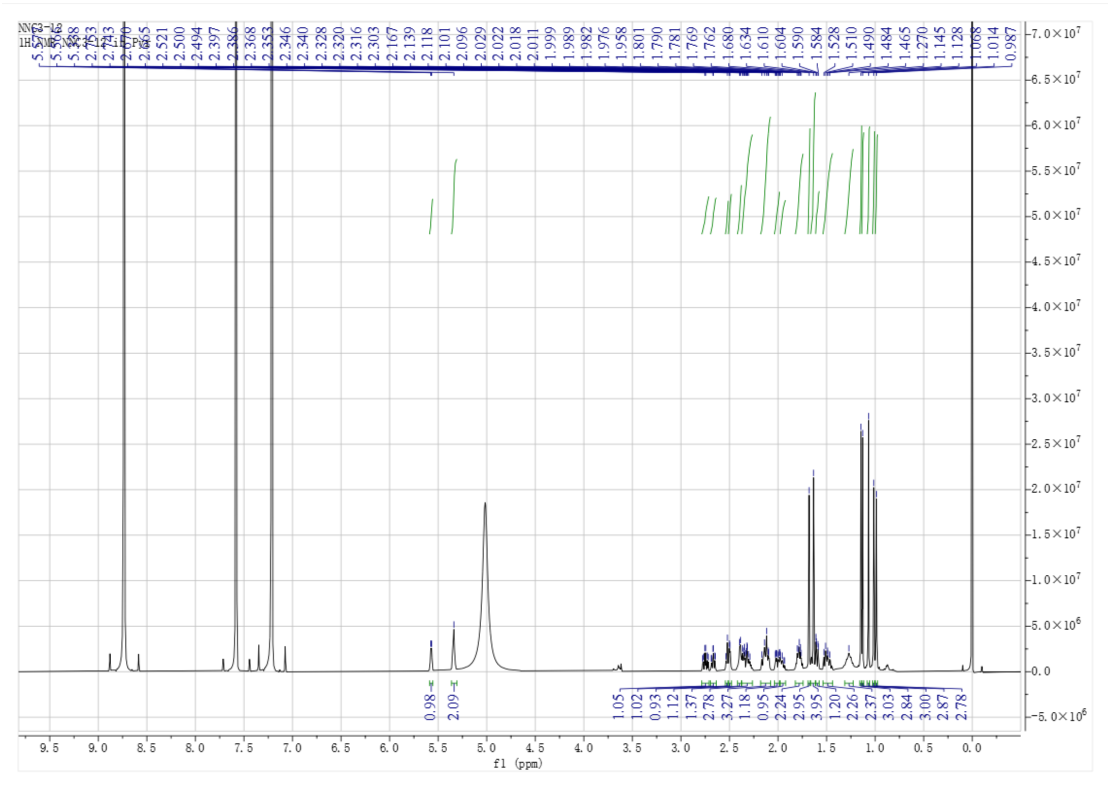

Figure S146. ^{1}H NMR spectrum (600 MHz, C_5D_5N) of compound **25**

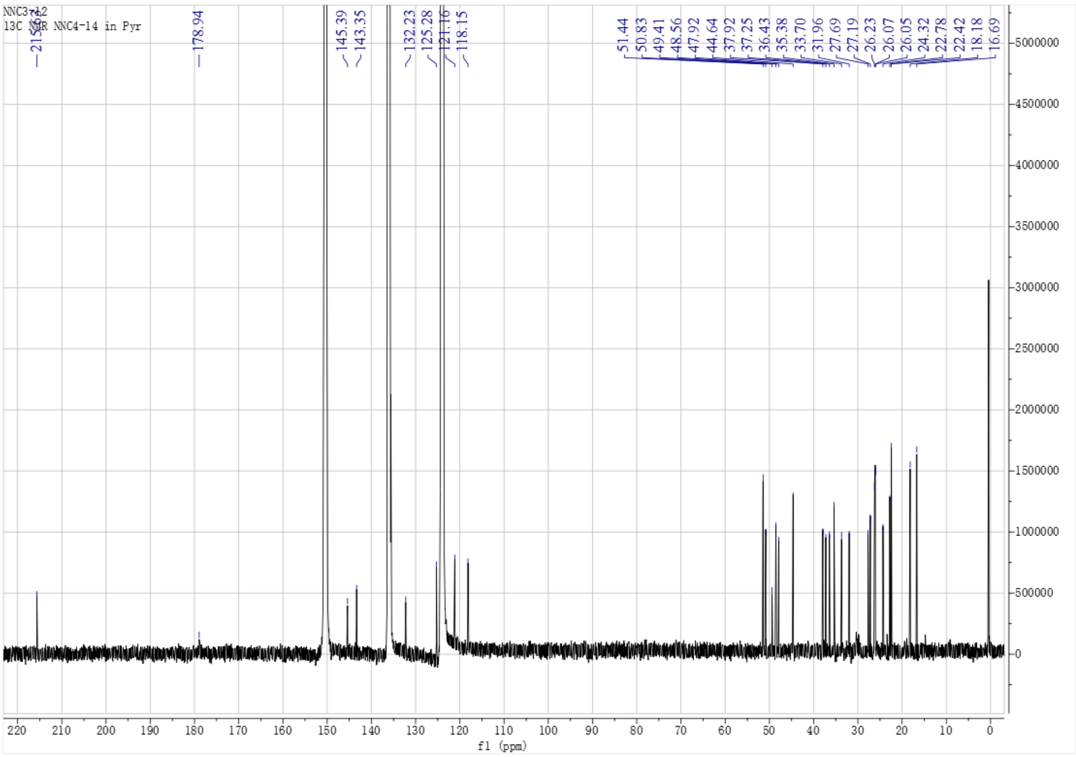

Figure S147. ^{13}C NMR spectrum (150 MHz, C_5D_5N) of compound **25**

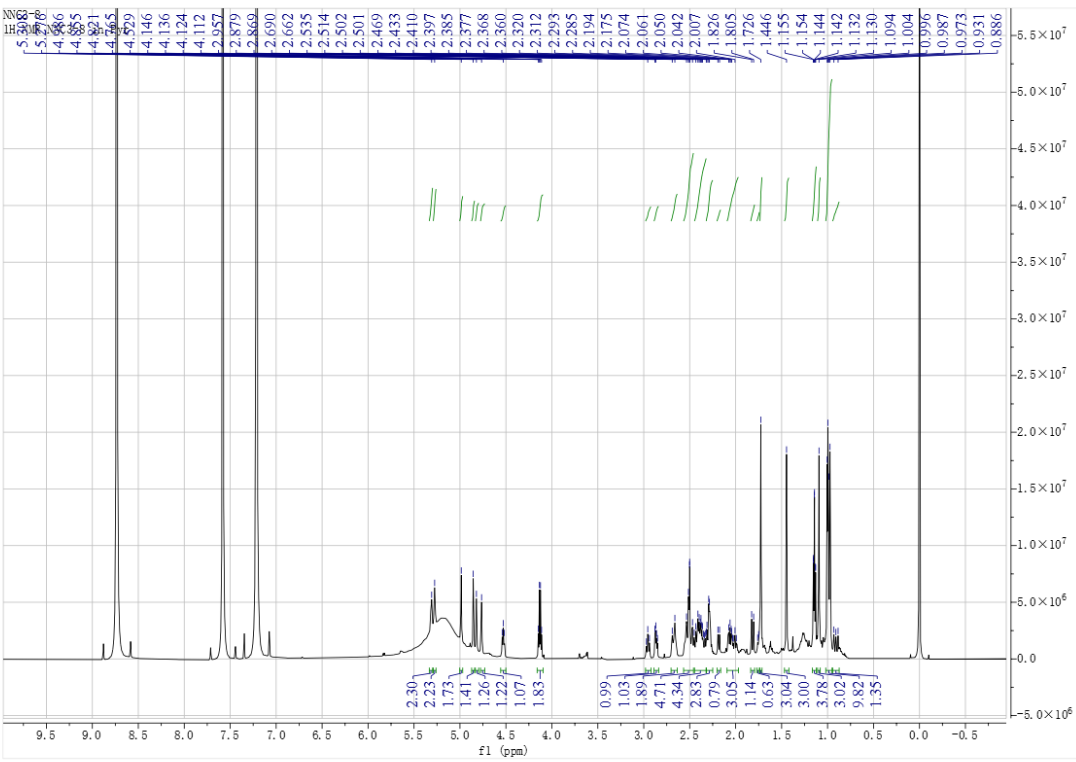

Figure S148. ^{1}H NMR spectrum (600 MHz, C_5D_5N) of compound **26**

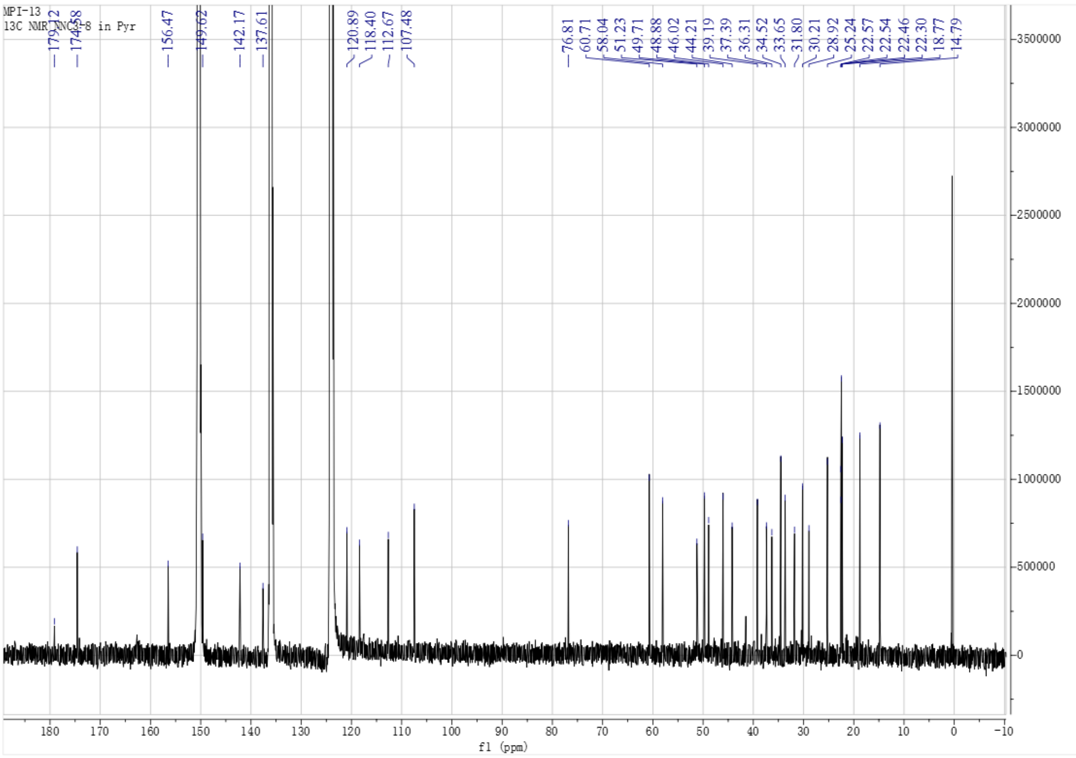

Figure S149. ^{13}C NMR spectrum (150 MHz, C_5D_5N) of compound **26**

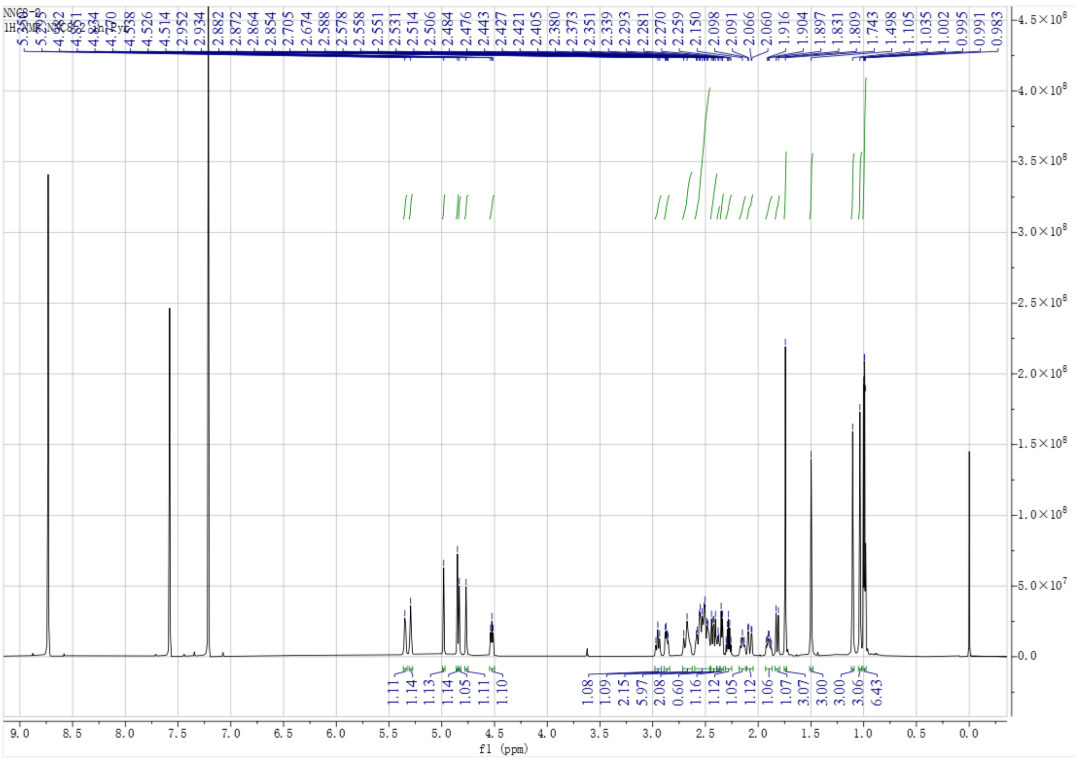

Figure S150. ^{1}H NMR spectrum (600 MHz, C_5D_5N) of compound **27**

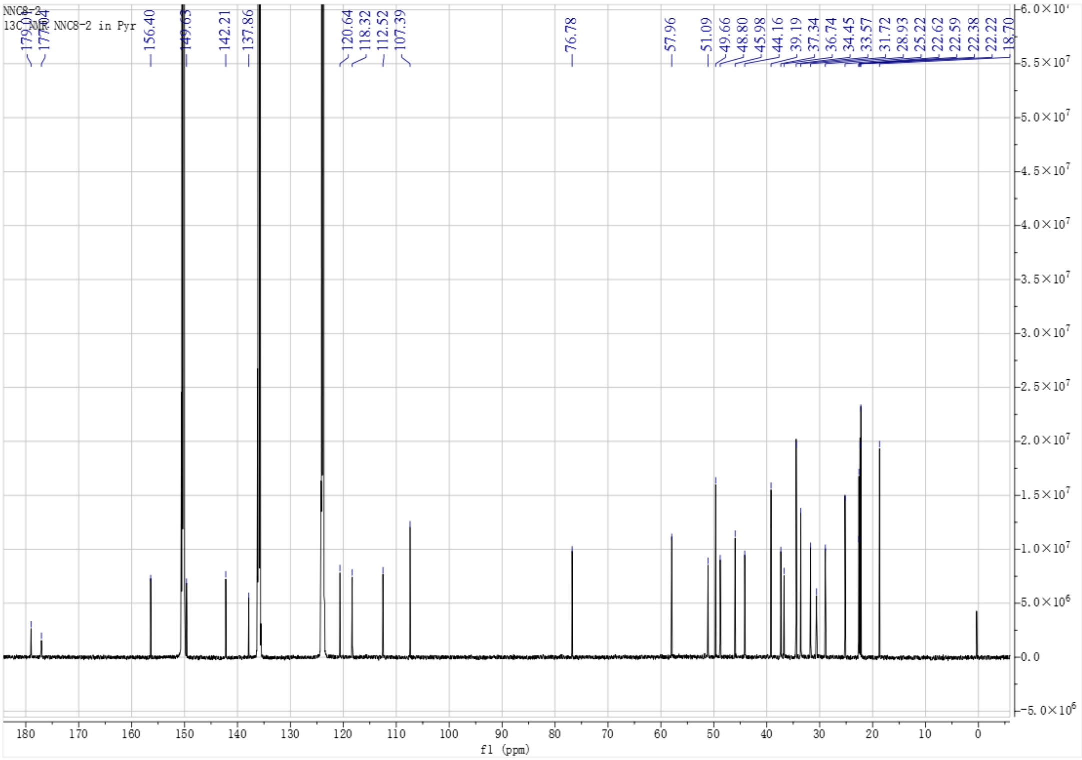

Figure S151. ^{13}C NMR spectrum (150 MHz, C_5D_5N) of compound **27**

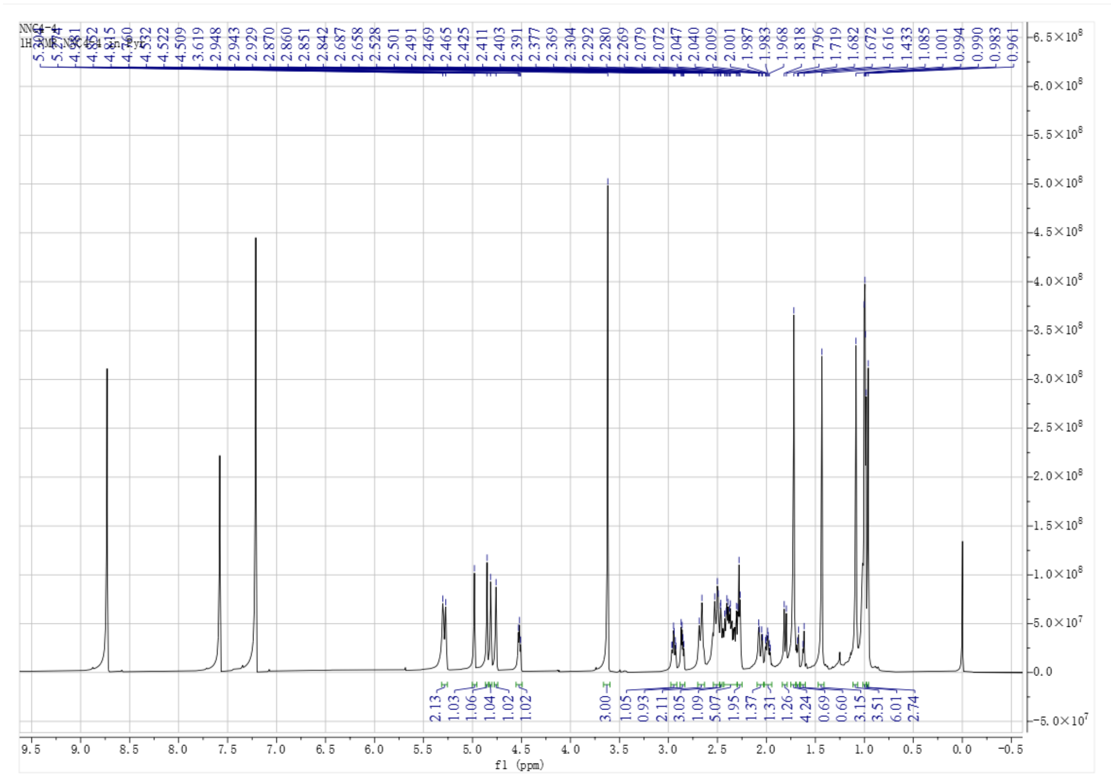

Figure S152. ^{1}H NMR spectrum (600 MHz, C_5D_5N) of compound **28**

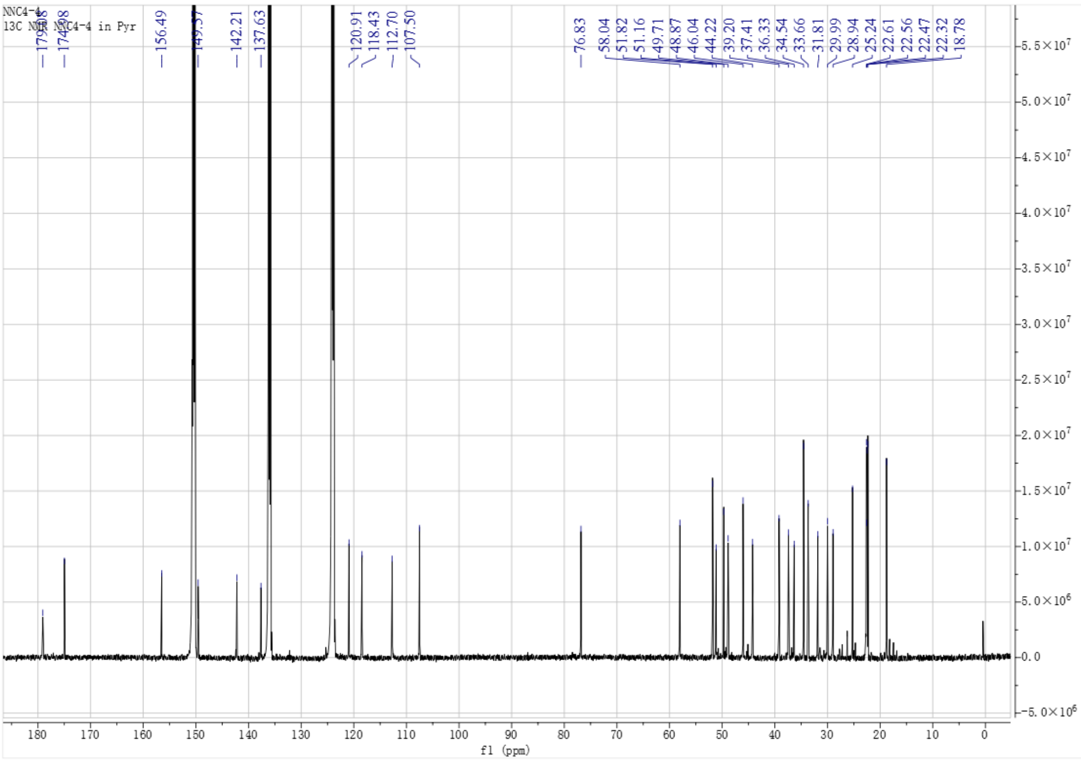

Figure S153. ^{13}C NMR spectrum (150 MHz, C_5D_5N) of compound **28**

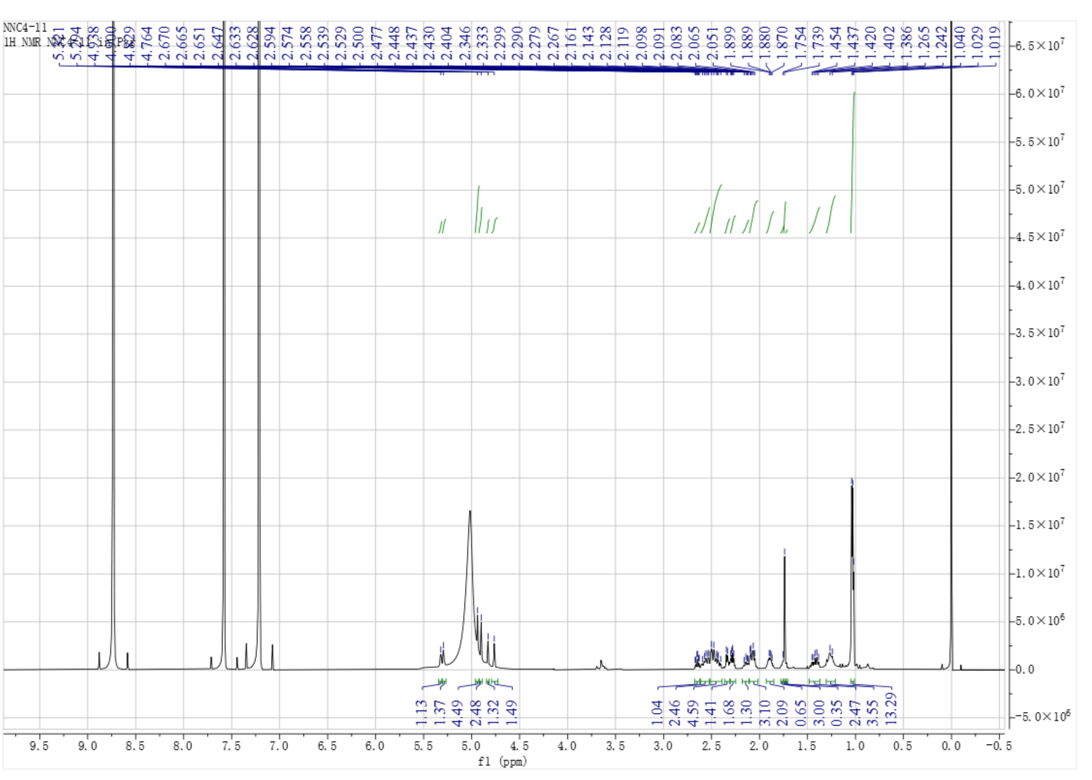

Figure S154. ^{1}H NMR spectrum (600 MHz, C_5D_5N) of compound **29**

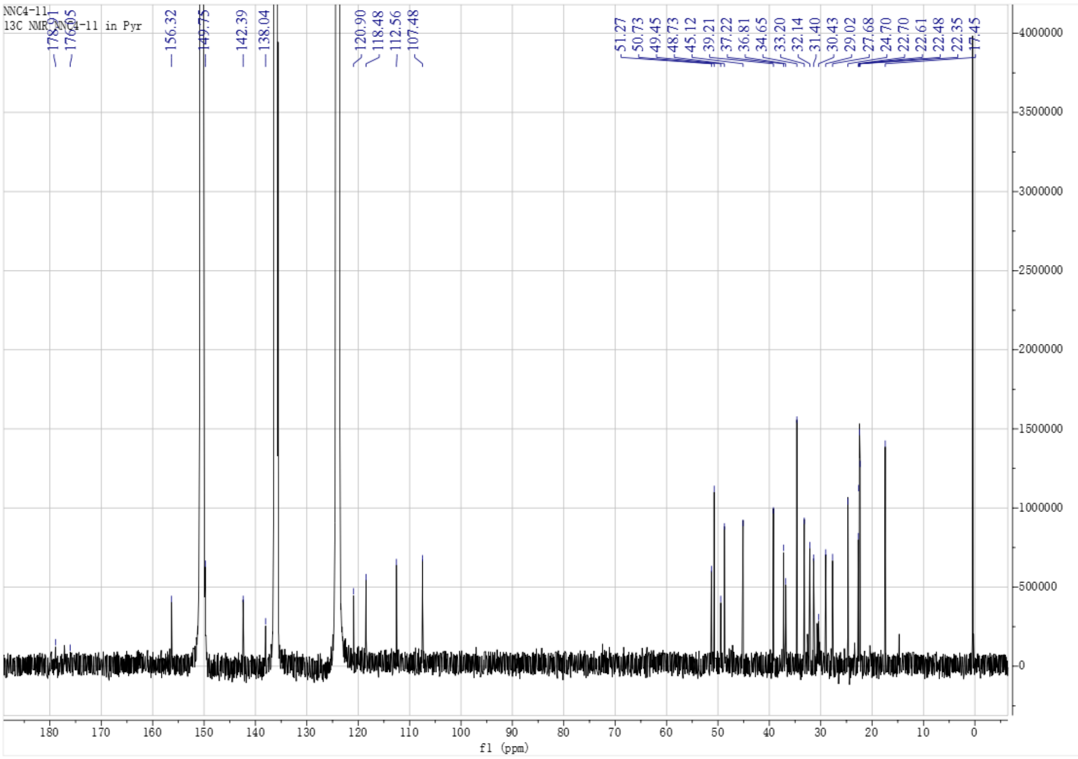

Figure S155. ^{13}C NMR spectrum (150 MHz, C_5D_5N) of compound **29**

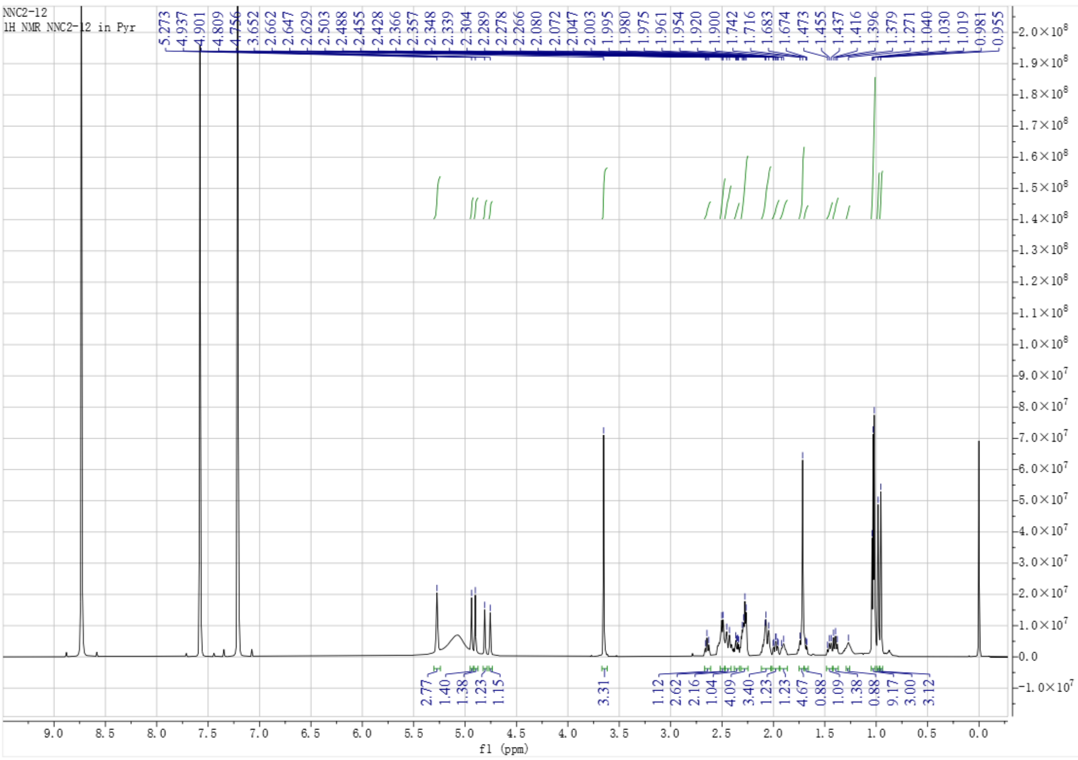

Figure S156. ^{1}H NMR spectrum (600 MHz, C_5D_5N) of compound **30**

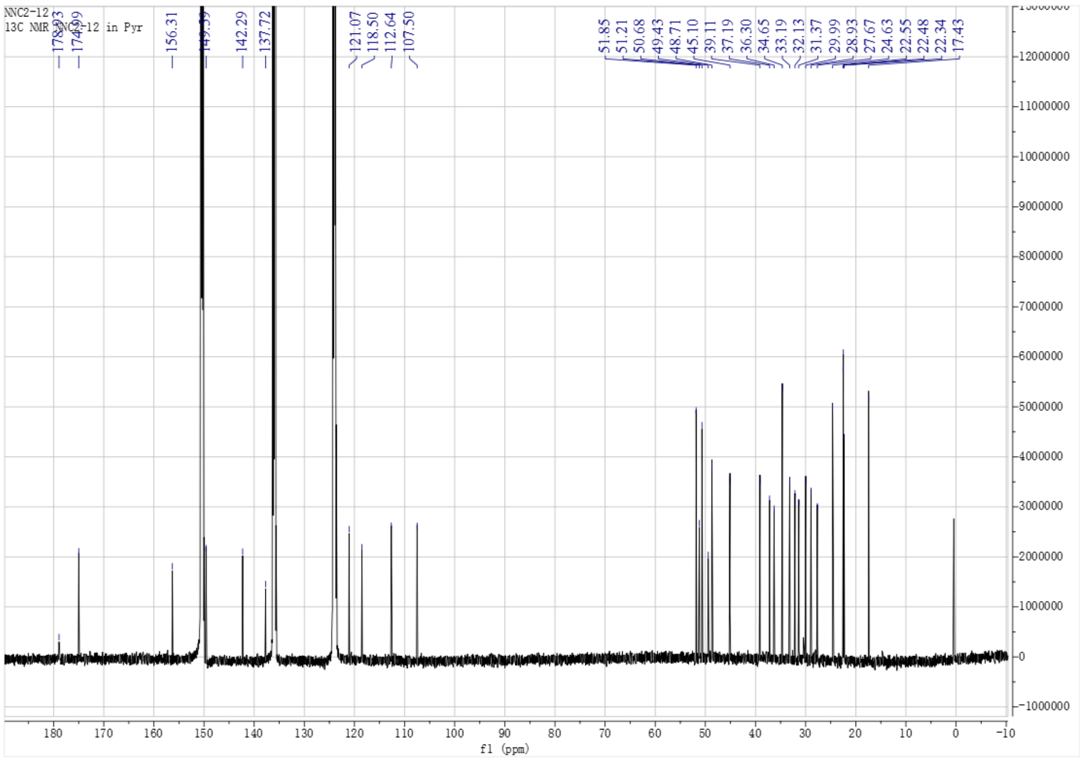

Figure S157. ^{13}C NMR spectrum (150 MHz, C_5D_5N) of compound **30**

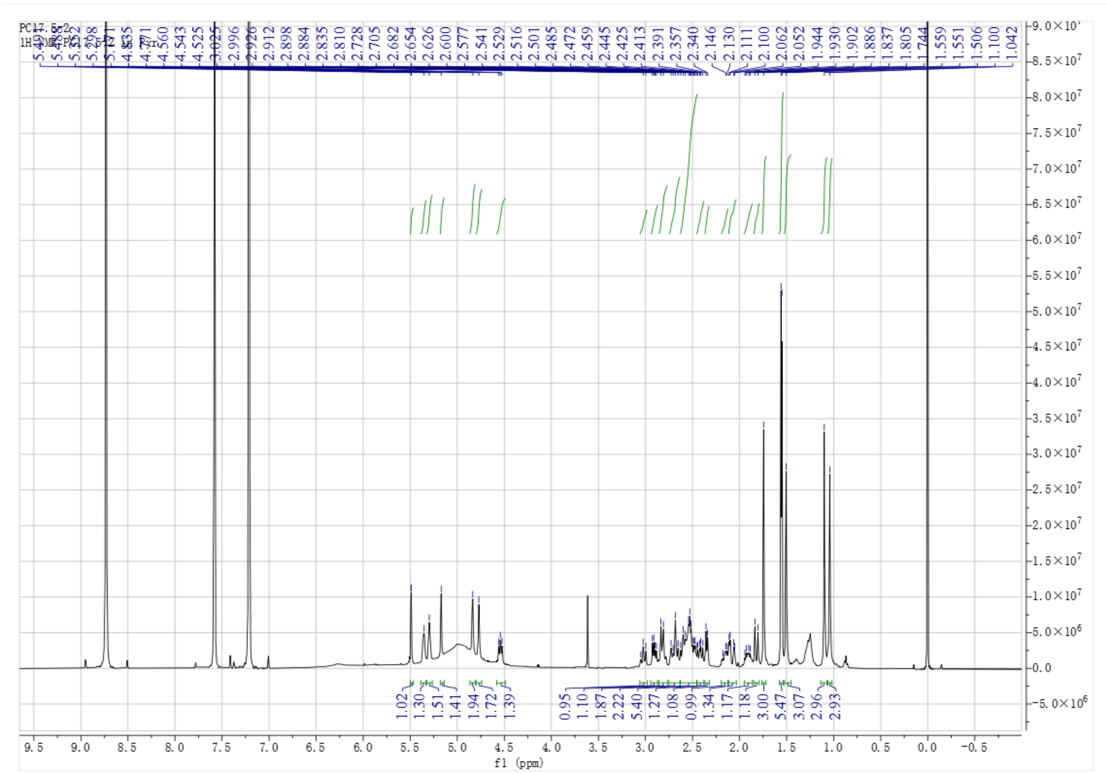

Figure S158. ^{1}H NMR spectrum (600 MHz, C_5D_5N) of compound **31**

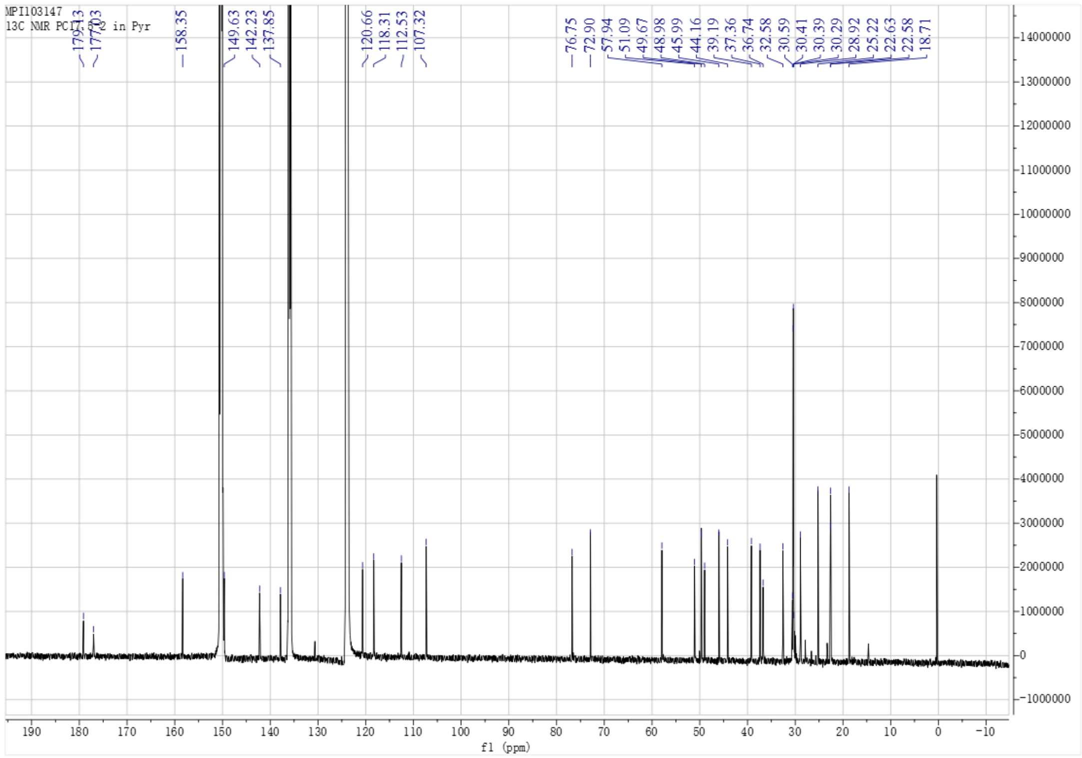

Figure S159. ^{13}C NMR spectrum (150 MHz, C_5D_5N) of compound **31**

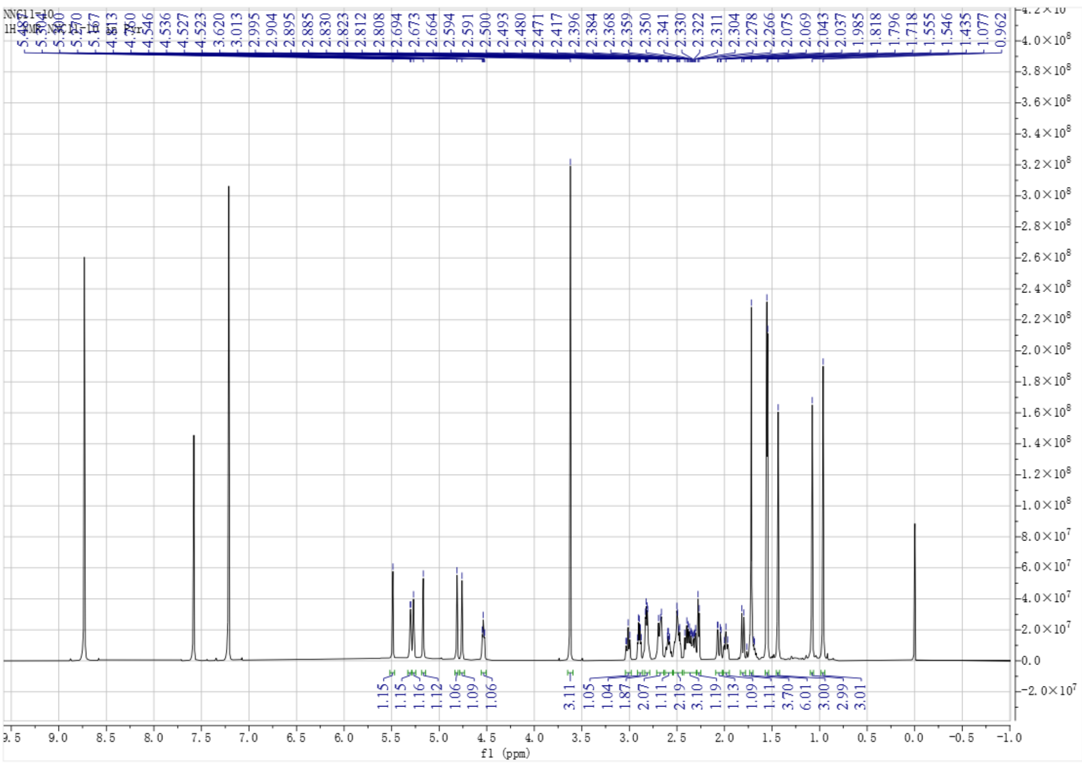

Figure S160. ^{1}H NMR spectrum (600 MHz, C_5D_5N) of compound **32**

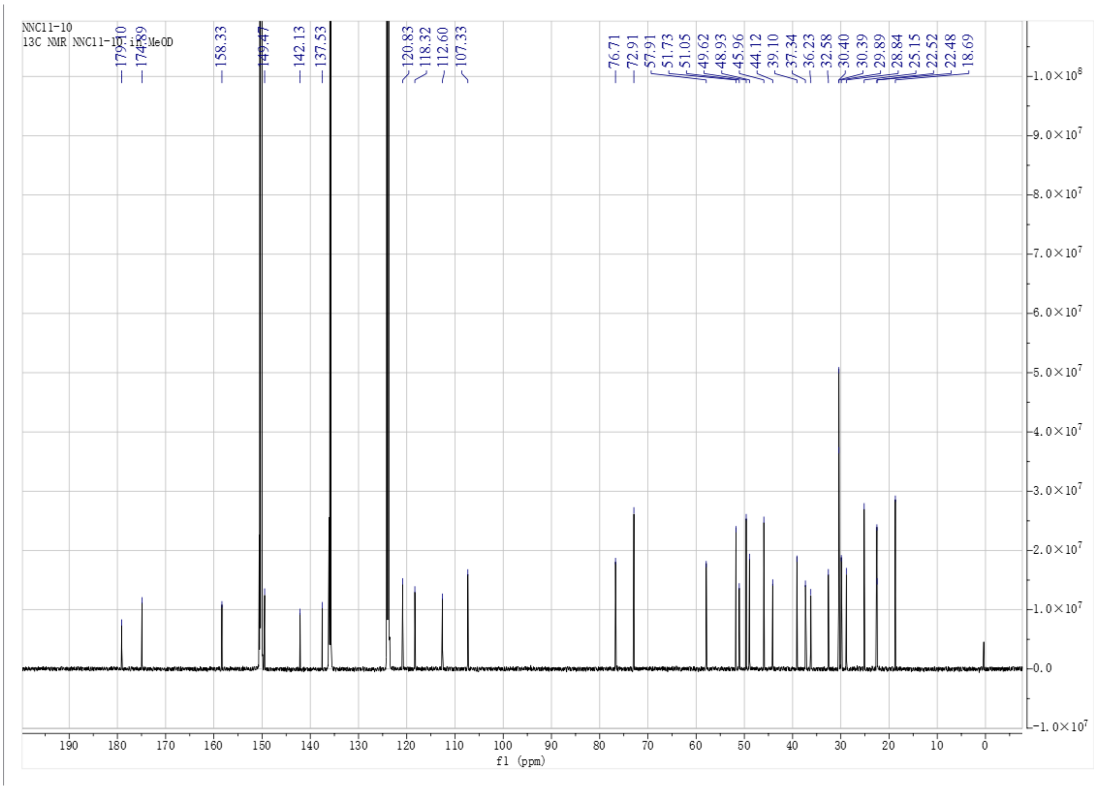

Figure S161. ^{13}C NMR spectrum (150 MHz, C_5D_5N) of compound **32**

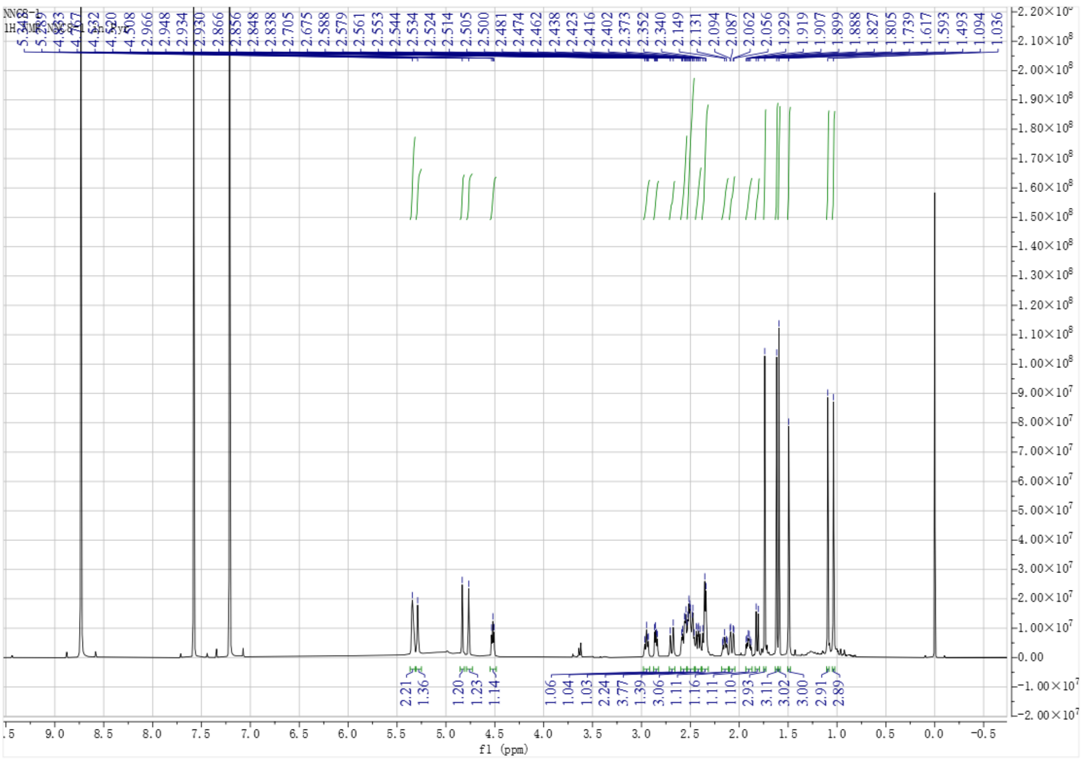

Figure S162. ^{1}H NMR spectrum (600 MHz, C_5D_5N) of compound **33**

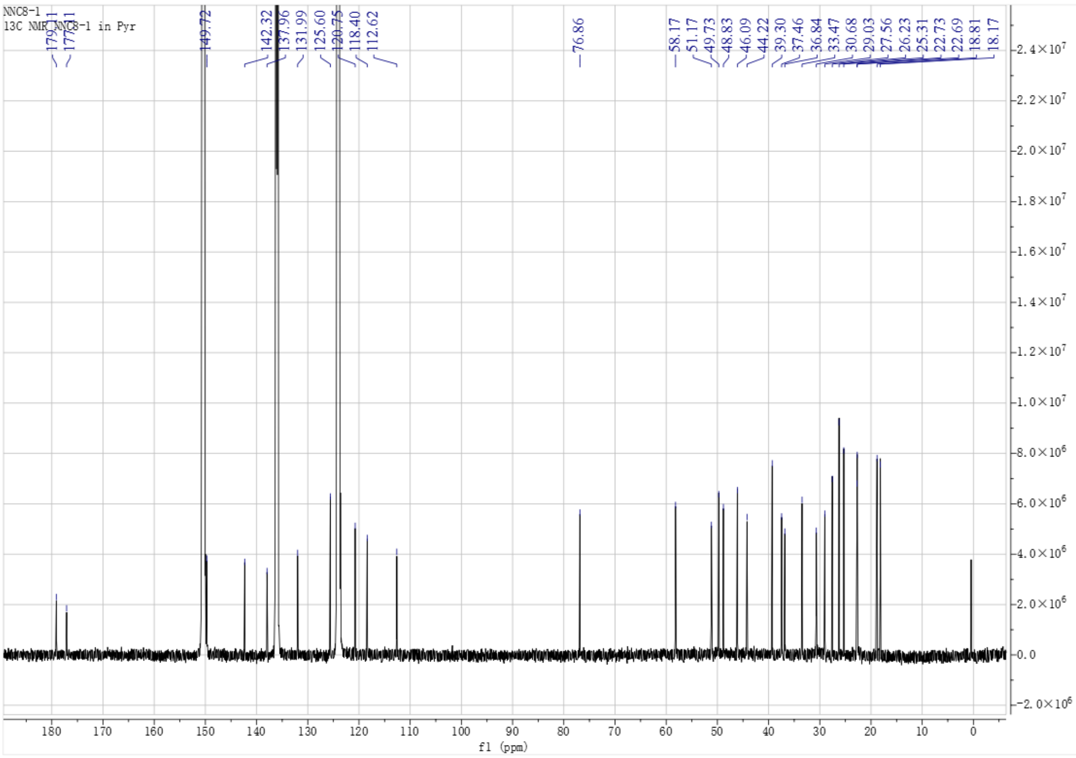

Figure S163. ^{13}C NMR spectrum (150 MHz, C_5D_5N) of compound **33**

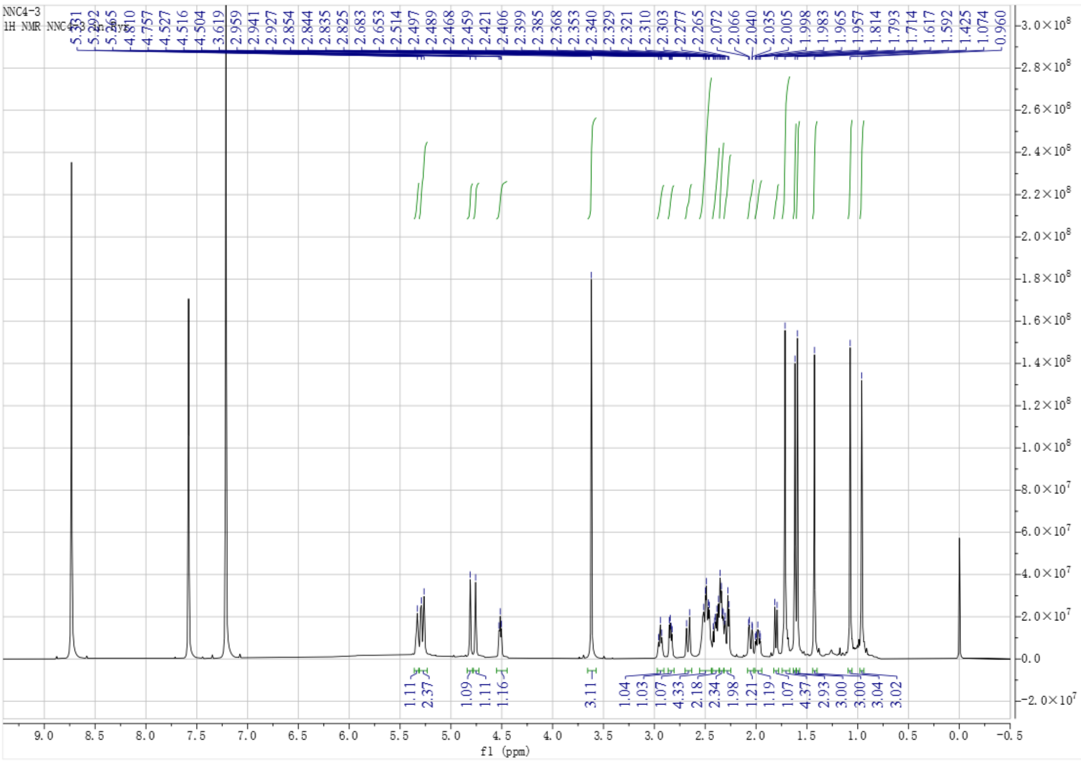

Figure S164. ^{1}H NMR spectrum (600 MHz, C_5D_5N) of compound **34**

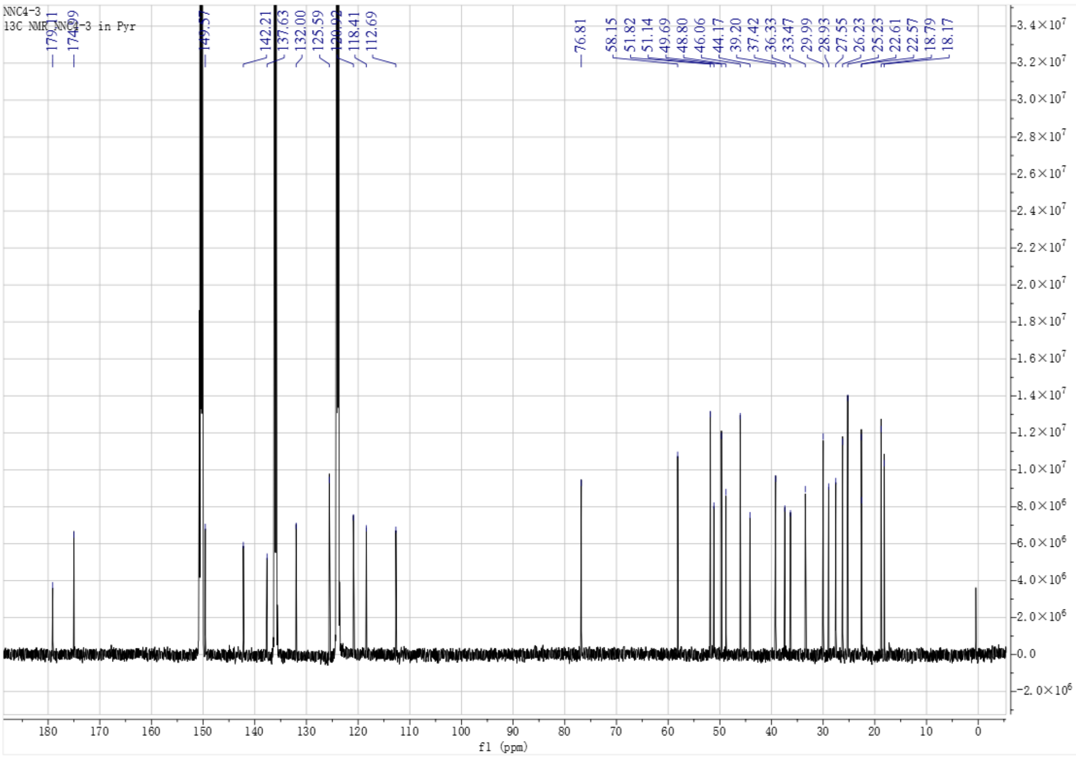

Figure S165. ^{13}C NMR spectrum (150 MHz, C_5D_5N) of compound **34**

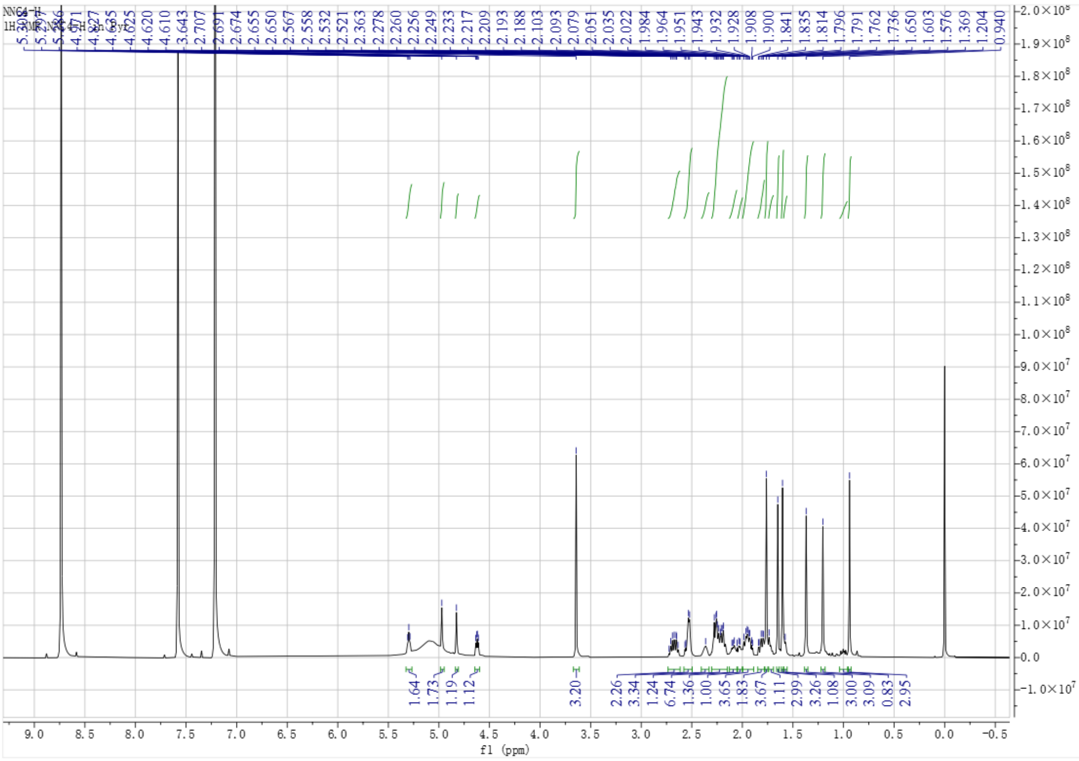

Figure S166. ^{1}H NMR spectrum (600 MHz, C_5D_5N) of compound **35**

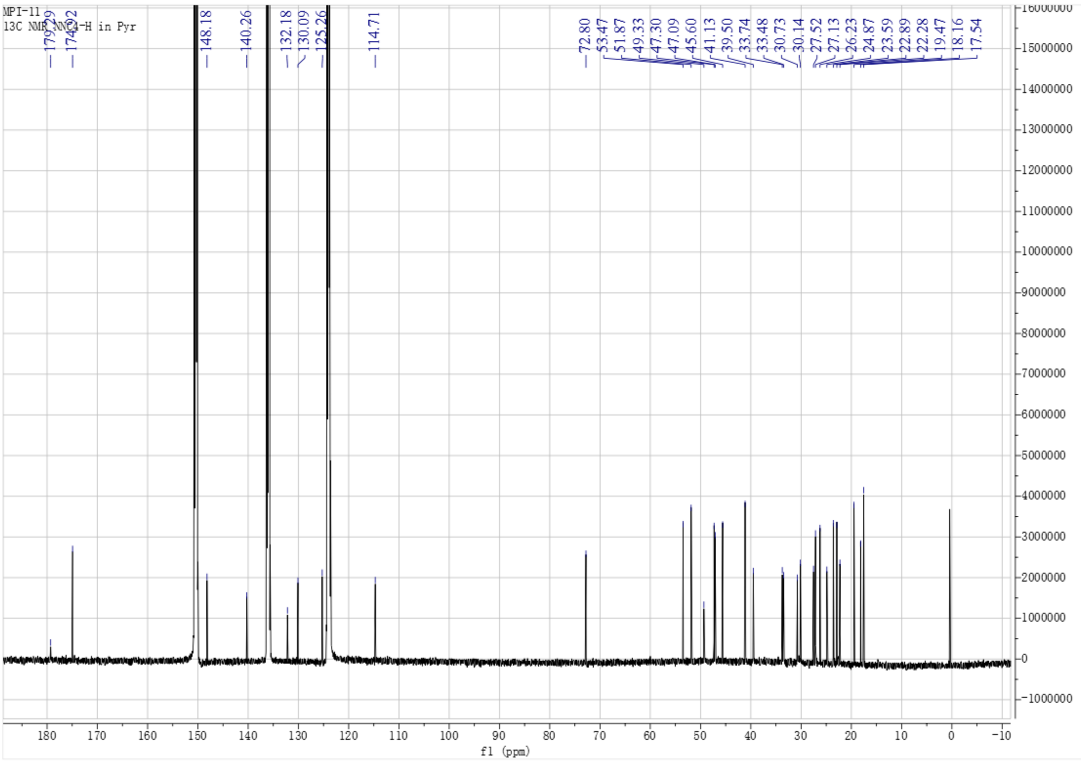

Figure S167. ^{13}C NMR spectrum (150 MHz, C_5D_5N) of compound **35**

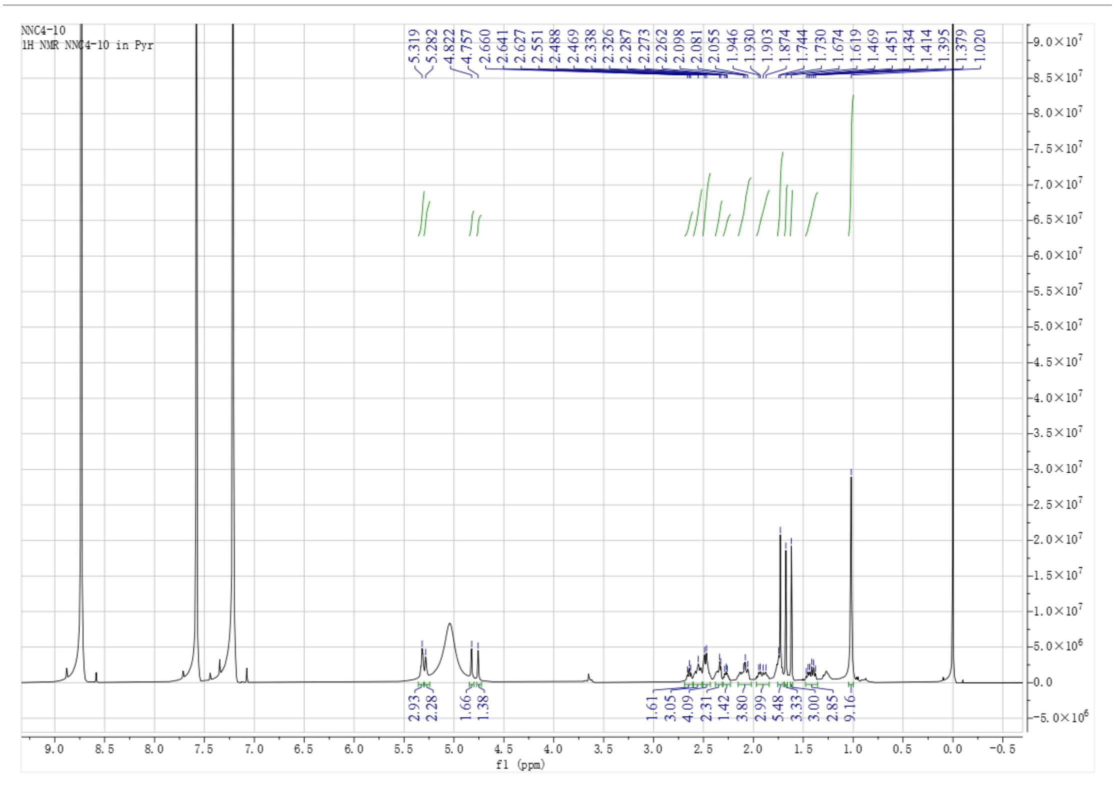

Figure S168. ^{1}H NMR spectrum (600 MHz, C_5D_5N) of compound **36**

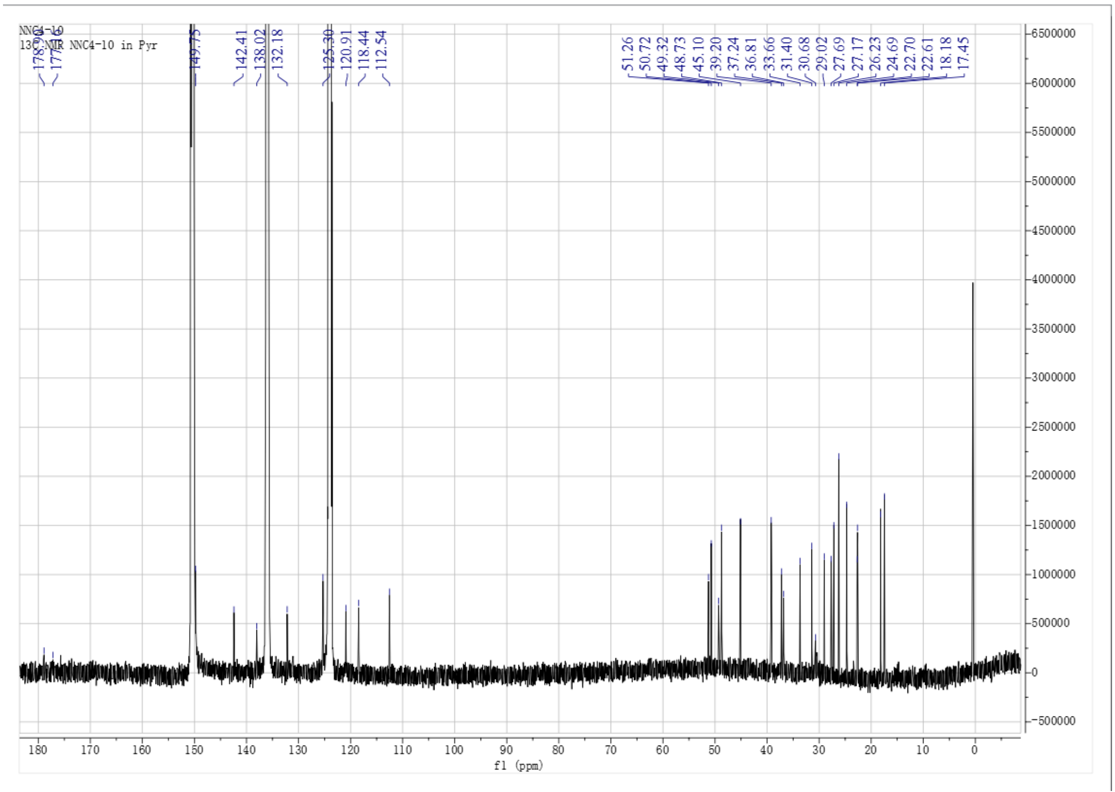

Figure S169. ^{13}C NMR spectrum (150 MHz, C_5D_5N) of compound **36**

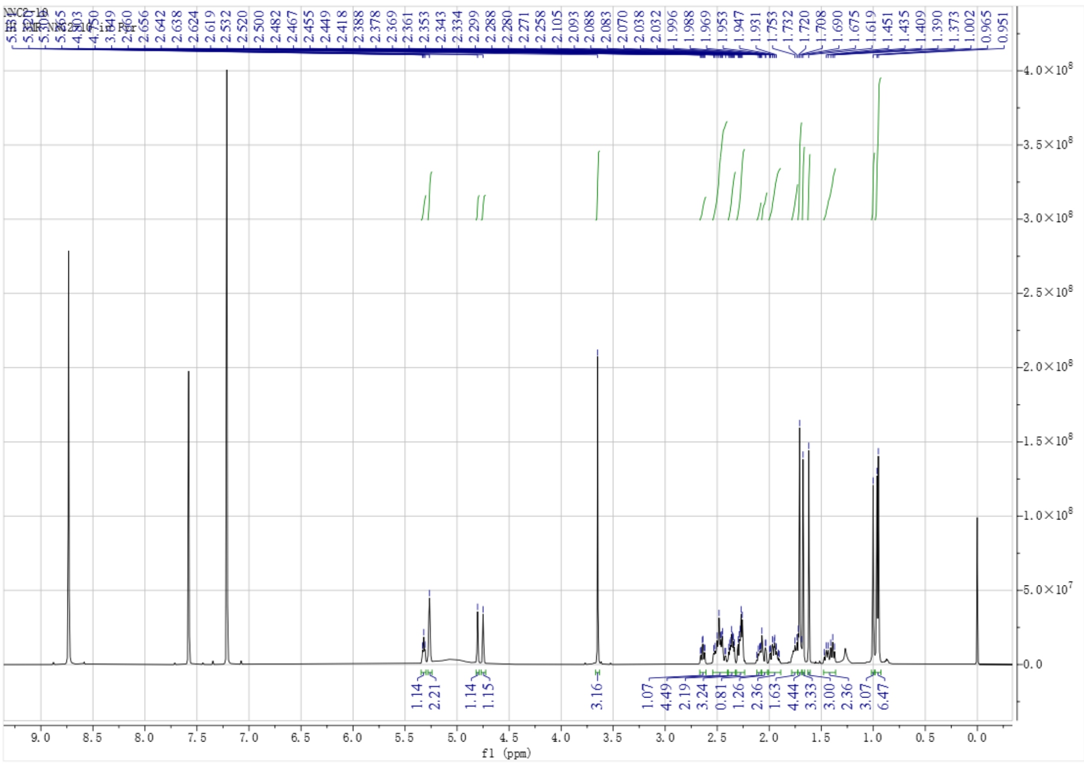

Figure S170. ^{1}H NMR spectrum (600 MHz, C_5D_5N) of compound **37**

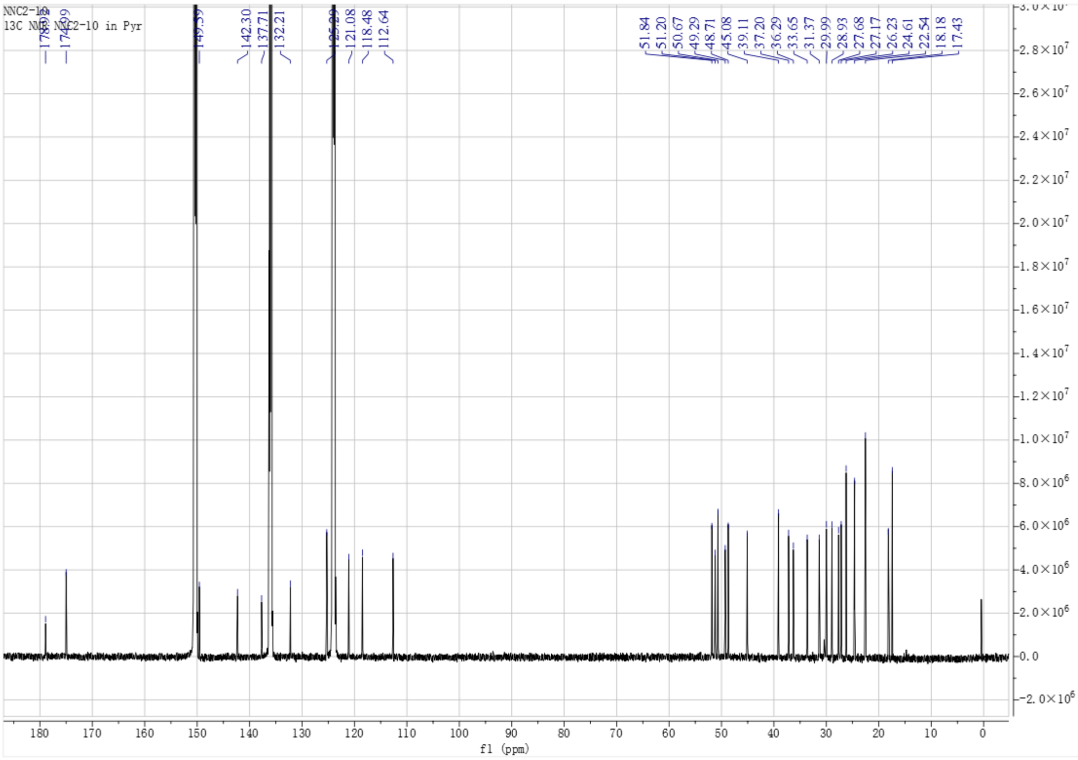

Figure S171. ^{13}C NMR spectrum (150 MHz, C_5D_5N) of compound **37**

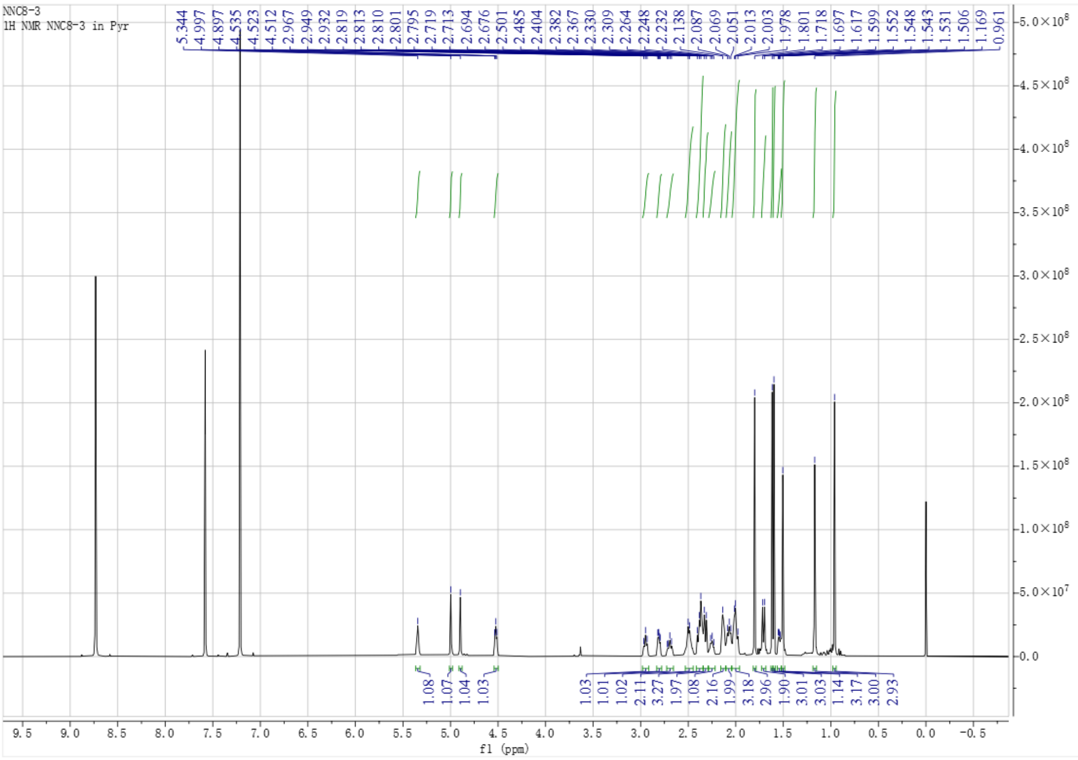

Figure S172. ^{1}H NMR spectrum (600 MHz, C_5D_5N) of compound **38**

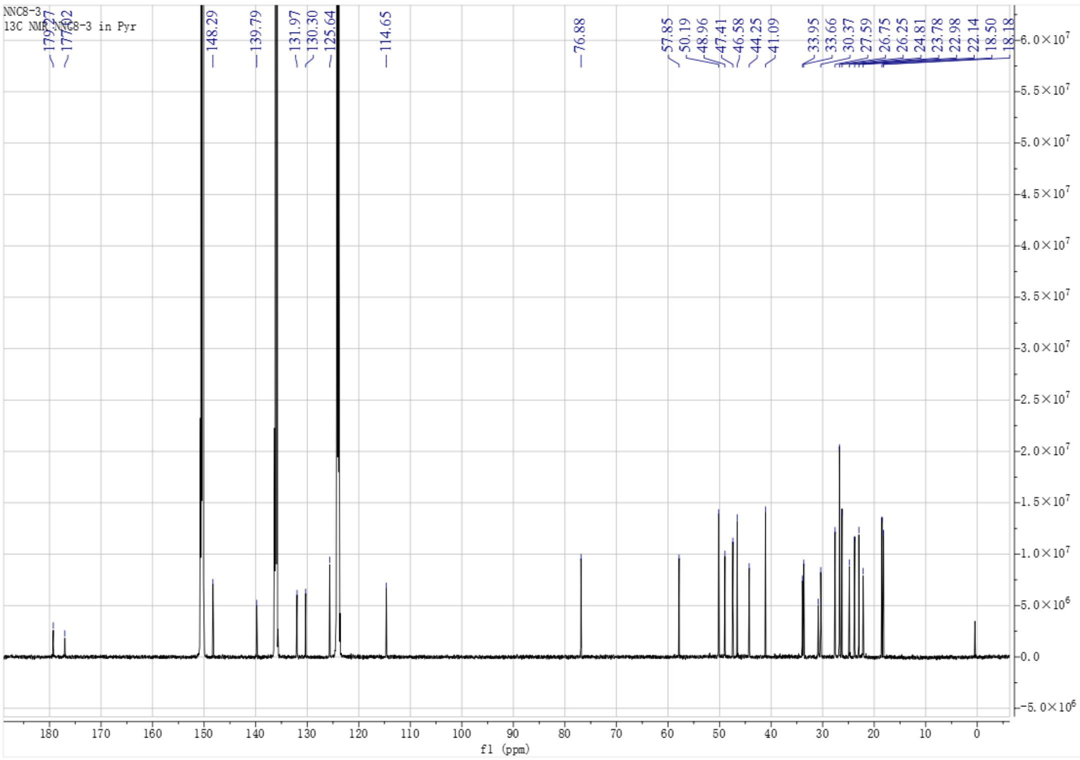

Figure S173. ^{13}C NMR spectrum (150 MHz, C_5D_5N) of compound **38**

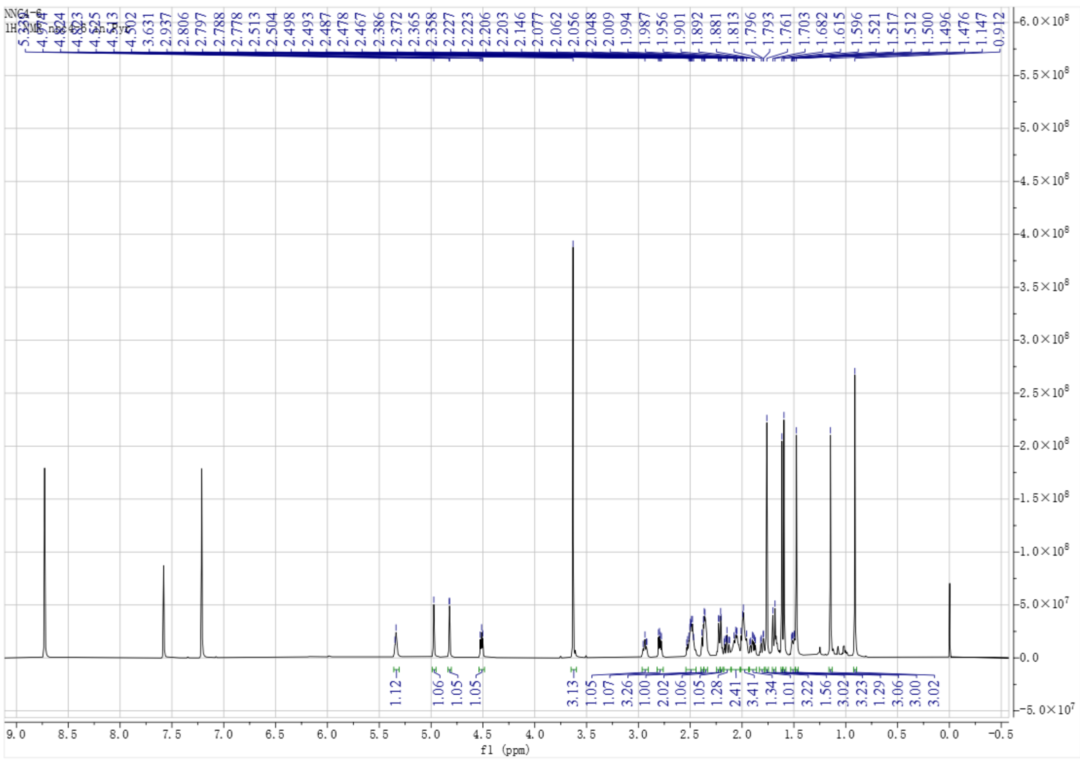

Figure S174. ^{1}H NMR spectrum (600 MHz, C_5D_5N) of compound **39**

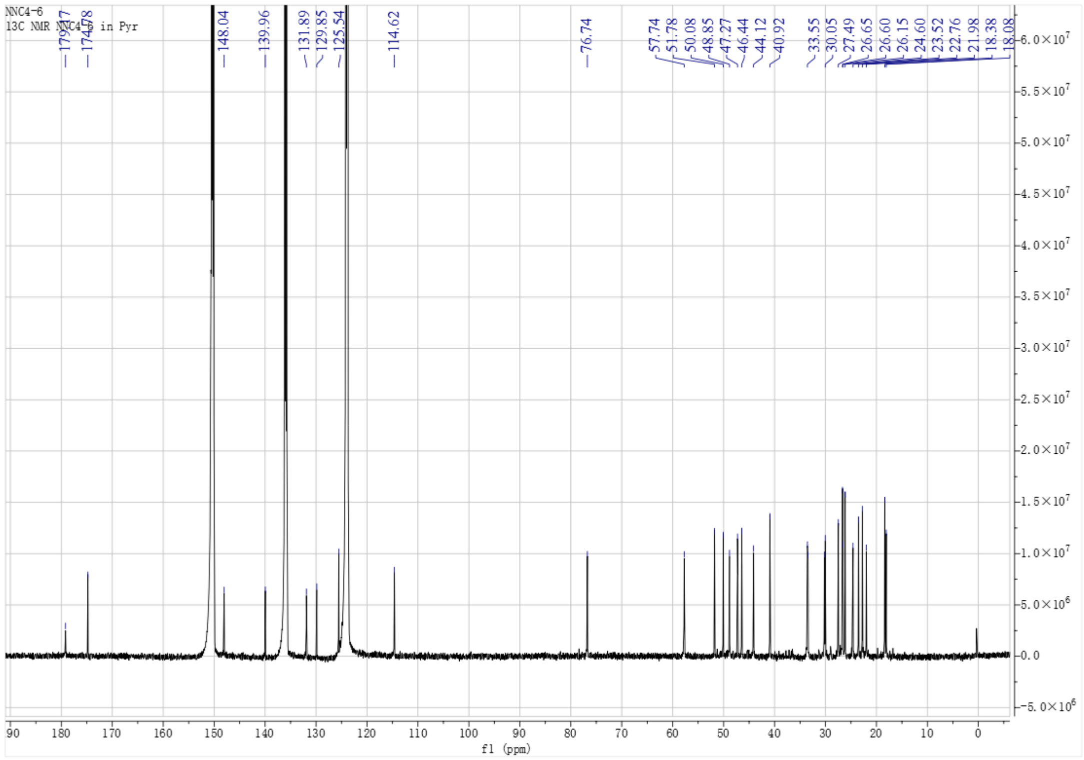

Figure S175. ^{13}C NMR spectrum (150 MHz, C_5D_5N) of compound **39**

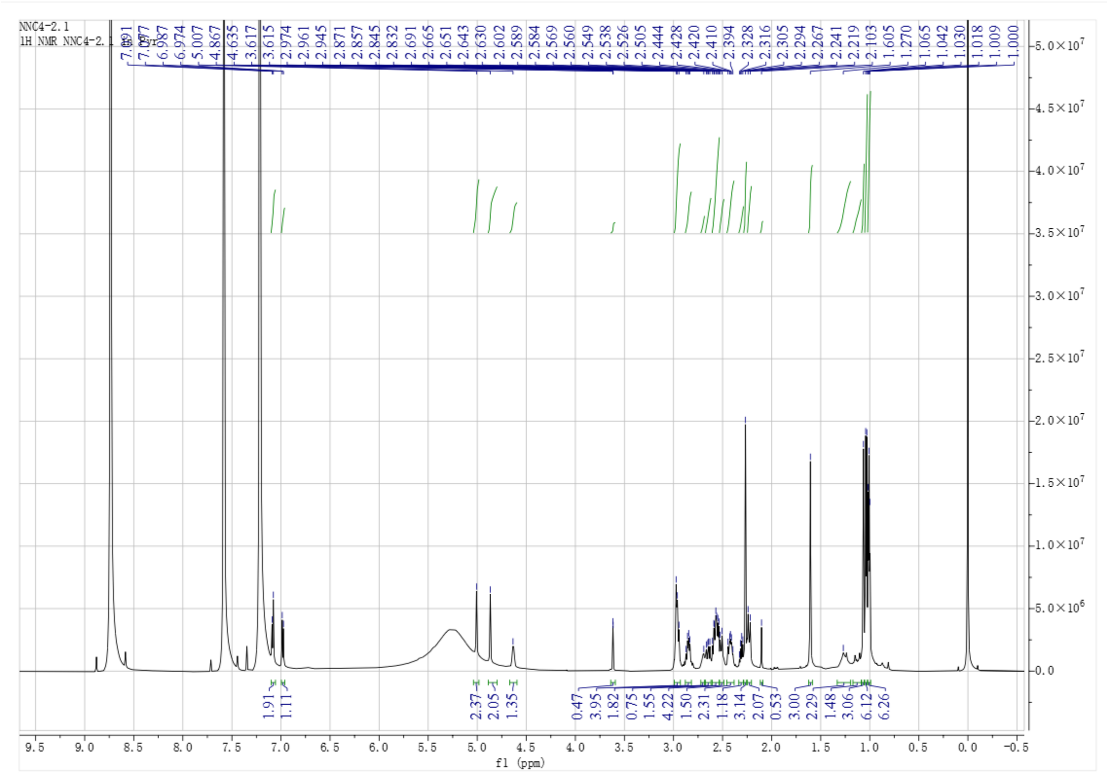

Figure S176. ^{1}H NMR spectrum (600 MHz, C_5D_5N) of compound **40**

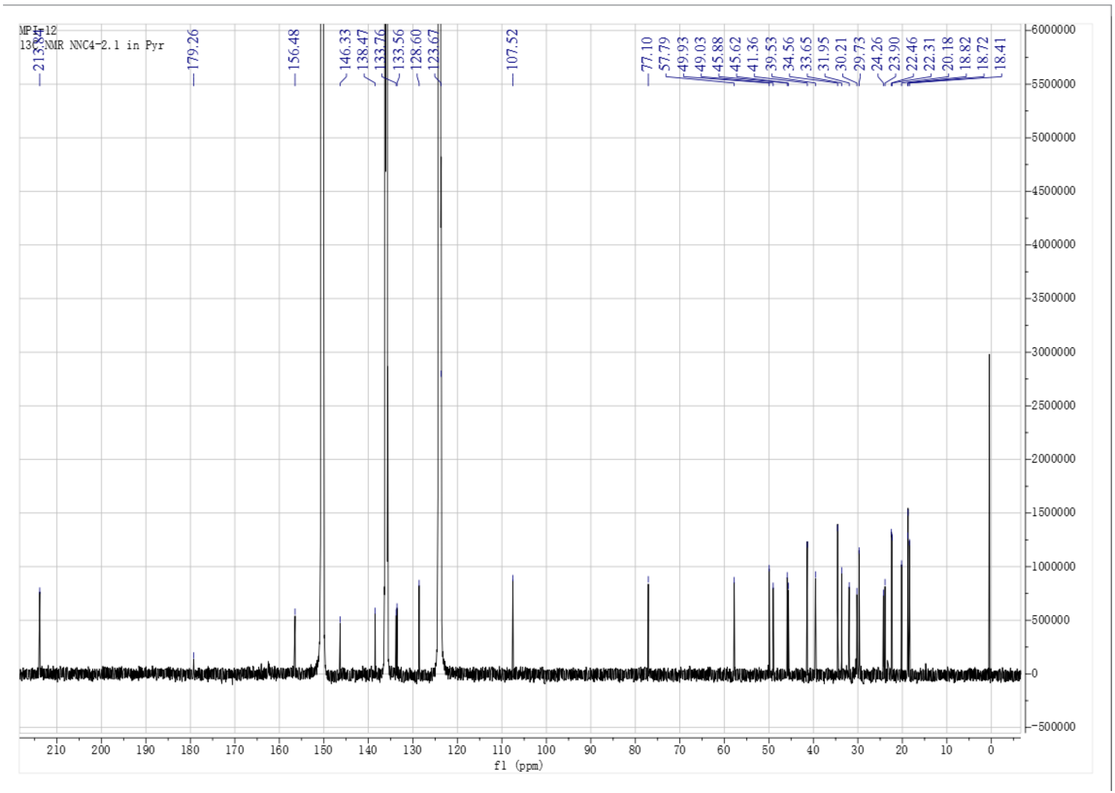

Figure S177. ^{13}C NMR spectrum (150 MHz, C_5D_5N) of compound **40**

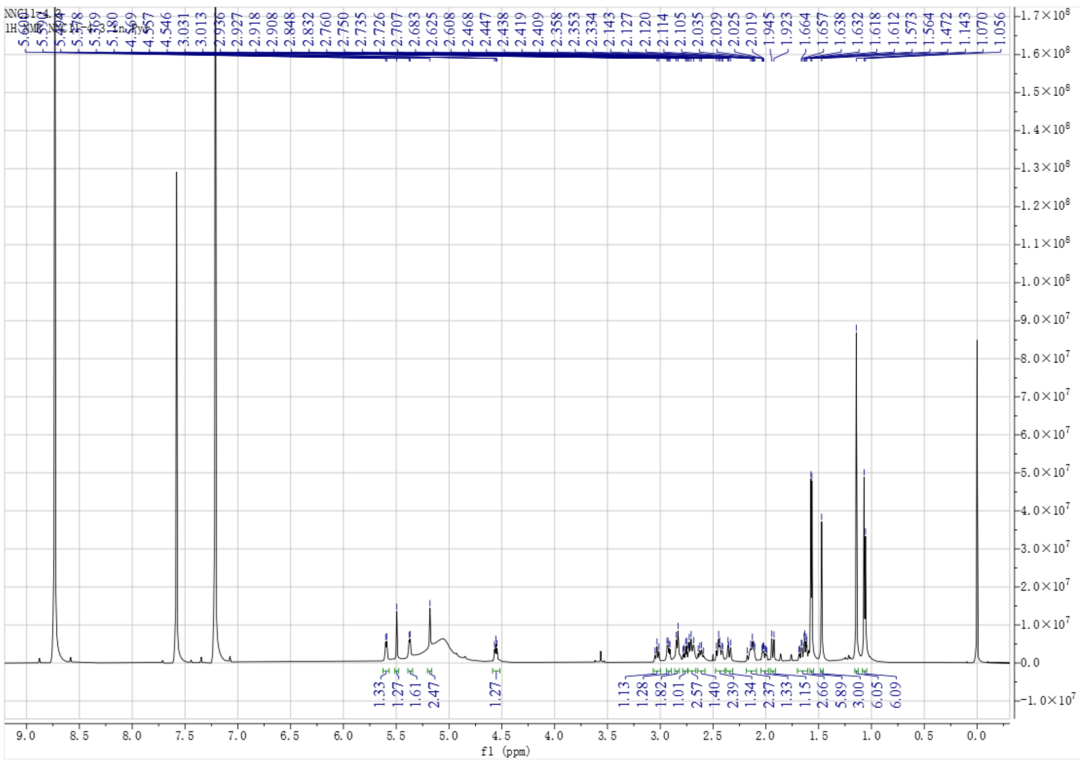

Figure S178. ^{1}H NMR spectrum (600 MHz, C_5D_5N) of compound **41**

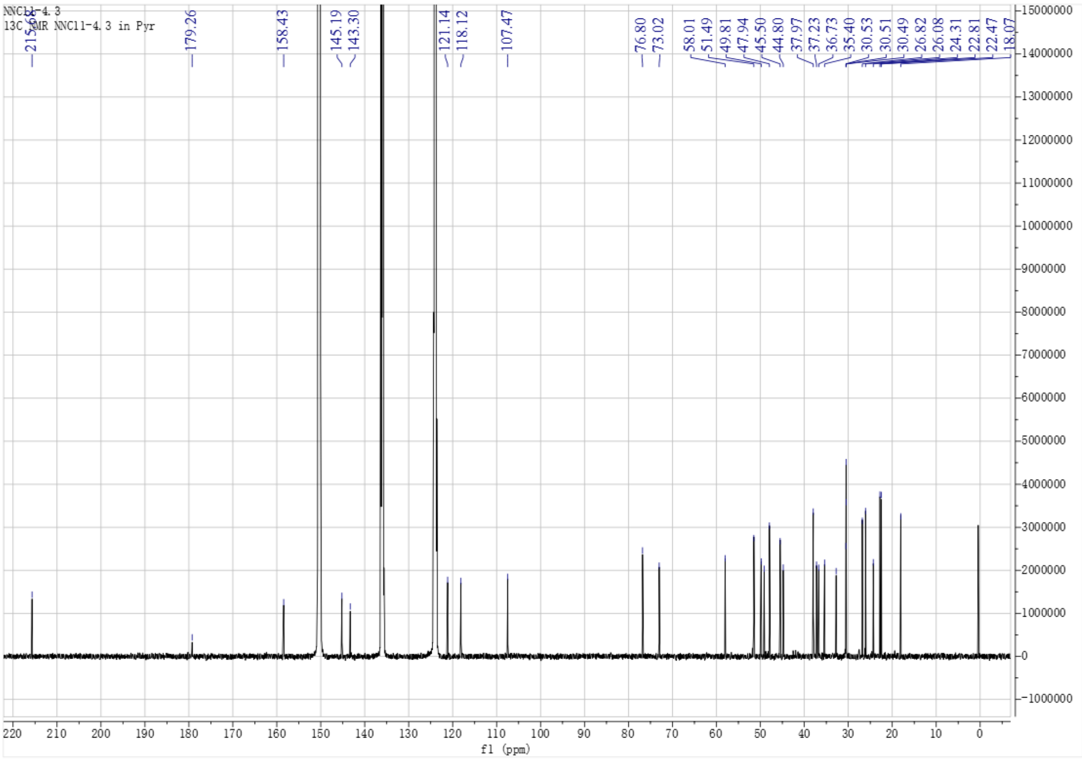

Figure S179. ^{13}C NMR spectrum (150 MHz, C_5D_5N) of compound **41**

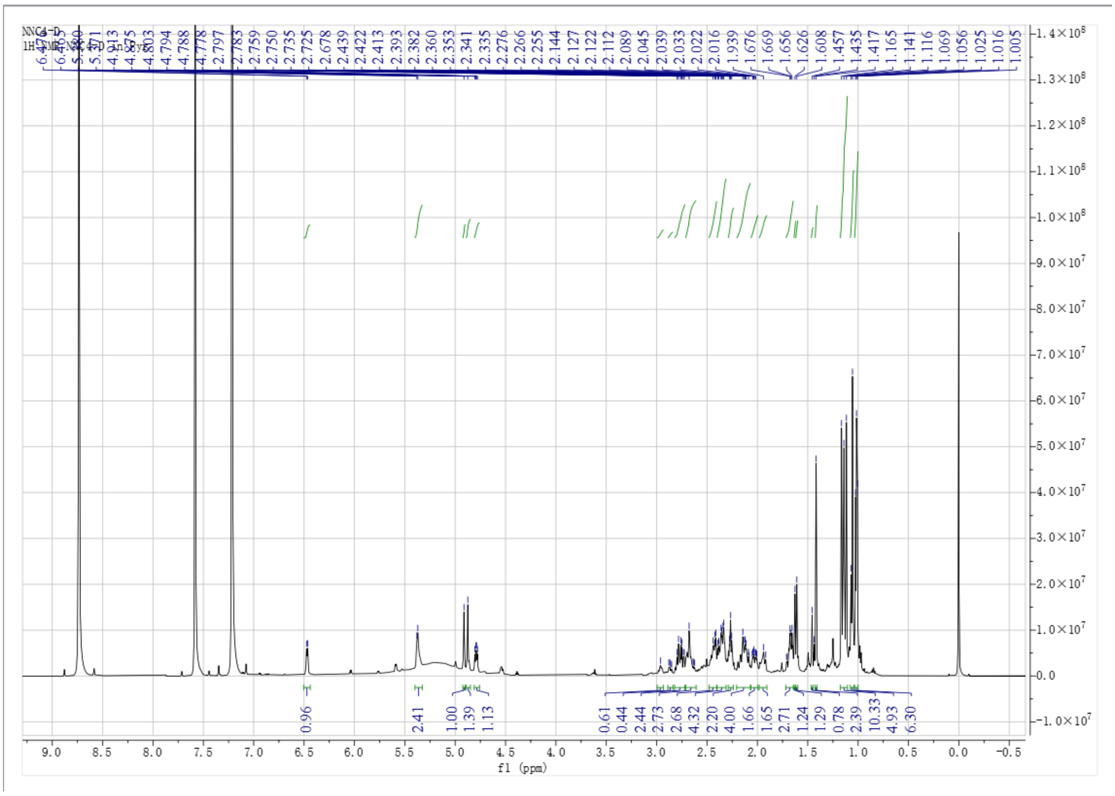

Figure S180. ^{1}H NMR spectrum (600 MHz, C_5D_5N) of compound **42**

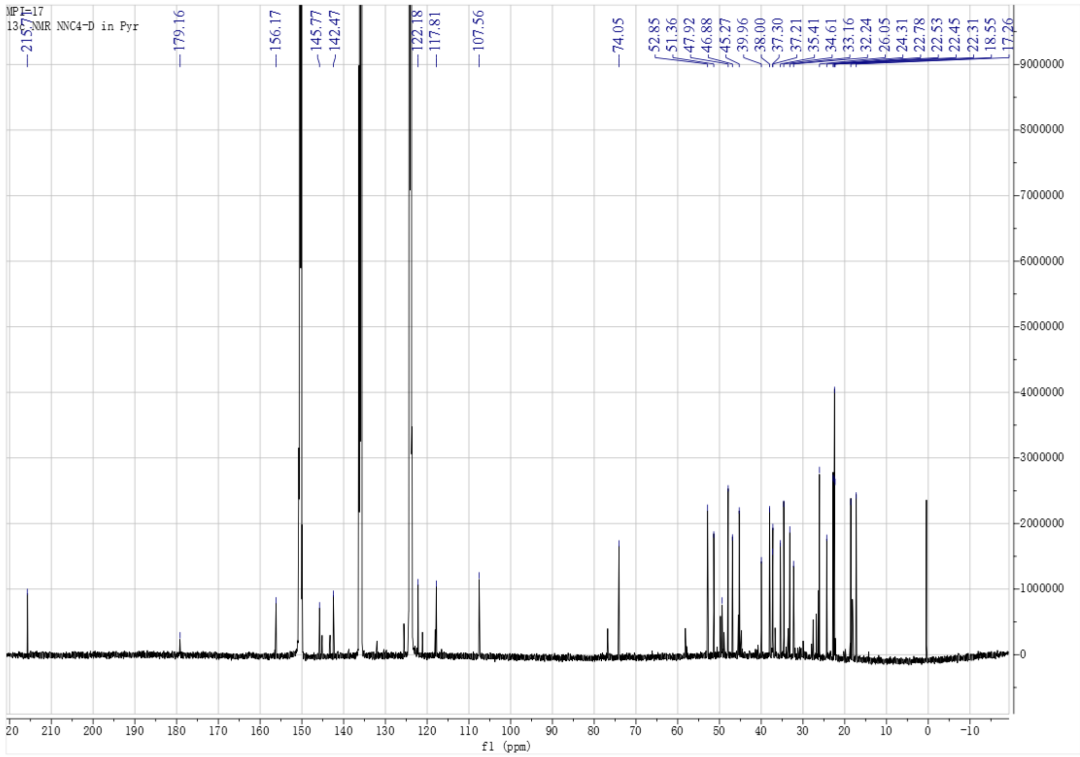

Figure S181. ^{13}C NMR spectrum (150 MHz, C_5D_5N) of compound **42**

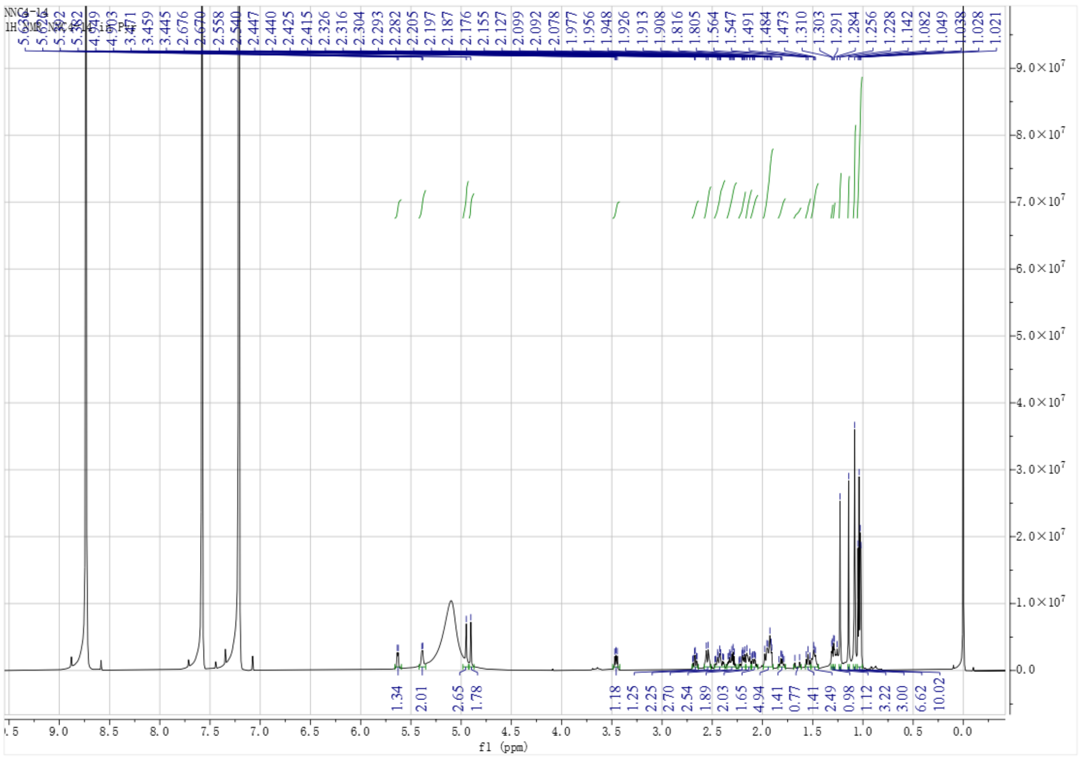

Figure S182. ^{1}H NMR spectrum (600 MHz, C_5D_5N) of compound **43**

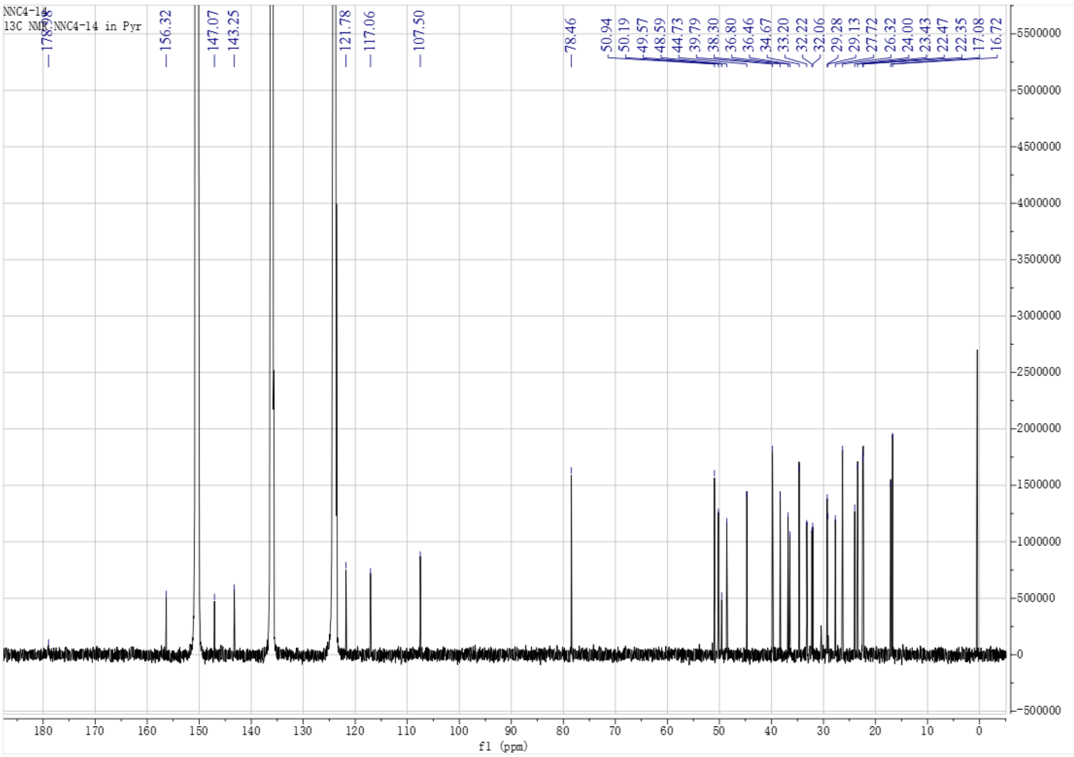

Figure S183. ^{13}C NMR spectrum (150 MHz, C_5D_5N) of compound **43**

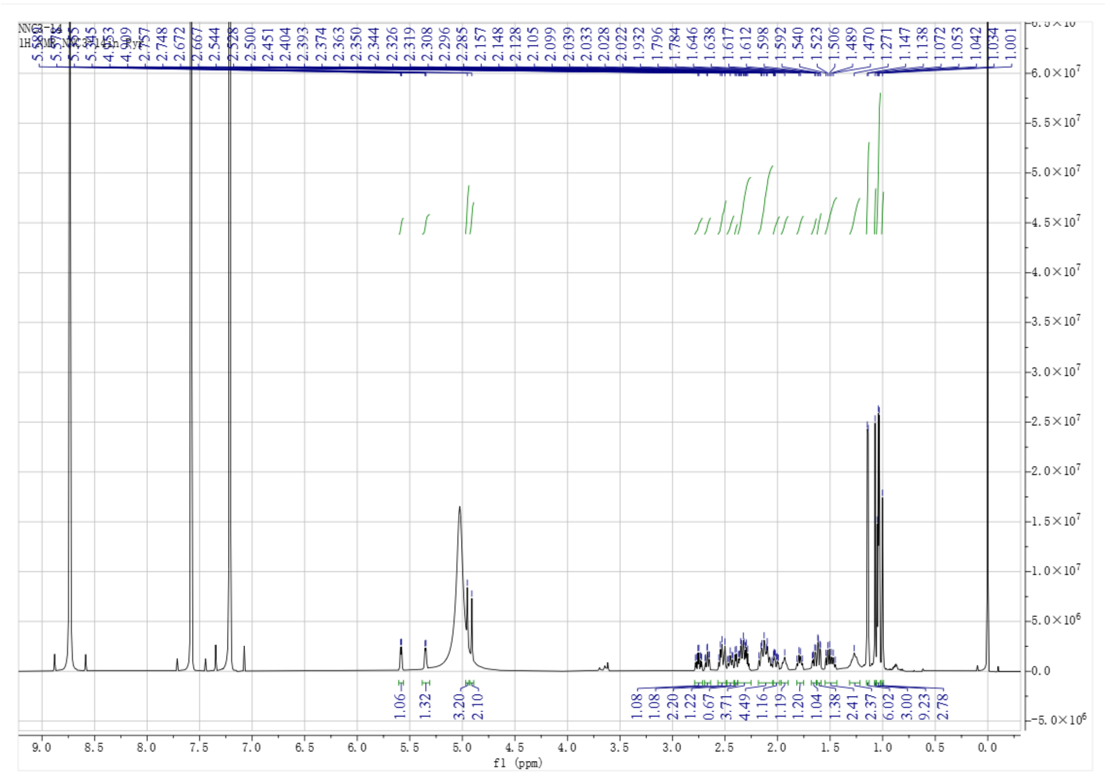

Figure S184. ^{1}H NMR spectrum (600 MHz, C_5D_5N) of compound **44**

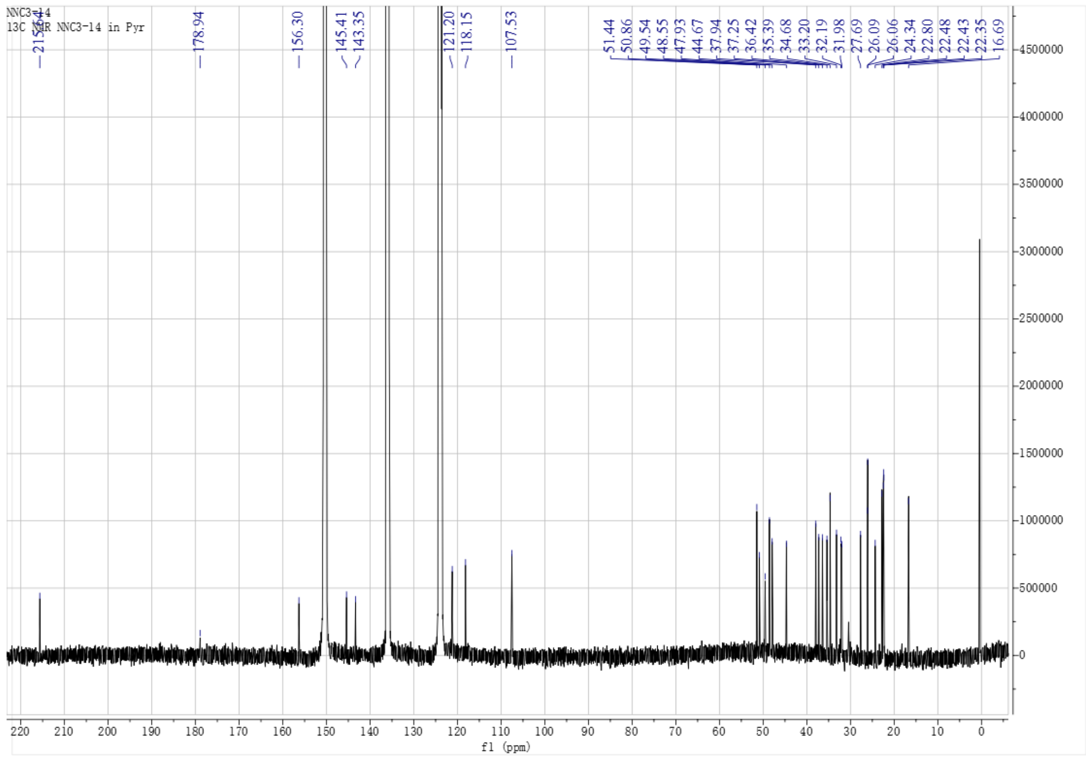

Figure S185. ^{13}C NMR spectrum (150 MHz, C_5D_5N) of compound **44**

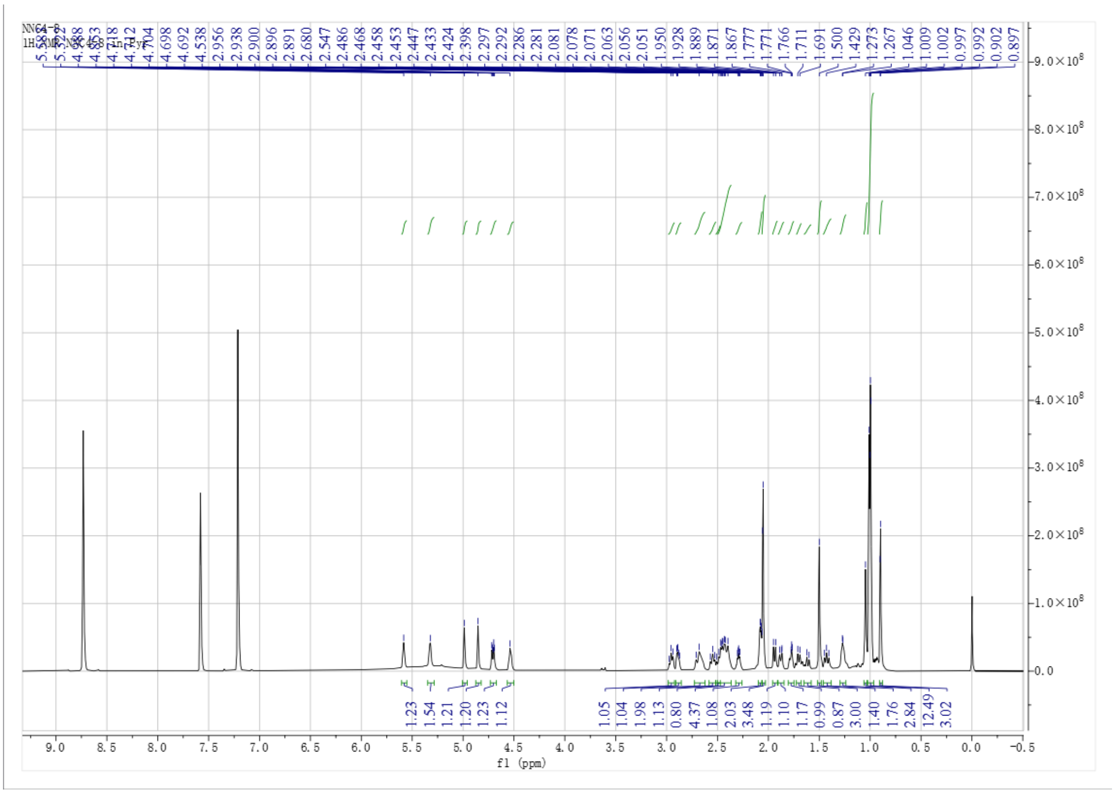

Figure S186. ^{1}H NMR spectrum (600 MHz, C_5D_5N) of compound **45**

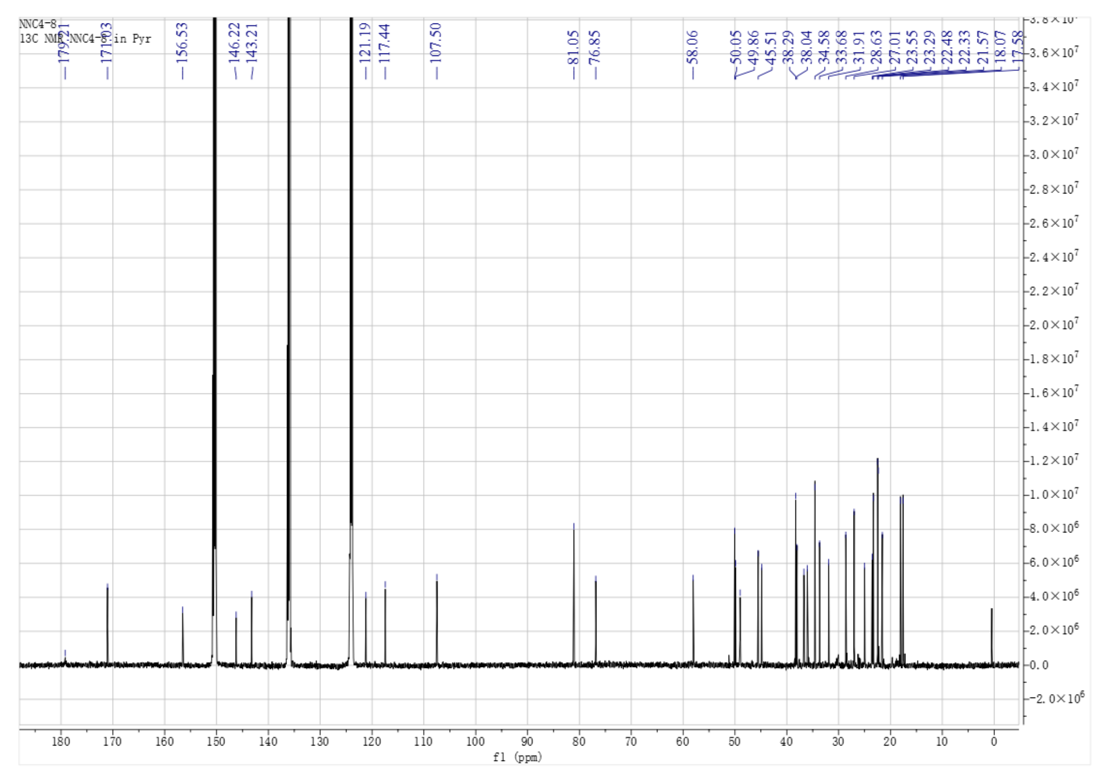

Figure S187. ^{13}C NMR spectrum (150 MHz, C_5D_5N) of compound **45**

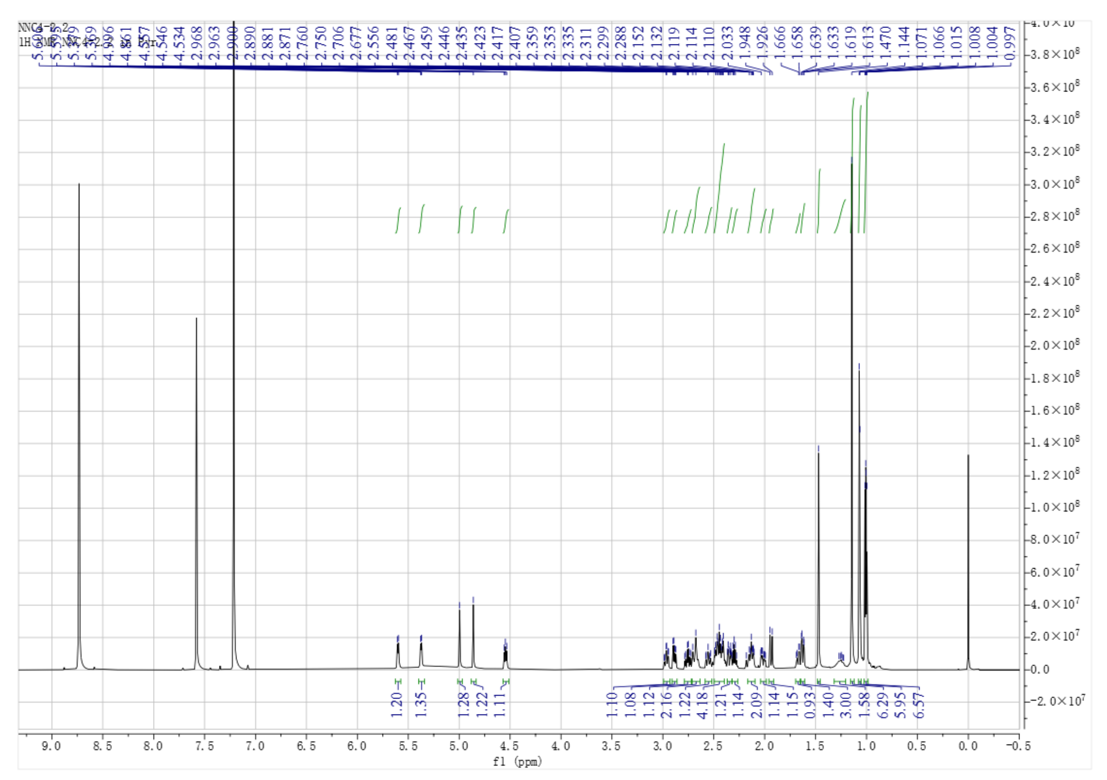

Figure S188. ^{1}H NMR spectrum (600 MHz, C_5D_5N) of compound **46**

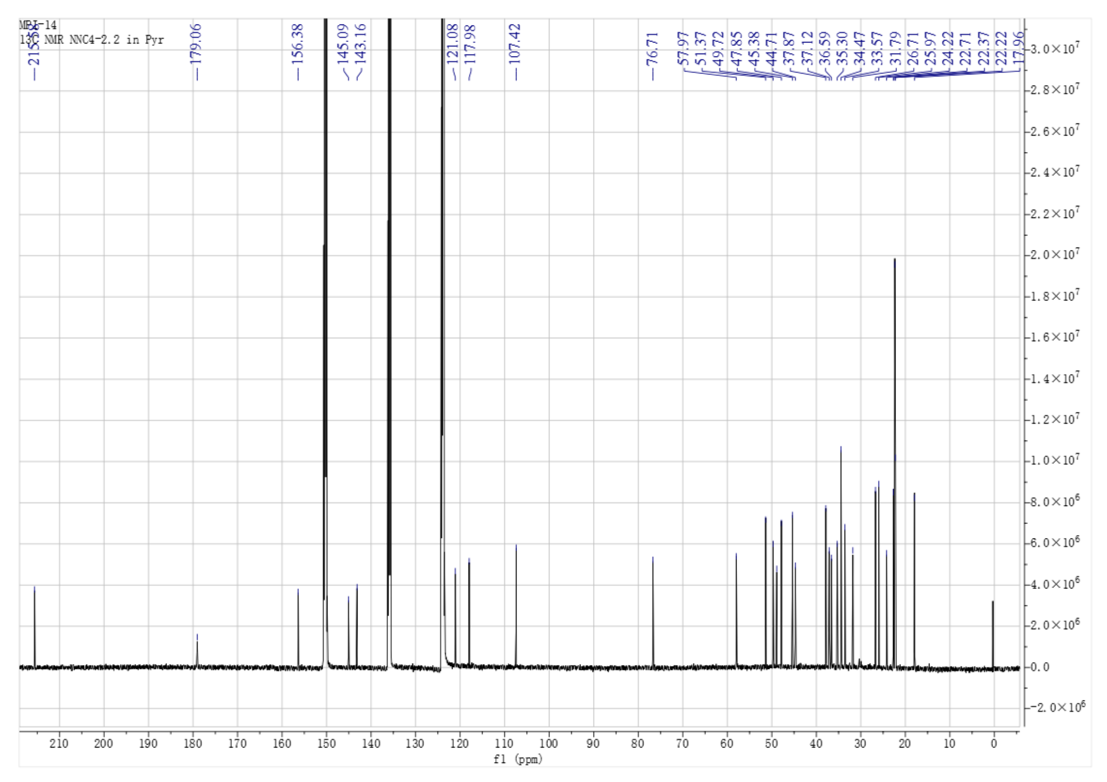

Figure S189. ^{13}C NMR spectrum (150 MHz, C_5D_5N) of compound **46**